# Modelling of postprandial glucose and insulin dynamics

# Modelling of postprandial glucose and insulin dynamics: the role of amino acids

Bart van Sloun

Cover design by Jelle Janssen (www.jellejanssen.nl)
Printed by Gildeprint Enschede, gildeprint.nl
Layout and design: jildou Hengst, persoonlijkproefschrift.nl

ISBN: 978-94-6419-896-6

# Modelling of postprandial glucose and insulin dynamics: the role of amino acids

DISSERTATION

to obtain the degree of Doctor at the Maastricht University,
on the authority of the Rector Magnificus, Prof. dr. Pamela Habibović
in accordance with the decision of the Board of Deans,
to be defended in public on

Friday 27th of October 2023, at 10:00 hours

by

Bart Johannes Hendrikus van Sloun

**Promotors**

Prof. Dr. Ir. Ilja. C.W. Arts

Prof. Dr. Ir. Natal A.W. van Riel (Eindhoven University of Technology)

**Co-promotor**

Dr. Gijs H. Goossens

**Assessment Committee**

Prof. Dr. Ir. Ralf L.M. Peeters (Chair)

Prof. Dr. Barbara M. Bakker (University of Groningen)

Dr. Aurélie M.F. Carlier

Prof. Dr. Peter A.J. Hilbers (Eindhoven University of Technology)

Dr. Lex B. Verdijk

The studies presented in this thesis were performed within the framework of TiFN

# TABLE OF CONTENTS

# 1 General introduction

The complexity of biological systems manifests itself in many features, including the large number of components involved and the intricate interactions between these components. As a consequence, reliable predictions can't be made based on intuition alone. Computational models can be combined with datasets containing information on biological parameters and variables such as genes, protein, and metabolites, to perform *in silico* simulations of complex biological systems [1]. This serves a variety of roles, including hypothesis testing and generating new insight in the biological processes that underlie health and disease [2]. Various computational modelling techniques exist, from mechanistic models to data-driven approaches, each having their own advantages and disadvantages [3-5]. Data-driven approaches such as machine learning, examine patterns in data to determine the best combination of input variables that predict the desired outcomes [6, 7]. Most data-driven approaches, however, are 'black box', meaning that a causal explanation for the prediction is absent. In contrast, mechanistic models are based on rate equations and describe how quantities of interest change in time, using an *a priori* understanding of the underlying biological system [8]. As biological processes are inherently dynamic, mechanistic modelling allows simulation and insight in complex metabolic systems, such as the glucose-insulin regulatory system, which includes various organs and tissues and maintains blood glucose to ensure normal body function [9, 10].

## FOOD INTAKE AND GLUCOSE HOMEOSTASIS

In the acute postprandial state, which means the period following meal intake, the body absorbs nutrients from the gastro-intestinal tract. Carbohydrates are the body's primary energy source and are ingested as simple carbohydrates like monosaccharides and disaccharides or as complex carbohydrates, such as oligosaccharides and polysaccharides [11]. Various organs, for example the brain, require a continues supply of the monosaccharide glucose to function properly [12]. If glucose concentrations in the blood fall too low (hypoglycemia) or rise too high (hyperglycemia) for a prolonged period of time, it can lead to major health problems [13, 14]. As such, a tightly-regulated feedback system, consisting of various hormones and neuropeptides released from the intestine, pancreas, brain, liver, muscle and adipose tissue, ensures tight control of blood glucose levels [15].

## GLUCOSE REGULATORY SYSTEM

The main processes involved in glucose regulation are illustrated in Figure 1. One of the major determinants of how quickly glucose appears in the circulation following ingestion of a meal is the gastric emptying rate, which is the speed at which gastric contents leave the stomach after ingestion [16, 17]. The rate of gastric emptying is mainly regulated by gastrointestinal peptide hormones, such as cholecystokinin (CCK) and Glucagon-like-peptide 1 (GLP-1) [18-20]. One of the roles of GLP-1 includes slowing down glucose entry into the bloodstream, thus reducing postprandial fluctuations in blood glucose levels [21]. However, to prevent an excessive increase in blood glucose concentrations after meal intake, the increase in glucose delivery requires a comparable increase in the removal of glucose from the circulation [22].

The most important hormones involved in blood glucose regulation are insulin, glucagon and adrenaline [15]. Insulin is a peptide hormone secreted by the β-cells of the pancreas that facilitates the uptake of glucose to insulin-dependent tissues, such as skeletal muscle and adipose tissue, and inhibits glucose production in the liver [23, 24].

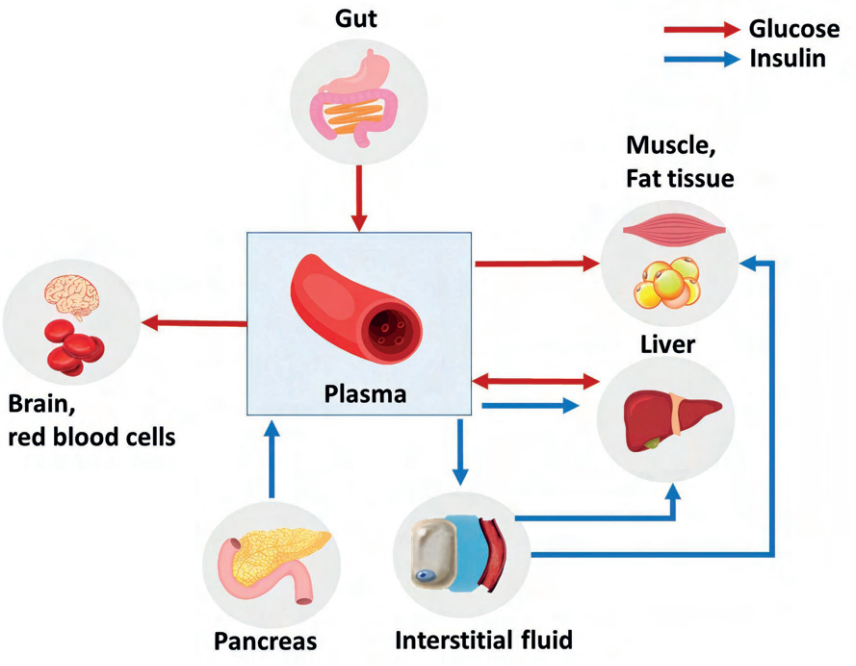


**Figure 1. Glucose regulatory system.** This figure depicts major processes involved in the glucose regulatory system. The red arrows indicate the flow of glucose. The blue arrows indicate the flow of insulin.

Glucose exerts insulin secretion from pancreatic β-cells by inducing a rise in ATP/ADP ratio, suppressing ATP-sensitive potassium channels and leading to the activation of voltage-gated $Ca^{2+}$ channels. The subsequent calcium influx enables exocytosis of the insulin granules from the β-cells [25, 26]. Glucagon is a peptide hormone secreted by the α-cells of the pancreas and plays an important role in maintaining glucose levels by stimulating liver glucose production [27]. In contrast to the effects of insulin, glucagon acts as a glucose-mobilizing hormone, which promotes the conversion of glycogen to glucose (glycogenolysis) in the liver, stimulates *de novo* glucose synthesis from non-carbohydrate precursors (gluconeogenesis) in the liver, and inhibits glucose breakdown (glycolysis) and glycogen formation (glycogenesis). Circulating glucose acts as the most potent regulator of glucagon secretion, as hypoglycemia stimulates the pancreatic α-cells to secrete glucagon, whereas hyperglycemia inhibits glucagon secretion [27]. Adrenaline is a hormone mainly produced in the adrenal glands and plays an important role in regulating glucose metabolism [28]. Adrenaline increases plasma glucose through promoting glycogenolysis in the liver and skeletal

muscle, gluconeogenesis in the liver, and inhibition of glucose uptake by tissues such as the skeletal muscle.

Thus, through the influence of various hormones, in particular the actions of insulin, glucagon and adrenaline, blood glucose is tightly controlled under different physiological conditions. Whilst providing a simplified overview of the main processes involved in postprandial glucose metabolism, several other factors have been shown to influence glucose metabolism, such as amino acids (AAs). Not all of these factors are well understood, and interactions between various physiological processes make it even more complex.



## INSULIN RESISTANCE: A KEY FACTOR IN GLUCOSE HOMEOSTASIS

In individuals with insulin resistance, the regulatory system that aims for glucose homeostasis is not functioning properly [29]. Insulin resistance is defined as an impairment in the uptake of glucose by the insulin-dependent tissues, and may lead to the development of type 2 diabetes mellitus (T2DM), which is characterized by persistent hyperglycemia [29, 30]. One of the major causes of insulin resistance is obesity, which is the result of an imbalance between energy intake and energy expenditure [31]. The long-term positive energy balance contributes to adipose tissue dysfunction, ectopic fat storage and may induce insulin resistance, in which the muscle, fat, and liver cells fail to respond normally to the effects of insulin, resulting in a compensatory increase in insulin secretion from β-cells [32]. Although insulin resistance often develops simultaneously in multiple organs, its severity and phenotype may differ between tissues [33]. Skeletal muscle, due to its high rate of insulin-stimulated glucose uptake, represents an important tissue in the development of insulin resistance [34, 35]. In individuals with the muscle insulin resistance (MIR) phenotype, the insulin-stimulated glucose uptake by the skeletal muscle is markedly impaired [36]. It is believed that this impaired glucose uptake, which characterizes muscle insulin resistance, results from impaired insulin receptor signaling and intracellular defects, including impaired glucose transport and glucose phosphorylation, reduced glucose oxidation and glycogen synthesis [36, 37]. Another important tissue in the development of insulin resistance is the liver, which aims to maintain a balance between glucose production and glucose storage in the form of glycogen [38]. In liver insulin resistance (LIR), insulin fails to appropriately regulate liver metabolism, resulting in excess

glucose production [39]. Furthermore, liver insulin resistance causes decreased glycogen synthesis and increased lipid accumulation [40]. If insulin resistance is left untreated and β-cell dysfunction is present, hyperglycemia is amplified leading to the progression to T2DM [41].

## THE EFFECTS OF PROTEIN AND AMINO ACID INTAKE ON GLUCOSE HOMEOSTASIS

Besides carbohydrates, foods contain other nutrients such as fat, protein, and fiber. Protein and their constituent AAs, which we focus on in the current thesis, have been shown to have a notable impact on both acute and long-term postprandial glucose metabolism [42]. AAs can be divided in various categories (Table 1). Essential AAs are defined as AAs that cannot be synthesized by humans and must come from the diet [43]. AAs can be glucogenic (i.e. AAs that can be converted into glucose through gluconeogenesis), and/or ketogenic (i.e. AAs that are converted into ketone bodies) [44]. Furthermore, there are the branched chain amino acids (BCAAs) which all have protein anabolic properties (enhanced protein synthesis and/or a decrease rate of protein degradation) [45, 46].

**Table 1. List of amino acids**

| Amino acid | Essential | Glucogenic | Ketogenic | BCAA |
|---|---|---|---|---|
| Alanine | | ✓ | | |
| Arginine | | ✓ | | |
| Asparagine | | ✓ | | |
| Aspartic Acid | | ✓ | | |
| Cysteine | | ✓ | | |
| Glutamic acid | | ✓ | | |
| Glutamine | | ✓ | | |
| Glycine | | ✓ | | |
| Histidine | ✓ | ✓ | | |
| Isoleucine | ✓ | ✓ | ✓ | ✓ |
| Leucine | ✓ | | ✓ | ✓ |
| Lysine | ✓ | | ✓ | |
| Methionine | ✓ | ✓ | | |
| Phenylalanine | ✓ | ✓ | ✓ | |

**Table 1. List of amino acids (continued)**

| Amino acid | Essential | Glucogenic | Ketogenic | BCAA |
|---|---|---|---|---|
| Proline | | ✓ | | |
| Serine | | ✓ | | |
| Threonine | ✓ | ✓ | ✓ | |
| Tryptophan | ✓ | ✓ | ✓ | |
| Tyrosine | | ✓ | ✓ | |
| Valine | ✓ | ✓ | | ✓ |



In most cases, proteins are consumed as part of foods, and not as isolated ingredients. The digestion of the majority of dietary proteins starts in the stomach and continues in the small intestine [47]. Through a variety of digestive enzymes, proteins are broken down into AAs that are absorbed across the small intestinal enterocytes into the bloodstream. AAs are transported directly to the liver by the liver portal vein [48]. AAs stimulate glucagon release from pancreatic α-cells to allow AA uptake and metabolism in the liver, where they are used as substrates for protein synthesis, nitrogen containing compounds, and gluconeogenesis [27, 49, 50]. AAs that pass through the liver (mainly BCAAs), are metabolized primarily in the peripheral tissues (particularly skeletal muscle), through the effects of insulin release from pancreatic β-cells [51-54]. Here, they are used as substrates for protein synthesis and suppress the breakdown of protein into smaller polypeptides or AAs (proteolysis) [55]. AAs exert some of their effects on insulin secretion via β-cell metabolism, allowing a rise in ATP/ADP ratio, suppression of ATP sensitive potassium ($K_{ATP}$) channels and activation of voltage-gated $Ca^{2+}$ channels, leading to stimulation of insulin granule release [56]. Furthermore, several AAs have been shown to have distinct mechanisms leading up to insulin secretion, as well as exert a synergistic effect on the postprandial insulin response and attenuation of the glucose response when co-ingested with glucose [57, 58]. The insulin secretion effect of AA intake has also been demonstrated in patients with T2DM [59]. In the long term, high protein diets have been shown to lead to a reduction in body weight, fat mass, and increase in the glucose metabolic clearance rate [60-62].

## NUTRITIONAL MANAGEMENT OF BLOOD GLUCOSE

Nutritional management of blood glucose levels is an important target in the prevention and management of metabolic diseases such as T2DM [63]. Dietary interventions can have significant and clinically relevant effects on blood glucose modulation. However, a large heterogeneity exists in an individual's response to a dietary intervention, which can be attributed to differences in genetic, environmental, and lifestyle factors [64]. Recent findings indicate that individuals with distinct metabolic phenotypes, for example, individuals with MIR or LIR, may have different outcomes regarding glucose homeostasis in response to dietary macronutrient modulation [65, 66]. The PERSonalized glucose Optimization through Nutritional intervention (PERSON) study was designed to investigate the effect of an optimal compared to a suboptimal dietary intervention, according to tissue-specific insulin resistant phenotype, on glucose metabolism and other metabolic health outcomes [67]. The participants of this study were extensively phenotyped before and after the intervention, including the use of various challenge tests (i.e. oral glucose tolerance test (OGTT) and high-fat mixed meal challenge). Such challenge tests are widely used in clinical metabolic research and diabetes drug development, and provide an assessment of glucose tolerance and β-cell function [68, 69]. In an OGTT, a standard dose of glucose is ingested orally and blood samples are collected at regular time-intervals to allow assessment of postprandial glucose and insulin profiles (illustrated in Figure 2). OGTTs have widely been used for evaluation of β-cell dysfunction in obesity, prediabetes, and T2DM [70].

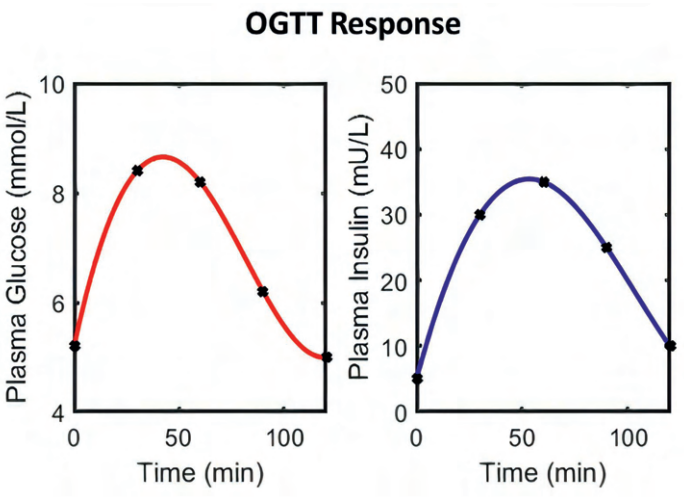


**Figure 2. Plasma glucose and insulin response following an OGTT.** This figure depicts plasma glucose (red) and insulin (blue) concentrations following an OGTT. Sampling points are indicated with an asterisk (*).

A mixed meal challenge test consists of a high caloric mixture of carbohydrates, fat, and protein. As nutrients other than glucose (e.g. protein, and fat) have been shown to affect glucose homeostasis, these mixed meals induce physiologically relevant postprandial responses and allow assessment of postprandial profiles of AAs, triglycerides, non-esterified fatty acids and their interplay with glucose and glucoregulatory hormones [71].

## MECHANISTIC MODELLING OF GLUCOSE HOMEOSTASIS

Physiology-based mechanistic models of the glucose regulatory system, as introduced before, are able to provide quantitative information on postprandial glucose and insulin dynamics, whilst taking the underlying mechanisms into account [10, 72]. Such models are constructed using a bottom up approach, using *a priori* understanding of the underlying biological system. The reactions in the model are described by equations, and the rates at which each reaction occurs are determined by parameters, often inferred from experimental data [73]. The estimation of these parameters, by fitting the model simulation to the measured time-series data, provides a parameter set corresponding to the state of the underlying system [74].

The glucose minimal model, developed by Bergman and colleagues [75], was one of the earliest mechanistic glucose models able to describe the effect of insulin action on glucose uptake and suppression of liver glucose production following an intravenous glucose tolerance test. More extensive models, like the meal simulation model from Dalla-Man and colleagues [9], were able to provide detailed information on the underlying processes governing glucose utilization in the postprandial state. The Dalla-Man meal model was parameterized on a population of healthy individuals and individuals with T2DM using gold-standard triple glucose tracer data and was approved by the FDA for *in silico* pre-clinical trials, for example to test closed loop control systems for Type 1 Diabetes Mellitus [76]. The Eindhoven Diabetes Education Simulator (E-DES), developed by Anne Maas and colleagues [10], provided a virtual practice environment for patients with diabetes, incorporating the most important factors influencing glycemic control. The E-DES model was developed through combining various models from literature and allows accurate simulation of glucose and insulin concentrations following an OGTT in healthy individuals, as well as type 1 and type 2 diabetes patients [77]. Currently, computational glucose models, such as the E-DES model, are able to only simulate glycemic responses to glucose ingestion, and do not include effects of other nutrients such as AAs and protein on glucose regulation.

## MACHINE LEARNING

Artificial intelligence, in particular machine learning, has seen a rapid growth due to increased data-availability and growth of computational power in the context of data-analysis [78, 79]. In contrast to bottom-up approaches, such as mechanistic modelling, which rely on pre-existing knowledge of the underlying system, machine-learning techniques are purely data-driven [80]. Machine learning involves a broad range of algorithms that perform prediction by utilizing patterns in the available data [81]. Machine learning is used in a wide variety of applications, such as in predictive analytics and decision making, E-commerce, cybersecurity, and healthcare [82]. In the field of nutrition, Zeevi and colleagues [64] devised a machine learning algorithm, integrating blood parameters, physical activity, dietary habits, gut microbiota and anthropometrics to provide a personalized postprandial prediction of glycemic responses to meals. However, while machine-learning based approaches are useful for prediction, they only provide limited insight into the biology underlying inter-individual differences in glucose homeostasis [83]. Combining mechanistic models with machine learning techniques might provide more detailed insight into the

biology underlying these inter-individual differences than machine learning approaches alone.

## THESIS OUTLINE



A complex glucose regulatory system is in play to maintain and control blood glucose levels under different physiological conditions. Current existing whole-body mechanistic models of the postprandial glucose regulatory system describe and provide quantitative information on glucose-insulin dynamics whilst capturing the mechanistic link between glucose and insulin. However, these models do not include the effect of AAs, which have been recognized as important factors influencing glucose homeostasis in various health phenotypes. In addition, these mechanistic models have mainly been applied to the population level, disregarding the heterogeneity in individual responses. In this thesis, we use a computational modelling approach to allow (personalized) simulation of postprandial glucose, insulin, and AA responses following challenge tests containing AAs or protein in various health phenotypes using a whole-body mechanistic model of the glucose homeostasis. Furthermore, we explored whether the addition of a data-driven model could improve the predictive performance of (personalized) mechanistic models.

The research in **Chapter 2** provides a systematic overview of the quantitative effects of isolated AAs (with and without glucose co-ingestion) and AA mixtures on postprandial glucose and insulin dynamics in humans with various health phenotypes. Here, we identified, extracted, and compared time-series data from intervention studies reporting glucose and insulin concentrations following acute ingestion and/or intravenous infusion of AAs in healthy adults and those living with obesity and/or type 2 diabetes. In **Chapter 3**, we personalized a physiology-based mechanistic model of the glucose regulatory system (E-DES) to elucidate the heterogeneity in individuals' responses following an OGTT using a large population of overweight/obese individuals from the DIOGenes study. In **Chapter 4**, we developed a mechanistic model of the glucose regulatory system (E-DES-PROT), which incorporates and captures the postprandial effects of AAs and protein intake. New terms, to account for the effect of AAs on insulin secretion and liver glucose production, were introduced and the novel model was applied to postprandial glucose and insulin time-series data following different AA challenges (identified in Chapter 2) and dried milk protein ingredients, and dairy products from a randomized, single-blind crossover trial.

While both “bottom-up” mechanistic and “top-down” data-driven techniques offer distinct benefits in untangling the complex interactions underlying disturbances in glucose homeostasis, a combined approach has yet to be explored. In **Chapter 5**, we use a sequential combination of a mechanistic (E-DES) and data-driven modelling approach to quantify individuals’ glucose and insulin responses to an OGTT, using data from a large observational prospective population-based cohort, the Maastricht Study. In **Chapter 6**, we applied the novel E-DES-PROT model to simulate and understand mechanistic differences between MIR and LIR, using postprandial glucose, insulin, and AA time-series data following a high-fat-mixed meal in individuals from the PERSON study. An overall evaluation of the findings can be found in **Chapter 7**.

## REFERENCES


1. Breitling, R., *What is systems biology?* Front Physiol, 2010. **1**: p. 9.
2. Atwell, K., S.J. Dunn, J.M. Osborne, H. Kugler, and E.J. Hubbard, *How computational models contribute to our understanding of the germ line.* Mol Reprod Dev, 2016. **83**(11): p. 944-957.
3. Pfau, T., N. Christian, and O. Ebenhöh, *Systems approaches to modelling pathways and networks.* Briefings in Functional Genomics, 2011. **10**(5): p. 266-279.
4. Klipp, E., *Systems biology : a textbook*. 2016, Weinheim: Wiley-VCH.
5. Kim, O.D., M. Rocha, and P. Maia, *A Review of Dynamic Modeling Approaches and Their Application in Computational Strain Optimization for Metabolic Engineering.* Frontiers in microbiology, 2018. **9**: p. 1690-1690.
6. Ellis, J.L., M. Jacobs, J. Dijkstra, H. van Laar, J.P. Cant, D. Tulpan, and N. Ferguson, *Review: Synergy between mechanistic modelling and data-driven models for modern animal production systems in the era of big data.* Animal, 2020. **14**: p. s223-s237.
7. Shah, P., F. Kendall, S. Khozin, R. Goosen, J. Hu, J. Laramie, M. Ringel, and N. Schork, *Artificial intelligence and machine learning in clinical development: a translational perspective.* NPJ digital medicine, 2019. **2**: p. 69-69.
8. Stalidzans, E., M. Zanin, P. Tieri, F. Castiglione, A. Polster, S. Scheiner, J. Pahle, B. Stres, M. List, J. Baumbach, et al., *Mechanistic Modeling and Multiscale Applications for Precision Medicine: Theory and Practice.* Network and Systems Medicine, 2020. **3**(1): p. 36-56.
9. Dalla Man, C., R.A. Rizza, and C. Cobelli, *Meal simulation model of the glucose-insulin system.* IEEE Trans Biomed Eng, 2007. **54**(10): p. 1740-9.
10. Maas, A.H., Y.J. Rozendaal, C. van Pul, P.A. Hilbers, W.J. Cottaar, H.R. Haak, and N.A. van Riel, *A physiology-based model describing heterogeneity in glucose metabolism: the core of the Eindhoven Diabetes Education Simulator (E-DES).* J Diabetes Sci Technol, 2015. **9**(2): p. 282-92.
11. Morris, A.L. and S.S. Mohiuddin, *Biochemistry, Nutrients*, in *StatPearls*. 2021, StatPearls Publishing LLC.
12. Berg, J.M., L. Stryer, and J.L. Tymoczko, *Biochemistry. 5th edition*. 2002: W. H. Freeman 2002.
13. Mouri, M. and M. Badireddy, *Hyperglycemia*, in StatPearls. 2021, StatPearls Publishing LLC.
14. Mathew, P. and D. Thoppil, *Hypoglycemia*, in StatPearls. 2021, StatPearls Publishing LLC.
15. Röder, P.V., B. Wu, Y. Liu, and W. Han, *Pancreatic regulation of glucose homeostasis.* Exp Mol Med, 2016. **48**(3): p. e219.
16. Hellström, P.M., P. Grybäck, and H. Jacobsson, *The physiology of gastric emptying.* Best Practice & Research Clinical Anaesthesiology, 2006. **20**(3): p. 397-407.
17. Goyal, R.K., Y. Guo, and H. Mashimo, *Advances in the physiology of gastric emptying.* Neurogastroenterology and motility : the official journal of the European Gastrointestinal Motility Society, 2019. **31**(4): p. e13546-e13546.
18. Camilleri, M., *Gastrointestinal hormones and regulation of gastric emptying.* Current opinion in endocrinology, diabetes, and obesity, 2019. **26**(1): p. 3-10.
19. Gribble, F.M. and F. Reimann, *Function and mechanisms of enteroendocrine cells and gut hormones in metabolism.* Nature Reviews Endocrinology, 2019. **15**(4): p. 226-237.

20. Wu, T., C.K. Rayner, R.L. Young, and M. Horowitz, *Gut motility and enteroendocrine secretion.* Curr Opin Pharmacol, 2013. **13**(6): p. 928-34.
21. Marathe, C.S., C.K. Rayner, K.L. Jones, and M. Horowitz, *Relationships between gastric emptying, postprandial glycemia, and incretin hormones.* Diabetes care, 2013. **36**(5): p. 1396-1405.
22. Alsahli, M. and J.E. Gerich, *Normal Glucose Physiology*☆, in *Encyclopedia of Endocrine Diseases (Second Edition)*, I. Huhtaniemi and L. Martini, Editors. 2014, Academic Press: Oxford. p. 72-86.
23. Thota, S. and A. Akbar, *Insulin*, in *StatPearls*. 2021, StatPearls Publishing LLC.
24. Leto, D. and A.R. Saltiel, *Regulation of glucose transport by insulin: traffic control of GLUT4.* Nature Reviews Molecular Cell Biology, 2012. **13**(6): p. 383-396.
25. Fridlyand, L.E., L. Ma, and L.H. Philipson, *Adenine nucleotide regulation in pancreatic beta-cells: modeling of ATP/ADP-Ca2+ interactions.* Am J Physiol Endocrinol Metab, 2005. **289**(5): p. E839-48.
26. Newgard, C.B., D. Lu, M.V. Jensen, J. Schissler, A. Boucher, S. Burgess, and A.D. Sherry, *Stimulus/secretion coupling factors in glucose-stimulated insulin secretion: insights gained from a multidisciplinary approach.* Diabetes, 2002. **51**(suppl 3): p. S389-S393.
27. Rix, I., C. Nexøe-Larsen, N.C. Bergmann, A. Lund, and F.K. Knop, *Glucagon physiology.* 2015.
28. Verberne, A.J.M., W.S. Korim, A. Sabetghadam, and I.J. Llewellyn-Smith, *Adrenaline: insights into its metabolic roles in hypoglycaemia and diabetes.* British journal of pharmacology, 2016. **173**(9): p. 1425-1437.
29. Freeman, A.M. and N. Pennings, *Insulin Resistance*, in StatPearls. 2021, StatPearls Publishing LLC.
30. Taylor, R., *Insulin resistance and type 2 diabetes.* Diabetes, 2012. **61**(4): p. 778-9.
31. Goossens, G.H., *The role of adipose tissue dysfunction in the pathogenesis of obesity-related insulin resistance.* Physiol Behav, 2008. **94**(2): p. 206-18.
32. Hudish, L.I., J.E. Reusch, and L. Sussel, β Cell dysfunction during progression of metabolic syndrome to type 2 diabetes. J Clin Invest, 2019. **129**(10): p. 4001-4008.
33. Abdul-Ghani, M.A., M. Matsuda, B. Balas, and R.A. DeFronzo, *Muscle and liver insulin resistance indexes derived from the oral glucose tolerance test.* Diabetes Care, 2007. **30**(1): p. 89-94.
34. Di Meo, S., S. Iossa, and P. Venditti, *Skeletal muscle insulin resistance: role of mitochondria and other ROS sources.* Journal of Endocrinology, 2017. **233**(1): p. R15-R42.
35. Paquin, J., J.C. Lagacé, M. Brochu, and I.J. Dionne, *Exercising for Insulin Sensitivity - Is There a Mechanistic Relationship With Quantitative Changes in Skeletal Muscle Mass?* Front Physiol, 2021. **12**: p. 656909.
36. Abdul-Ghani, M.A. and R.A. DeFronzo, *Pathogenesis of insulin resistance in skeletal muscle.* Journal of biomedicine & biotechnology, 2010. **2010**: p. 476279-476279.
37. Fazakerley, D.J., J.R. Krycer, A.L. Kearney, S.L. Hocking, and D.E. James, *Muscle and adipose tissue insulin resistance: malady without mechanism?* Journal of Lipid Research, 2019. **60**(10): p. 1720-1732.
38. Sharabi, K., C.D.J. Tavares, A.K. Rines, and P. Puigserver, *Molecular pathophysiology of hepatic glucose production.* Molecular aspects of medicine, 2015. **46**: p. 21-33.

39. Santoleri, D. and P.M. Titchenell, *Resolving the Paradox of Hepatic Insulin Resistance.* Cellular and Molecular Gastroenterology and Hepatology, 2019. **7**(2): p. 447-456.
40. Mu, W., X.F. Cheng, Y. Liu, Q.Z. Lv, G.L. Liu, J.G. Zhang, and X.Y. Li, *Potential Nexus of Non-alcoholic Fatty Liver Disease and Type 2 Diabetes Mellitus: Insulin Resistance Between Hepatic and Peripheral Tissues.* Front Pharmacol, 2018. **9**: p. 1566.
41. Galicia-Garcia, U., A. Benito-Vicente, S. Jebari, A. Larrea-Sebal, H. Siddiqi, K.B. Uribe, H. Ostolaza, and C. Martín, *Pathophysiology of Type 2 Diabetes Mellitus.* Int J Mol Sci, 2020. **21**(17).
42. Ranawana, V. and B. Kaur, *Role of proteins in insulin secretion and glycemic control.* Adv Food Nutr Res, 2013. **70**: p. 1-47.
43. Hou, Y. and G. Wu, *Nutritionally Essential Amino Acids.* Adv Nutr, 2018. **9**(6): p. 849-851.
44. Litwack, G., *Chapter 13 - Metabolism of Amino Acids*, in *Human Biochemistry*, G. Litwack, Editor. 2018, Academic Press: Boston. p. 359-394.
45. Holeček, M., *Branched-chain amino acids in health and disease: metabolism, alterations in blood plasma, and as supplements.* Nutrition & Metabolism, 2018. **15**(1): p. 33.
46. Manders, R.J., J.P. Little, S.C. Forbes, and D.G. Candow, *Insulinotropic and muscle protein synthetic effects of branched-chain amino acids: potential therapy for type 2 diabetes and sarcopenia.* Nutrients, 2012. **4**(11): p. 1664-1678.
47. Dallas, D.C., M.R. Sanctuary, Y. Qu, S.H. Khajavi, A.E. Van Zandt, M. Dyandra, S.A. Frese, D. Barile, and J.B. German, *Personalizing protein nourishment.* Crit Rev Food Sci Nutr, 2017. **57**(15): p. 3313-3331.
48. Carlson, B.M., *The human body : linking structure and function.* 2019.
49. Just, P.-A., S. Charawi, R.G.P. Denis, M. Savall, M. Traore, M. Foretz, S. Bastu, S. Magassa, N. Senni, P. Sohier, et al., *Lkb1 suppresses amino acid-driven gluconeogenesis in the liver.* Nature Communications, 2020. **11**(1): p. 6127.
50. Lee, D.-Y. and E.-H. Kim, *Therapeutic Effects of Amino Acids in Liver Diseases: Current Studies and Future Perspectives.* Journal of cancer prevention, 2019. **24**(2): p. 72-78.
51. Newsholme, P., K. Bender, A. Kiely, and L. Brennan, *Amino acid metabolism, insulin secretion and diabetes.* Biochemical Society Transactions, 2007. **35**(5): p. 1180-1186.
52. van der Zijl, N.J., C.C. Moors, G.H. Goossens, M.M. Hermans, E.E. Blaak, and M. Diamant, *Valsartan improves {beta}-cell function and insulin sensitivity in subjects with impaired glucose metabolism: a randomized controlled trial.* Diabetes Care, 2011. **34**(4): p. 845-51.
53. Han, G., H. Takahashi, N. Murao, G. Gheni, N. Yokoi, Y. Hamamoto, S.-I. Asahara, Y. Seino, Y. Kido, and S. Seino, *Glutamate is an essential mediator in glutamine-amplified insulin secretion.* Journal of diabetes investigation, 2021. **12**(6): p. 920-930.
54. Park, S.Y., J.-F. Gautier, and S. Chon, *Assessment of Insulin Secretion and Insulin Resistance in Human.* Diabetes & metabolism journal, 2021. **45**(5): p. 641-654.
55. Mann, G., S. Mora, G. Madu, and O.A.J. Adegoke, *Branched-chain Amino Acids: Catabolism in Skeletal Muscle and Implications for Muscle and Whole-body Metabolism.* Front Physiol, 2021. **12**: p. 702826.
56. Newsholme, P. and M. Krause, *Nutritional regulation of insulin secretion: implications for diabetes.* Clin Biochem Rev, 2012. **33**(2): p. 35-47.

57. Newsholme, P., L. Brennan, and K. Bender, *Amino Acid Metabolism, β-Cell Function, and Diabetes.* Diabetes, 2006. **55**(Supplement_2): p. S39-S47.
58. Kalogeropoulou, D., L. Lafave, K. Schweim, M.C. Gannon, and F.Q. Nuttall, *Leucine, when ingested with glucose, synergistically stimulates insulin secretion and lowers blood glucose.* Metabolism, 2008. **57**(12): p. 1747-52.
59. van Loon, L.J., M. Kruijshoop, P.P. Menheere, A.J. Wagenmakers, W.H. Saris, and H.A. Keizer, *Amino acid ingestion strongly enhances insulin secretion in patients with long-term type 2 diabetes.* Diabetes Care, 2003. **26**(3): p. 625-30.
60. Drummen, M., L. Tischmann, B. Gatta-Cherifi, T. Adam, and M. Westerterp-Plantenga, *Dietary Protein and Energy Balance in Relation to Obesity and Co-morbidities.* Frontiers in endocrinology, 2018. **9**: p. 443-443.
61. Marco-Benedí, V., S. Pérez-Calahorra, A.M. Bea, I. Lamiquiz-Moneo, L. Baila-Rueda, A. Cenarro, F. Civeira, and R. Mateo-Gallego, *High-protein energy-restricted diets induce greater improvement in glucose homeostasis but not in adipokines comparing to standard-protein diets in early-onset diabetic adults with overweight or obesity.* Clin Nutr, 2020. **39**(5): p. 1354-1363.
62. Coussa, A., M. Bassil, R. Gougeon, E.B. Marliss, and J.A. Morais, *Glucose and protein metabolic responses to an energy- but not protein- restricted diet in type 2 diabetes.* Diabetes Obes Metab, 2020. **22**(8): p. 1278-1285.
63. Russell, W.R., A. Baka, I. Björck, N. Delzenne, D. Gao, H.R. Griffiths, E. Hadjilucas, K. Juvonen, S. Lahtinen, M. Lansink, et al., *Impact of Diet Composition on Blood Glucose Regulation.* Crit Rev Food Sci Nutr, 2016. **56**(4): p. 541-90.
64. Zeevi, D., T. Korem, N. Zmora, D. Israeli, D. Rothschild, A. Weinberger, O. Ben-Yacov, D. Lador, T. Avnit-Sagi, M. Lotan-Pompan, et al., *Personalized Nutrition by Prediction of Glycemic Responses.* Cell, 2015. **163**(5): p. 1079-1094.
65. Trouwborst, I., S.M. Bowser, G.H. Goossens, and E.E. Blaak, *Ectopic fat accumulation in distinct insulin resistant phenotypes; targets for personalized nutritional interventions.* Frontiers in nutrition, 2018: p. 77.
66. Goossens, G.H., C. Moors, J.W. Jocken, N.J. Van der Zijl, A. Jans, E. Konings, M. Diamant, and E.E. Blaak, *Altered skeletal muscle fatty acid handling in subjects with impaired glucose tolerance as compared to impaired fasting glucose.* Nutrients, 2016. **8**(3): p. 164.
67. Gijbels, A., I. Trouwborst, K.M. Jardon, G.B. Hul, E. Siebelink, S.M. Bowser, D. Yildiz, L. Wanders, B. Erdos, D.H.J. Thijssen, et al., *The PERSonalized Glucose Optimization Through Nutritional Intervention (PERSON) Study: Rationale, Design and Preliminary Screening Results.* Front Nutr, 2021. **8**: p. 694568.
68. Wile, D.B. and J.P.H. Wilding, *CHAPTER 15 - Glucose metabolism and the pathophysiology of diabetes mellitus*, in *Clinical Biochemistry: Metabolic and Clinical Aspects (Third Edition)*, W.J. Marshall, et al., Editors. 2014, Churchill Livingstone. p. 273-304.
69. Bacha, F., N. Gungor, and S.A. Arslanian, *Measures of beta-cell function during the oral glucose tolerance test, liquid mixed-meal test, and hyperglycemic clamp test.* The Journal of pediatrics, 2008. **152**(5): p. 618-621.
70. Utzschneider, K.M., R.L. Prigeon, M.V. Faulenbach, J. Tong, D.B. Carr, E.J. Boyko, D.L. Leonetti, M.J. McNeely, W.Y. Fujimoto, and S.E. Kahn, *Oral disposition index predicts the development of future diabetes above and beyond fasting and 2-h glucose levels.* Diabetes Care, 2009. **32**(2): p. 335-41.

71. Brodovicz, K.G., C.J. Girman, A.M.C. Simonis-Bik, J.M. Rijkelijkhuizen, M. Zelis, M.C. Bunck, A. Mari, G. Nijpels, E.M.W. Eekhoff, and J.M. Dekker, *Postprandial metabolic responses to mixed versus liquid meal tests in healthy men and men with type 2 diabetes.* Diabetes Research and Clinical Practice, 2011. **94**(3): p. 449-455.
72. Parkinson, J., B. Hamrén, M.C. Kjellsson, and S. Skrtic, *Application of the integrated glucose-insulin model for cross-study characterization of T2DM patients on metformin background treatment.* Br J Clin Pharmacol, 2016. **82**(6): p. 1613-1624.
73. Banga, J.R., *Optimization in computational systems biology.* BMC Systems Biology, 2008. **2**(1): p. 47.
74. van Riel, N.A.W., *Dynamic modelling and analysis of biochemical networks: mechanism-based models and model-based experiments.* Briefings in Bioinformatics, 2006. **7**(4): p. 364-374.
75. Bergman, R.N., Y.Z. Ider, C.R. Bowden, and C. Cobelli, *Quantitative estimation of insulin sensitivity.* Am J Physiol, 1979. **236**(6): p. E667-77.
76. Kovatchev, B.P., M. Breton, C.D. Man, and C. Cobelli, *In silico preclinical trials: a proof of concept in closed-loop control of type 1 diabetes.* J Diabetes Sci Technol, 2009. **3**(1): p. 44-55.
77. AH, M., *Playing with numbers: the development of an educational diabetes game.* Technische Universiteit Eindhoven, 2017.
78. Choi, R.Y., A.S. Coyner, J. Kalpathy-Cramer, M.F. Chiang, and J.P. Campbell, *Introduction to Machine Learning, Neural Networks, and Deep Learning.* Transl Vis Sci Technol, 2020. **9**(2): p. 14.
79. Sarker, I.H., M.H. Furhad, and R. Nowrozy, *AI-Driven Cybersecurity: An Overview, Security Intelligence Modeling and Research Directions.* SN Computer Science, 2021. **2**(3): p. 173.
80. Baker, R.E., J.-M. Peña, J. Jayamohan, and A. Jérusalem, *Mechanistic models versus machine learning, a fight worth fighting for the biological community?* Biology Letters, 2018. **14**(5): p. 20170660.
81. Bhavsar, P., I. Safro, N. Bouaynaya, R. Polikar, and D. Dera, *Chapter 12 - Machine Learning in Transportation Data Analytics*, in *Data Analytics for Intelligent Transportation Systems*, M. Chowdhury, A. Apon, and K. Dey, Editors. 2017, Elsevier. p. 283-307.
82. Sarker, I.H., *Machine Learning: Algorithms, Real-World Applications and Research Directions.* SN Comput Sci, 2021. **2**(3): p. 160.
83. Alber, M., A. Buganza Tepole, W. Cannon, S. De, S. Dura-Bernal, K. Garikipati, G. Karniadakis, W. Lytton, P. Perdikaris, L. Petzold, et al., *Integrating machine learning and multiscale modeling—perspectives, challenges, and opportunities in the biological, biomedical, and behavioral sciences.* npj Digital Medicine, 2019. **2**.

# The impact of amino acids on postprandial glucose and insulin kinetics in humans: a quantitative overview

# 2

**Bart van Sloun, Gijs H. Goossens, Balázs Erdõs, Michael Lenz, Natal van Riel and Ilja C.W. Arts**

*Nutrients 2020, 12(10), 3211*

## ABSTRACT

Different amino acids (AAs) may exert distinct effects on postprandial glucose and insulin concentrations. A quantitative comparison of the effects of AAs on glucose and insulin kinetics in humans is currently lacking. PubMed was queried to identify intervention studies reporting glucose and insulin concentrations after acute ingestion and/or intravenous infusion of AAs in healthy adults and those living with obesity and/or type 2 diabetes (T2DM). The systematic literature search identified 55 studies that examined the effects of L-leucine, L-isoleucine, L-alanine, L-glutamine, L-arginine, L-lysine, glycine, L-proline, L-phenylalanine, L-glutamate, branched-chain AAs (i.e. L-leucine, L-isoleucine, and L-valine), and multiple individual L-AAs on glucose and insulin concentrations. Oral ingestion of most individual AAs induced an insulin response but did not alter glucose concentrations in healthy participants. Specific AAs (i.e. leucine, and isoleucine) co-ingested with glucose exerted a synergistic effect on the postprandial insulin response, and attenuated the glucose response compared to glucose intake alone in healthy participants. Oral AAs ingestion as well as intravenous AA infusion was able to stimulate an insulin response and decrease glucose concentrations in T2DM and obese individuals. The extracted information is publicly available and can serve multiple purposes such as computational modelling.

## INTRODUCTION

Glucose is a key substrate for many different types of cells and tissues, and as such plays an important role in human metabolism [1]. Blood glucose concentrations are tightly regulated to prevent hypoglycemia and hyperglycemia, thereby ensuring normal body functions. Glucagon and adrenalin are the key hormones responsible for elevating blood glucose concentration (for example during fasting or exercise), whereas insulin lowers blood glucose concentrations (for example following meal intake) [2]. This complex regulatory system involves various organs, including the gut, pancreas, liver, adipose tissue and skeletal muscle. Impairment of glucose homeostasis increases the risk of developing chronic cardiometabolic diseases such as type 2 diabetes (T2DM) and cardiovascular disease, highlighting the importance of adequate control of blood glucose concentrations [3].



Amino acids (AAs) are involved in the regulation of insulin secretion through their effects on β-cells, causing a rise in the ATP/ADP ratio, suppression of ATP-sensitive potassium channels and activation of voltage-gated Ca2+ channels [4]. The resulting calcium influx allows exocytosis of insulin granules from the β-cells. The insulinotropic effect of AA administration in humans was studied already in the 1960s by Floyd and colleagues [5, 6]. An intravenous infusion of an AA mixture, consisting of essential L-AA increased plasma insulin concentration and subsequently lowered blood glucose concentrations in healthy people [5]. A similar response was also demonstrated following infusion of single AAs [5, 6]. Interestingly, however, there seemed to be large differences in the capacity of the various AAs to stimulate insulin secretion [5]. A synergistic effect of simultaneous glucose and AA ingestion was found in several studies, where co-ingestion of AAs with glucose increased insulin secretion more than the sum of the individual effects [6-9]. The insulinotropic effect of AA administration has also been demonstrated in patients with T2DM. For example, co-ingestion of a protein hydrolysate/AA mixture with carbohydrates induced a more pronounced increase in plasma insulin concentrations compared to intake of carbohydrates alone, not only in healthy people but also in patients with T2DM [9]. Of note, the metabolic phenotype may influence the magnitude of the glucose and insulin responses following ingestion of AAs.

Despite decades of research, there is no quantitative overview available that describes the effects of individual AAs on glucose and insulin kinetics in individuals with different metabolic phenotypes. These data are needed as

the type and amount of AA intake, the administration route (i.e. oral versus intravenous) and study population seems to affect the insulin and glucose responses to AAs. We hypothesize that AAs exert distinct effects on glucose and insulin dynamics, which is further influenced by the metabolic phenotype as well as route of administration. A better mechanistic understanding would therefore allow for more targeted nutrition studies. This information could also aid in the improvement of physiology-based computational models of the glucose regulatory system, which have been developed and approved for pre-clinical research [10]. Therefore, we performed a systematic literature search and extracted the original data, which we made publicly available, to obtain better insight into the quantitative acute effects of individual AAs on postprandial glucose and insulin dynamics in humans, taking the metabolic phenotype into account.

## MATERIALS AND METHODS

Details of the systematic review were registered in the PROSPERO International Prospective Register of Systematic Reviews (registration number CRD42020155067).

### Search Strategy

Studies assessing the quantitative acute effects of AAs on postprandial plasma glucose and insulin concentrations were retrieved from the PubMed database between February 2018 and February 2020. The search strategy contained multiple (combinations of) main keywords appropriate for the topic of interest (("Amino acids" AND "Postprandial" AND ("Glucose" OR "Insulin")). The detailed search strategy is provided in the Supplemental File 1. Searches were not limited by article publication date. From the identified articles, the titles and abstract were assessed first, and if considered relevant for the present systematic review, the full text of the article was examined in detail.

### Selection Criteria

Criteria for study inclusion were set according to the Population-Intervention-Comparator-Outcomes-Study design (PICOS) format (Table 1). Eligible studies included healthy adults as well as people living with overweight/obesity and T2DM. Only acute studies that evaluated the effects of oral AA ingestion and/or intravenous AA administration on glucose and insulin concentrations were included. Studies had to be original research and be written in English. Labels

were added to the eligible articles, describing the subject characteristics, type of AA and route of AA administration.

**Table 1.** Selection criteria.

| | Inclusion criteria | Exclusion criteria |
|---|---|---|
| Population | Healthy adults | Children and adolescents |
| | Adults with T2DM | Pregnant females |
| | Adults with overweight/obesity | Animals |
| | | Cells |
| Intervention | Oral AA ingestion | |
| | Intravenous AA infusion | |
| Comparison | Control (i.e. water, saline) | |
| Outcomes | Glucose concentrations (repeated measurements) | |
| | Insulin concentrations (repeated measurements) | |
| Trial design | Intervention study | |
| Type of publication | Original research articles | Non-English articles |
| | Published in a peer-reviewed international journal, regardless of publication year | Review articles |

T2DM: Type 2 diabetes mellitus, AA: Amino acid.

## Data extraction

Data were extracted from eligible studies and entered into an Excel (2016, Microsoft Corporation) spreadsheet. The following items were extracted: bibliographic details (title; authors; year; journal), study population (health status; number of subjects; sex; age; body mass index (BMI); weight), intervention (type; dose; method of administration; duration), study design and the outcome measurements of interest (glucose concentrations; insulin concentrations). In the absence of exact numerical values for the outcome measurements of interest in the original articles, figures were digitized using a graph digitizing software (Graph Grabber version 2.0, Quintessa). After loading the figures in the digitizing software, the x- and y-axis was set to correctly map the image pixels to the corresponding data values in the figure. Data points (i.e. means and their corresponding standard errors or standard deviations) were determined

by manually clicking them and were subsequently stored in Excel data sheets for further processing. The extracted data from the 55 studies is publicly available (https://doi.org/10.34894/RNZI0A) and can serve multiple purposes such as computational modelling.

### Data processing

The extracted data was imported into MATLAB [11]. Measurements units were converted to mg/dL for glucose and μU/mL for insulin. The iAUC was calculated according to the trapezoidal rule in MATLAB, and normalized to one minute by dividing with the time span of the response. The time to glucose and insulin peaks, and their concentrations were identified from the extracted data by selecting the data-points with the highest glucose and insulin concentrations, and their corresponding time points in MATLAB. No statistical analysis was performed. The mention of significance in this review refers to the statistical analysis performed in the original studies.

## RESULTS

### Literature search

The PubMed search identified 10311 unique records (Figure 1). Titles and/or abstracts were screened, which resulted in the exclusion of 9678 studies. Three additional records were identified through searching reference lists. The remaining 636 full-text articles were retrieved and assessed for eligibility based on the selection criteria (Table 1). From these full-text articles, a total of 548 articles were excluded. Reasons for exclusion were related to the target population, intervention, time-scale, outcome parameters, and article language. An additional 33 articles were excluded due to accessibility restrictions and could not be retrieved via the university library. Thus, a total of 55 studies were included in the analysis. In the studies, the effects of L-leucine ($n$=6), L-isoleucine ($n$=1), L-alanine ($n$=6), L-glutamine ($n$=1), L-arginine ($n$=28), L-lysine ($n$=1), glycine ($n$=2), L-proline ($n$=1), L-phenylalanine ($n$=1), L-glutamate ($n$=3), branched-chain AAs (BCAAs) (i.e. L-leucine, L-isoleucine, and L-valine) ($n$=4), multiple L-AAs ingested separately (i.e. L-leucine, L-arginine, L-lysine, and L-phenylalanine) ($n$=1) on postprandial glucose and insulin concentrations were determined. When mentioning the different AAs throughout the present manuscript, with the exception of glycine that has no enantiomers because it has two hydrogen atoms attached to the central carbon atom, we refer to the L-isoforms of the respective AA.

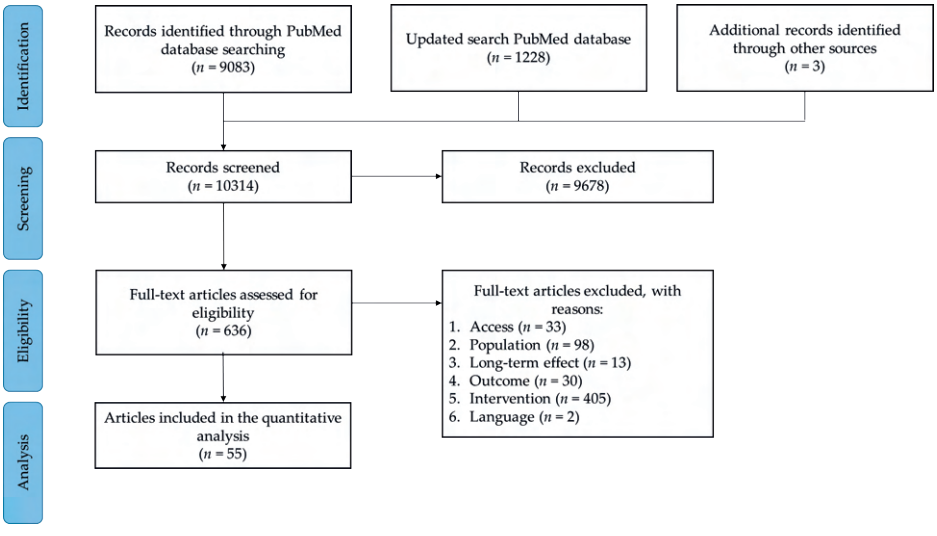


**Figure 1.** Flow diagram of the systematic literature search

## Leucine

Leucine study details are provided in Table 2 (section A). The time series data and the calculated kinetic parameters are visualized in Figure 2. The effect of oral leucine intake (Figure 2-A) has only been examined in healthy individuals [8, 12, 13]. Two out of the three studies showed increased insulin concentrations (iAUC range, 0.85 to 0.95 µU/mL/min) from baseline [12] and compared to a water control group (0.28 µU/mL/min) [8]. Glucose concentrations were unchanged compared to the water control group. The study with the lowest oral leucine dose showed decreased insulin (iAUC, -1.22 µU/mL/min) [13]. Here, the insulin reached a peak (5.35 µU/mL at 15 min), followed by a decrease below baseline values.

Kalogeropoulou et al. [8] demonstrated that co-ingestion of leucine+glucose (Figure 2-B) increased the insulin concentration (iAUC, 21.25 µU/mL/min) more than the sum of their individual effects (iAUC, 12.87 and 0.95 µU/mL/min for glucose and leucine ingestion, respectively), and attenuated the glucose response. The insulin concentrations increased more rapidly and reached a higher insulin peak (53.1 µU/mL) after co-ingestion of leucine+glucose compared to glucose ingestion alone (31.0 µU/mL).

The effect of intravenous leucine infusion (Figure 2-C) has also been examined in healthy people only [14-17]. Three out of the four studies showed increased

insulin (iAUC range, 4.47 to 8.90 μU/mL/min) [14, 15, 17], and decreased glucose concentrations (iAUC range, -2.52 to -6.31 mg/dL/min) compared to baseline. The study with the lowest intravenous leucine dose did not show increased insulin concentrations (iAUC, -0.45 μU/mL/min) [16]. To our knowledge, no kinetic data are available concerning leucine intake in people with obesity and/or T2DM.

**Table 2.** Characteristics of the 55 included studies

| Section | First author, Year of Publication | *n* | Age (yrs) | BMI (kg/m$^2$) | Body Weight (kg) | Lean body mass (kg) | Subject condition | Group | Dose | Route of administration | Duration (min) | Glucose measurements | Insulin measurements | Blood sampling |
|---|---|---|---|---|---|---|---|---|---|---|---|---|---|---|
| | Floyd, 1970 [17] | 11 | 22.9 | - | - | - | Healthy | Leucine | 15g | IV | 0-30 | Blood | Plasma | Forearm vein |
| | | 11 | 22.9 | - | - | - | Healthy | Arginine | 15g | IV | 0-30 | Blood | Plasma | Forearm vein |
| | | 11 | 22.9 | - | - | - | Healthy | Lysine | 15g | IV | 0-30 | Blood | Plasma | Forearm vein |
| | | 11 | 22.9 | - | - | - | Healthy | Phenylalanine | 15g | IV | 0-30 | Blood | Plasma | Forearm vein |
| A | Kalogeropoulou, 2008 [8] | 13 | 24 | 24 | 70.9 | 51 | Healthy | Leucine | 7g | Oral | Acute | Serum | Serum | Antecubital or forearm vein |
| | | 13 | 24 | 24 | 70.9 | 51 | Healthy | Leucine+ Glucose | 7g +25g | Oral | Acute | Serum | Serum | Antecubital or forearm vein |
| | | 13 | 24 | 24 | 70.9 | 51 | Healthy | Glucose | 25g | Oral | Acute | Serum | Serum | Antecubital or forearm vein |
| | | 13 | 24 | 24 | 70.9 | 51 | Healthy | Water | - | Oral | Acute | Serum | Serum | Antecubital or forearm vein |
| | Wilkenson, 2013 [12] | 7 | 21±0.3 | 25±0.6 | - | - | Healthy | Leucine | 3.42g | Oral | Acute | Plasma | Plasma | Arterialized blood from dorsal capillary bed of the hand |
| | Yoshii, 2018 [13] | 10 | 25±1 | - | 65.8 ±1.5 | - | Healthy | Leucine | 2g | Oral | Acute | Blood | Plasma | Cutaneous forearm vein |
| | Abumrad, 1982 [14] | 13 | 27±1 | - | 68±2 | - | Healthy | Leucine | 5.6g | IV | 0-300 | Plasma | Plasma | - |
| | Eriksson, 1983 [15] | 18 | 26±1 | 22.9 | 76±2 | - | Healthy | Leucine | 5.9g | IV | 0-150 | Blood | Serum | Arterial blood samples |
| | Sherwin, 1978 [16] | 11 | 21-35 | - | - | - | Healthy | Leucine | 3.7g[1] | IV | 0-180 | Plasma | Plasma | Antecubital vein |

**Table 2.** Characteristics of the 55 included studies (continued)

| Section | First author, Year of Publication | *n* | Age (yrs) | BMI (kg/m²) | Body Weight (kg) | Lean body mass (kg) | Subject condition | Group | Dose | Route of administration | Duration (min) | Glucose measurements | Insulin measurements | Blood sampling |
|---|---|---|---|---|---|---|---|---|---|---|---|---|---|---|
| **B** | Nuttall, 2008 [18] | 9 | 33.8±6.5 | 28±6.6 | 81±20.8 | 56.5±12.3 | Healthy | Isoleucine | 7.4g | Oral | Acute | Plasma | Serum | Antecubital vein |
| | | 9 | 33.8±6.5 | 28±6.6 | 81±20.8 | 56.5±12.3 | Healthy | Isoleucine+Glucose | 7.4g +25g | Oral | Acute | Plasma | Serum | Antecubital vein |
| | | 9 | 33.8±6.5 | 28±6.6 | 81±20.8 | 56.5 ±12.3 | Healthy | Glucose | 25g | Oral | Acute | Plasma | Serum | Antecubital vein |
| | | 9 | 33.8±6.5 | 28±6.6 | 81±20.8 | 56.5±12.3 | Healthy | Water | - | Oral | Acute | Plasma | Serum | Antecubital vein |
| **C** | Rossini, 1975 [19] | 6 | 20-32 | - | - | - | Healthy | Alanine | 10g | Oral | Acute | Blood | Serum | Antecubital vein |
| | | 6 | 20-32 | - | - | - | Healthy | Alanine | 10g | IV | 0-60 | Blood | Serum | Antecubital vein |
| | Rose, 1977 [20] | 13 | 23±4 | - | 59.5±5.6 | - | Healthy | Alanine | 11.9g | Oral | Acute | Plasma | Plasma | Forearm vein |
| | Sato, 1980 [21] | 5 | 25 | - | - | - | Healthy | Alanine | 64.6g[2] | Oral | Acute | Blood | Plasma | Antecubital vein |
| | Genuth, 1974 [22] | 10 | 20-46 | - | - | - | Healthy | Alanine | 33.8g[2] | Oral | Acute | Plasma | Plasma | - |
| | | 10 | 20-46 | - | - | - | Healthy | Alanine | 6.8g[2] | Oral | Acute | Plasma | Plasma | - |
| | | 10 | 20-72 | - | - | - | T2DM | Alanine | 37.5g[2] | Oral | Acute | Plasma | Plasma | - |
| | | 10 | 40-71 | - | - | - | T2DM | Alanine | 8.2g[2] | Oral | Acute | Plasma | Plasma | - |
| | Genuth, 1973 [23] | 6 | 42.5±9.3 | - | 151±39.6 | - | Obese | Alanine | 50g | Oral | Acute | Plasma | Plasma | - |
| | Asano, 1989 [24] | 9 | 21±0.7 | 19.8 ±0.3 | 53±5 | - | Healthy | Alanine | 5.3g | IV | 0-2 | Plasma | Plasma | Forearm vein |
| | | 6 | 28±3.5 | 31.3±3 | 89±12 | - | Obese | Alanine | 8.9g | IV | 0-2 | Plasma | Plasma | Forearm vein |
| **D** | Greenfield, 2008 [25] | 8 | 30±5.8 | 21.9±2.2 | 70.3±8.6 | - | Healthy | Glutamine | 30g | Oral | Acute | Plasma | Plasma | Antecubital vein |
| | | 8 | 30±5.8 | 21.9±2.2 | 70.3±8.6 | - | Healthy | Water | 300mL | Oral | Acute | Plasma | Plasma | Antecubital vein |
| | | 8 | 38.5±8 | 38.5±6.5 | 120.6 ±24.2 | - | T2DM | Glutamine | 30g | Oral | Acute | Plasma | Plasma | Antecubital vein |

**Table 2.** Characteristics of the 55 included studies (continued)

| Section | First author, Year of Publication | *n* | Age (yrs) | BMI (kg/m²) | Body Weight (kg) | Lean body mass (kg) | Subject condition | Group | Dose | Route of administration | Duration (min) | Glucose measurements | Insulin measurements | Blood sampling |
|---|---|---|---|---|---|---|---|---|---|---|---|---|---|---|
| | | 8 | 38.5±8 | 38.5±6.5 | 120.6 ±24.2 | - | T2DM | Water | 300mL | Oral | Acute | Plasma | Plasma | Antecubital vein |
| | | 8 | 39±9.8 | 34.5±4.4 | 106±14.8 | - | Obese | Glutamine | 30g | Oral | Acute | Plasma | Plasma | Antecubital vein |
| | | 8 | 39±9.8 | 34.5±4.4 | 106±14.8 | - | Obese | Water | 300mL | Oral | Acute | Plasma | Plasma | Antecubital vein |
| E | Gannon, 2002 [26] | 9 | 21-52 | 25.9±0.5 | 75 | 61 | Healthy | Arginine | 10.6g | Oral | Acute | Plasma | Serum | Forearm vein |
| | | 9 | 21-52 | 25.9±0.5 | 75 | 61 | Healthy | Arginine +Glucose | 10.6g +25g | Oral | Acute | Plasma | Serum | Forearm vein |
| | | 9 | 21-52 | 25.9±0.5 | 75 | 61 | Healthy | Glucose | 25g | Oral | Acute | Plasma | Serum | Forearm vein |
| | | 9 | 21-52 | 25.9±0.5 | 75 | 61 | Healthy | Water | - | Oral | Acute | Plasma | Serum | Forearm vein |
| | Tang, 2013 [27] | 8 | 30.5±3.7 | 21.0±2.4 | 56.8±6.8 | - | Healthy | Arginine | 30g | Oral | Acute | Serum | Serum | - |
| | | 8 | 30.5±3.7 | 21.0±2.4 | 56.8±6.8 | - | Healthy | Arginine +Glucose | 30g +75g | Oral | Acute | Serum | Serum | - |
| | | 8 | 30.5±3.7 | 21.0±2.4 | 56.8±6.8 | - | Healthy | Glucose | 75g | Oral | Acute | Serum | Serum | - |
| | | 8 | 30.5±3.7 | 21.0±2.4 | 56.8±6.8 | - | Healthy | Water | 300mL | Oral | Acute | Serum | Serum | - |
| | Giugliano, 1997 [28] | 10 | 24±1 | 23±0.4 | 67±1.8 | - | Healthy | Arginine | 30g | IV | 0-30 | Plasma | Plasma | Dorsal vein |
| | Coiro, 1997 [29] | 14 | 24-35 | - | - | - | Healthy | Arginine | 30g | IV | 0-30 | Blood | - | Antecubital vein |
| | Broglio, 2003 [30] | 7 | 28.3±3.1 | 29.1±0.9 | - | - | Healthy | Arginine | 34g[3] | IV | 0-30 | Blood | Blood | Antecubital vein |
| | | 7 | 28.3±3.1 | 29.1±0.9 | - | - | Healthy | Saline | 3mL | IV | Acute | Blood | Blood | Antecubital vein |
| | Dela, 1990 [31] | 7 | 22 | 23.2 | 76 | - | Healthy-untrained | Arginine | 68.4g | IV | 0-90 | Plasma | Plasma | Retrograde direction in a dorsal hand vein (arterialized blood samples) |

**Table 2.** Characteristics of the 55 included studies (continued)

| Section | First author, Year of Publication | *n* | Age (yrs) | BMI (kg/m²) | Body Weight (kg) | Lean body mass (kg) | Subject condition | Group | Dose | Route of administration | Duration (min) | Glucose measurements | Insulin measurements | Blood sampling |
|---|---|---|---|---|---|---|---|---|---|---|---|---|---|---|
| | | 7 | 23 | 21.6 | 70 | - | Healthy-trained | Arginine | 63g | IV | 0-90 | Plasma | Plasma | Retrograde direction in a dorsal hand vein (arterialized blood samples) |
| | Penny, 1970* [32] | 8 | - | - | 69.5±14.3 | - | Healthy | Arginine | 34g | IV | 0-30 | Plasma | - | Peripheral vein |
| | | 8 | - | - | 69.5±14.3 | - | Healthy | Saline | - | IV | 0-30 | Plasma | - | Peripheral vein |
| | Levin, 1971 [33] | 6 | 23-50 | - | - | - | Healthy | Arginine | 20g | IV | 0-20 | Blood | - | Antecubital vein |
| | | 6 | 23-50 | - | - | - | Healthy | Arginine | 20g | IV | 0-20 | Blood | - | Antecubital vein |
| | Bratusch-Marrain, 1979 [34] | 9 | 21-42 | - | - | - | Healthy | Arginine | 30g | IV | 0-30 | Blood | - | Glucose: arterial Insulin: hepatic venous |
| | Imura, 1976 [35] | 15 | - | - | - | - | Healthy | Arginine | 30g | IV | 0-45 | Blood | Plasma | Antecubital vein |
| | Hasselblatt, 2006 [36] | 15 | 39 | 24.9 | - | - | Healthy | Arginine | 30g | IV | 0-30 | Blood | Plasma | Glucose: capillary blood Insulin: Forearm vein |
| | Berger, 1974 [37] | 9 | - | - | - | - | Healthy | Arginine | 30g | IV | 0-30 | Blood | Plasma | - |
| | Dupre, 1968 [38] | 13 | - | - | - | - | Healthy | Arginine | 15g | IV | 0-40 | Blood | Serum | - |
| | | 6 | - | - | - | - | Healthy | Arginine | 3.9g | IV | 0-40 | Blood | Serum | - |
| | Dupre, 1969 [39] | 4 | 18-35 | - | - | - | Healthy | Arginine | 15g | IV | 0-40 | Blood | Serum | Forearm vein |
| | | 6 | 18-35 | - | - | - | Healthy | Arginine | 15g | IV | 0-40 | Blood | Serum | Forearm vein |

**Table 2.** Characteristics of the 55 included studies (continued)

| Section | First author, Year of Publication | *n* | Age (yrs) | BMI (kg/m²) | Body Weight (kg) | Lean body mass (kg) | Subject condition | Group | Dose | Route of administration | Duration (min) | Glucose measurements | Insulin measurements | Blood sampling |
|---|---|---|---|---|---|---|---|---|---|---|---|---|---|---|
| | Kimber, 2001 [40] | 5 | 58 | - | - | - | Healthy | Arginine | 31.8g[2] | IV | 0-30 | Plasma | Plasma | Antecubital vein |
| | Ohneda, 1972 [41] | 8 | - | - | - | - | Healthy | Arginine | 30g | IV | 0-30 | Blood | Plasma | - |
| | Efendic, 1974 [42] | 7 | 30.6±4.4 | - | - | - | Healthy | Arginine | 27.9g[2] | IV | 0-30 | Blood | Plasma | Brachial vein |
| | | 6 | 36.5±15.3 | - | - | - | T2DM | Arginine | 29.8g[2] | IV | 0-30 | Blood | Plasma | Brachial vein |
| | Kawamori, 1980 [43] | 9 | 25-35 | - | - | - | Healthy | Arginine | 32.3g[2] | IV | 0-30 | Blood | Plasma | Antecubital vein |
| | | 5 | 48-70 | - | - | - | T2DM | Arginine | 33.5g[2] | IV | 0-30 | Blood | Plasma | Antecubital vein |
| | Sparks, 1967 [44] | 10 | 25±1 | - | 66±3 | - | Healthy | Arginine | 30g | IV | 0-30 | Blood | Serum | Venous blood samples |
| | | 6 | 57±3 | - | 66±9 | - | T2DM | Arginine | 30g | IV | 0-30 | Blood | Serum | Venous blood samples |
| | Kawamori, 1985 [45] | 9 | 25-30 | - | - | - | Healthy | Arginine | 32.3g[2] | IV | 0-30 | Blood | Serum | Venous blood samples |
| | | 7 | 48-71 | - | - | - | T2DM | Arginine | 32.3g[2] | IV | 0-30 | Blood | Plasma | Antecubital vein |
| | Maccario, 1996 [46] | 7 | 26-32 | 20.6±1.3 | - | - | Healthy | Arginine | 27.2g[3] | IV | 0-30 | Plasma | Serum | Antecubital vein |
| | | 7 | 23-52 | 38.3±2.6 | - | - | Obese | Arginine | 50.6g[3] | IV | 0-30 | Plasma | Serum | Antecubital vein |
| | Marfella, 1996 [47] | 10 | 47±0.8 | 28.1±0.7 | 78±2.9 | - | T2DM | Arginine | 30g | IV | 0-30 | Plasma | Plasma | Dorsal vein |
| | Raskin, 1976 [48] | 6 | 48 | - | 85 | - | T2DM | Arginine | 20g | IV | 0-40 | Plasma | Plasma | Antecubital vein |
| | Maejima, 2002 [49] | 12 | 58.5±3.3 | - | 57.0±3.6 | - | T2DM | Arginine | 30g | IV | 0-30 | Blood | - | - |

**Table 2.** Characteristics of the 55 included studies (continued)

| Section | First author, Year of Publication | *n* | Age (yrs) | BMI (kg/m²) | Body Weight (kg) | Lean body mass (kg) | Subject condition | Group | Dose | Route of administration | Duration (min) | Glucose measurements | Insulin measurements | Blood sampling |
|---|---|---|---|---|---|---|---|---|---|---|---|---|---|---|
| | Ohneda, 1975 [50] | 5 | 63.2±5.9 | - | - | - | T2DM | Arginine | 30g | IV | 0-30 | Blood | Plasma | Glucose: capillary blood Insulin: antecubital vein |
| | Carpentier, 2001 [51] | 14 | 44.4±2 | 36.2±1.9 | - | - | Obese | Arginine | 30g | IV | -0.75-30 | Plasma | Plasma | Forearm distal vein (arterialized venous blood) |
| | Maccario, 1997 [52] | 6 | - | - | - | - | Obese | Arginine | 49.3g[3] | IV | 0-30 | Plasma | Serum | - |
| | Walter, 1980 [53] | 5 | 26-40 | - | 135-227 | - | Obese | Arginine | 5g | IV | 0-1 | Serum | Serum | Antecubital vein |
| **F** | Kalogeropoulou 2009 [54] | 13 | 30 | 26 | 80 | 60 | Healthy | Lysine | 11g | Oral | Acute | Serum | Serum | Antecubital vein |
| | | 13 | 30 | 26 | 80 | 60 | Healthy | Lysine+ Glucose | 11g +25g | Oral | Acute | Serum | Serum | Antecubital vein |
| | | 13 | 30 | 26 | 80 | 60 | Healthy | Glucose | 25g | Oral | Acute | Serum | Serum | Antecubital vein |
| | | 13 | 30 | 26 | 80 | 60 | Healthy | Water | - | Oral | Acute | Serum | Serum | Antecubital vein |
| **G** | Gannon, 2002 [55] | 9 | 21-52 | 25.9±0.5 | 75 | 61 | Healthy | Glycine | 4.6g | Oral | Acute | Plasma | Serum | Forearm vein |
| | | 9 | 21-52 | 25.9±0.5 | 75 | 61 | Healthy | Glycine+ Glucose | 4.6g +25g | Oral | Acute | Plasma | Serum | Forearm vein |
| | | 9 | 21-52 | 25.9±0.5 | 75 | 61 | Healthy | Glucose | 25g | Oral | Acute | Plasma | Serum | Forearm vein |
| | | 9 | 21-52 | 25.9±0.5 | 75 | 61 | Healthy | Water | - | Oral | Acute | Plasma | Serum | Forearm vein |
| | Kasai, 1978 [56] | 19 | 20-70 | - | - | - | Healthy | Glycine | 22.5g | Oral | Acute | Blood | Serum | Venous blood samples |
| **H** | Nuttall, 2004 [57] | 8 | 28 | 23 | 80 | 53 | Healthy | Proline | 6g | Oral | Acute | Plasma | Serum | Forearm vein |

**Table 2.** Characteristics of the 55 included studies (continued)

| Section | First author, Year of Publication | *n* | Age (yrs) | BMI (kg/m²) | Body Weight (kg) | Lean body mass (kg) | Subject condition | Group | Dose | Route of administration | Duration (min) | Glucose measurements | Insulin measurements | Blood sampling |
|---|---|---|---|---|---|---|---|---|---|---|---|---|---|---|
| | | 8 | 28 | 23 | 80 | 53 | Healthy | Proline+ Glucose | 6g+25g | Oral | Acute | Plasma | Serum | Forearm vein |
| | | 8 | 28 | 23 | 80 | 53 | Healthy | Glucose | 25g | Oral | Acute | Plasma | Serum | Forearm vein |
| | | 8 | 28 | 23 | 80 | 53 | Healthy | Water | - | Oral | Acute | Plasma | Serum | Forearm vein |
| I | Nuttall, 2006 [58] | 6 | 26 | 24 | - | 59 | Healthy | Phenylalanine | 9.7g | Oral | Acute | Plasma | Serum | Antecubital vein |
| | | 6 | 26 | 24 | - | 59 | Healthy | Phenylalanine+ Glucose | 9.7g +25g | Oral | Acute | Plasma | Serum | Antecubital vein |
| | | 6 | 26 | 24 | - | 59 | Healthy | Glucose | 25g | Oral | Acute | Plasma | Serum | Antecubital vein |
| | | 6 | 26 | 24 | - | 59 | Healthy | Water | - | Oral | Acute | Plasma | Serum | Antecubital vein |
| J | Di Sabastiano, 2013 [59] | 9 | 23.9±1.9 | 25±2.4 | 79.4±9 | - | Healthy | Glutamate | 11.9g | Oral | Acute | Serum | Serum | Antecubital vein |
| | | 9 | 23.9±1.9 | 25±2.4 | 79.4±9 | - | Healthy | Gelatin capsules (containing NaCl in the same proportions as in the MSG capsules) | - | Oral | Acute | Serum | Serum | Antecubital vein |
| | Fernstrom, 1996 [60] | 8 | 25.6±4.1 | 25.1±1.8 | 79.7±7.5 | - | Healthy | Glutamate | 12.7g | Oral | Acute | Plasma | Plasma | - |
| | | 8 | 25.6±4.1 | 25.1±1.8 | 79.7±7.5 | - | Healthy | Cold flavored vehicle (containing 3g sodium chloride instead of MSG) | 300mL | Oral | Acute | Plasma | Plasma | - |
| | Graham, 2000 [61] | 9 | 26 | - | 76.9 | - | Healthy | Glutamate | 11.5g | Oral | Acute | - | Plasma | Antecubital vein |

**Table 2.** Characteristics of the 55 included studies (continued)

| Section | First author, Year of Publication | *n* | Age (yrs) | BMI (kg/m²) | Body Weight (kg) | Lean body mass (kg) | Subject condition | Group | Dose | Route of administration | Duration (min) | Glucose measurements | Insulin measurements | Blood sampling |
|---|---|---|---|---|---|---|---|---|---|---|---|---|---|---|
| K | Zhang, 2011 [62] | 5 | 22-25 | 19.7 | 61±3 | - | Healthy | BCAA (weight ratio of 1 : 2.3 : 1.2 for isoleucine : leucine: valine) | 1g | Oral | Acute | Plasma | Plasma | - |
| | | 5 | 22-25 | 19.7 | 61±3 | - | Healthy | BCAA (weight ratio of 1 : 2.3 : 1.2 for isoleucine : leucine: valine) | 5g | Oral | Acute | Plasma | Plasma | - |
| | Gojda, 2017 [63] | 18 | 25.5±1.4 | - | 76.7±2.6 | - | Healthy | BCAA (50% leucine, 25% isoleucine, 25% valine) | 30.7 ± 1.1g | Oral | Acute | Plasma | Serum | - |
| | | 18 | 25.5±1.4 | - | 76.7±2.6 | - | Healthy | Gelatin Capsule (methylcellulose in gelatin capsule, prepared by University Hospital pharmacy) | - | Oral | Acute | Plasma | Serum | - |
| | | 18 | 25.5±1.4 | - | 76.7±2.6 | - | Healthy | BCAA (43% leucine, 24% isoleucine, 33% valine) | 30.7 ±1.1g | IV | 0-120 | Plasma | Serum | - |
| | Tatpati, 2010 [64] | 12 | 23.4±0.8 | 24.4±1 | 74.5±4.2 | 47.6 ±3.5 | Healthy | BCAA (equimolar mixture of valine, leucine and isoleucine) | 18.5g | IV | 0-510 | Blood | Plasma | Dorsal hand vein (arterialized venous blood samples) |
| | | 12 | 70.7±1.1 | 24.5±0.7 | 72.7±3.3 | 42.2 ±3.1 | Healthy | BCAA (equimolar mixture of valine, leucine and isoleucine) | 16.35g | IV | 0-510 | Blood | Plasma | Dorsal hand vein (arterialized venous blood samples) |

**Table 2.** Characteristics of the 55 included studies (continued)

| Section | First author, Year of Publication | *n* | Age (yrs) | BMI (kg/m²) | Body Weight (kg) | Lean body mass (kg) | Subject condition | Group | Dose | Route of administration | Duration (min) | Glucose measurements | Insulin measurements | Blood sampling |
|---|---|---|---|---|---|---|---|---|---|---|---|---|---|---|
| | | 12 | 23.4±0.8 | 24.4±1 | 74.5±4.2 | 47.6 ±3.5 | Healthy | Saline | - | IV | 0-510 | Blood | Plasma | Dorsal hand vein (arterialized venous blood samples) |
| | | 12 | 70.7±1.1 | 24.5±0.7 | 72.7±3.3 | 42.2 ±3.1 | Healthy | Saline | - | IV | 0-510 | Blood | Plasma | Dorsal hand vein (arterialized venous blood samples) |
| | Louard, 1990 [65] | 10 | - | - | - | - | Healthy | BCAA (equimolar mixture of valine, leucine and isoleucine) | 3.4g[2] | IV | 0-180 | Blood | Plasma | Arterial samples |

[1] Estimated based on the average body surface area for males and females [66]. [2] Estimated based on height/weight tables for males and females [67]. [3] Estimated based on average height for males and females [68].
*Two subjects were excluded due to missing time series values. BMI: Body Mass Index, IV: Intravenous, T2DM: Type 2 diabetes mellitus, BCAA: Branched-chain amino acids, *n:* number of participants, -: Data not reported


**Figure 2.** Leucine infograph consisting of study details with postprandial glucose and insulin time-series data and iAUC after oral leucine ingestion (A), leucine co-ingested with glucose (B), and intravenous leucine infusion (C) in healthy individuals. No data are available for T2DM patients, and obese individuals.

### Isoleucine

Isoleucine study details are provided in Table 2 (section B). The time series data and the calculated kinetic parameters are visualized in Supplemental Figure 1. Nuttall et al. [18] demonstrated that oral isoleucine ingestion alone (Supplemental Figure 1-A) had no significant effect on insulin concentrations, but decreased glucose (iAUC, -4.15 mg/dL/min) compared to ingestion of water (iAUC, 0.30 mg/dL/min) in healthy individuals. Co-ingestion of isoleucine+glucose (Supplemental Figure 1-B) increased the insulin concentrations (iAUC, 21.38 μU/mL/min) more than the sum of their individual effects (iAUC, 19.0 and 0.00 μU/mL/min for glucose, and isoleucine ingestion respectively), and attenuated the glucose-stimulated glucose response in healthy individuals [18]. To our knowledge, no kinetic data are available concerning intravenous isoleucine infusion, nor for isoleucine intake in people with obesity and/or T2DM.



### Alanine

Alanine study details are provided in Table 2 (section C). The time series data and the calculated kinetic parameters are visualized in Supplemental Figure 2. The effect of oral alanine ingestion has been examined in healthy individuals [19-22], T2DM patients [22], and obese individuals [23] (Supplemental Figure 2-A). All four studies showed increased insulin concentrations (iAUC range, 1.01 to 10.53 μU/mL/min) from baseline following oral ingestion of alanine in healthy individuals. Alanine was found to lower glucose concentrations (iAUC, -3.33 mg/dL/min) in one study [21] that had the highest alanine dose. Genuth et al. [22] demonstrated that the effect of oral ingestion of alanine on insulin is dose-dependent, with high dosing (33.8g) leading to a larger postprandial insulin response (iAUC, 10.53 μU/mL/min) compared to low dosing (6.8g) (iAUC, 1.01 μU/mL/min). Plasma glucose concentrations were unchanged in both interventions, with the exception of a slight but significant decrease in glucose concentrations 240 min after oral ingestion for the low alanine dose. The initial insulin response to oral alanine ingestion was similar in healthy individuals and T2DM patients, but the insulin concentrations remained elevated over a prolonged period of time in the latter [22]. Glucose concentrations were decreased (iAUC range, -12.99 to -12.29 mg/dL/min) from baseline in T2DM patients. Oral ingestion of alanine also increased insulin (iAUC, 42.67 μU/mL/min), and decreased glucose concentrations (iAUC, -10.49 mg/dL/min) from baseline in people with obesity [23]. To our knowledge, no kinetic data are available concerning co-ingestion of alanine with glucose in individuals.

Additionally, the effect of intravenous alanine infusion was examined in healthy [19, 24] and obese individuals [24] (Supplemental Figure 2-C). Rossini et al. [19] showed that, in contrast to oral alanine ingestion, intravenous alanine infusion did not alter insulin and glucose concentrations from baseline. Asano et al. [24] showed increased insulin concentrations in both obese participants (iAUC, 12.02 μU/mL/min) and healthy individuals (iAUC, 3.42 μU/mL/min). Glucose concentrations were also increased, despite not being different between groups.

### Glutamine

Glutamine study details are provided in Table 2 (section D). The time series data and the calculated kinetic parameters are visualized in Supplemental Figure 3. Greenfield et al. [25] demonstrated that oral ingestion of glutamine increased insulin concentrations compared to ingestion of water only in healthy, T2DM and obese individuals (Supplemental Figure 3-A). The effects found were most pronounced in T2DM individuals (iAUC, 13.35 and -0.23 μU/mL/min for glutamine, and water ingestion, respectively), intermediate in obese individuals (iAUC, 6.16 and -2.73 μU/mL/min for glutamine, and water ingestion, respectively), and modest in healthy individuals (iAUC, 1.62 and -1.06 μU/mL/min for glutamine, and water ingestion, respectively). The glucose concentrations were comparable to water ingestion in these groups. To our knowledge, no kinetic data are available concerning individuals co-ingesting glutamine with glucose, nor for intravenous glutamine infusion.

### Arginine

Arginine study details are provided in Table 2 (section E). The time series data and the calculated kinetic parameters are visualized in Supplemental Figure 4. The effects of oral arginine ingestion have been investigated in healthy individuals only [26, 27] (Supplemental Figure 4-A). One out of the two studies [27], with the largest oral arginine dose, showed increased insulin concentrations (iAUC, 1.41 μU/mL/min) compared to water intake (iAUC, 0.06 μU/mL/min), with no significant effect on glucose concentrations.

Co-ingestion of arginine+glucose (Supplemental Figure 4-B) resulted in a similar iAUC for insulin compared to glucose ingestion alone and attenuated the glucose-stimulated glucose response [26]. Despite the lower insulin peak, the insulin concentrations remained elevated for a longer time after co-ingestion of arginine+glucose. Tang et al. [27] showed a non-significant increase in insulin concentrations when glucose was co-ingested with arginine (iAUC, 28.62 μU/

mL/min) compared to glucose ingestion alone (iAUC, 19.05 μU/mL/min). Glucose concentrations were unchanged.

The effect of intravenous arginine infusion has been examined in healthy individuals [17, 28-46], T2DM patients [42-45, 47-50], and obese individuals [46, 51-53] (Supplemental Figure 4-C). All twenty studies [17, 28-46] on intravenous arginine infusion in healthy individuals showed increased insulin concentrations (iAUC range, 1.58 to 45.75 μU/mL/min) from baseline. Glucose concentrations increased (iAUC range, 1.79 to 18.65 mg/dL/min) from baseline in fourteen studies [17, 28, 29, 31, 33-35, 38-43, 45]. Four additional studies showed an increase in glucose concentrations in the beginning of the study followed by a drop below baseline, resulting in a negative iAUC [36, 37, 44, 46]. Two studies [30, 32] included an intravenous saline infusion control group and showed increased insulin concentrations after intravenous arginine infusion (iAUC, 11.42 and 25.98 μU/mL/min, respectively) compared to intravenous saline infusion (iAUC, -0.64 and 5.33 μU/mL/min, respectively). Broglio et al. [30] also showed increased glucose concentrations (iAUC, 4.45 mg/dL/min) after intravenous arginine infusion compared to intravenous saline infusion (iAUC, -1.64 mg/dL/min), however no dynamic data were provided for both insulin and glucose. Dela et al. [31] found that intravenous arginine infusion increased insulin and glucose concentrations from baseline in trained and untrained, healthy individuals, with lower insulin concentrations in trained males (iAUC, 18.40 μU/mL/min and 45.75 μU/mL/min, for trained and untrained individuals respectively). The glucose concentrations did not differ between the two groups.

All eight studies [42-45, 47-50] investigating intravenous arginine infusion in T2DM individuals showed increased insulin (iAUC range, 4.09 to 21.66 μU/mL/min) and glucose concentrations (iAUC range, 5.00 to 29.75 mg/dL/min). Three studies [43-45] demonstrated that insulin responses were lower in T2DM patients (iAUC range, 4.09 to 13.17 μU/mL/min) compared to healthy individuals (iAUC range, 21.84 to 31.25 μU/mL/min) during intravenous arginine infusion. Efendić et al. [42] demonstrated a slightly lower insulin response in T2DM patients (iAUC, 21.66 μU/mL/min) compared to healthy individuals (iAUC, 22.49 μU/mL/min) who received intravenous arginine infusion, but the insulin concentrations remained elevated over a prolonged period of time in T2DM patients. Glucose concentrations were increased from baseline in both healthy individuals (iAUC, 5.04 mg/dL/min) and T2DM patients (iAUC, 8.44 mg/dL/min). All four studies [46, 51-53] on intravenous arginine infusion in obese individuals showed increased insulin (iAUC range, 6.10 to 22.07 μU/mL/min) and glucose concentrations (iAUC

range, 1.37 to 9.08 mg/dL/min). Maccario et al. [46] demonstrated that the arginine induced insulin response was higher in obese participants (iAUC, 22.07 μU/mL/min) than in healthy individuals (iAUC, 8.30 μU/mL/min). Glucose concentrations did not decrease below baseline values in obese participants (iAUC, 1.60 mg/dL/min) compared to healthy individuals (iAUC, -3.20 mg/dL/min).

### Lysine

Lysine study details are provided in Table 2 (section F). The time series data and the calculated kinetic parameters are visualized in Supplemental Figure 5. The effects of oral lysine ingestion [54] (Supplemental Figure 5-A) and intravenous lysine infusion [17] (Supplemental Figure 5-C) were examined in healthy individuals. Kalogeropoulou et al. [54] demonstrated that oral ingestion of lysine increased insulin (iAUC, 0.67 μU/mL/min) and decreased glucose concentrations (iAUC, -1.73 mg/dL/min) compared to individuals that ingested water (iAUC, -0.62 μU/mL/min, 0.35 mg/dL/min). Co-ingestion of lysine+glucose (Supplemental Figure 5-B) resulted in a similar iAUC for insulin compared to glucose ingestion alone and attenuated the glucose-stimulated glucose response. However, insulin concentrations increased more rapidly and reached higher peak insulin concentrations (38.7 μU/mL) compared to glucose ingestion alone (35.4 μU/mL).

Intravenous lysine infusion (Supplemental Figure 5-C) increased insulin (iAUC, 8.83 μU/mL/min) and decreased glucose concentrations (iAUC, -2.23 mg/dL/min) from baseline in healthy individuals [17]. To our knowledge, no kinetic data are available concerning lysine intake in people with obesity and/or T2DM.

### Glycine

Glycine study details are provided in Table 2 (section G). The time series data and the calculated kinetic parameters are visualized in Supplemental Figure 6. The effects of oral glycine ingestion have been examined in healthy individuals [55, 56] (Supplemental Figure 6-A). One out of the two studies showed increased insulin concentrations (iAUC, 2.29 μU/mL/min) compared to water (iAUC, -1.66 μU/mL/min), with no change in glucose concentrations [55]. Co-ingestion of glycine+glucose (Supplemental Figure 6-B) resulted in a similar iAUC for insulin compared to glucose ingestion alone and attenuated the glucose-stimulated glucose response. However, insulin concentrations increased more slowly and reached lower peak insulin concentrations (76.7 μU/mL) compared to glucose ingestion alone (92.4 μU/mL). To our knowledge, no kinetic data are available

concerning intravenous glycine infusion, nor for glycine intake in people with obesity and/or T2DM patients.

### Proline

Proline study details are provided in Table 2 (section H). The time series data and the calculated kinetic parameters are visualized in Supplemental Figure 7. Nuttall et al. [57] demonstrated that oral ingestion of proline (Supplemental Figure 7-A) increased insulin (iAUC, 0.46 μU/mL/min) compared to intake of water (iAUC, -0.99 μU/mL/min), with no change in glucose concentrations in healthy individuals. Co-ingestion of proline+glucose (Supplemental Figure 7-B) resulted in a comparable iAUC for insulin compared to glucose ingestion alone, and attenuated the glucose-stimulated glucose response. However, insulin concentrations increased more rapidly and reached higher peak insulin concentrations (41.2 μU/mL) compared to glucose ingestion alone (33.0 μU/mL) in healthy individuals. To our knowledge, no kinetic data are available concerning intravenous proline infusion, nor for proline intake in people with obesity and/or T2DM patients.



### Phenylalanine

Phenylalanine study details are provided in Table 2 (section I). The time series data and the calculated kinetic parameters are visualized in Supplemental Figure 8. The effect of oral phenylalanine ingestion [58] (Supplemental Figure 8-A) and intravenous phenylalanine infusion [17] (Supplemental Figure 8-C) has been examined in healthy individuals. Nuttal et al. [58] found that oral phenylalanine ingestion increased insulin concentrations (iAUC, 3.88 μU/mL/min) compared to water (iAUC, -1.52 μU/mL/min), while glucose concentrations remained unaltered. Co-ingestion of phenylalanine+glucose (Supplemental Figure 8-B) resulted in a similar iAUC for insulin compared to glucose ingestion alone, and attenuated the glucose-stimulated glucose response. However, insulin concentrations increased more rapidly and reached higher peak insulin concentrations (64.8 μU/mL) compared to glucose ingestion alone (49.3 μU/mL). Finally, intravenous phenylalanine infusion increased insulin (iAUC, 6.48 μU/mL/min), and decreased glucose concentrations (iAUC, -2.89 mg/dL/min) from baseline in healthy individuals [17]. To our knowledge, no kinetic data are available concerning phenylalanine intake in people with obesity and/or T2DM.

### Glutamate

Glutamate study details are provided in Table 2 (section J). The time series data and the calculated kinetic parameters are visualized in Supplemental Figure 9. The effects of oral glutamate ingestion have been examined in healthy individuals

only [59-61] (Supplemental Figure 9-A).Two out of three studies showed that oral glutamate ingestion increased insulin concentrations (iAUC range, 1.95 to 3.80 μU/mL/min) from baseline [60, 61]. Fernstrom et al. [60] showed increased insulin concentrations (iAUC, 1.95 μU/mL/min) after oral glutamate ingestion, compared to the control, whereas the control (a cold flavored vehicle containing 3g sodium chloride instead of glutamate) did not (iAUC, -0.95 μU/mL/min). Glucose values were not reported. Di Sebastiano [59] showed a non-significant increase in insulin (iAUC, 1.70 μU/mL/min) compared to the control group (gelatin capsules containing NaCl) (iAUC, 0.21 μU/mL/min). Glucose concentrations were unchanged compared to the control group. To our knowledge, no kinetic data are available concerning intravenous glutamate infusion, nor for glutamate intake in people with obesity and/or T2DM patients.

### Branched-chain amino acids

BCAA study details (including BCAA composition) are provided in Table 2 (section K). The time series data and the calculated kinetic parameters are visualized in Supplemental Figure 10. The effect of oral BCAA ingestion (mixtures containing leucine, isoleucine, and valine) has been investigated in healthy individuals only [62, 63] (Supplemental Figure 10-A). Both studies (excluding the low dose, 1g, BCAA dose intervention [62]), showed that oral BCAA ingestion increased insulin (iAUC range, 0.47 to 1.51 μU/mL/min), and decreased glucose concentrations (iAUC, -9.22 to -3.67 mg/dL/min) from baseline and the control group (iAUC, -0.29 μU/mL/min, -0.30 mg/dL/min). Furthermore, the 5g BCAA dose resulted in a higher insulin peak concentration (8.5 μU/mL) than the 1g BCAA dose (7.3 μU/mL) [62]. The highest insulin response was observed in the study that had the largest BCAA dose [63].

The effect of intravenous BCAA infusion (mixtures containing leucine, isoleucine, and valine) has also been investigated in healthy individuals [63-65] (Supplemental Figure 10-C). Two out of the three studies showed increased insulin (iAUC range, 0.18 to 0.50 μU/mL/min) [63, 64]. Glucose concentrations consistently decreased from baseline in these studies (iAUC, range, -12.05 to -8.37 mg/dL/min). Gojda et al. [63] demonstrated that oral BCAA ingestion increased insulin concentrations (iAUC, 1.51 μU/mL/min) more than the same dose (30.7g) infused intravenously in healthy individuals (iAUC, 0.42 μU/mL/min). Glucose concentrations declined in the same pattern during both BCAA tests. To our knowledge, no kinetic data are available concerning BCAA intake in people with obesity and/or T2DM.

## DISCUSSION

AAs have been recognized as important factors involved in glucose homeostasis. In the present systematic review, we aimed to provide a detailed overview of the quantitative effects of oral ingestion and intravenous administration of AAs on postprandial glucose and insulin concentrations in humans. A summary of the results is provided in Table 3.

**Table 3.** Summary of the findings.

| | | | | | | | | | | | | | | | | |
|---|---|---|---|---|---|---|---|---|---|---|---|---|---|---|---|---|
| -- | All studies show decrease from control/baseline | | | | | | | | | | | | | | | |
| - | One or more studies show decrease from control/baseline | | | | | | | | | | | | | | | |
| +/- | No change from control/baseline; contrasting outcomes | | | | | | | | | | | | | | | |
| + | One or more studies show increase from control/baseline | | | | | | | | | | | | | | | |
| ++ | All studies show increase from control/baseline | | | | | | | | | | | | | | | |
| AA | Oral ingestion | | | | | | Co-ingestion with glucose | | Intravenous infusion | | | | | | | |
| | Healthy | | T2DM | | Obese | | Healthy | | Healthy | | T2DM | | Obese | | | |
| | I | G | I | G | I | G | I | G | I | G | I | G | I | G | | |
| Leucine | + | +/- | | | | | ++ | -- | + | -- | | | | | | |
| Isoleucine | +/- | -- | | | | | ++ | -- | | | | | | | | |
| Alanine | ++ | - | ++ | -- | ++ | -- | | | + | + | | | ++ | ++ | | |
| Glutamine | ++ | +/- | ++ | +/- | ++ | +/- | | | | | | | | | | |
| Arginine | + | +/- | | | | | +/- | +/- | ++ | + | ++ | ++ | ++ | ++ | | |
| Lysine | ++ | -- | | | | | +/- | -- | ++ | -- | | | | | | |
| Glycine | + | +/- | | | | | +/- | -- | | | | | | | | |
| Proline | ++ | +/- | | | | | +/- | -- | | | | | | | | |
| Phenylalanine | ++ | +/- | | | | | +/- | -- | ++ | -- | | | | | | |
| Glutamate | + | +/- | | | | | | | | | | | | | | |
| BCAA mixture (leucine, isoleucine, and valine) | + | -- | | | | | | | + | -- | | | | | | |

AA: Amino acid, T2DM: Type 2 diabetes mellitus, BCAA: Branched-chain amino acids, G: Glucose concentrations, I: Insulin concentrations. An overview of the studies is provided in Table 2.

In total, 55 studies that assessed the effects of 10 AAs, i.e. leucine, isoleucine, alanine, glutamine, arginine, lysine, glycine, proline, phenylalanine, glutamate, and BCAA mixtures were included in this review. The majority of orally ingested

AAs, except isoleucine, induced an insulin response when ingested in isolation. Glucose concentrations, with the exception of isoleucine, and lysine, remained unchanged.

The increase in insulin concentrations through AAs has long been recognized, though their mechanisms of action are diverse and not fully elucidated yet [4, 69]. It has been shown that AAs affect β-cell insulin secretion through mitochondrial metabolism linked to the TCA cycle, and subsequent generation of ATP (e.g. for leucine, glutamine, and alanine) [70, 71]. The rise in the ATP/ADP ratio suppresses ATP-sensitive potassium channels, causing depolarization of the β-cell plasma membrane. This in turn activates voltage-gated $Ca^{2+}$ channels, and through the influx of $Ca^{2+}$ leads to insulin exocytosis. Other AAs, like arginine via its mCAT2A AA transporter, directly depolarize the β-cell plasma membrane ([4, 72]. Co-transport of AA with $Na^{+}$ (e.g. alanine, and proline) also depolarize the β-cell plasma membrane, ultimately leading to $Ca^{2+}$ activated insulin exocytosis [69, 73-75]. The seemingly unaffected glucose concentrations despite the presence of an insulin response are somewhat surprising. However, compensatory glucagon production and gluconeogenesis to prevent hypoglycemia may at least partly explain these observations [76]. Indeed, multiple studies included in the present systematic review showed increased glucagon concentrations after ingestion of isolated AAs [8, 18, 19, 24-26, 28, 29, 31, 34, 36, 37, 41, 43, 45, 48, 50, 53-55, 58]. Digitizing postprandial glucagon responses found in these studies was, however, outside the scope of the present review. Furthermore, the carbon chain of AA can be used in the liver for gluconeogenesis (i.e. generating glucose from non-carbohydrate carbon substrates), which might further contribute to the lack in suppression of postprandial glucose concentrations [25].

While oral ingestion of most AAs did not alter postprandial glucose responses, oral intake of isoleucine, lysine and BCAA mixtures evoked a clear decrease in plasma glucose concentrations. Remarkably, the decrease in glucose concentration following isoleucine ingestion occurred without a change in insulin concentrations, suggesting glucose uptake by tissues independent of insulin, as has previously been found *in vivo* [77]. In the latter study, isoleucine increased glucose uptake in rat skeletal muscle cells through activation of phosphatidylinositol 3-kinase, and independent of mTOR, indicative of insulin-independent glucose uptake.

Co-ingestion of most identified AAs (lysine, glycine, proline, phenylalanine) with glucose did not significantly increase the insulin response compared to

the ingestion of glucose alone. However, for these AAs, co-ingestion with glucose prompted a reduction in the glucose response of up to ~70% for phenylalanine. The mechanisms remain to be determined, as it is unclear whether the attenuation of glucose is due to an increased removal rate of glucose (i.e. insulin-independent mechanisms), or due to decreased endogenous glucose production by the liver [55]. Despite the unchanged insulin responses (iAUCs), the postprandial insulin dynamics were frequently altered, indicating a sharper, and more pronounced peak after co-ingestion of AAs (i.e. lysine, proline, and phenylalanine) with glucose as compared to glucose ingesting alone. The greater early rise in insulin concentrations observed after co-ingestion of AAs may imply increased first-phase insulin secretion [54, 58], which certainly influences the postprandial glucose concentrations. Co-ingestion of glucose with leucine or isoleucine increased the postprandial insulin concentrations more than the sum of their individual effects, reaching a ~50% increase in iAUC for leucine [8]. This synergistic stimulating effect of the combined intake of AAs and glucose on plasma insulin concentrations was already described by Floyd et al. [6] many years ago. Maximizing insulin secretion could be important in the treatment of T2DM to promote glucose disposal and improve glucose homeostasis [69]. Van Loon and colleagues [9] showed that co-ingestion of a mixture of protein hydrolysate, leucine, and phenylalanine in long-term T2DM patients, resulted in a considerable (+189%) increase in insulin response compared to the healthy control group (+114%), implying functional β-cells secretory capacity to stimuli other than glucose. Manders and coworkers [78] applied continuous infusion with labeled [6,6-$^{2}H_{2}$] glucose to determine blood glucose appearance and disappearance rates following carbohydrate ingestion with or without addition of a protein, leucine, and phenylalanine mixture in T2DM patients. A substantial (~3-fold) greater insulin response was observed following co-ingestion of carbohydrates with AA/protein, with a 28% reduction in blood glucose response, attributed to an increase in plasma glucose disposal.

Intravenous infusion of leucine, arginine, lysine, phenylalanine, and BCAAs infusion induced a plasma insulin response, and with the exception of arginine, evoked a decrease in plasma glucose concentrations. These AAs were thus able to induce a substantial increase in insulin response, also observed after oral ingestion, independent from the gut. However, intravenous alanine infusion, unlike oral alanine ingestion, did not induce an insulin response, suggesting that alanine may increase postprandial insulin concentrations through an incretin effect [19]. An incretin effect indicates the release of insulin-inducing substances from the gut and plays a major part in the regulation of postprandial glucose

concentrations [79, 80]. Incretin hormones, like gastric inhibitory polypeptide (GIP) and glucagon-like peptide-1 (GLP-1), are shown to rapidly stimulate insulin secretion from β-cells in response to nutrients in order to control meal-related glycemic excursions [81]. This incretin effect was also observed by others [82, 83], demonstrating that oral ingestion of an AA mixture increased insulin concentrations more than comparable intravenous AA infusion, with increased GIP concentrations. A large number of studies were found that investigated the effects of intravenous arginine infusion, which is often used to evaluate β-cell function (i.e. during hyperglycemic clamp) and allows for simultaneous examination of acute insulin, c-peptide, and glucagon response [84]. Intravenous arginine infusion stimulated insulin release to a greater extent than oral arginine ingestion, however, studies comparing oral and intravenous administrations are lacking. The larger arginine content in the blood circulation, by avoiding gut metabolism, might have led to increased β-cell stimulation [85, 86].

Although limited data are available on the effect of AAs on glucose and insulin responses across different population, studies in obese and T2DM individuals focused on alanine, glutamine, and arginine. Abnormalities in β-cell function are present in prediabetes and T2DM, whereas insulin sensitivity already declines decades before T2DM onset [87]. Furthermore, insulin resistance through excess adiposity is linked to several abnormalities, impacting β-cell function and viability [4]. The studies included here showed that AAs are able to stimulate insulin secretion and lower glucose concentrations in T2DM, and obese individuals. Greenfield et al. [25] observed the greatest insulin response after oral glutamine ingestion in T2DM patients, followed by obese and healthy people. In addition, increased GLP-1 concentrations were found following oral ingestion of glutamine, with no significant differences between T2DM, obese, and healthy individuals. Samocha-Bonet et al. [88] showed that in patients with well-controlled T2DM, the stimulatory action of GLP-1 on insulin secretion is preserved, reducing the postprandial glycemia in T2DM [89]. Whereas oral ingestion of alanine resulted in a comparable insulin response in both healthy and T2DM patients, the insulin dynamics showed considerable differences. More specific, a lower but prolonged elevation in insulin concentrations was observed in T2DM patients [22]. This prolonged elevation in insulin was also observed in obese individuals following intravenous alanine infusion [24]. Intravenous infusion of arginine showed a blunted insulin response in T2DM, as compared to healthy individuals in three out the four studies. This impairment in insulin secretion might be explained by insufficient β-cell mass, and/or functional

defects within the β-cells themselves, in patients with T2DM and individuals at risk for diabetes [4].

In this review, we systematically investigated the effects of AAs on postprandial insulin and glucose dynamics. An extensive approach, consisting of the extraction and utilization of time series data, with a focus on the link between glucose and insulin kinetics was employed. In the present review, the effects of ten distinct AAs and BCAA mixtures from 55 articles were included. As the AA composition in protein and whole foods largely contributes to the variability observed in glycemic responses, we decided to focus on the glycemic effects of individual AAs. However, the diversity of the included studies, e.g. differences in study set-up, participant characteristics, and measurement instruments, made it difficult to draw quantitative conclusions based on the data. Furthermore, the large heterogeneity in AA dosages used in the studies was not accounted for, when calculating and comparing the postprandial responses, as this would incorrectly assume a linear relationship between AA dosage and postprandial glucose and insulin responses, which we believe is not true. Nevertheless, this might have contributed to a certain extent to the variability observed in postprandial glucose and insulin responses between the different studies. While glucagon measurements were outside the scope of the present systematic review, future studies investigating the effect of AAs on glucose and insulin responses should also include postprandial glucagon concentrations. Notably, since we have made the digitized data on insulin and glucose concentrations publicly available, other parameters such as glucagon concentrations can easily be incorporated in this database. A large difference in the number of identified studies per AA was found in the literature. There was ample information on some AAs (e.g. 28 articles on arginine) and very little information on others (e.g. 1 article on isoleucine), yet several distinct effects were found for the studied AAs. Furthermore, a better understanding of the effects of different AAs on postprandial plasma glucose and insulin responses, as well as putative synergistic effects of co-ingestion of different AAs with glucose, may contribute to the development of more optimal dietary intervention to improve (postprandial) glucose homeostasis.

## REFERENCES


1. Pena, M., J. Rocha, and N. Borges, *Amino acids, glucose metabolism and clinical relevance for phenylketonuria management.* 2015.
2. Röder, P.V., B. Wu, Y. Liu, and W. Han, *Pancreatic regulation of glucose homeostasis.* Experimental & molecular medicine, 2016. **48**(3): p. e219.
3. Bröer, S. and A. Bröer, *Amino acid homeostasis and signalling in mammalian cells and organisms.* Biochemical Journal, 2017. **474**(12): p. 1935-1963.
4. Newsholme, P. and M. Krause, *Nutritional regulation of insulin secretion: implications for diabetes.* The Clinical Biochemist Reviews, 2012. **33**(2): p. 35.
5. Floyd, J., S.S. Fajans, J.W. Conn, R.F. Knopf, and J. Rull, *Stimulation of insulin secretion by amino acids.* The Journal of clinical investigation, 1966. **45**(9): p. 1487-1502.
6. Floyd, J.C., S.S. Fajans, S. Pek, C.A. Thiffault, R.F. Knopf, and J.W. Conn, *Synergistic effect of essential amino acids and glucose upon insulin secretion in man.* Diabetes, 1970. **19**(2): p. 109-115.
7. Nilsson, M., J.J. Holst, and I.M. Björck, *Metabolic effects of amino acid mixtures and whey protein in healthy subjects: studies using glucose-equivalent drinks.* The American journal of clinical nutrition, 2007. **85**(4): p. 996-1004.
8. Kalogeropoulou, D., L. LaFave, K. Schweim, M.C. Gannon, and F.Q. Nuttall, *Leucine, when ingested with glucose, synergistically stimulates insulin secretion and lowers blood glucose.* Metabolism-Clinical and Experimental, 2008. **57**(12): p. 1747-1752.
9. van Loon, L.J., M. Kruijshoop, P.P. Menheere, A.J. Wagenmakers, W.H. Saris, and H.A. Keizer, *Amino acid ingestion strongly enhances insulin secretion in patients with long-term type 2 diabetes.* Diabetes care, 2003. **26**(3): p. 625-630.
10. Kovatchev, B.P., M. Breton, C.D. Man, and C. Cobelli, *In silico preclinical trials: a proof of concept in closed-loop control of type 1 diabetes.* J Diabetes Sci Technol, 2009. **3**(1): p. 44-55.
11. MATLAB, *R2018b.* The MathWorks Inc. Natick, Massachusetts, United States.
12. Wilkinson, D.J., T. Hossain, D. Hill, B. Phillips, H. Crossland, J. Williams, P. Loughna, T. Churchward-Venne, L. Breen, and S.M. Phillips, *Effects of leucine and its metabolite β-hydroxy-β-methylbutyrate on human skeletal muscle protein metabolism.* The Journal of physiology, 2013. **591**(11): p. 2911-2923.
13. Yoshii, N., K. Sato, R. Ogasawara, Y. Nishimura, Y. Shinohara, and S. Fujita, *Effect of Mixed Meal and Leucine Intake on Plasma Amino Acid Concentrations in Young Men.* Nutrients, 2018. **10**(10): p. 1543.
14. Abumrad, N.N., R.P. Robinson, B.R. Gooch, and W. Lacy, *The effect of leucine infusion on substrate flux across the human forearm.* Journal of Surgical Research, 1982. **32**(5): p. 453-463.
15. Eriksson, L.S., L. Hagenfeldt, P. Felig, and J. Wahren, *Leucine uptake by splanchnic and leg tissues in man: relative independence of insulin levels.* Clinical Science, 1983. **65**(5): p. 491-498.
16. Sherwin, R.S., *Effect of starvation on the turnover and metabolic response to leucine.* The Journal of clinical investigation, 1978. **61**(6): p. 1471-1481.
17. Floyd, J.C., Jr., S.S. Fajans, S. Pek, C.A. Thiffault, R.F. Knopf, and J.W. Conn, *Synergistic effect of certain amino acid pairs upon insulin secretion in man.* Diabetes, 1970. **19**(2): p. 102-8.

18. Nuttall, F.Q., K. Schweim, and M.C. Gannon, *Effect of orally administered isoleucine with and without glucose on insulin, glucagon and glucose concentrations in non-diabetic subjects.* European e-Journal of Clinical Nutrition and Metabolism, 2008. **3**(4): p. e152-e158.
19. Rossini, A.A., T.T. Aoki, O.P. Ganda, J.S. Soeldner, and G.F. Cahill Jr, *Alanine-induced amino acid interrelationships.* Metabolism, 1975. **24**(10): p. 1185-1192.
20. Rose, D.P., J.E. Leklem, L. Fardal, R.B. Baron, and E. Shrago, *Effect of oral alanine loads on the serum triglycerides of oral contraceptive users and normal subjects.* Am J Clin Nutr, 1977. **30**(5): p. 691-4.
21. Sato, T., S. Saito, M. Kokubun, T. Saito, M. Ito, M. Yamamoto, K. Kaise, and N. Kaise, *Gluconeogenesis from glycerol and alanine in thyrotoxicosis.* The Tohoku journal of experimental medicine, 1980. **132**(4): p. 369-373.
22. Genuth, S.M. and J. Castro, *Effect of oral alanine on blood beta-hydroxybutyrate and plasma glucose, insulin, free fatty acids, and growth hormone in normal and diabetic subjects.* Metabolism, 1974. **23**(4): p. 375-386.
23. Genuth, S.M., *Effects of oral alanine administration in fasting obese subjects.* Metabolism, 1973. **22**(7): p. 927-937.
24. Asano, T., H. Ninomiya, K. Kan, T. Yamamoto, and M. Okumura, *Plasma glucagon response to intravenous alanine in obese and non-obese subjects.* Endocrinologia japonica, 1989. **36**(5): p. 767-773.
25. Greenfield, J.R., I.S. Farooqi, J.M. Keogh, E. Henning, A.M. Habib, A. Blackwood, F. Reimann, J.J. Holst, and F.M. Gribble, *Oral glutamine increases circulating glucagon-like peptide 1, glucagon, and insulin concentrations in lean, obese, and type 2 diabetic subjects.* The American journal of clinical nutrition, 2008. **89**(1): p. 106-113.
26. Gannon, M.C., J.A. Nuttall, and F.Q. Nuttall, *Oral arginine does not stimulate an increase in insulin concentration but delays glucose disposal.* The American journal of clinical nutrition, 2002. **76**(5): p. 1016-1022.
27. Tang, Z.Q., T. Wu, S.W. Cui, X.H. Zhu, T. Yin, C.F. Wang, J.Y. Zhu, and A.J. Wu, *Stimulation of insulin secretion by large-dose oral arginine administration in healthy adults.* Exp Ther Med, 2013. **6**(1): p. 248-252.
28. Giugliano, D., R. Marfella, G. Verrazzo, R. Acampora, L. Coppola, D. Cozzolino, and F. D'Onofrio, *The vascular effects of L-Arginine in humans. The role of endogenous insulin.* The Journal of clinical investigation, 1997. **99**(3): p. 433-438.
29. Coiro, V., R. Volpi, L. Capretti, G. Speroni, G. Caffarri, and P. Chiodera, *Involvement of nitric oxide in arginine, but not glucose, induced insulin secretion in normal men.* Clinical endocrinology, 1997. **46**(1): p. 115-119.
30. Broglio, F., C. Gottero, A. Benso, F. Prodam, S. Destefanis, C. Gauna, M. Maccario, R. Deghenghi, A. Van Der Lely, and E. Ghigo, *Effects of ghrelin on the insulin and glycemic responses to glucose, arginine, or free fatty acids load in humans.* The Journal of Clinical Endocrinology & Metabolism, 2003. **88**(9): p. 4268-4272.
31. Dela, F., K.J. Mikines, B. Tronier, and H. Galbo, *Diminished arginine-stimulated insulin secretion in trained men.* Journal of Applied Physiology, 1990. **69**(1): p. 261-267.
32. Penny, R., R.M. Blizzard, and W.T. Davis, *Sequential study of arginine monochloride and normal saline as stimuli to growth hormone release.* metabolism, 1970. **19**(2): p. 165-169.
33. Levin, S.R., J.H. Karam, S. Hane, G.M. Grodsky, and P.H. Forsham, *Enhancement of arginine-induced insulin secretion in man by prior administration of glucose.* Diabetes, 1971. **20**(3): p. 171-176.

34. Bratusch-Marrain, P., O. Björkman, L. Hagenfeldt, W. Waldhäusl, and J. Wahren, *Influence of arginine on splanchnic glucose metabolism in man.* Diabetes, 1979. **28**(2): p. 126-131.
35. Imura, H., Y. Seino, M. Ikeda, T. Taminato, Y. Miyamoto, and Y. Goto, *Impaired plasma insulin response to arginine in hyperthyroidism: Important role of the rise of blood glucose in the second phase of insulin release induced by arginine.* Diabetes, 1976. **25**(10): p. 961-968.
36. Hasselblatt, M., H. Krampe, S. Jacobs, H. Sindram, V.W. Armstrong, M. Hecker, and H. Ehrenreich, *Arginine challenge unravels persistent disturbances of urea cycle and gluconeogenesis in abstinent alcoholics.* Alcohol and Alcoholism, 2006. **41**(4): p. 372-378.
37. Berger, W., M. Stahl, E. Ohnhaus, and H. Goschke, *Pancreatic glucagon, plasma insulin and blood glucose responses to arginine infusion in nondiabetic subjects following biguanide pretreatment.* Horm Metab Res, 1974. **6**(2): p. 165.
38. Dupre, J., J.D. Curtis, R.W. Waddell, and J.C. Beck, *Alimentary factors in the endocrine response to administration of arginine in man.* Lancet, 1968. **2**(7558): p. 28-9.
39. Dupre, J., J.D. Curtis, R.H. Unger, R.W. Waddell, and J.C. Beck, *Effects of secretin, pancreozymin, or gastrin on the response of the endocrine pancreas to administration of glucose or arginine in man.* J Clin Invest, 1969. **48**(4): p. 745-57.
40. Kimber, J., L. Watson, and C.J. Mathias, *Cardiovascular and neurohormonal responses to i. v. l-arginine in two groups with primary autonomic failure.* J Neurol, 2001. **248**(12): p. 1036-41.
41. Oneda, A., M. Sato, K. Matsuda, A. Yanbe, and Y. Maruhama, *Plasma glucagon response to blood glucose fall, gastrointestinal hormones and arginine in man.* Tohoku J Exp Med, 1972. **107**(3): p. 241-51.
42. Efendić, S., E. Cerasi, and R. Luft, *Quantitative study on the potentiating effect of arginine on glucose-induced insulin response in healthy, prediabetic, and diabetic subjects.* Diabetes, 1974. **23**(3): p. 161-171.
43. Kawamori, R., M. Shichiri, M. Kikuchi, Y. Yamasaki, and H. Abe, *Perfect normalization of excessive glucagon responses to intravenous arginine in human diabetes mellitus with the artificial beta-cell.* Diabetes, 1980. **29**(9): p. 762-765.
44. Sparks, L.L., G. Copinschi, C.L. Donaldson, A.S. Blum, and P.H. Forsham, *Hyperglycemic response to intravenous arginine in prematurity-onset diabetes*. 1967, Am Diabetes Assoc.
45. Kawamori, R., M. Shichiri, M. Kikuchi, Y. Yamasaki, and H. Abe, *The mechanism of exaggerated glucagon response to arginine in diabetes mellitus.* Diabetes Research and Clinical Practice, 1985. **1**(3): p. 131-137.
46. Maccario, M., S. Grottoli, P. Razzore, M. Procopio, S.E. Oleandri, E. Ciccarelli, F. Camanni, and E. Ghigo, *Effects of glucose load and/or arginine on insulin and growth hormone secretion in hyperprolactinemia and obesity.* Eur J Endocrinol, 1996. **135**(2): p. 205-10.
47. Marfella, R., R. Acampora, G. Verrazzo, P. Ziccardi, N. De Rosa, R. Giunta, and D. Giugliano, *Metformin improves hemodynamic and rheological responses to L-arginine in NIDDM patients.* Diabetes Care, 1996. **19**(9): p. 934-939.
48. Raskin, P., I. Aydin, and R.H. Unger, *Effect of insulin on the exaggerated glucagon response to arginine stimulation in diabetes mellitus.* Diabetes, 1976. **25**(3): p. 227-229.

49. Maejima, K., M. Himeno, T. Ishibashi, S. Nakano, M. Nishio, and K. Uchida, *Paradoxical decrease in plasma NOx by L-arginine load in diabetic and non-diabetic subjects.* Clinical and Experimental Hypertension, 2002. **24**(3): p. 155-167.
50. Ohneda, A., S. Ishii, K. Horigome, and S. Yamagata, *Glucagon response to arginine after treatment of diabetes mellitus.* Diabetes, 1975. **24**(9): p. 811-819.
51. Carpentier, A., A. Giacca, and G. Lewis, *Effect of increased plasma non-esterified fatty acids (NEFAs) on arginine-stimulated insulin secretion in obese humans.* Diabetologia, 2001. **44**(11): p. 1989-1997.
52. Maccario, M., S. Grottoli, M. Procopio, S. Oleandri, G. Boffano, P. Savio, F. Camanni, and E. Ghigo, *Effects of cholinergic blockade by pirenzepine on insulin and glucose response to oral and intravenous glucose and to arginine load in obesity.* Journal of endocrinological investigation, 1997. **20**(1): p. 8-12.
53. Walter, R.M., Jr., E.M. Gold, C.A. Michas, and J.W. Ensinck, *Portal and peripheral vein concentrations of insulin and glucagon after arginine infusion in morbidly obese subjects.* Metabolism, 1980. **29**(11): p. 1037-40.
54. Kalogeropoulou, D., L. LaFave, K. Schweim, M.C. Gannon, and F.Q. Nuttall, *Lysine ingestion markedly attenuates the glucose response to ingested glucose without a change in insulin response.* The American journal of clinical nutrition, 2009. **90**(2): p. 314-320.
55. Gannon, M.C., J.A. Nuttall, and F.Q. Nuttall, *The metabolic response to ingested glycine.* The American journal of clinical nutrition, 2002. **76**(6): p. 1302-1307.
56. Kasai, K., M. Kobayashi, and S.-I. Shimoda, *Stimulatory effect of glycine on human growth hormone secretion.* Metabolism, 1978. **27**(2): p. 201-208.
57. Nuttall, F.Q., M.C. Gannon, and K. Jordan, *The metabolic response to ingestion of proline with and without glucose.* Metabolism, 2004. **53**(2): p. 241-246.
58. Nuttall, F., K. Schweim, and M. Gannon, *Effect of orally administered phenylalanine with and without glucose on insulin, glucagon and glucose concentrations.* Hormone and metabolic research, 2006. **38**(08): p. 518-523.
59. Di Sebastiano, K.M., K.E. Bell, T. Barnes, A. Weeraratne, T. Premji, and M. Mourtzakis, *Glutamate supplementation is associated with improved glucose metabolism following carbohydrate ingestion in healthy males.* British Journal of Nutrition, 2013. **110**(12): p. 2165-2172.
60. Fernstrom, J.D., J.L. Cameron, M.H. Fernstrom, C. McConaha, T.E. Weltzin, and W.H. Kaye, *Short-term neuroendocrine effects of a large oral dose of monosodium glutamate in fasting male subjects.* J Clin Endocrinol Metab, 1996. **81**(1): p. 184-91.
61. Graham, T.E., V. Sgro, D. Friars, and M.J. Gibala, *Glutamate ingestion: the plasma and muscle free amino acid pools of resting humans.* Am J Physiol Endocrinol Metab, 2000. **278**(1): p. E83-9.
62. Zhang, Y., H. Kobayashi, K. Mawatari, J. Sato, G. Bajotto, Y. Kitaura, and Y. Shimomura, *Effects of branched-chain amino acid supplementation on plasma concentrations of free amino acids, insulin, and energy substrates in young men.* Journal of nutritional science and vitaminology, 2011. **57**(1): p. 114-117.
63. Gojda, J., R. Strakova, A. Plihalova, P. Tuma, J. Potockova, J. Polak, and M. Andel, *Increased Incretin But Not Insulin Response after Oral versus Intravenous Branched Chain Amino Acids.* Ann Nutr Metab, 2017. **70**(4): p. 293-302.
64. Tatpati, L.L., B.A. Irving, A. Tom, M.L. Bigelow, K. Klaus, K.R. Short, and K.S. Nair, *The effect of branched chain amino acids on skeletal muscle mitochondrial function in young and elderly adults.* The Journal of Clinical Endocrinology & Metabolism, 2010. **95**(2): p. 894-902.

65. Louard, R.J., E.J. Barrett, and R.A. Gelfand, *Effect of infused branched-chain amino acids on muscle and whole-body amino acid metabolism in man.* Clinical Science, 1990. **79**(5): p. 457-466.
66. Mosteller, R.D., *Simplified calculation of body-surface area.* N Engl J Med, 1987. **317**(17): p. 1098.
67. *1983 metropolitan height and weight tables.* Stat Bull Metrop Life Found, 1983. **64**(1): p. 3-9.
68. Fryar, C.D., D. Kruszan-Moran, Q. Gu, and C.L. Ogden, *Mean body weight, weight, waist circumference, and body mass index among adults: United States, 1999–2000 through 2015–2016.* 2018.
69. van Loon, C. and J. Luc, *Amino acids as pharmaco-nutrients for the treatment of type 2 diabetes.* Immunology, Endocrine & Metabolic Agents in Medicinal Chemistry (Formerly Current Medicinal Chemistry-Immunology, Endocrine and Metabolic Agents), 2007. **7**(1): p. 39-48.
70. Panten, U., E. Kriegstein, W. Poser, J. Schönborn, and A. Hasselblatt, *Effects of L-leucine and alpha-ketoisocaproic acid upon insulin secretion and metabolism of isolated pancreatic islets.* FEBS Lett, 1972. **20**(2): p. 225-228.
71. Newsholme, P., C. Gaudel, and N. McClenaghan, *Nutrient regulation of insulin secretion and β-cell functional integrity.* Advances in Experimental Medicine and Biology, 2010. **654**: p. 91-114.
72. Sener, A., L.C. Best, A.P. Yates, M.M. Kadiata, E. Olivares, K. Louchami, H. Jijakli, L. Ladrière, and W.J. Malaisse, *Stimulus-secretion coupling of arginine-induced insulin release.* Endocrine, 2000. **13**(3): p. 329-340.
73. Dunne, M.J., D.I. Yule, D.V. Gallacher, and O.H. Petersen, *Effects of alanine on insulin-secreting cells: patch-clamp and single cell intracellular Ca2+ measurements.* Biochim Biophys Acta, 1990. **1055**(2): p. 157-64.
74. McClenaghan, N.H., C.R. Barnett, and P.R. Flatt, *Na+ cotransport by metabolizable and nonmetabolizable amino acids stimulates a glucose-regulated insulin-secretory response.* Biochemical and biophysical research communications, 1998. **249**(2): p. 299-303.
75. Newsholme, P., L. Brennan, and K. Bender, *Amino acid metabolism, β-cell function, and diabetes.* Diabetes, 2006. **55**(Supplement 2): p. S39-S47.
76. Bankir, L., N. Bouby, R.C. Speth, G. Velho, and G. Crambert, *Glucagon revisited: Coordinated actions on the liver and kidney.* Diabetes Research and Clinical Practice, 2018. **146**: p. 119-129.
77. Doi, M., I. Yamaoka, T. Fukunaga, and M. Nakayama, *Isoleucine, a potent plasma glucose-lowering amino acid, stimulates glucose uptake in C2C12 myotubes.* Biochemical and Biophysical Research Communications, 2003. **312**(4): p. 1111-1117.
78. Manders, R.J., A.J. Wagenmakers, R. Koopman, A.H. Zorenc, P.P. Menheere, N.C. Schaper, W.H. Saris, and L.J. van Loon, *Co-ingestion of a protein hydrolysate and amino acid mixture with carbohydrate improves plasma glucose disposal in patients with type 2 diabetes.* The American Journal of Clinical Nutrition, 2005. **82**(1): p. 76-83.
79. Holst, J.J., F. Gribble, M. Horowitz, and C.K. Rayner, *Roles of the Gut in Glucose Homeostasis.* Diabetes Care, 2016. **39**(6): p. 884-92.
80. Nauck, M.A. and J.J. Meier, *The incretin effect in healthy individuals and those with type 2 diabetes: physiology, pathophysiology, and response to therapeutic interventions.* Lancet Diabetes Endocrinol, 2016. **4**(6): p. 525-36.

81. Gérard, C. and H. Vidal, *Impact of Gut Microbiota on Host Glycemic Control.* Front Endocrinol (Lausanne), 2019. **10**: p. 29.
82. Lindgren, O., G. Pacini, A. Tura, J.J. Holst, C.F. Deacon, and B. Ahrén, *Incretin effect after oral amino acid ingestion in humans.* The Journal of Clinical Endocrinology & Metabolism, 2015. **100**(3): p. 1172-1176.
83. Abdulla, H., J.J. Bass, T. Stokes, S.H.M. Gorissen, C. McGlory, B.E. Phillips, S.M. Phillips, K. Smith, I. Idris, and P.J. Atherton, *The effect of oral essential amino acids on incretin hormone production in youth and ageing.* Endocrinology, Diabetes & Metabolism, 2019. **2**(4): p. e00085.
84. Robertson, R.P., L.D. Bogachus, E. Oseid, S. Parazzoli, M.E. Patti, M.R. Rickels, C. Schuetz, T. Dunn, T. Pruett, A.N. Balamurugan, et al., *Assessment of β-cell mass and α- and β-cell survival and function by arginine stimulation in human autologous islet recipients.* Diabetes, 2015. **64**(2): p. 565-72.
85. Tangphao, O., M. Grossmann, S. Chalon, B.B. Hoffman, and T.F. Blaschke, *Pharmacokinetics of intravenous and oral L-arginine in normal volunteers.* Br J Clin Pharmacol, 1999. **47**(3): p. 261-6.
86. Castillo, L., T.E. Chapman, Y.M. Yu, A. Ajami, J.F. Burke, and V.R. Young, *Dietary arginine uptake by the splanchnic region in adult humans.* Am J Physiol, 1993. **265**(4 Pt 1): p. E532-9.
87. Roden, M. and G.I. Shulman, *The integrative biology of type 2 diabetes.* Nature, 2019. **576**(7785): p. 51-60.
88. Samocha-Bonet, D., O. Wong, E.-L. Synnott, N. Piyaratna, A. Douglas, F.M. Gribble, J.J. Holst, D.J. Chisholm, and J.R. Greenfield, *Glutamine Reduces Postprandial Glycemia and Augments the Glucagon-Like Peptide-1 Response in Type 2 Diabetes Patients.* The Journal of Nutrition, 2011. **141**(7): p. 1233-1238.
89. Wang, X., H. Liu, J. Chen, Y. Li, and S. Qu, *Multiple Factors Related to the Secretion of Glucagon-Like Peptide-1.* International journal of endocrinology, 2015. **2015**: p. 651757-651757.

## SUPPLEMENTARY MATERIAL

**Supplemental File 1: PubMed search strategy**: ((“Amino Acids” [MeSH Terms] OR “Amino Acid” OR “Amino Acids” OR “Branched-Chain Amino Acids” OR “Branched-Chain Amino Acid” OR Alanine OR Arginine OR Asparagine OR “Aspartic Acid” OR Cysteine OR Glutamine OR “Glutamic Acid” OR Glycine OR Histidine OR Isoleucine OR Leucine OR Lysine OR Methionine OR Phenylalanine OR Proline OR Serine OR Threonine OR Tryptophan OR Tyrosine OR Valine OR Whey OR Casein) AND (Ingestion OR Ingested OR Infused OR Infusion OR Infusions OR Response OR Stimulation OR Elevation OR Elevated OR Oral OR Altered OR Alter OR Absorption OR Absorbed OR Postprandial OR Post-Prandial OR “Post Prandial” OR Supplemented OR Supplementation OR Supplement OR Eating OR Administration OR Administered OR Intravenous OR Intravenously OR Intake OR Food OR Consumption OR Consumed OR Dynamics OR Dynamic OR “Glucose Tolerance Test” OR “Tolerance Test” OR “Challenge Test”) AND (Insulinotropic OR Insulin OR Glucose OR Glycaemic OR Glycemia OR Glycaemia OR “Glycemic Control”) AND (Glucose [ti] OR Insulin [ti] OR Glycaemic [ti] OR Glycemia [ti] OR Glycaemia [ti] OR “Glycemic Control” [ti] OR “Amino Acids” [ti] OR “Amino Acid” [ti] OR Whey [ti] OR Casein [ti] OR Protein [ti] OR Proteins [ti] OR Alanine [ti] OR Arginine [ti] OR Asparagine [ti] OR “Aspartic Acid” [ti] OR Cysteine [ti] OR Glutamine [ti] OR “Glutamic Acid” [ti] OR Glycine [ti] OR Histidine [ti] OR Isoleucine [ti] OR Leucine [ti] OR Lysine [ti] OR Methionine [ti] OR Phenylalanine [ti] OR Proline [ti] OR Serine [ti] OR Threonine [ti] OR Tryptophan [ti] OR Tyrosine [ti] OR Valine [ti]) NOT Review [ptyp] AND English AND “loattrfull text”[sb] AND humans)

**Supplemental Figure 1-10:** The following are available online at http://www.mdpi.com/2072-6643/12/10/3211/s1 (Zip, 8917KB). Figure S1: Isoleucine infograph, Figure S2: Alanine infograph, Figure S3: Glutamine infograph, Figure S4: Arginine infograph, Figure S5: Lysine infograph, Figure S6: Glycine infograph, Figure S7: Proline infograph, Figure S8: Phenylalanine infograph, Figure S9: Glutamate infograph, Figure S10: BCAA infograph.

# Personalized computational model quantifies heterogeneity in postprandial responses to oral glucose challenge

# 3

**Balázs Erdõs*, Bart van Sloun*, Michiel E. Adriaens, Shauna D. O'Donovan, Dominique Langin, Arne Astrup, Ellen E. Blaak, Ilja C.W. Arts and Natal A. W. van Riel** *These authors contributed equally to this work

*PLoS Comput Biol 17(3): e1008852*

## ABSTRACT

Plasma glucose and insulin responses following an oral glucose challenge are representative of glucose tolerance and insulin resistance, key indicators of type 2 diabetes mellitus pathophysiology. A large heterogeneity in individuals' challenge test responses has been shown to underlie the effectiveness of lifestyle intervention. Currently, this heterogeneity is overlooked due to a lack of methods to quantify the interconnected dynamics in the glucose and insulin time-courses. Here, a physiology-based mathematical model of the human glucose-insulin system is personalized to elucidate the heterogeneity in individuals' responses using a large population of overweight/obese individuals (n = 738) from the DIOGenes study. The personalized models are derived from population level models through a systematic parameter selection pipeline that may be generalized to other biological systems. The resulting personalized models showed a 4-5 fold decrease in discrepancy between measurements and model simulation compared to population level. The estimated model parameters capture relevant features of individuals' metabolic health such as gastric emptying, endogenous insulin secretion and insulin-dependent glucose disposal into tissues, with the latter also showing a significant association with the Insulinogenic index and the Matsuda insulin sensitivity index, respectively.

## INTRODUCTION

Glucose homeostasis is maintained by the complex interplay between several tissues and organs including the brain, pancreas, skeletal muscle, liver and adipose tissue. The evolution of plasma glucose and insulin concentrations during an oral glucose tolerance test (OGTT) provide a readout of the metabolic health of these underlying tissues capturing the effects of insulin sensitivity and metabolic resilience status [1]. Certain features of the standard 75g OGTT response curves are widely accepted to be representative of glycemic control, most notably the fasting and 2 hour post-load glucose values are used in the diagnosis of prediabetes and type 2 diabetes mellitus (T2DM) [2]. The area under the plasma glucose/insulin response curve (AUC) is an extensively employed measure to compare responses [3] and has been successfully used in targeted and even personalized nutrition approaches [4–6]. However, the AUC is a somewhat crude measure that may often lead to ambiguous classifications [7]. Therefore, certain dynamic properties of the glucose response curves e.g. peak time, have been nominated as relevant for pathophysiological characterization [6, 8–11]. In addition, the post-load glucose and insulin trajectories may be used to derive proxy measures of whole-body and tissue-specific insulin sensitivity to serve as a surrogate to the hyperinsulinemic-euglycemic clamp. The HOMA-IR [12] and Matsuda insulin sensitivity indices [13, 14] have been widely utilized to quantify whole-body insulin resistance from fasting and average postprandial glucose/insulin levels, respectively. In recent years, the increased recognition of tissue-specific insulin resistance [15] leading to metabolically distinct phenotypes, has resulted in the development of the HIRI and MISI indices, quantifying hepatic and skeletal muscle insulin resistance from OGTT responses [16–18]. While these measures capture certain aspects of metabolic resilience, they rely upon single time-point or average glucose and insulin values taken from the response curves, as a result the dynamics of the time-courses are largely disregarded. Recently, Hulman et al. have shown that using a latent class mixed models framework, the glucose trajectories of healthy individuals following an OGTT may be classified into four distinct insulin sensitive phenotypes [19]. This approach—making use of the complete time-courses—highlights the importance of the dynamics of the glucose responses, however it does not allow for an individualized exploration due to the limited number of prospective classes.

The move towards personalized interventions requires the characterization of the large heterogeneity in individuals' glycemic regulation. Therefore, a holistic approach, accounting for the dynamic properties of the response curves is

needed on the individual level. Furthermore, the close interplay between plasma glucose and insulin concentrations calls for the evaluation of glucose and insulin trajectories as a whole, rather than as disjoint indicators.

Physiology-based mathematical models of the human glucose-insulin regulatory system can provide quantitative information on the dynamics while capturing the mechanistic link between glucose and insulin. Such models are built to describe the physiological processes by which insulin regulates glucose levels using a priori understanding of the underlying biological system. The detail to which the model can accurately simulate the glucose-insulin response mechanism depends on the desired scope and the availability of quantitative data. The Bergman model, a simplistic model of glucose disappearance containing only 5 parameters, has been extensively used to approximate insulin sensitivity and β-cell function using plasma glucose and insulin values following a frequently sampled intravenous glucose tolerance test [20]. The integrated glucose-insulin model has been used to describe population as well as individual responses to a frequently sampled OGTT [21], however its applicability (to nutritional and metabolic studies) is limited due to the complexity in the model's glucose absorption term that is made possible by an unusually frequent sampling strategy. A more complex model built by Dalla-Man et al. provides a detailed account of the underlying processes governing glucose utilization following a meal [22]. Here, the complexity of the model is enabled by the availability of triple tracer glucose data, quantifying the glucose fluxes between tissues. While the Bergman model can be applied to individual data, the Dalla-Man model has mostly been applied to population average data for *in silico* simulation and testing of insulin pump systems. The Eindhoven-Diabetes Education Simulator (E-DES) is a comparatively simple multi-compartmental model containing 12 parameters that has been used to describe the dynamics of the glucose homeostasis in healthy, type 1 and type 2 diabetic populations [23, 24].

Quantifying uncertainty in model parameters is essential to understand the limitations and predictive power of the model [25]. It is particularly important to consider parameter identifiability when estimating model parameters on the individual level—where sensitivity to measurement error may be high—to retain parameters that can be reliably estimated. Identifiability analysis may be carried out through methods such as Profile Likelihood Analysis (PLA) to evaluate how well parameter values can be determined given the available data [26, 27].

The aim of the current work is to explore the heterogeneity in the glucose and insulin responses to an OGTT in a large population of individuals by developing personalized dynamic models of the insulin mediated glucose metabolism, using an adapted E-DES model. The model parameters are estimated from measured postprandial trajectories of both glucose and insulin, and represent physiologically relevant properties that in turn may be used in the early identification of deterioration in the glucose homeostasis. Furthermore, the workflow presented here for transitioning a dynamic model away from describing population averages and towards individual response patterns may prove useful in numerous other applications, as it is generalizable to other biological models and systems.



## MATERIALS AND METHODS

### Ethics statement

The Medical Ethical Committees of the respective countries approved the DIOGenes study protocol. Participants provided informed written consent, and all procedures were conducted in accordance with the Declaration of Helsinki. Trial registration number: NCT00390637.

### Data

Data from the DIOGenes study (NCT00390637), a pan-European, multi-center, randomized controlled dietary intervention study were used in this work [28]. At the baseline of the intervention, following an overnight fast (n = 1118) overweight/obese (BMI > 27$kg/m^2$) but otherwise healthy adult participants underwent a two hour 75g OGTT, with plasma samples taken at the fasting state (t = 0) and 30, 60, 90 and 120 minutes after the glucose ingestion. The plasma samples were subsequently analyzed for glucose and insulin concentrations. Responses at the baseline of the intervention were used. Individuals with an incomplete set of glucose and/or insulin measurements were excluded from the analysis.

### Adapted E-DES model

The Eindhoven-Diabetes Education Simulator is a physiology-based mathematical model of the human insulin mediated glucose regulatory system in healthy, type 1 diabetes, and T2DM phenotypes [24]. The two compartment model describes the following physiological processes through coupled differential equations (see model schematic and details in S1 Fig, S1 and S2 Appendices): Glucose mass

is emptied into the gut according to an exponential decay function, followed by uptake into the plasma proportionally to the amount of glucose present in the gut. Both glucose and insulin fluxes are considered in the plasma compartment. Insulin secretion from the pancreas is modelled through a proportional-integral-derivative (PID) controller, responding to elevated plasma glucose levels. The insulin response facilitates the insulin-dependent glucose disposal to tissues such as the muscle. In addition, there is a constant glucose removal from the plasma by obligate glucose oxidizers such as the brain or the red blood cells. While the plasma glucose levels are elevated, endogenous glucose production (EGP) in the liver is suppressed. Finally, insulin is cleared by the liver proportionally to the plasma insulin concentration, as well as by a transfer and degradation in the interstitial fluid. The parameters corresponding to these physiological parameters control the rate of change in glucose or insulin concentrations. Through modulation of the parameters, responses of metabolically different phenotypes may be simulated *in silico*. The model has been previously parameterized and validated on multiple OGTT data sets from healthy populations [24]. The E-DES model was implemented and analyzed in MATLAB 2018b (The Mathworks, Inc., Natick, Massachusetts, United States). For the current study population, an adapted E-DES model is used. Model equations, including a description of parameters and modifications are described in detail in S1 Appendix.

### Parameter estimation

Parameters were estimated through minimizing the combined sum of squared residual (SSR) in the model prediction for glucose and insulin (Eq. 1) using *lsqnonlin*, a non-linear least squares solver in MATLAB. To avoid becoming trapped in erroneous local minima, the optimal parameter sets were obtained following fifty initializations of the optimization algorithm with 25% random noise starting from the original parameter value for the average healthy population from the publication [24].

$$SSR = \sum_{j=1}^{m} \sum_{i=1}^{N} (\gamma((y_{i,j}|\vec{\theta}) - d_{i,j}))^2$$

Where m, and N represent the number of metabolites and the number of time-points, respectively. The measured data point is denoted by d, while $y$ is the corresponding model prediction given the parameter vector $\vec{\theta}$. A weight factor $\gamma = 0.1$ was used in the case of insulin ($\gamma = 1$ in case of glucose) to account for the unit difference (*mmol/L*, *mU/L* for glucose and insulin, respectively) between the molecules.

## Model selection

A model selection approach was implemented in order to systematically identify parameters for personalized model fitting. The aim of the approach is to maintain parameter functionality and identifiability when transitioning from modelling population average responses to individual responses. The workflow involves systematically reducing the number of parameters to estimate for each individual response to ensure reliable, accurate parameter estimates. The parameters that are not selected in the approach for personalized fitting are fixed to reference population values [24] across all individuals. The subset of model parameters to be estimated was selected based on the following criteria: the selected parameters had to (i) exhibit high sensitivity, (ii) demonstrate good model fit while maintaining parsimony, (iii) be identifiable. The steps to meet these criteria are detailed below and a flowchart of the approach is shown on Fig 1.



(i). Sensitivity analysis. We carried out local parameter sensitivity analysis (LPSA) by varying one parameter in both directions while maintaining the others at a constant value, inspecting the effect on the resulting model outcome. A threshold of 75% in both directions compared to the average healthy population values was selected as the limit of sensitivity. Parameters that exhibit sensitivity at this level are expected to have a large modulatory effect on the model outcome. Parameters that are not sensitive at the threshold were fixed as a constant to their respective values (reported in [24]), as they have little impact on the model behavior. Only sensitive parameters were considered in subsequent steps of the model selection.

(ii). Model fit. The set of all possible combinations of 3 or more sensitive parameters were generated. Subsequently models were fit on a set of representative responses from the DIOGenes data set with these candidate parameter sets estimated from the data, while the rest of the parameters were fixed to the population reference values. The representative responses comprised of the median normal glucose tolerant (NGT), impaired fasting glucose (IFG), impaired glucose tolerant (IGT), both IFG and IGT (IFG&IGT) and T2DM responses in the data, based on the American Diabetes Association (ADA) diagnosis criteria [29]. The median responses were calculated by taking the median glucose and insulin values per time-point across all individuals in the respective groups. In addition to the median responses, both extreme responses (largest and smallest response in the data set by area under the glucose curve) were also included. The model with the candidate parameter set that showed the lowest Akaike Information Criterion (AIC) score across the set of representative curves (i.e. NGT, IFG, IGT, IFG&IGT, T2DM, Min, Max) was selected as most parsimonious model.

(iii). Parameter identifiability. The parameter set that produced the most parsimonious model was finally evaluated for identifiability using Profile Likelihood Analysis (PLA) [27]. In PLA the value of one parameter is changed iteratively from its optimal value and the remaining parameters are re-estimated. An increase in the cost function (SSR) for the model fit indicates that a reliable parameter estimate has been obtained and the parameter is identifiable given the model structure and data. Confidence intervals were derived using a Chi-squared threshold on the likelihood (Eq. 2).

$$-2\log\left(\frac{\mathcal{L}(\vec{\theta}_{PL})}{\mathcal{L}(\vec{\theta}_{opt})}\right) \leq x^2(\alpha, df)$$

Where $x^2$ $(\alpha, df)$ is the $\alpha$ quantile of the $x^2$-distribution with $df$ degrees of freedom, $\vec{\theta}_{PL}$ and $\vec{\theta}_{opt}$ are the profiled path and optimal parameter vectors, respectively. The threshold $\alpha$ was set to 0.95 and $df$ equals one or the number of parameters (see S3 and S4 Figs)

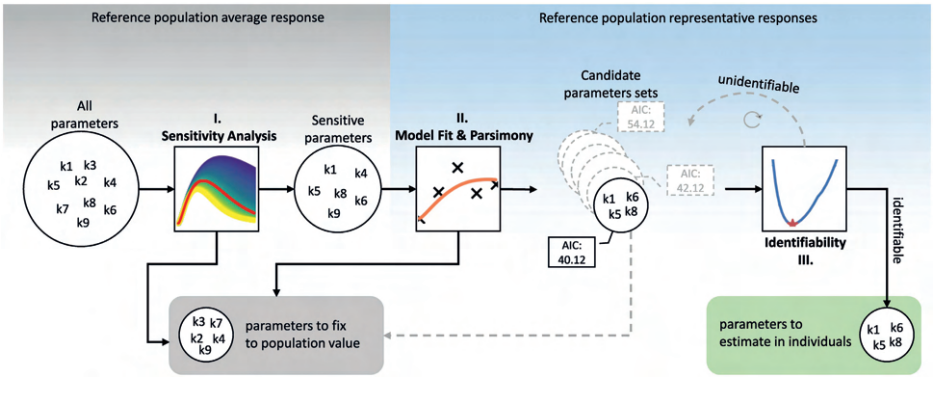


**Figure 1. Flowchart of the model selection approach.**

## Principal component analysis

The parameter space of the personalized E-DES model is visualized by reducing the number of dimensions from the number of estimated parameters to two dimensions using principal component analysis (PCA). Prior to PCA, the parameter values were normalized to zero mean and unit standard deviation.

## RESULTS

A total of 738 participants were included in the analysis, after excluding participants with incomplete OGTT measurements (n = 373) and participants with physiologically implausible responses (i.e. where the OGTT failed; n = 7). The identification of physiologically implausible responses was carried out by independent experts. The remaining 738 responses were characterized by the ADA criterion for prediabetes and diabetes as summarized in Table 1.

**Table 1. Classification of participant's responses based on ADA diabetes criteria**

| Diagnosis[1] | NGT | IFG | IGT | IFG&IGT | T2DM |
|---|---|---|---|---|---|
| N | 496 | 42 | 41 | 119 | 40 |
| Age[2][*years*] | 40.7 (6.4) | 42.0 (5.3) | 43.6 (4.8) | 41.8 (6.2) | 45.0 (6.7) |
| Sex [%*female*] | 65.8 | 42.9 | 53.7 | 68.1 | 55.0 |
| BMI[2] [$kg\,m^{-2}$] | 34.5 (4.8) | 34.7 (4.5) | 36.5 (5.8) | 34.2 (4.5) | 35.1 (5.1) |

[1] NGT: normal glucose tolerant, IFG: impaired fasting glucose, IGT: impaired glucose tolerant, T2DM: type 2 diabetes mellitus. For details about the criteria, see S1 Table. [2] Age and BMI are reported as mean and (standard deviation).

In general, DIOGenes contains overweight/obese but otherwise healthy participants [28]. However, characterization by the ADA guidelines shows that in fact, several participants may be diagnosed as prediabetic or type 2 diabetic.

### Model selection

Out of the eleven parameters contained in the adjusted E-DES model, only the physiological parameters $k1$ to $k9$ (defined in Table C of S1 Appendix) were considered in the personalization, while the two remaining parameters, the shape factor and Michaelis-Menten constant for glucose uptake, were fixed to their respective population values. As the first step of the model selection approach local parameter sensitivity analysis was carried out. The outcome of the sensitivity analysis on the plasma glucose response is shown in Fig 2. The effect on plasma insulin can be seen in S2 Fig.

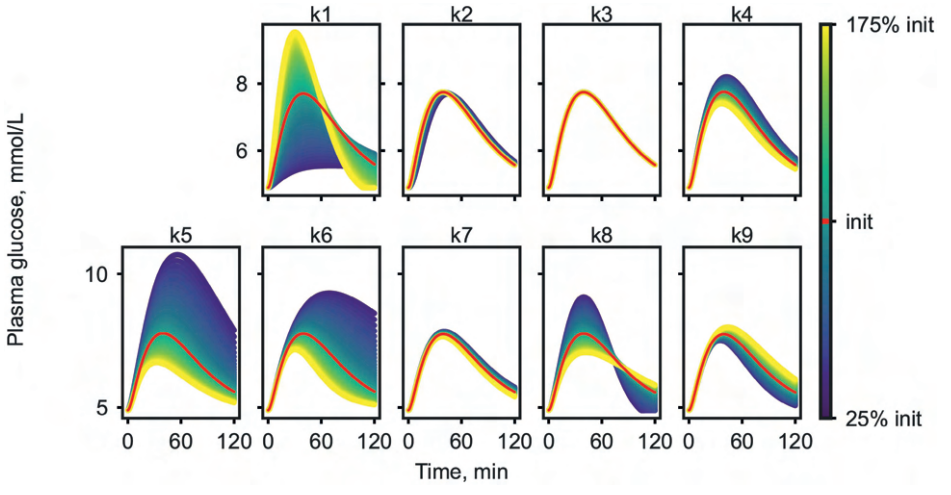


**Figure 2. Local parameter sensitivity analysis demonstrated on simulated plasma glucose response.**

Parameters *k*1, *k*4, *k*5, *k*6, *k*8, *k*9 were found to be sensitive at the ±75% threshold, and therefore were considered for further analyses, while the remainder of the parameters were kept constant in all subsequent analysis. As the second step of the model selection, the set of all possible combinations of 3, 4, 5, and 6 sensitive parameters were generated and models with these parameters estimated from data were assessed. This way a total of 42 different models were examined for model fit according to AIC on the median NGT, IFG, IGT, IFG&IGT, and T2DM responses as well as the largest and smallest response in the data set. The ten best per- forming candidate models with the resulting SSR and AIC values are shown in S2 Table.

The highest scoring model according to our criteria contained the parameters *k*1, *k*5, *k*6, and *k*8 with a SSR of 41.39. Visual inspection of the model output displayed good accordance with the majority of the data on the various group median and extreme responses as seen in Fig 3. The extreme responses are simulated less accurately compared to the median responses. Specifically, the model struggles with accurately capturing the part of the response that goes below basal. The best scoring model was subsequently evaluated for parameter identifiability in the last step of the model selection approach.

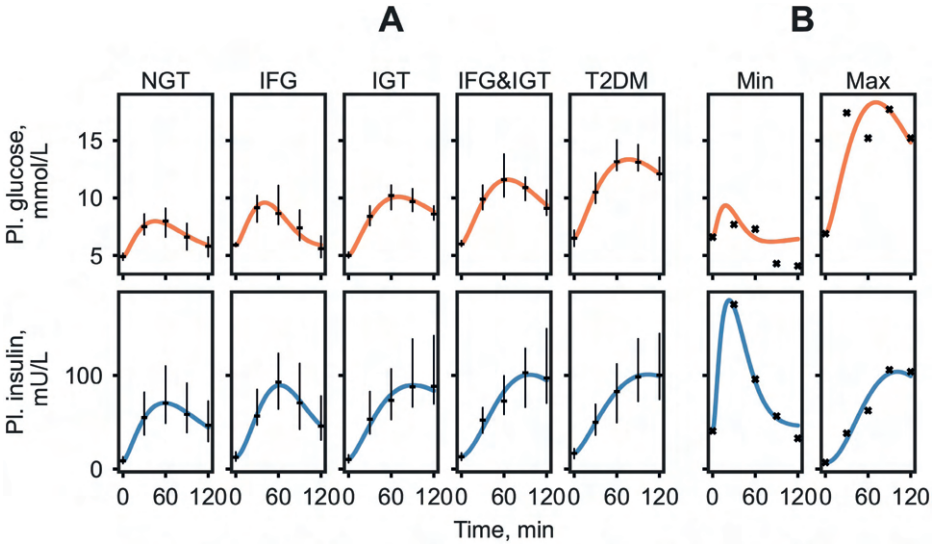


**Figure 3. Plasma glucose and insulin simulation of the set of representative responses in the DIOGenes study with estimated parameters *k*1, *k*5, *k*6, *k*8.**

The median responses were calculated as the median plasma glucose value of the ADA diabetes classification group at each time point (A). The 'Min' and 'Max' are the smallest and largest glucose responses in the data set, determined by area under the curve (B). Median measured values are shown as black dashes with the interquartile range and measured responses are indicated by black crosses.

The identifiability of the parameters *k*1, *k*5, *k*6, *k*8 was assessed on the median NGT, IFG, IGT, IFG&IGT, T2DM and the extreme responses to infer the reliability in estimating the selected parameters. The PLA profiles indicated that parameters were identifiable, with the exception of parameters *k*6 and *k*8, which were practically non-identifiable [27] for the lowest response. The parameter profiles can be found in S3 Fig. Additionally, to verify the choice of the 4 parameter model, the best performing 5 parameter candidate model (with parameters *k*1, *k*5, *k*6, *k*8, *k*9) was also evaluated for parameter identifiability. The PLA profiles from the 5 parameter model indicate that *k*9 was structurally non-identifiable in 6 out of 7 representative responses, with further two parameters (*k*6 and *k*8) proving to be non-identifiable in 2 out of 7 cases (S4 Fig).

The model selection pipeline resulted in a model with parameters *k*1, *k*5, *k*6, *k*8 to be estimated from experimental data in personalized models. The selected parameters describe the rate constant of glucose appearance in the gut (*k*1), the

rate constant of insulin-dependent glucose uptake (*k*5), the proportional rate constant of insulin secretion due to the difference in the actual plasma glucose level compared to baseline (*k*6), and the insulin secretion dependent of the rate of change in plasma glucose (*k*8).

## Individual simulation

A population of 738 personalized models were generated *in silico* through estimating the selected parameters on post-load time series of glucose and insulin in participants from the DIOGenes study. To evaluate the success of simulating individual responses, we compared the discrepancy of population specific simulations to that of individualized simulations. The median response was calculated in every group (NGT, IFG, IGT, IFG&IGT, and T2DM) and the selected 4 parameter model was used to simulate the median glucose and insulin trajectories on the calculated responses. The individuals' measured data were then compared to the median simulations per group. The SSRs in the personalized model simulations were substantially lower than those of the median simulations in every group (Table 2), indicating that the personalized models were able to capture a wide range of response curves.

**Table 2. Mean (standard deviation) of sum of squared residuals in the model simulations**

| | NGT | IFG | IGT | IFG&IGT | T2DM |
|---|---|---|---|---|---|
| Group simulation | 149.87 | 213.52 | 205.15 | 153.46 | 195.93 |
| | (153.11) | (205.15) | (134.92) | (126.97) | (181.90) |
| Individual simulation | 32.37 | 44.29 | 35.33 | 43.54 | 36.69 |
| | (36.26) | (32.11) | (47.89) | (29.92) | (33.56) |

The best and worst personalized model simulations by SSR are shown in Fig 4A and 4B, respectively. While the measured glucose and insulin responses ranged from 1.8 to 18.3 mmol/L and from 2.0 to 749.0 mU/L, the simulations show good agreement with the measured data in most cases. To highlight other striking model behavior, additional, hand selected example responses and their corresponding simulations are shown in Fig 4C.

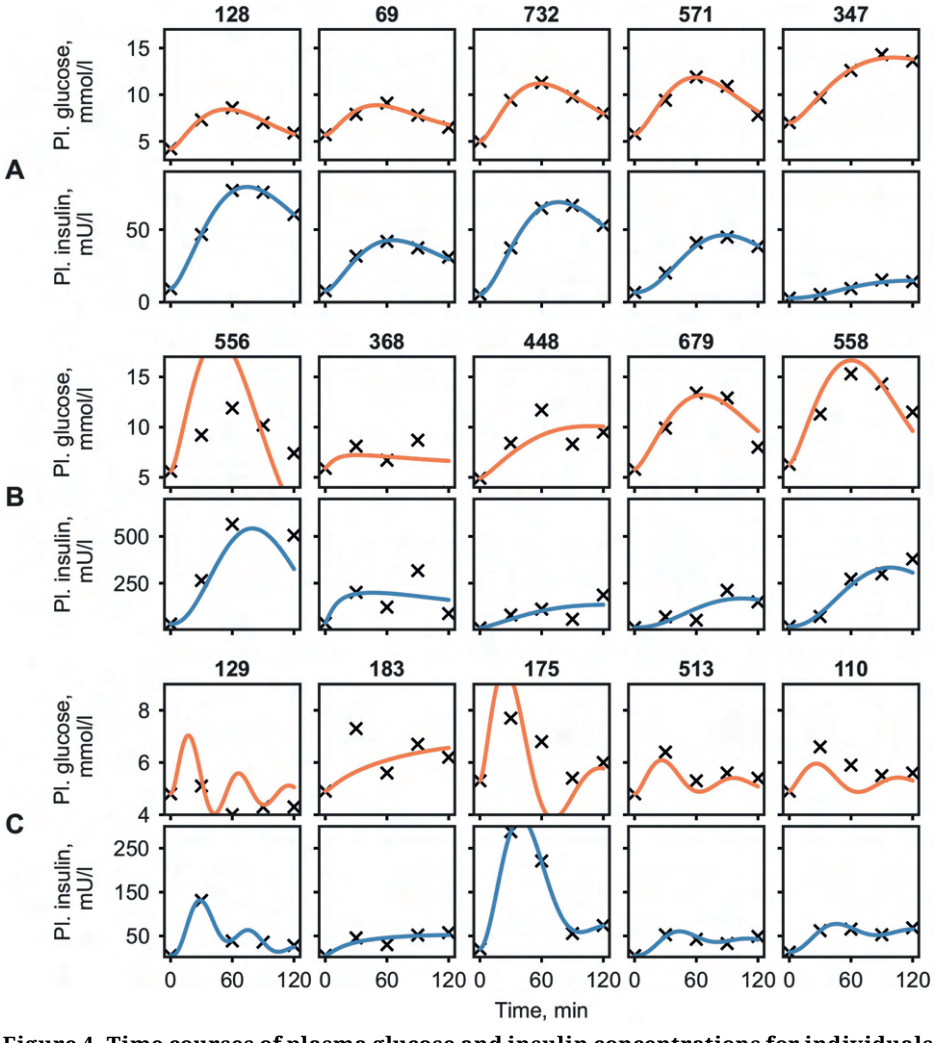


**Figure 4. Time courses of plasma glucose and insulin concentrations for individuals with the lowest and highest simulation error (quantified by the SSR) in each ADA category, and other interesting model behaviour (A, B and C respectively).** Black crosses and orange/blue lines correspond to measurement and model simulation of glucose/insulin, respectively.

In particular, metabolite responses with an intermediate dip between two values were found to be difficult to capture using the 4 parameter model (e.g. participant 183, Fig 4C). However, there were cases of such bi-phasic curves, that the model could replicate accurately (e.g. participant 513, Fig 4C). In some cases, the model predicted a fast response, with a probable peak between the 0 and 30 minute measurements (e.g. participants 129, Fig 4C). Furthermore, the success of simulating complex shapes appeared to depend on the scale of the insulin values

in the responses, where higher insulin values lead to difficulties in accurately fitting the glucose response (e.g. participant 175, Fig 4C).

The distribution of parameter values estimated from individuals' responses are shown by subgroup in Fig 5. In general, the range of estimated parameters was greatest in the group that was NGT according to the ADA diabetes criteria, with values spanning the whole range of the other groups. The rate constant of glucose appearance in the gut ($k1$) was largest in the NGT and IFG groups. Similarly, insulin-dependent glucose uptake ($k5$), and glucose-dependent insulin production ($k6$) were lower in the IGT, IFG&IGT, and T2DM groups compared to the NGT and the IFG groups. The plasma glucose rate of change-dependent insulin production ($k8$) was lower in the IFG&IGT, and T2DM groups compared to the other groups. Additionally, the association of the parameter values with frequently used measures of insulin secretion and insulin resistance were evaluated to assess model structure. Parameters $k6$ and $k8$ associated with the insulinogenic index ($r = 0.56$, $p < 0.001$ and $r = 0.49$, $p < 0.001$, respectively; S7 Fig), a frequently used measure of first-phase insulin secretion [30]. Additionally, parameter $k5$, describing insulin mediated uptake of glucose into the periphery showed a significant positive correlation with the Matsuda index (Pearson $r = 0.68$, $p < 0.001$; S7 Fig).

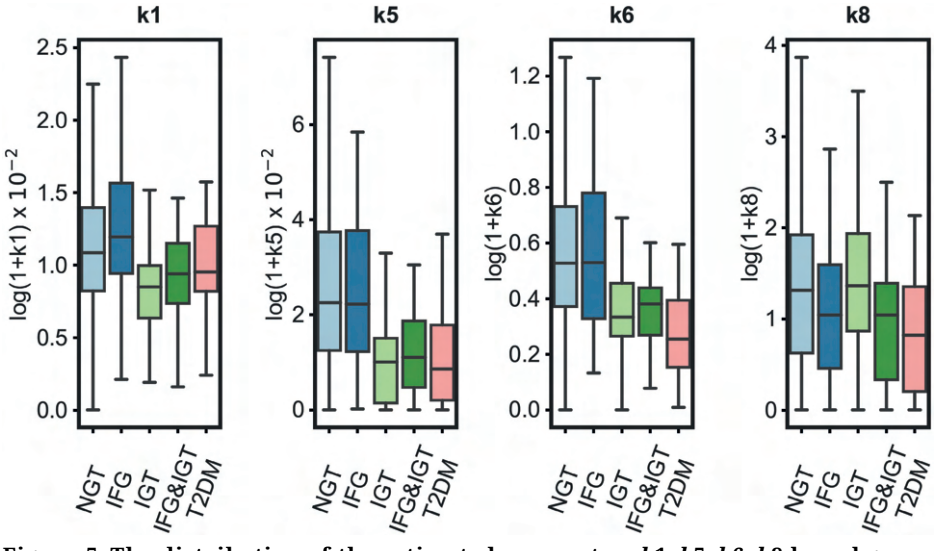


**Figure 5. The distribution of the estimated parameters *k*1, *k*5, *k*6, *k*8 by subgroup based on ADA diabetes criteria.** *k*1—rate constant of glucose appearance in the gut, *k*5—rate constant of insulin-dependent glucose uptake, *k*6—rate constant of insulin secretion proportional to glucose elevation, *k*8—rate constant of insulin secretion by the rate of change in glucose elevation. For details, see S1 Appendix. Observations outside the interquartile range of the $25^{th}$ and $75^{th}$ percentile of each group are visualized in S5 Fig. The boxes represent the 25th and 75th percentiles, the whiskers represent the min, and max values, and the horizontal line represents the median.

A better grasp of the parameter space of the model can be obtained by visualizing it after reducing the four dimensional space to two dimensions via principal component analysis. The personalized models in the resulting space are shown in Fig 6. The unique parameter set in each model defines the model's place in the parameter space, where the model is colored according to the ADA criteria (A) and the participants' Matsuda index (B). The explained variance and the loading vectors indicate that the parameters pertain to distinct mechanisms and retain their functionality (Fig 6B insert). The spread over the first two principal components demonstrate the large heterogeneity in the modelled population. Furthermore, the additional insight gained by the personalized models is illustrated when coloring the parameter space by the ADA criterion for prediabetes and diabetes (Fig 6A). The featured examples highlight the large heterogeneity that remains hidden when considering only the single time-point measures of the diagnosis categories, but is captured by the person specific models. Fig 6B shows examples of participants with different states of insulin sensitivity. The examples positioned along the direction of the loading vectors of *k*5 show responses with increasing insulin sensitivity noted by the rapid

clearance of glucose from plasma (i.e. curve rapidly approaching baseline) as well as lower insulin secretion. Responses of individuals with varying levels of first-phase insulin secretion are shown on S8 Fig with the corresponding models in the parameter space colored by the insulinogenic index. Responses along the loading vectors of both *k*6 and *k*8 indicate increasing first-phase secretion of insulin, with highlighted examples of low (e.g. participant 347) moderate (e.g. participant 693) and high (e.g. participant 51) secretion. Additionally, S9 Fig highlights examples in the parameter space colored by the error in the simulation of the individual as measured by SSR.

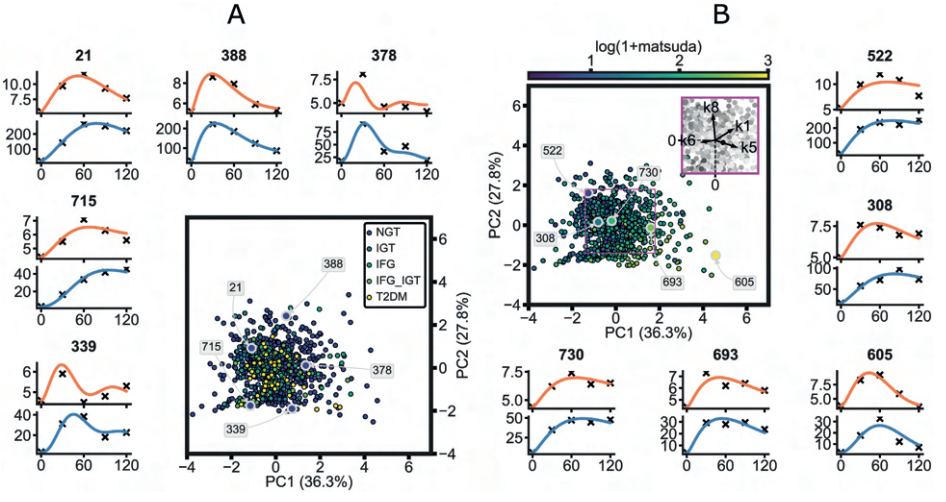


**Figure 6. Individual parameter sets in the parameter space of the model colored by the ADA diabetes criterion (A) and the Matsuda index (B) after reduction to 2d via principal component analysis.** The personalized model simulations of five participants' responses are highlighted (individuals 21, 388, 378, 715, 339 on panel A and 522, 308, 730, 693, 605 on panel B). Orange and blue lines correspond to glucose and insulin model simulation, while crosses represent measured data. The loading vectors of k1, k5, k6, and k8 are shown in the purple insert in panel B.

## DISCUSSION

In this work, we implemented a pipeline to convert a physiological model of the postprandial glucose-insulin dynamics describing population averages into a personalizable model. A key aspect of the parameter selection process was to maintain certainty in the parameter estimates and consequent model predictions by systematically reducing the number of parameters to be estimated in personalized models, taking into account the availability of quantitative data.

Furthermore, our approach allows the comparison of personalized models due to retaining the same model structure across individuals. The protocol does not require biological knowledge and may be generalized to models of other systems. The resulting personalized models were able to accurately describe a wide variety of responses from the DIOGenes data set, a large population of overweight/obese but otherwise healthy individuals. Furthermore, the estimated parameter values of the model allowed mechanistic insight into the differences in individuals' glucose metabolism.

Parameters exhibiting high sensitivity exert a large effect on model outcome, whereas not sensitive parameters may be fixed to a constant value. Sensitivity of the parameters was assessed through their modulatory effect on glucose and insulin concentrations of an average healthy simulation, to keep in line with the study population. Due to the structure of the model, different responses might indicate different parameters to be sensitive, such as the parameter controlling the rate of endogenous glucose production, which is expected to behave differently when the glucose response goes below the basal level. However, in the current study population such behavior is rare (66/738 responses) and thus an average healthy simulation was considered adequate for sensitivity analysis. Following the selection of the sensitive parameters, parsimony and model fit was considered. The ADA group median and extreme responses were chosen to promote the model to be able to fit a wide range of responses. We hypothesize, that these responses are representative of the parameter space that we aim to capture with the model. Thus, if the model is able to capture these responses accurately, it is likely to be able to simulate arbitrary responses in intermediate states as well. In order to impose a criterion towards parsimony, we used the AIC to introduce a penalty term on the number of parameters in the model. As shown in S2 Table, candidate models with more parameters had a lower SSR. However, the top 5 and 6 parameter models performed only marginally better than the 4 parameter ones, with a SSR of 37.02, 35.20, 41.39 respectively. The best scoring 3 parameter model ($k1$, $k5$, $k9$) had more than twice the SSR (87.00) of the best 4 parameter model. Based on the AIC, the 4 parameter candidate model containing parameters $k1$, $k5$, $k6$ and $k8$ to be estimated was selected as the most parsimonious model. Finally, the identifiability of the candidate model was examined via PLA on the representative median and extreme responses. Besides the smallest response, PLA profiles showed that the parameters were identifiable (S3 Fig) indicating that a unique solution exists in the tested range.

The parameters identified in the model selection process indicate that the most discriminating processes in this population are transition of glucose from the stomach to the gut ($k1$), the insulin-dependent glucose uptake to the periphery ($k5$), and the processes representative of insulin secretion ($k6$ and $k8$). It is known that gastric emptying is a major determinant of postprandial glycemia that has been shown to exhibit large intra- and interindividual variability [31, 32]. The decline in insulin mediated glucose disposal into tissues such as the muscle, liver or adipose tissue is acknowledged as one of the key process leading to the development of T2DM [15]. Furthermore, defects in the first phase insulin secretion are known to appear in the early stages of deteriorating glucose control compared to abnormalities in second phase insulin secretion, which is more prevalent in advanced stages of T2DM [33]. The ability to potentially quantify these otherwise difficult to measure processes from time-series of postprandial glucose and insulin using a computation model may prove incredibly useful in the advent of personalized medicine and targeted nutritional interventions.

Following the identification of the model structure to be personalized, we elected to generate our population of personalized models by fitting the model to the individuals' corresponding meal response data via maximum likelihood estimation (MLE) while fixing other parameters to population averages. Here, it is important to note that, approaches such as non-linear mixed effects modelling, where population and individual level dynamics are estimated simultaneously, may provide a valuable alternative to our approach [34, 35]. In addition, future applications may benefit from integrating regularization in the MLE as proposed by Dolejsch et al. [36].

The personalized models showed a 4-5 fold decrease in SSR in all groups compared to group simulations, confirming that the model personalization was successful, as well as re-enforcing the need for a personalized approach when assessing such dynamic responses. A good accordance with data was further confirmed by visually inspecting the model output (Fig 3 and S6 Fig). However, the SSR does not always give a realistic overview of the model fit, for instance, it can be susceptible to bias towards responses with extreme glucose and especially insulin values. Thus, to further highlight the limits of the model, a manual selection of responses and corresponding model simulations were shown in Fig 4C. The model frequently struggled with accurately predicting an intermediate dip in the glucose response (e.g. participant 183, Fig 4C). The more complex bi-phasic shapes were only accurately modelled in a few cases (e.g. participants 513, Fig 4C), although it is thought that, this lack of fit could be avoided by estimating

additional parameters. Responses with high insulin values drove the model to fail at accurately capturing the glucose response. This is partly due to the combined glucose and insulin error function used in model fitting, in which insulin values were multiplied by 0.1 to account for the difference in scale compared to glucose. However, in case of extremely high insulin responses, the insulin values are still favored during the optimization (e.g. participants 175, 556, Fig 4B and 4C). By estimating additional glucose parameters, such as the parameter handling endogenous glucose production ($k3$), these responses might be captured more accurately. Additionally, in some cases where the glucose levels quickly returned below the basal value the model exhibited oscillatory behaviour (e.g. participants 129, Fig 4C). This may originate from the parameter estimates relating to the insulin secretion term in the model, however further examination of this was outside the scope of the current study. Furthermore, it is worth noting that the outlying parameter estimates not necessarily indicate erroneous simulations but rather unusual or extreme responses as can be seen on Fig 6, S8 and S9 Figs.



Each of the 738 personalized models contain a unique parameter set pertaining to the physiological state of the participant's glucose homeostasis. The largest range for all of the estimated parameters was found in the NGT group, which could partly be explained due to the data set containing more normo-glycemic individuals (see Table 1) resulting in a larger variability. Furthermore, normo-glycemic individuals are also known to be more likely to exhibit bi-phasic responses [11], raising the variability of responses, and thereby the range of estimated parameters values in this category. In addition, the groupings defined by the ADA criteria only consider the fasting and 2h plasma glucose values while ignoring the insulin levels. Thus, individuals that exhibit normal glucose levels at the fasting and 2h time-points due to unusually high insulin values still end up in the NGT group. This lack of consideration for the dynamics and insulin values make it difficult to detect early deterioration in individuals' responses indicative of insulin resistance. However, taking into account the complete dynamics of both glucose and insulin the personalized models outlined here are able to indicate such transitions before they are detected by steady state or single time-point measures (e.g. 221, 522 Fig 6). By screening for the parameter estimates of $k6$ and $k8$ one can identify cases where the glucose response appears normoglycemic, however the insulin levels are abnormally high.

Variation in gastric emptying linked to obesity has been previously reported, however we found no difference in the parameter estimates for $k1$ between overweight and obese participants as well as no association between the

parameter $k1$ and BMI [37]. Importantly, the model parameters corresponding to insulin secretion ($k6$, $k8$) were found to be lower for individuals with more severe metabolic conditions (IGT, IFG&IGT, T2DM). The insulin secretion parameters also showed a significant association with the insulinogenic index, a frequently used measure of insulin secretion. While the parameter controlling the insulin-dependent glucose uptake $k5$ was lower in IGT, IFG&IGT and T2DM compared to the other groups and showed a significant association with the Matsuda index. These findings reinforce that the model structure captures relevant features of the insulin mediated glucose homeostasis and the personalized models can distinguish between divergent impairments in the insulin regulated glucose control. Therefore, our modelling framework might prove beneficial in revealing nuanced behaviour specifically for the early detection of decline in the glucose homeostasis from a standard five time-point OGTT. Moreover, the personalized models may be used to assess the effects of lifestyle and diet interventions, where the observed effects can be quite subtle. Our results also highlights the possibility of using such an approach to generate cohorts of virtual patients with varying glucose homeostasis for potential *in silico* testing.

The population in the study may be considered relatively homogeneous in terms of glucose homeostasis, as measured by current single time-point measures such as the ADA criterion. However, the personalized models utilizing the dynamic, intertwined plasma glucose and insulin responses of individuals, allowed the quantification of an immense heterogeneity in the responses even within the ADA groups. Furthermore, the mechanistic nature of the model promotes the identification and allows comparison of distinctive processes underlying individuals' metabolic health. We believe that such personalized modelling approaches will be essential in advancing personalized nutrition.

## CONCLUSION

The systematic model selection pipeline implemented in this work allows the personalization of a mathematical model through reducing the number of parameters to be estimated in personalized models. The approach results in the most parsimonious model that contains identifiable parameters. The selection pipeline is generalizable in the sense, that it does not require biological insight to implement, therefore it may be applied to other systems or models to gain insight on the individual level. The E-DES model, a computational model of the human glucose-insulin system, was personalized using the approach and

subsequently a population of personalized models were simulated from a large data set of overweight/obese but otherwise healthy individuals. The personalized models, consisting of only four parameters estimated from experimental data were capable of simulating a wide variety of postprandial glucose and insulin responses to a standard OGTT from the DIOGenes data set. Taking advantage of a frequently sampled time-series of both glucose and insulin the dynamic models were able to capture a large, previously overlooked heterogeneity in the population. The mechanistic aspect of the model allows the description and comparison of the physiological state of the individuals' glucose homeostasis and provide mechanistic insight into the glycemic variability observed in the responses.

## REFERENCES


1. van Ommen B, van der Greef J, Ordovas JM, Daniel H. *Phenotypic flexibility as key factor in the human nutrition and health relationship*. Genes & Nutrition. 2014;**9**(5):423. pmid:25106484
2. Tabák AG, Herder C, Rathmann W, Brunner EJ, Kivimäki M. *Prediabetes: a high-risk state for diabetes development*. The Lancet. 2012;**379**(9833):2279–2290. pmid:22683128
3. Meng H, Matthan NR, Ausman LM, Lichtenstein AH. *Effect of macronutrients and fiber on postprandial glycemic responses and meal glycemic index and glycemic load value determinations*. The American Journal of Clinical Nutrition. 2017;**105**(4):842–853. pmid:28202475
4. Zeevi D, Korem T, Zmora N, Israeli D, Rothschild D, Weinberger A, et al. *Personalized Nutrition by Prediction of Glycemic Responses*. Cell. 2015;**163**(5):1079–1094. pmid:26590418
5. Astrup A, Hjorth MF. *Classification of obesity targeted personalized dietary weight loss management based on carbohydrate tolerance*. European Journal of Clinical Nutrition. 2018;**72**(9):1300–1304. pmid:30185850
6. Berry SE, Valdes AM, Drew DA, Asnicar F, Mazidi M, Wolf J, et al. *Human postprandial responses to food and potential for precision nutrition*. Nature Medicine. 2020.
7. Potteiger J, Jacobsen D, Donnelly J. *A comparison of methods for analyzing glucose and insulin areas under the curve following nine months of exercise in overweight adults*. International Journal of Obesity. 2002;**26**(1):87–89. pmid:11791151
8. Tschritter O, Fritsche A, Shirkavand F, Machicao F, Haring H, Stumvoll M. *Assessing the Shape of the Glucose Curve During an Oral Glucose Tolerance Test*. Diabetes Care. 2003;**26**(4):1026–1033. pmid:12663568
9. Tura A, Morbiducci U, Sbrignadello S, Winhofer Y, Pacini G, Kautzky-Willer A. *Shape of glucose, insulin, C-peptide curves during a 3-h oral glucose tolerance test: any relationship with the degree of glucose tolerance*? American Journal of Physiology-Regulatory, Integrative and Comparative Physiology. 2011;**300**(4):R941–R948. pmid:21248305
10. Frøslie KF, Røislien J, Qvigstad E, Godang K, Bollerslev J, Voldner N, et al. *Shape information from glucose curves: Functional data analysis compared with traditional summary measures*. BMC Medical Research Methodology. 2013;**13**(1). pmid:23327294
11. Cheng X, Yang N, Li Y, Sun Q, Qiu L, Xu L, et al. *The shape of the glucose response curve during an oral glucose tolerance test heralds β–cell function in a large Chinese population*. BMC Endocrine Disorders. 2019;**19**(1):119. pmid:31690291
12. Matthews DR, Hosker JP, Rudenski AS, Naylor BA, Treacher DF, Turner RC. *Homeostasis model assessment: insulin resistance and beta-cell function from fasting plasma glucose and insulin concentrations in man.* Diabetologia. 1985;**28**(7):412–419. pmid:3899825
13. Matsuda M, DeFronzo RA. *Insulin sensitivity indices obtained from oral glucose tolerance testing: comparison with the euglycemic insulin clamp*. Diabetes Care. 1999;**22**(9):1462–1470. pmid:10480510
14. Blaak EE. *Current metabolic perspective on malnutrition in obesity: towards more subgroup-based nutritional approaches?* Proceedings of the Nutrition Society. 2020; p. 1–7.

15. Roden M, Shulman GI. *The integrative biology of type 2 diabetes. Nature*. 2019;**576**(7785):51–60. pmid:31802013
16. Abdul-Ghani MA, Matsuda M, Balas B, DeFronzo RA. *Muscle and Liver Insulin Resistance Indexes Derived From the Oral Glucose Tolerance Test*. Diabetes Care. 2007;**30**(1):89–94. pmid:17192339
17. Blanco-Rojo R, Alcala-Diaz JF, Wopereis S, Perez-Martinez P, Quintana-Navarro GM, Marin C, et al. *The insulin resistance phenotype (muscle or liver) interacts with the type of diet to determine changes in disposition index after 2 years of intervention: the CORDIOPREV-DIAB randomised clinical trial. Diabetologia*. 2016;**59**(1):67–76. pmid:26474775
18. O'Donovan SD, Lenz M, Goossens GH, van der Kallen CJH, Eussen SJMP, Stehouwer CDA, et al. *Improved quantification of muscle insulin sensitivity using oral glucose tolerance test data: the MISI Calculator*. Scientific Reports. 2019;**9**(1):9388. pmid:31253846
19. Hulman A, Witte DR, Vistisen D, Balkau B, Dekker JM, Herder C, et al. *Pathophysiological Characteristics Underlying Different Glucose Response Curves: A Latent Class Trajectory Analysis From the Prospective EGIR-RISC Study*. Diabetes Care. 2018;**41**(8):1740–1748. pmid:29853473
20. Bergman RN, Ider YZ, Bowden CR, Cobelli C. *Quantitative estimation of insulin sensitivity*. The American journal of physiology. 1979;**236**(6):E667–677. pmid:443421
21. Silber HE, Frey N, Karlsson MO. *An Integrated Glucose-Insulin Model to Describe Oral Glucose Tolerance Test Data in Healthy Volunteers*. The Journal of Clinical Pharmacology. 2010;**50**(3):246–256. pmid:19940230
22. Dalla Man C, Rizza RA, Cobelli C. *Meal Simulation Model of the Glucose-Insulin System*. IEEE Transactions on Biomedical Engineering. 2007;**54**(10):1740–1749. pmid:17926672
23. Maas AH, Rozendaal YJW, van Pul C, Hilbers PAJ, Cottaar WJ, Haak HR, et al. *A Physiology-Based Model Describing Heterogeneity in Glucose Metabolism: The Core of the Eindhoven Diabetes Education Simulator (E-DES)*. Journal of Diabetes Science and Technology. 2015;**9**(2):282–292. pmid:25526760
24. Maas AH. *Playing with numbers: the development of an educational diabetes game*. Technische Universiteit Eindhoven; 2017.
25. Kreutz C, Raue A, Kaschek D, Timmer J. *Profile likelihood in systems biology*. FEBS Journal. 2013;**280**(11):2564–2571. pmid:23581573
26. Raue A, Kreutz C, Maiwald T, Bachmann J, Schilling M, Klingmüller U, et al. *Structural and practical identifiability analysis of partially observed dynamical models by exploiting the profile likelihood. Bioinformatics*. 2009;**25**(15):1923–1929. pmid:19505944
27. Vanlier J, Tiemann CA, Hilbers PAJ, van Riel NAW. *Parameter uncertainty in biochemical models described by ordinary differential equations*. Mathematical Biosciences. 2013;**246**(2):305–314. pmid:23535194
28. Larsen TM, Dalskov S, Van Baak M, Jebb S, Kafatos A, Pfeiffer A, et al. *The Diet, Obesity and Genes (Diogenes) Dietary Study in eight European countries—a comprehensive design for long-term intervention*. Obesity Reviews. 2010;**11**(1):76–91. pmid:19470086
29. American Diabetes Association. *2. Classification and Diagnosis of Diabetes*. Diabetes Care. 2015;**38**(Supplement_1):S8–S16.

30. Yeckel CW, Weiss R, Dziura J, Taksali SE, Dufour S, Burgert TS, et al. *Validation of Insulin Sensitivity Indices from Oral Glucose Tolerance Test Parameters in Obese Children and Adolescents*. The Journal of Clinical Endocrinology & Metabolism. 2004;**89**(3):1096–1101. pmid:15001593
31. Marathe CS, Rayner CK, Jones KL, Horowitz M. *Relationships Between Gastric Emptying, Postprandial Glycemia, and Incretin Hormones. Diabetes Care*. 2013;**36**(5):1396–1405. pmid:23613599
32. Grimm M, Koziolek M, Kühn JP, Weitschies W. *Interindividual and intraindividual variability of fasted state gastric fluid volume and gastric emptying of water*. European Journal of Pharmaceutics and Biopharmaceutics. 2018;127:309–317. pmid:29522898
33. Seino S, Shibasaki T, Minami K. *Dynamics of insulin secretion and the clinical implications for obesity and diabetes. Journal of Clinical Investigation*. 2011;**121**(6):2118–2125. pmid:21633180
34. P Denti, A Bertoldo, P Vicini, C Cobelli. *Nonlinear Mixed Effects to Improve Glucose Minimal Model Parameter Estimation: A Simulation Study in Intensive and Sparse Sampling*. IEEE Transactions on Biomedical Engineering. 2009;**56**(9):2156–2166.
35. Fröhlich F, Reiser A, Fink L, Woschée D, Ligon T, Theis FJ, et al. *Multi-experiment nonlinear mixed effect modeling of single-cell translation kinetics after transfection*. npj Systems Biology and Applications. 2018;**4**(1):42. pmid:30564456
36. Dolejsch P, Hass H, Timmer J. *Extensions of l1 regularization increase detection specificity for cell-type specific parameters in dynamic models*. BMC Bioinformatics. 2019;**20**(1):395. pmid:31311516
37. Oberoi A, Giezenaar C, Jensen C, Lange K, Hausken T, Jones KL, et al. *Acute effects of whey protein on energy intake, appetite and gastric emptying in younger and older, obese men*. Nutrition & Diabetes. 2020;**10**(1):37. pmid:33004790

## SUPPLEMENTARY MATERIAL

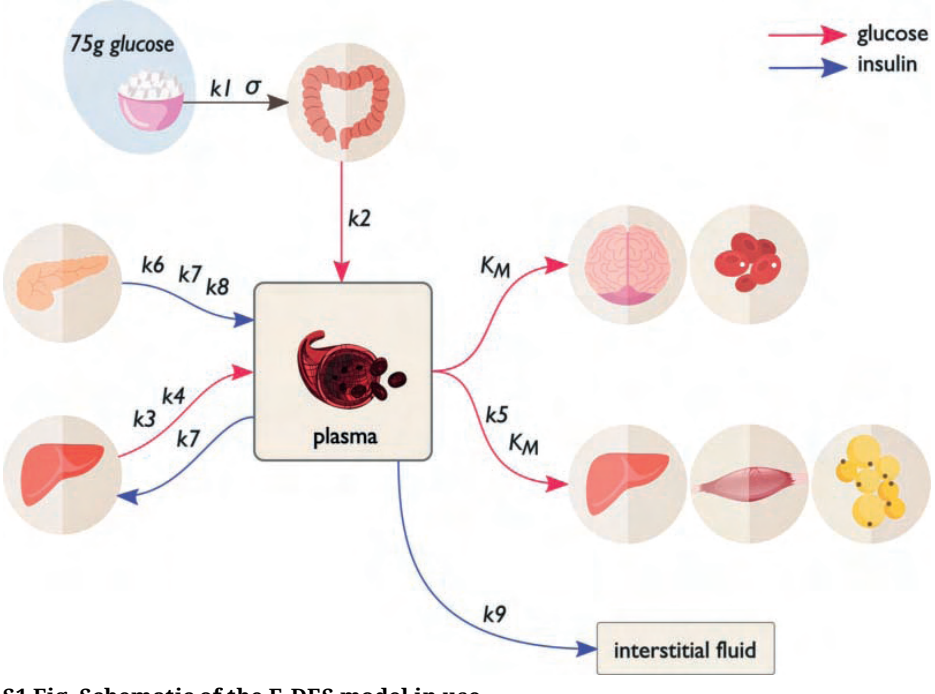


**S1 Fig. Schematic of the E-DES model in use**

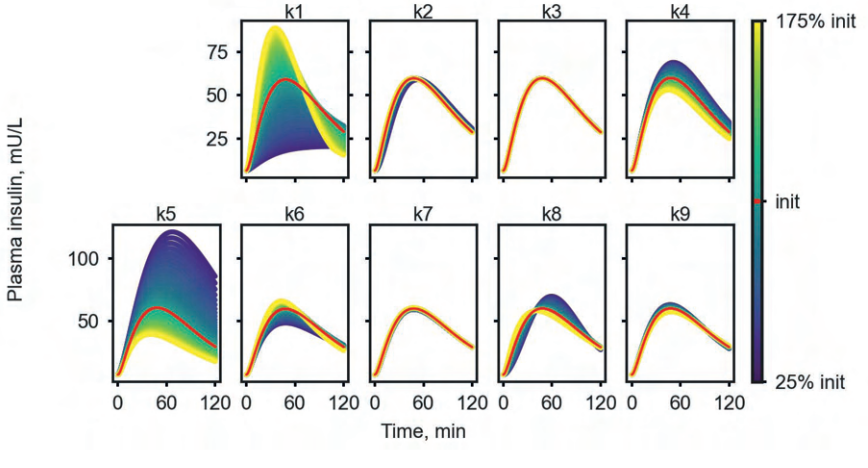


**S2 Fig. Local parameter sensitivity analysis on the simulated plasma insulin response**

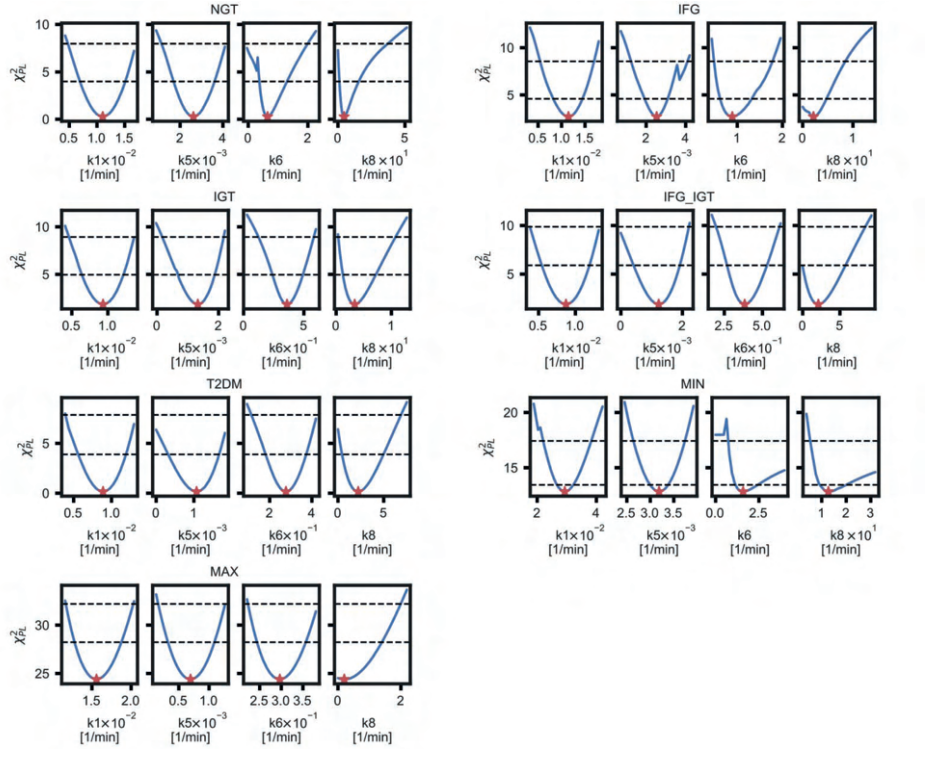


**S3 Fig. Profile Likelihood Analysis results of the 4 parameter model (*k*1, *k*5, *k*6, *k*8) on the median NGT, IFG, IGT, IFG&IGT, T2DM, min and max responses.** The red star indicates the SSR of the model fitted using the optimal parameter values estimated from data, while the blue line corresponds to the error as the other parameter values are being re-estimated after adjusting the parameter value iteratively. The dashed lines indicate confidence intervals where the degrees of freedom equals one (lower), and the number of parameters (upper), respectively.

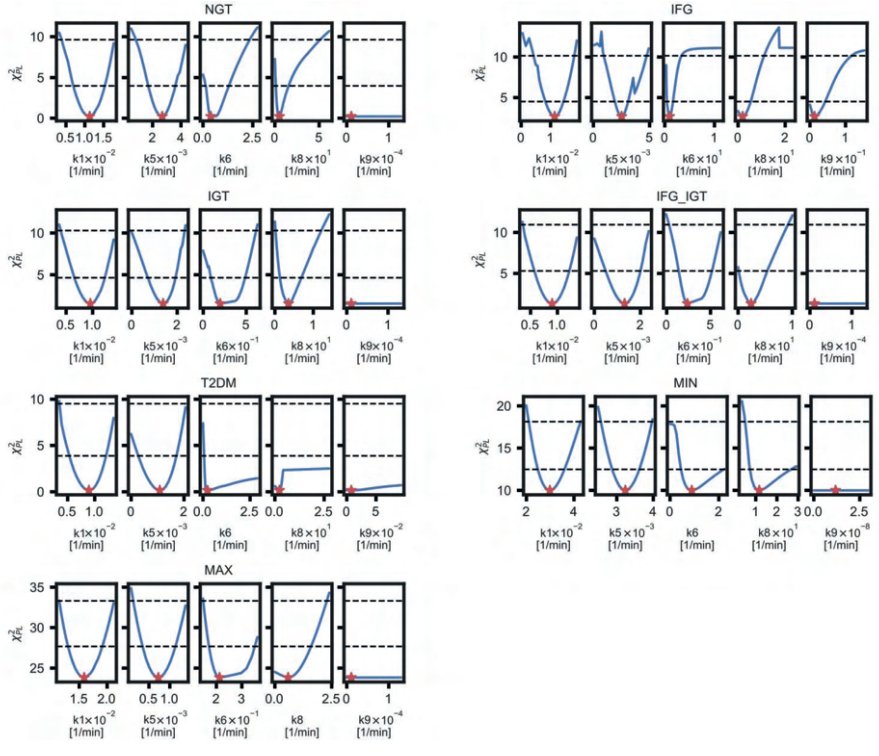


**S4 Fig. Profile Likelihood Analysis results of the 5 parameter model (*k*1, *k*5, *k*6, *k*8, *k*9) on the median NGT, IFG, IGT, IFG&IGT, T2DM, min and max responses**. The red star indicates the SSR of the model fitted using the optimal parameter values estimated from data, while the blue line corresponds to the error as the other parameter values are being re-estimated after adjusting the parameter value iteratively. The dashed lines indicate confidence intervals where the degrees of freedom equals one (lower), and the number of parameters (upper), respectively.

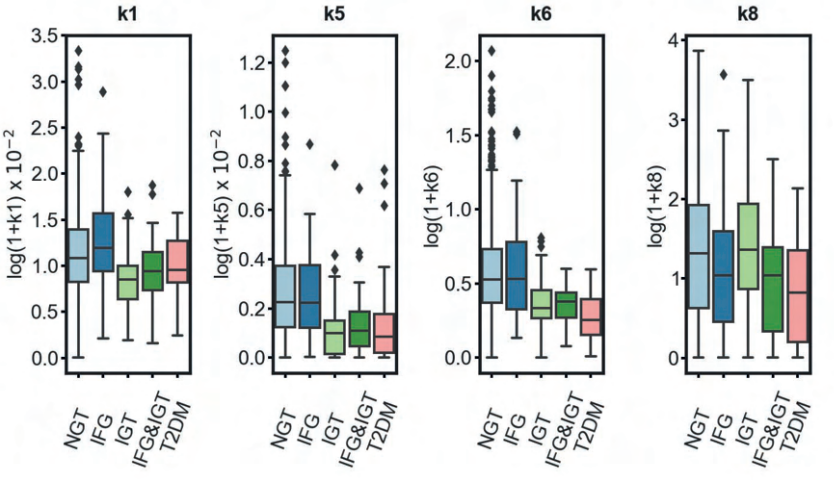


**S5 Fig. The distribution of parameters *k*1, *k*5, *k*6, *k*8 by subgroup (based on ADA diabetes criteria) with the outliers highlighted.** The boxes represent the 25th and 75th percentiles, the whiskers represent the min, and max values, and the horizontal line represents the median.

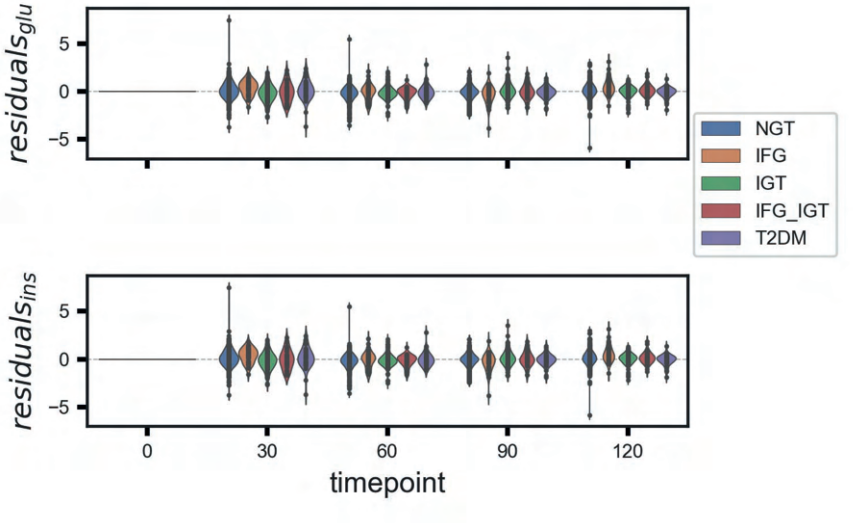


**S6 Fig. Pooled residuals in the personalized models per time-point per metabolite, colored by the ADA prediabetes and diabetes diagnosis criteria.**

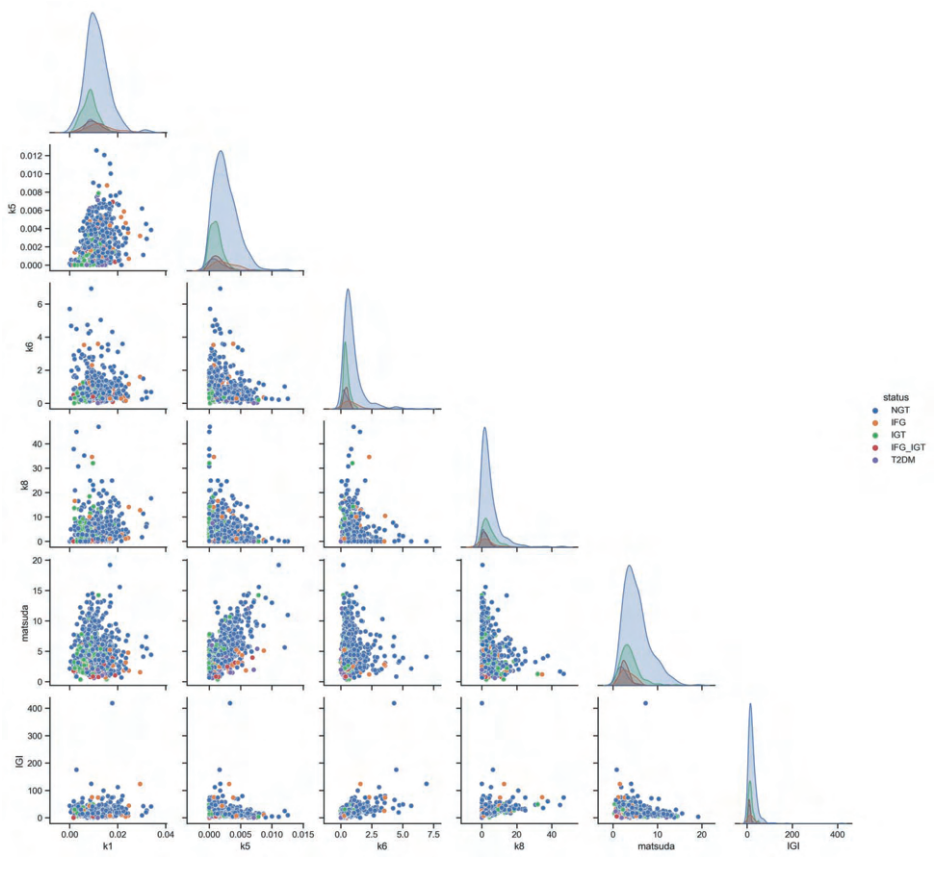


**S7 Fig. Pairwise scatter plots and density plots of the personalized model parameters, the Insulinogenic index and the Matsuda index from the DIOGenes study colored by the ADA prediabetes and diabetes diagnosis criteria.**

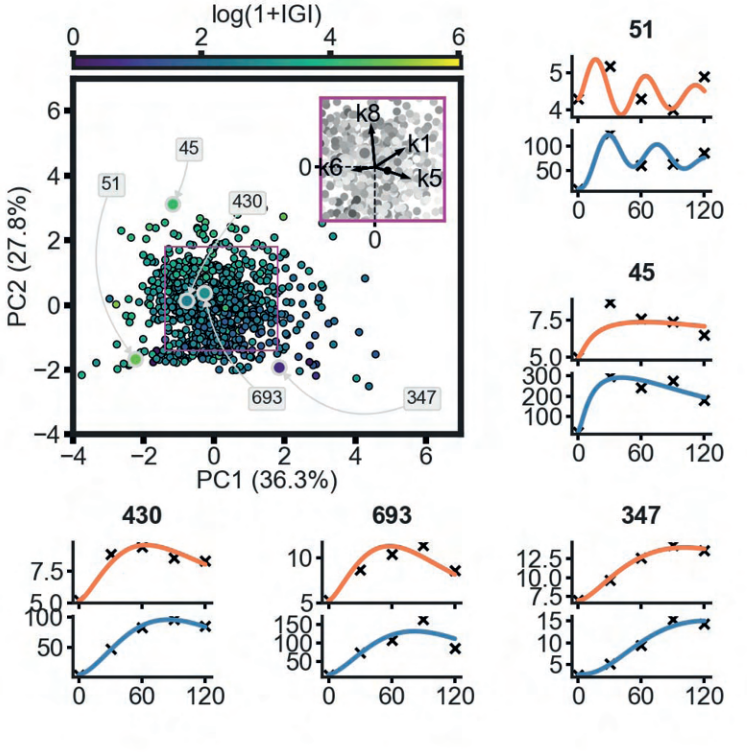


**S8 Fig. Personalized models colored by the Insulinogenic index in the parameter space of the model after reduction to 2d via principal component analysis.** The personalized model simulations of five participants with varying first-phase insulin secretion are highlighted (individuals 51, 45, 347, 430, 693). Orange and blue lines correspond to plasma glucose and insulin model simulation, while crosses represent measured data.

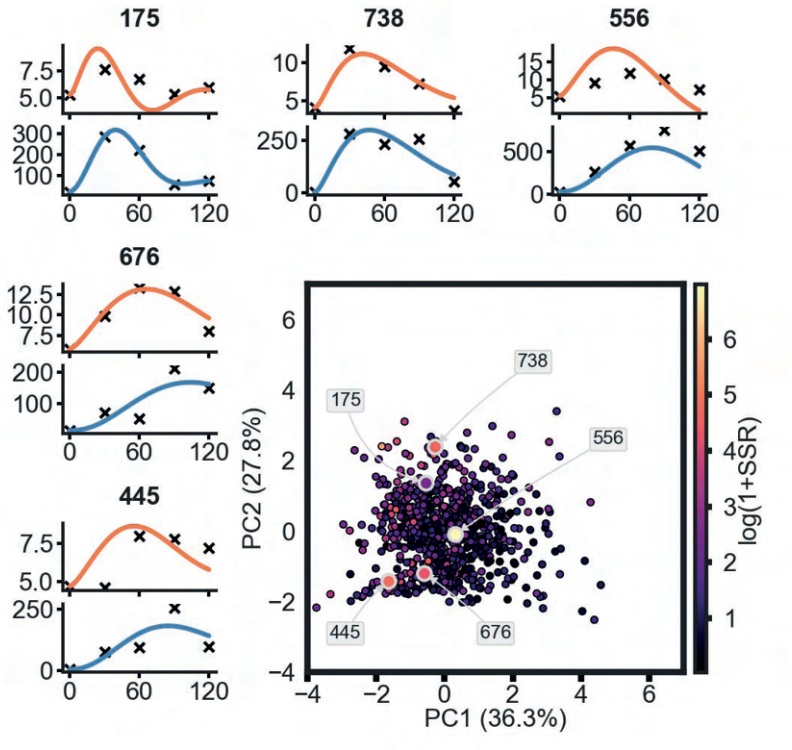


**S9 Fig. Personalized models colored by SSR in the parameter space of the model after reduction to 2d via principal component analysis.** The personalized model simulations of five participants with varying first-phase insulin secretion are highlighted (individuals 175, 738, 556, 676, 445). Orange and blue lines correspond to plasma glucose and insulin model simulation, while crosses represent measured data.

**S1 Table: Criteria for prediabetes and diabetes classification used in this study.** Based on the standard two hour OGTT by the American Diabetes Association [1].

| Group[1] | Fasting plasma glucose | 2hr plasma glucose |
|---|---|---|
| IFG | 5.6 – 6.9 mmol/L | - |
| IGT | - | 7.8 – 11.0 mmol/L |
| IFG&IGT | 5.6 – 6.9 mmol/L | 7.8 – 11.0 mmol/L |
| T2DM | 7.0 mmol/L ≤ | 11.1 mmol/L ≤ |

[1]IFG: impaired fasting glucose, IGT: impaired glucose tolerant, T2DM: type 2 diabetes mellitus

[1] American Diabetes Association. 2. Classification and Diagnosis of Diabetes. Diabetes Care. 2015;38(Supplement_1):S8– S16. doi:10.2337/dc15-S005.

**S2 Table: Results of step two of the model selection approach.** Sum of squared residuals (SSR) and Akaike Information Criterion (AIC) of the ten best performing candidate models.

| Rank | Estimated parameters | SSR | AIC |
|---|---|---|---|
| 1 | $k1$, $k5$, $k6$, $k8$ | 41.39 | 20.44 |
| 2 | $k1$, $k5$, $k8$, $k9$ | 44.46 | 20.94 |
| 3 | $k1$, $k5$, $k6$, $k8$, $k9$ | 37.02 | 21.66 |
| 4 | $k1$, $k4$, $k5$, $k6$, $k8$ | 39.15 | 22.05 |
| 5 | $k1$, $k4$, $k5$, $k8$, $k9$ | 42.57 | 22.64 |
| 6 | $k1$, $k4$, $k5$, $k6$, $k8$, $k9$ | 35.20 | 23.31 |
| 7 | $k1$, $k5$, $k9$ | 87.00 | 23.64 |
| 8 | $k1$, $k5$, $k6$ | 89.75 | 23.86 |
| 9 | $k1$, $k5$, $k6$, $k9$ | 67.94 | 23.91 |
| 10 | $k5$, $k6$, $k8$ | 93.84 | 24.17 |

**S1 Appendix:** E-DES model structure, fluxes, inputs, parameters and constants is available online at https://doi.org/10.1371/journal.pcbi.1008852.s010

**S2 Appendix:** MATLAB implementation of the model used in the manuscript is available online at https://doi.org/10.1371/journal.pcbi.1008852.s011 (Zip, 110KB)

# E-DES-PROT: A novel computational model to describe the effects of amino acids and protein on postprandial glucose and insulin dynamics in humans

# 4

**Bart van Sloun, Gijs H. Goossens, Balázs Erdõs, Shauna D. O'Donovan, Cécile M. Singh-Povel , Jan M.W. Geurts, Natal A.W. van Riel and Ilja C.W. Arts**

*iScience. 2023 Feb 18:26(3):106218*

## SUMMARY

Current computational models of whole-body glucose homeostasis describe physiological processes by which insulin regulates circulating glucose concentrations. While these models perform well in response to oral glucose challenges, interaction with other nutrients that impact postprandial glucose metabolism, such as amino acids (AAs), are not considered. Here, we developed a computational model of the human glucose-insulin system, which incorporates the effects of AAs on insulin secretion and hepatic glucose production. This model was applied to postprandial glucose and insulin time-series data following different AA challenges (with and without co-ingestion of glucose), dried milk protein ingredients, and dairy products. Our findings demonstrate that this model allows accurate description of postprandial glucose and insulin dynamics and provides insight into the physiological processes underlying meal responses. This model may facilitate the development of computational models that describe glucose homeostasis following the intake of multiple macronutrients, whilst capturing relevant features of an individual's metabolic health.

## INTRODUCTION

Glucose homeostasis is primarily regulated by the hormones insulin and glucagon, which act in antagonistic fashion to maintain circulating glucose concentrations within a healthy range (Qaid and Abdelrahman, 2016; Röder et al., 2016). When glucose concentrations are elevated (i.e. following meal intake), pancreatic β-cells secrete insulin to suppress hepatic glucose output and promote glucose uptake in peripheral organs, predominantly in the skeletal muscle (Chadt and Al-Hasani, 2020). In contrast, when glucose concentrations drop (i.e. during fasting or physical exercise), pancreatic α-cells secrete glucagon to stimulate glycogen breakdown and gluconeogenesis (formation of glucose from non-carbohydrate precursors), allowing glucose release from the liver into the circulation, thereby preventing hypoglycemia (Rix et al., 2015). As such, glucagon and insulin exert opposing actions on glucose metabolism and are part of a tightly-regulated feedback system to maintain glucose homeostasis.



Computational models of whole-body glucose homeostasis describe and incorporate the current mechanistic understanding of insulin-mediated regulation of circulating glucose concentrations (Bergman et al., 1979; Dalla Man et al., 2007; Maas et al., 2015). These processes are represented by model parameters, which can be estimated from postprandial time-series data without requiring direct invasive measurements. One of the earliest computational glucose models, the Bergman minimal model (Bergman *et al.*, 1979), was able to determine *insulin sensitivity* (i.e. the capability of insulin to suppress hepatic glucose output and increase glucose disposal in insulin-sensitive tissues) and *glucose effectiveness* (i.e. the ability of glucose to enhance its own disposal at basal insulin levels) in response to an intravenous glucose tolerance test. The Bergman minimal model formed the basis of the Food and Drug Administration approved glucose-insulin model by Dalla Man and colleagues (Dalla Man *et al.*, 2007; Kovatchev et al., 2009), which is used for *in silico* simulation and testing of insulin pump systems. The Dalla Man model has been parameterized using triple tracer glucose data to allow quantification of glucose fluxes between tissues.

The Eindhoven-Diabetes Education Simulator (E-DES), a multi-compartmental ordinary differential equation model, has been used to describe glucose dynamics following a glucose challenge in healthy individuals as well as patients with type 1 and type 2 diabetes (Maas, 2017; Maas *et al.*, 2015; Rozendaal et al., 2018). We have previously individualized the E-DES model to allow accurate description of individual postprandial responses compared to population-based

models, demonstrating it is capable of providing mechanistic insight into glucose homeostasis of individuals (Erdős et al., 2021). Whilst the E-DES model performs very well in response to an oral glucose challenge, modelling the response to more complex meals is still challenging because these contain fat and protein, which also influence glucose homeostasis.

Dietary protein consists of amino acids (AAs) which are used for synthesis of body protein and of nitrogen-containing compounds, such as creatine, peptide hormones, and several neurotransmitters (Case et al., 2011). AAs have been shown to influence glucose metabolism by inducing insulin secretion to facilitate AA uptake and incorporation into protein in muscle tissue, and secreting glucagon to enhance hepatic AA uptake, production of ketone bodies from AAs, and formation of glucose from AAs (i.e. gluconeogenesis) (Qaid and Abdelrahman, 2016; Rix *et al.*, 2015). In a systematic review, we have recently summarized available studies describing postprandial glucose and insulin responses to AAs (van Sloun et al., 2020).

In the present study, we aimed to extend an existing computational model of the glucose-insulin regulatory system to account for the postprandial effects of AAs. To parameterize the model, we used time-series data of postprandial AA, glucose and insulin concentrations following AA challenges (with and without glucose), dried milk protein ingredients, and dairy products, derived both from a previously performed randomized, single-blind crossover trial (Horstman et al., 2021) as well as data extracted from available literature (van Sloun *et al.*, 2020). Here, we show that this novel model, which we termed E-DES-PROT, accurately describes postprandial glucose and insulin dynamics, outperforms the original E-DES model and allows insight into the physiological processes underlying meal responses.

## RESULTS

### Postprandial simulation of AA, glucose, and insulin dynamics following AA challenges and intake of protein ingredients

We investigated whether our newly developed model was able to capture AA and protein challenges, estimating only the model parameters accounting for AAs ($k11$-$k13$). The parameters pertaining to the original E-DES model were kept to their healthy average population value and the measured plasma AA

concentration (pertaining to the challenge) were interpolated and provided to the model as an input (Rozendaal *et al.*, 2018).

The simulated glucose and insulin responses, parameterized on the AA challenges (1 mmol/kg body weight) are shown in Figure S1. The simulated glucose and insulin responses, parameterized on the milk protein ingredients (i.e. WPC, MCI) containing 25g of protein in a 700mL solution, are shown in Figure 1. Here, the leftmost column pertains to the average population responses, whereas the other columns show selected individual responses highlighting striking model behavior. The complete overview of all the individual glucose and insulin responses is shown in Supplemental Section S1.

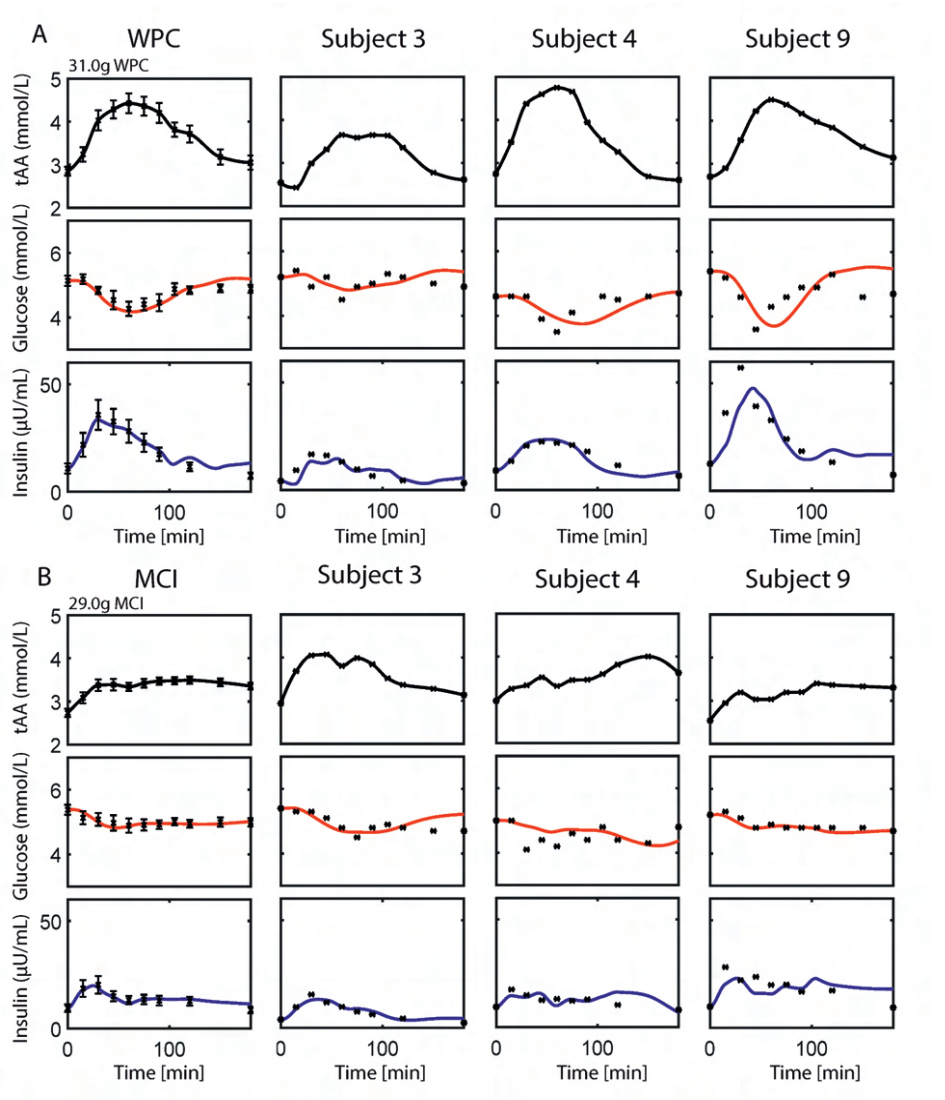


**Figure 1. Plasma glucose and insulin simulation following intake of whey protein concentrate (WPC) and micellar casein isolate (MCI) in the average healthy study population and selected individuals**. The model parameters pertaining to amino acids (AAs, *k*11-*k*13) were estimated, whereas the other model parameters were kept to their original population value. The tAA input is shown in black (data and polynomial interpolation). The simulated glucose and insulin concentrations are shown in red and blue, respectively. The measured concentrations, obtained from (Horstman *et al.*, 2021), are shown as black asterisks with corresponding standard errors of the means. The leftmost column in panel A & B pertains to average study population, whereas the other columns represent selected individuals.

Visual inspection of the plasma glucose and insulin simulations following the AA challenges and protein ingredients displays good agreement with the measured data. In general, our new model is able to capture the postprandial glucose and insulin following AA challenges, as well as protein ingredients. In addition, our model is also able to capture individual glucose and insulin concentrations following the intake of protein ingredients, being able to capture more pronounced glucose and insulin responses (Figure 1A, subject 9), but also less prominent responses (Figure 1A, subject 3).

## E-DES-PROT improves upon the original E-DES model in capturing glucose dynamics following the intake of AA+glucose and dairy products

We investigated whether our newly developed model was able to capture meals that in addition to AAs and protein also contained glucose and carbohydrates. The E-DES-PROT model was compared to the original E-DES model using the AIC and BIC, with the lowest AIC and BIC value pertaining to the preferred model.



*Amino acids + glucose challenge*

The simulated glucose and insulin responses using the original E-DES and the newly developed E-DES-PROT model, parameterized on the AA+glucose challenges (1 mmol/kg body weight + 25g glucose), are shown in Figure 2. For the original E-DES model, parameters ($k1$, $k5$, $k6$, $k8$) were estimated. For the E-DES-PROT model, these model parameters were estimated in conjunction with the model parameters accounting for AAs ($k11$-$k13$). The measured plasma AA concentration (pertaining to the challenge) were interpolated and provided to the model as an input (Rozendaal *et al.*, 2018).

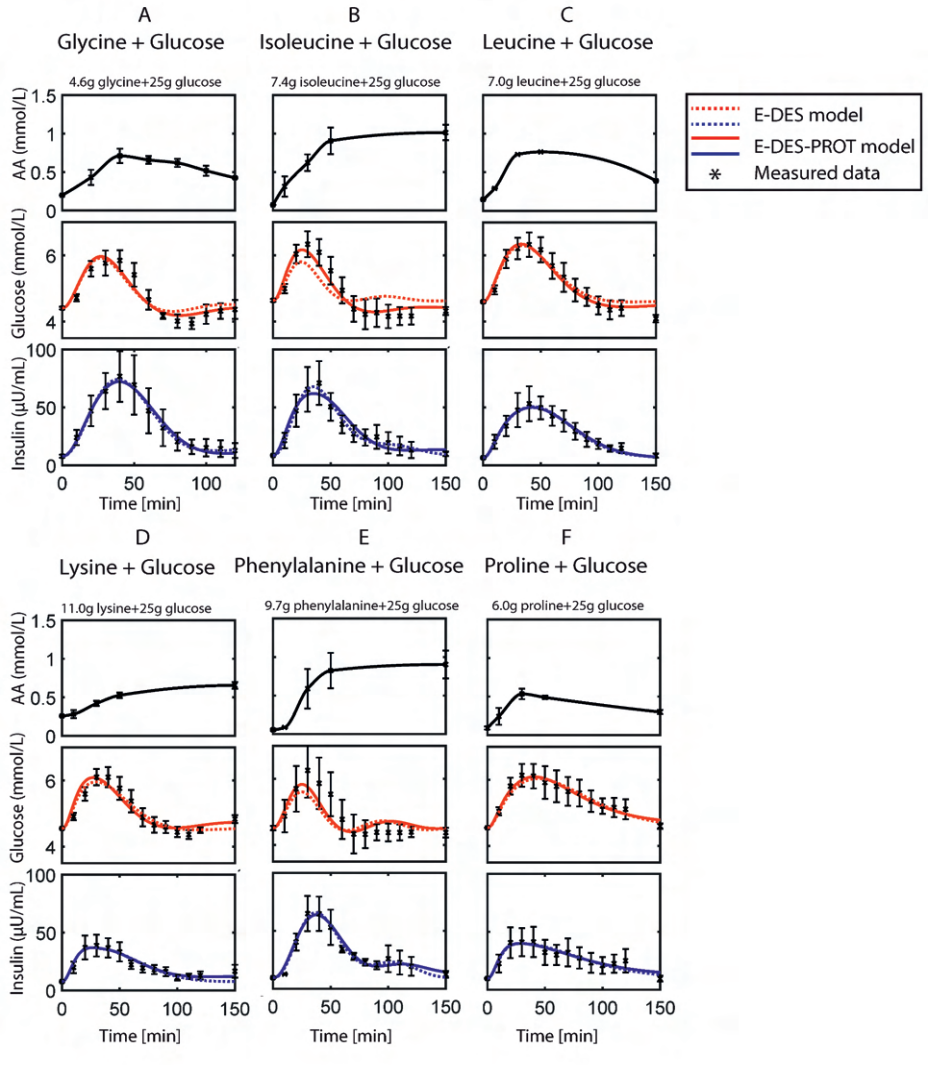


**Figure 2. Plasma glucose and insulin simulation following intake of different amino acids (AAs) together with glucose in healthy individuals, using the original E-DES and E-DES-PROT model.** The AA input is shown in black (data and polynomial interpolation). The simulated glucose and insulin concentrations following parameter estimation ($k1$, $k5$, $k6$, $k8$) using the original E-DES model, are shown in dashed red and blue, respectively. The simulated glucose and insulin concentrations following parameter estimation ($k1$, $k5$, $k6$, $k8$, $k11$-$k13$) using the E-DES-PROT model, are shown in red and blue, respectively. The other model parameters were kept to their original population value. The measured concentrations, obtained from (van Sloun et al., 2020), are shown as black asterisks with corresponding standard errors of the means.

Visual inspection of the plasma glucose and insulin simulations following the AA+glucose challenges displays good agreement with the measured data using the E-DES and E-DES-PROT model. The E-DES-PROT model is able to capture AA+glucose challenges and improves in capturing the measured postprandial glucose data (Figure 2, AIC, 1.05 and -1.45; BIC, 3.31 and 2.50 for E-DES, and E-DES-PROT, respectively across all challenges). For glycine+glucose (Figure 2A), the improvement pertained to the period from 60 min after intake onwards, whereas the E-DES-PROT model improved the overall postprandial glucose response for isoleucine+glucose (Figure 2B). The postprandial insulin data was nicely captured using both models. Thus, both the E-DES and E-DES-PROT model are able to describe postprandial responses to simple meal challenges consisting of single AAs co-ingested with glucose. The complete overview of the AIC and BIC for the AA+glucose challenges using the E-DES and E-DES-PROT model is shown in Table S1.



### Dairy products

The simulated glucose and insulin responses using the original E-DES and the newly developed E-DES-PROT model, parameterized on responses to selected dairy food products (i.e. LF-UHT and yoghurt) containing 25g of protein and a variable amount of carbohydrates in a 700mL solution are shown in Figure 3. Here, the leftmost column pertains to the average population responses, whereas the other columns show selected individual responses highlighting striking model behavior. The complete overview of the individual glucose and insulin responses for the dairy products (i.e. LF-UHT, LF-PAS, FF-UHT, FF-PAS, and yoghurt) are shown in Supplemental Section S2. For the original E-DES model, parameters ($k1$, $k5$, $k6$, $k8$) were estimated. For the E-DES-PROT model, these parameters were estimated in conjunction with the model parameters accounting for AAs ($k11$-$k13$). The measured plasma AA concentration (pertaining to the challenge) were interpolated and provided to the model as an input (Rozendaal *et al.*, 2018).

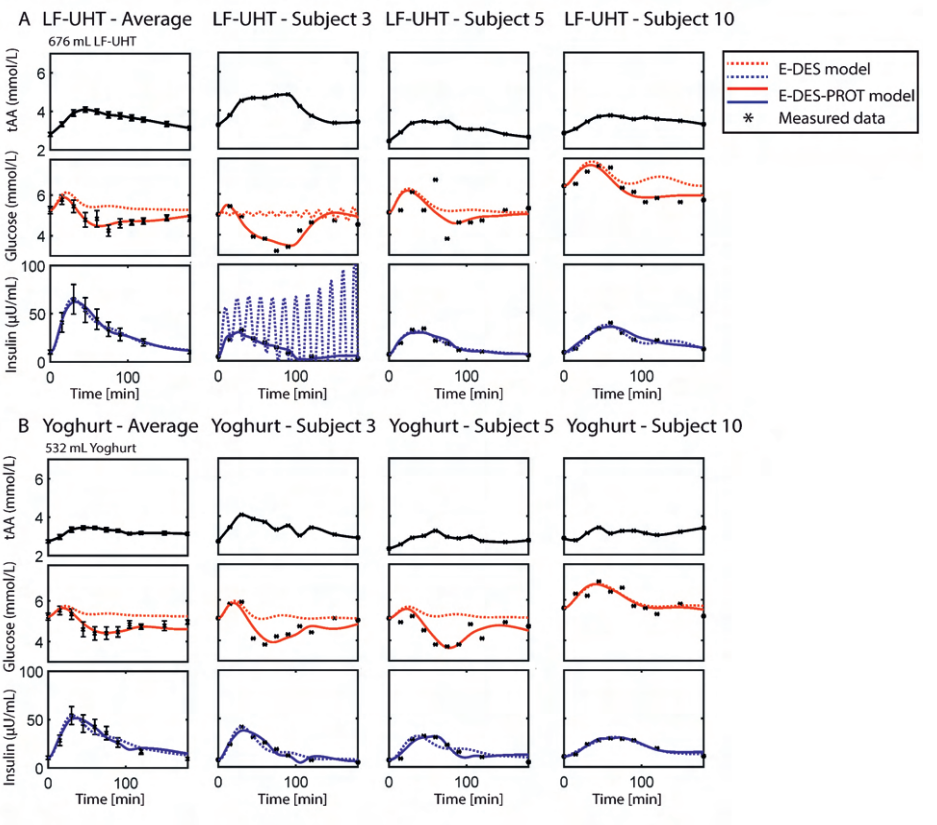


**Fig 3. Plasma glucose and insulin simulation following intake of low-fat untreated treated milk (LF-UHT) and Yoghurt in the average healthy study population and selected individuals using the original E-DES and E-DES-PROT model.** The tAA input is shown in black (data and polynomial interpolation). The simulated glucose and insulin concentrations following parameter estimation ($k1$, $k5$, $k6$, $k8$) using the original E-DES model, are shown in dashed red and blue, respectively. The simulated glucose and insulin concentrations following parameter estimation ($k1$, $k5$, $k6$, $k8$, $k11$-$k13$) using the E-DES-PROT model, are shown in red and blue, respectively. The other model parameters were kept to their original population value. The measured concentrations, obtained from (Horstman et al., 2021), are shown as black asterisks with corresponding standard errors of the means. The leftmost column in panel A & B pertains to average study population, whereas the other columns represent selected individuals.

The plasma glucose and insulin simulations following LF-UHT and yoghurt ingestion are in good agreement with the measured data using the E-DES-PROT model. In particular, the original E-DES model was less able to capture the measured postprandial glucose data compared the E-DES-PROT model (Figure 3, AIC, 16.01 and -5.44; BIC, 17.21 and -3.32 for E-DES and E-DES-PROT, respectively,

across all challenges). Whereas the first glucose data point after intake (t=15min) is accurately captured with the original E-DES model, the remainder of the response is not, and appears to overshoot the measured concentration. The postprandial insulin data was captured well using both models. Looking at the individual level, the E-DES-PROT model was able capture a wide variety of measured postprandial glucose and insulin responses. Here, the E-DES-PROT model was better able to capture the measured data, for instance for subject 3, 10 (Figure 3A) and subject 3, 5 (Figure 3B). The E-DES-PROT model thus allows capture of more complex meals containing protein as well as carbohydrates, which the original E-DES model was unable to do. The complete overview of the AIC and BIC for the dairy products using the E-DES and E-DES-PROT model is shown in Table S2.

Model fluxes were compared between E-DES-PROT and the original E-DES model following LF-UHT intake in the average healthy population (Figure S2). The fluxes for endogenous glucose production and insulin-dependent glucose uptake increased more in the E-DES-PROT model compared to the original E-DES model. Despite the small increase in the insulin-dependent glucose uptake flux, a minor change greatly affects the postprandial glucose and insulin concentrations (Figure S3). In addition, model fluxes were compared for different types of meals, ranging from simple AA challenges to more complex dairy products in the average healthy study populations, using the E-DES-PROT model (Figure 4).

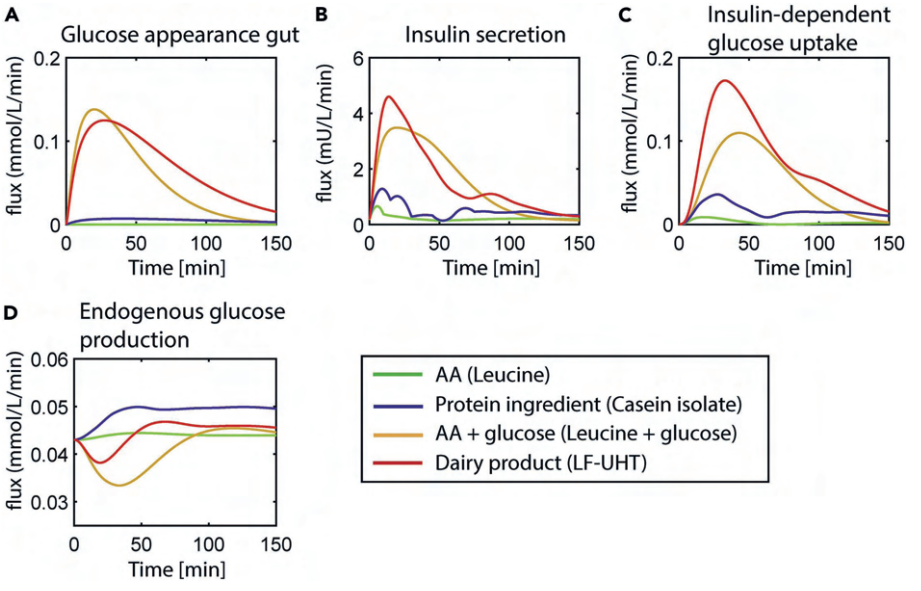


**Figure 4. Model fluxes following intake of various meal challenges in the average healthy study populations using the E-DES-PROT model.** The corresponding model fluxes pertaining to the E-DES-PROT model simulations for leucine (green), micellar casein isolate (blue), leucine+glucose (brown), and LF-UHT (red) intake are shown in panels A, B, C, and D.

The glucose appearance in the gut appears to be more spread out following LF-UHT intake, as compared to leucine+glucose co-ingestion, which has an earlier peak. Insulin secretion and insulin-dependent glucose uptake are substantially lower for leucine and micellar casein isolate ingestion compared to co-ingestion of leucine with glucose and LF-UHT intake, with the largest peak in insulin secretion in the latter. Furthermore, a clear increase from baseline in endogenous glucose production is observed for micellar casein isolate intake, in contrast to LF-UHT and in particular leucine+glucose, which shows the largest decrease from baseline. Leucine ingestion alone only slightly increased endogenous glucose production.

## DISCUSSION

Dietary protein and AAs play an important role in glucose metabolism through stimulating both insulin and glucagon secretion (Ang et al., 2019; Lindgren et al., 2015; van Sloun *et al.*, 2020). In this study, we developed a novel computational model of the glucose-insulin regulatory system, taking the effects of AAs into account, and used this novel model to describe postprandial glucose and insulin dynamics following a variety of simple to complex meals containing AAs and

protein. Here, we show that our E-DES-PROT model accurately describes the measured glucose and insulin concentrations, allows insight into the underlying model fluxes, and outperforms the original E-DES model that only takes the postprandial effects of glucose ingestion into account.

The Eindhoven-Diabetes Education Simulator (E-DES) model by Maas et al. (Maas *et al.*, 2015) was selected as a basis for model extension due to its relatively simple description of glucose metabolism. Other models that have previously been reported such as the model of Dalla Man et al. (Dalla Man *et al.*, 2007) requires data derived from complex, costly measurements (i.e. stable isotope studies) to allow estimation of its model parameters, making it challenging models to parameterize. In contrast, the E-DES model is less complex in terms of the number of parameters included in the model, and has so far been shown to describe glucose homeostasis in different populations as well as individuals, whilst including the most important metabolic fluxes (Erdős *et al.*, 2021; Maas *et al.*, 2015; Rozendaal *et al.*, 2018). The present E-DES-PROT model introduces several novel terms accounting for the postprandial effects of both individual and total AAs on glucose and insulin regulation. More specifically, the equation regulating liver glucose production was extended to increase glucose output with increasing plasma AA levels, representing the physiological effects of AAs on glucagon secretion, and consequently hepatic glucose output (Holst et al., 2017). Secondly, the equation regulating pancreatic insulin secretion was extended to increase insulin secretion with increasing plasma AA levels, representing the physiological effects of AAs on β-cells, causing a rise in the ATP/ADP ratio, ultimately leading to the stimulation of insulin granule exocytosis (Newsholme and Krause, 2012). These extensions were necessary to capture the characteristics of the postprandial data, whilst adhering to established human physiology (Holst *et al.*, 2017; Newsholme et al., 2007). To prevent the development of an overly complex model, we modeled these processes using simple linear and derivative terms; in this way the model can still be readily individualized using standard plasma glucose, insulin, and AA measurements. With the addition of only three parameters, the E-DES-PROT model was able to accurately capture postprandial glucose and insulin data following various challenge tests containing AAs and protein ingredients. The E-DES-PROT model outperforms the original E-DES model in capturing postprandial glucose data, particularly in the case of the dairy challenges, where both AIC and BIC showed a preference for the E-DES-PROT model. For the AA+glucose challenges, both E-DES and E-DES-PROT were able to accurately capture the insulin response, explaining why the AIC and BIC

preferred the E-DES model. However, in contrast to the insulin response, the E-DES model was not able to accurately capture the glucose response.

These results confirm the necessity of including the effects of AAs and protein in the models to be able to capture glycemic responses to foods such as to yoghurt. A model based on E-DES that incorporates dietary fat has been developed in parallel and was recently published (O'Donovan *et al.*, 2022). A next step would be to merge these two models into a model able to fully capture the effects of a complex meal, taking into account all three macronutrient classes (i.e. carbohydrate, protein, and fat) (Laxminarayan et al., 2015).

Despite only slightly improving in capturing the glucose response following AA+glucose challenges, the E-DES-PROT model is physiologically more accurate and provides more detailed insight into the underlying physiological processes (i.e. insulin secretion and endogenous glucose production). Besides being able to describe average postprandial responses to the various challenges, the E-DES-PROT showed the ability to reproduce a wide variety of individual postprandial glucose and insulin responses as well. However, there were some exceptions in which the model did not perfectly capture certain individual postprandial responses. This was observed for responses in which the data points following meal ingestion (t=0) were below basal glucose concentration (e.g. participant 5, Figure 3B). Furthermore, the model struggled accurately predicting an intermediate dip in the glucose response (e.g. participant 5, Figure 3A).

The mechanistic nature of the model also allows the investigation of non-measured variables such as metabolite fluxes between tissues. Inspecting the metabolite fluxes, we found that there was an increase in insulin-dependent glucose uptake using the E-DES-PROT model compared to the original E-DES model, resulting in accurate description of the postprandial glucose data. The model fluxes calculated for various meals included in this study provide information on physiological processes underlying the dynamic responses. For example, glucose appearance in the gut seems to be more spread out for the dairy product (i.e. LF-UHT) compared to the more simple AA+glucose co-ingestion test (i.e. leucine + glucose). Furthermore, endogenous glucose production was increased for protein only meals (i.e. micellar casein isolate), corresponding with findings from literature (Ang *et al.*, 2019; Khan et al., 1992). Whilst beyond the scope of the present study, investigating model parameters and corresponding fluxes at the individual level with the new E-DES-PROT model might provide further insight into the glucometabolic status of individuals.

In conclusion, we present a new physiology-based computational model of the glucose homeostasis that extends the E-DES model with the postprandial effects of AAs and protein. The E-DES-PROT model allows, for the first time, to accurately describe postprandial responses following different AA challenges (with and without co-ingestion of glucose), dried milk protein ingredients and dairy challenges, and is able to provide information on physiological processes underlying the meal responses. Introducing AAs in these models is important to move towards describing physiologically relevant complex meals. In addition, our model outperforms the original E-DES model in terms of describing postprandial glucose responses following dairy products. As the model covers two out of three macronutrient classes (carbohydrates and protein), future studies should explore the possibility to further extend the E-DES-PROT model with fat to allow model-based prediction of glucose responses to complex meals varying in macronutrient composition and content.



## LIMITATIONS OF THE STUDY

The increased liver glucose output was modeled to be dependent on the AA concentration in the plasma. However, AAs are known to stimulate glucagon secretion, which in turn increases liver glucose output (Holst *et al.*, 2017). As glucagon is not explicitly accounted for in the E-DES model, future work should consider incorporating glucagon in the E-DES model, as has been implemented before in the Dalla Man model (Man et al., 2014). Secondly, as the objective of our research was to quantify the effect of AAs on postprandial glucose-insulin dynamics, a forcing function is used to describe the rate of appearance of AAs in E-DES-PROT. In future research, the addition of a function to explicitly describe the rate of appearance could increase the functionality of our model. This rate of appearance function would allow simulation of plasma AAs, without the need for measured plasma AAs to be provided as input. Furthermore, this would allow refinement of the glucose rate of appearance, as protein (and fat) have been known to delay gastric emptying (Sun et al., 2017).

Individual AAs have been shown to have distinct effects on the glucose and insulin response (Newsholme *et al.*, 2007; van Sloun *et al.*, 2020), but also interact with each other when provided together (Iverson et al., 2014). In this study, we added up the AA profiles (tAA) for the protein ingredients and dairy products, and did not include possible interactions between individual AAs in the E-DES-PROT model. Furthermore, not only AAs but also fat influences the blood glucose

response in response to complex meals (Garonzi et al., 2021; Savage et al., 2007). However, incorporating the postprandial effects of fat on glucose metabolism was beyond the scope of this present study. Identifiability analysis showed that the parameters related to AAs ($k11$ – $k13$) were identifiable for AA challenges and milk protein ingredients (examples are shown in Figure S4). However, for the AA+glucose challenges as well as for the dairy products, only the parameters $k1$, $k5$, $k6$, $k8$, and $k13$ were consistently deemed identifiable. The unidentifiability of the $k11$ and $k12$ parameter in several of these challenges might have resulted from functional relationships between parameters.

## STAR⋆METHODS

### Study workflow

The study workflow is illustrated in Figure S5. Briefly, the existing E-DES model was extended to a model that accounts for the postprandial effects of AAs and protein on glucose and insulin dynamics. Model equations were adjusted and additional parameters were introduced to take the effects of AAs on insulin secretion and liver glucose production, as observed from literature, into account. Subsequently, postprandial time-series data, extracted from the literature (van Sloun *et al.*, 2020), and obtained from a previously performed randomized, single-blind crossover trial in healthy elderly males and females (RCT; NCT02546141) (Horstman *et al.*, 2021) were used to estimate the model parameters. The ability of the model to describe the measured data was evaluated using the sum of squared residuals (SSR), the Akaike Information Criterion (AIC) and the Bayesian Information Criterion (BIC). Model fluxes were compared between the E-DES and the newly developed E-DES-PROT model, as well as for various meal challenges.

### Collection of data

Publicly available datasets, containing postprandial time-series data of AAs, glucose, and insulin following various AA challenge tests (leucine, isoleucine, lysine, glycine, proline, and phenylalanine; with or without glucose) in healthy individuals were included in the present study (summarized in (van Sloun *et al.*, 2020)). In all experiments, plasma samples were taken from the antecubital vein in the fasting state (t=0) and 10, 20, 30, 40, 50, 60, 70, 80, 90, 100, 110, 120, and 150 minutes after ingestion of 1 mmol AA per kg of lean body weight (with or without 25g glucose). In addition, we used data on postprandial AAs (arginine, glutamine, serine, asparagine, glycine, threonine, alanine, methionine, proline, lysine, aspartic acid, histidine, valine, glutamic acid, tryptophan, leucine,

phenylalanine, isoleucine, cysteine and tyrosine), glucose, and insulin time-series from a randomized single-blind crossover trial (RCT; NCT02546141), in which ten participants (five male) received two spray dried milk protein ingredients (whey protein concentrate, WPC; micellar casein isolate, MCI) and six dairy products (low-fat untreated milk (LF-UHT); low-fat pasteurized milk (LF-PAS); full-fat untreated milk (FF-UHT); full-fat pasteurized milk (FF-PAS); low-fat yoghurt; full-fat cheese) in random order, as previously described (Horstman *et al.*, 2021). The dairy products and protein ingredients were supplied on eight separate test days, with a one-week washout period in between. For each meal, an appropriate amount of the product to ensure 25g of protein intake was consumed. For the milk protein ingredients (i.e. WPC and MCI), this was achieved by dissolving an appropriate amount of powder in water to attain a solution of 700mL containing 25g of protein. To standardize the volume for all products, water was added to a total of 700mL of volume ingested. Plasma samples were taken from the antecubital vein in the fasting state (t=0) and 15, 30, 45, 60, 75, 90, 105, 120, 150, 180, 210, 240, and 300 minutes after ingesting the protein ingredients and dairy products. An overview of the datasets included in the present study is given in Table S3.



## Development of a novel physiology-based computational model of glucose homeostasis

The Eindhoven Diabetes Education Simulator (E-DES, version 1.1) published by Maas et al. (Maas *et al.*, 2015; Rozendaal *et al.*, 2018) formed the basis for the model extension with AAs in the present study. The E-DES model is a physiology-based computational model of the glucose regulatory system in healthy individuals and patients with type 1 and type 2 diabetes (Maas, 2017). It consists of a system of coupled differential equations, which describe the change of the mass or concentration of either glucose or insulin over time. Each of these equations consists of a positive inflow and negative outflow term and can be summarized as follows: (i) glucose balance in the gut is determined through the inflow of glucose mass from the stomach and glucose leaving the gut through uptake by the plasma (ii) glucose balance in the plasma is determined by glucose inflow from the gut in conjunction with glucose output from the liver and glucose uptake by insulin-(in)dependent tissues (iii) insulin balance in the plasma is determined by inflow of endogenously produced insulin from the pancreas and uptake of insulin by the interstitial fluid (iv) insulin balance in the interstitial fluid is determined by insulin inflow from the plasma and removal of insulin from the interstitial fluid proportional to the interstitial insulin fluid concentration. The rates through which these processes occur are controlled by parameters (denoted with *k*),

which have been estimated and validated on multiple oral glucose tolerance tests (OGTTs) in healthy populations (Maas, 2017). The model parameters are described in Table S4. The model inputs, equations, fluxes, constants are described in detail in Supplemental Section S3.

## Model development

In this study, we extended the previously developed E-DES model to also account for the postprandial effects of AAs on glucose and insulin dynamics (illustrated in Figure S6). Firstly, the equation regulating glucose production from the liver (Eq. 1) was extended with a proportional (*k*11) term to accommodate an increase in liver glucose production proportional to the AA concentration present in the plasma ($AA^{pl}(t)$) relative to the basal concentration ($AA_b^{pl}$).

$$g^{liv}(t) = g_b^{liv} - k_3\left(G^{pl}(t) - G_b^{pl}\right) - k_4\beta\left(I^{if}(t)\right) + k_{11}\left(AA^{pl}(t) - AA_b^{pl}\right) \quad (1)$$

Secondly, the equation regulating insulin secretion from the pancreas (Eq. 2) was extended with a derivative (*k*12) and proportional (*k*13) term to accommodate an increase in insulin secretion (i) based on the rate of change of plasma AAs $(\frac{dAA^{pl}}{dt})$, and (ii) proportional to the AA concentration present in the plasma ($AA^{pl}(t)$) relative to the basal concentration ($AA_b^{pl}$).

$$i^{pnc}(t) = k_6(G^{pl}(t) - G_b^{pl}) + \left(\frac{k_7}{\tau_i}\right)\int (G^{pl}(t) - G_b^{pl})dt + \left(\frac{k_7}{\tau_i}\right)G_b^{pl} + (k_8\tau_d)\frac{dG^{pl}}{dt} + k_{12}\frac{dAA^{pl}}{dt} + k_{13}(AA^{pl}(t) - AA_b^{pl}) \quad (2)$$

The extended equations (1) and (2) described above require plasma AA concentrations as model input. Therefore, measured AA concentrations following the challenge tests were interpolated via a fitted piecewise cubic Hermite interpolating polynomial (pchip), and provided to the model as $AA^{pl}(t)$. For the RCT (NCT02546141), the following AA measurements were added up, interpolated, and denoted as total AA (tAA): arginine, glutamine, serine, asparagine, glycine, threonine, alanine, methionine, proline, lysine, aspartic acid, histidine, valine, glutamic acid, tryptophan, leucine, phenylalanine, isoleucine, cysteine, and tyrosine.

## Model calibration

Model calibration was performed by generating parameter values that resulted in an optimal description of measured data. This was done through minimizing a cost function, representing the sum of squared residual (SSR) in the model prediction for glucose and insulin (Eq. 3). The SSR is minimized using *lsqnonlin*,

a local, gradient-based least squares solver in MATLAB (Version R2018b). Optimal parameter sets were obtained using twenty-five initializations of the optimization algorithm with 25% random noise starting from the original parameter value for the average healthy population (Rozendaal *et al.*, 2018).

$$SSR = \sum_{j=1}^{m}\sum_{i=1}^{N}(\gamma((y_{i,j}|\vec{\theta}) - d_{i,j}))^2 \quad (3)$$

Where $m$, and $N$ represent the number of metabolites and the number of time-points, respectively. The measured data is denoted by $d$, while $y$ is the corresponding model prediction given the parameter vector $\vec{\theta}$. A weight factor

$\gamma = 0.1$ was used in the case of insulin ($\gamma = 1$ in case of glucose) to account for the unit difference (mmol/L, mU/L for glucose and insulin, respectively) between the molecules. As the *lsqnonlin* function, that minimizes the sum of squared error, does this simultaneously for glucose and insulin, the $\gamma$ factor aims to bring the units for glucose and insulin closer together to avoid prioritizing one or the other in the optimization process.



### Model selection and analysis

Visual inspection was performed to evaluate the goodness-of-fit of the simulated glucose and insulin responses to the measured data. In order to compare the E-DES and the E-DES-PROT model, we selected the parameters identified from our previous work (Erdős *et al.*, 2021). In that work, a systematic model selection pipeline was implemented to allow personalization of the E-DES model through reducing the number of parameters to be estimated, resulting in a model containing parameters $k1$, $k5$, $k6$, and $k8$ (sensitivity is shown in Figure S7). In the current work, we estimated those parameters, both for the systematic review datasets and the randomized single-blind crossover trial. The selected parameters represent distinct physiological processes involved in glucose and insulin regulation, described in Table 2. For the E-DES-PROT model simulation, the AA parameters ($k11$-$k13$) were also estimated. Parameters $G_b^{pl}$ and $I_b^{pl}$ (sensitivity is shown in Figure S8) were set to be equal to the first data-point (t = 0 min) of the measured responses, whereas the other parameters were set to the average healthy population values from the original publication (Rozendaal *et al.*, 2018).

Model performance was evaluated using the Akaike Information Criterion (AIC) and the Bayesian Information Criterion (BIC), in which model complexity (i.e. number of estimated parameters) was penalized (Eq. 4 & 5 respectively).

$$AIC = N * \ln(\frac{SSR}{N}) + 2 * K \quad (4)$$

$$BIC = N * \ln(\frac{SSR}{N}) + \ln(N) * K \quad (5)$$

N represents the number of observations, and K the number of parameters. Given a set of candidate models that describe the postprandial time-series data, the preferred model is the one with the lowest AIC and BIC value, indicating the better-fit model whilst taking the number of parameters into account. In addition, model fluxes were calculated and compared between the E-DES and E-DES-PROT model, as well as for the various meal challenges. Parameter identifiability was assessed using Profile Likelihood Analysis (PLA). In PLA, the value of one parameter is changed iteratively from its optimal value and the remaining parameters are re-estimated. An increase in the cost function for the model fit indicates that a reliable parameter estimate has been obtained and the parameter is identifiable given the model structure and data.

### Computer software

The model was implemented and analyzed in MATLAB (MATLAB, Version R2018b, The Mathworks, Inc., Natick, Massachusetts, United States). The ordinary differential equation model was simulated using the variable step solver ode15s.

## REFERENCES


1. Ang, T., Bruce, C.R., and Kowalski, G.M. (2019). Postprandial Aminogenic Insulin and Glucagon Secretion Can Stimulate Glucose Flux in Humans. Diabetes *68*, 939-946. 10.2337/db18-1138.
2. Bergman, R.N., Ider, Y.Z., Bowden, C.R., and Cobelli, C. (1979). Quantitative estimation of insulin sensitivity. Am J Physiol *236*, E667-677. 10.1152/ajpendo.1979.236.6.E667.
3. Case, L.P., Daristotle, L., Hayek, M.G., and Raasch, M.F. (2011). Chapter 4 - Protein and Amino Acids. In Canine and Feline Nutrition (Third Edition), L.P. Case, L. Daristotle, M.G. Hayek, and M.F. Raasch, eds. (Mosby), pp. 21-25. https://doi.org/10.1016/B978-0-323-06619-8.10004-0.
4. Chadt, A., and Al-Hasani, H. (2020). Glucose transporters in adipose tissue, liver, and skeletal muscle in metabolic health and disease. Pflügers Archiv - European Journal of Physiology *472*, 1273-1298. 10.1007/s00424-020-02417-x.
5. Dalla Man, C., Rizza, R.A., and Cobelli, C. (2007). Meal simulation model of the glucose-insulin system. IEEE Trans Biomed Eng *54*, 1740-1749. 10.1109/tbme.2007.893506.
6. Erdős, B., van Sloun, B., Adriaens, M.E., O'Donovan, S.D., Langin, D., Astrup, A., Blaak, E.E., Arts, I.C., and van Riel, N.A. (2021). Personalized computational model quantifies heterogeneity in postprandial responses to oral glucose challenge. PLoS computational biology *17*, e1008852.
7. Garonzi, C., Forsander, G., and Maffeis, C. (2021). Impact of Fat Intake on Blood Glucose Control and Cardiovascular Risk Factors in Children and Adolescents with Type 1 Diabetes. Nutrients *13*. 10.3390/nu13082625.
8. Holst, J.J., Albrechtsen, N.J.W., Pedersen, J., and Knop, F.K. (2017). Glucagon and amino acids are linked in a mutual feedback cycle: the liver–α-cell axis. Diabetes *66*, 235-240.
9. Horstman, A.M., Ganzevles, R.A., Kudla, U., Kardinaal, A.F., van den Borne, J.J., and Huppertz, T. (2021). Postprandial blood amino acid concentrations in older adults after consumption of dairy products: The role of the dairy matrix. International Dairy Journal *113*, 104890.
10. Iverson, J.F., Gannon, M.C., and Nuttall, F.Q. (2014). Interaction of ingested leucine with glycine on insulin and glucose concentrations. Journal of amino acids *2014*, 521941. 10.1155/2014/521941.
11. Khan, M.A., Gannon, M.C., and Nuttall, F.Q. (1992). Glucose appearance rate following protein ingestion in normal subjects. Journal of the American College of Nutrition *11*, 701-706. 10.1080/07315724.1992.10718270.
12. Kovatchev, B.P., Breton, M., Man, C.D., and Cobelli, C. (2009). In silico preclinical trials: a proof of concept in closed-loop control of type 1 diabetes. Journal of diabetes science and technology *3*, 44-55. 10.1177/193229680900300106.
13. Laxminarayan, S., Reifman, J., Edwards, S.S., Wolpert, H., and Steil, G.M. (2015). Bolus Estimation--Rethinking the Effect of Meal Fat Content. Diabetes technology & therapeutics *17*, 860-866. 10.1089/dia.2015.0118.
14. Lindgren, O., Pacini, G., Tura, A., Holst, J.J., Deacon, C.F., and Ahrén, B. (2015). Incretin Effect After Oral Amino Acid Ingestion in Humans. The Journal of Clinical Endocrinology & Metabolism *100*, 1172-1176. 10.1210/jc.2014-3865.
15. Maas, A.H. (2017). Playing with numbers: the development of an educational diabetes game. Technische Universiteit Eindhoven.

16. Maas, A.H., Rozendaal, Y.J., van Pul, C., Hilbers, P.A., Cottaar, W.J., Haak, H.R., and van Riel, N.A. (2015). A physiology-based model describing heterogeneity in glucose metabolism: the core of the Eindhoven Diabetes Education Simulator (E-DES). Journal of diabetes science and technology *9*, 282-292. 10.1177/1932296814562607.
17. Man, C.D., Micheletto, F., Lv, D., Breton, M., Kovatchev, B., and Cobelli, C. (2014). The UVA/PADOVA Type 1 Diabetes Simulator: New Features. Journal of diabetes science and technology *8*, 26-34. 10.1177/1932296813514502.
18. Newsholme, P., Bender, K., Kiely, A., and Brennan, L. (2007). Amino acid metabolism, insulin secretion and diabetes. Biochemical Society Transactions *35*, 1180-1186. 10.1042/bst0351180.
19. Newsholme, P., and Krause, M. (2012). Nutritional regulation of insulin secretion: implications for diabetes. The Clinical biochemist. Reviews *33*, 35-47.
20. O'Donovan, S.D., Erdős, B., Jacobs, D.M., Wanders, A.J., Thomas, E.L., Bell, J.D., Rundle, M., Frost, G., Arts, I.C.W., Afman, L.A., and van Riel, N.A.W. (2022). Quantifying the contribution of triglycerides to metabolic resilience through the mixed meal model. iScience *25*, 105206. https://doi.org/10.1016/j.isci.2022.105206.
21. Qaid, M.M., and Abdelrahman, M.M. (2016). Role of insulin and other related hormones in energy metabolism—A review. Cogent Food & Agriculture *2*, 1267691.
22. Rix, I., Nexøe-Larsen, C., Bergmann, N.C., Lund, A., and Knop, F.K. (2015). Glucagon physiology.
23. Röder, P.V., Wu, B., Liu, Y., and Han, W. (2016). Pancreatic regulation of glucose homeostasis. Experimental & molecular medicine *48*, e219. 10.1038/emm.2016.6.
24. Rozendaal, Y.J., Maas, A.H., van Pul, C., Cottaar, E.J., Haak, H.R., Hilbers, P.A., and van Riel, N.A. (2018). Model-based analysis of postprandial glycemic response dynamics for different types of food. Clinical Nutrition Experimental *19*, 32-45. https://doi.org/10.1016/j.yclnex.2018.01.003.
25. Savage, D.B., Petersen, K.F., and Shulman, G.I. (2007). Disordered lipid metabolism and the pathogenesis of insulin resistance. Physiological reviews *87*, 507-520. 10.1152/physrev.00024.2006.
26. Sun, L., Tan, K.W.J., Han, C.M.S., Leow, M.K., and Henry, C.J. (2017). Impact of preloading either dairy or soy milk on postprandial glycemia, insulinemia and gastric emptying in healthy adults. European journal of nutrition *56*, 77-87. 10.1007/s00394-015-1059-y.
27. van Sloun, B., Goossens, G.H., Erdos, B., Lenz, M., van Riel, N., and Arts, I.C.W. (2020). The Impact of Amino Acids on Postprandial Glucose and Insulin Kinetics in Humans: A Quantitative Overview. Nutrients *12*, 3211.

## SUPPLEMENTAL INFORMATION

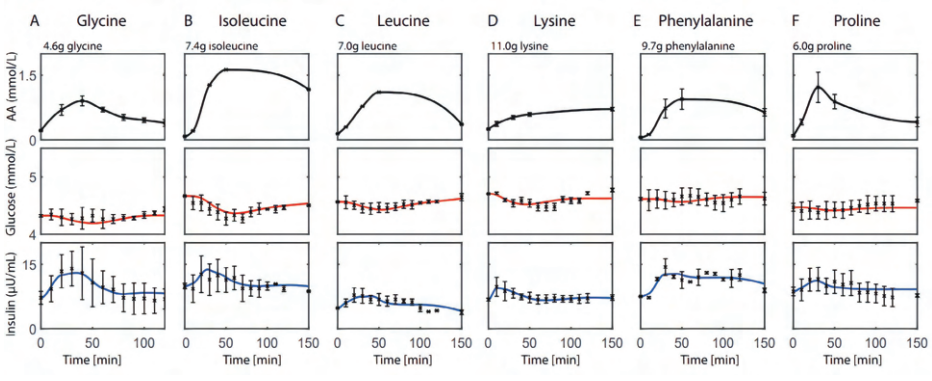


**Supplemental Figure S1: Simulated postprandial responses in the literature study following ingestion of amino acids as described in the Results section.** The model parameters pertaining to amino acids (AAs, k11-k13) were estimated, whereas the other model parameters were kept to their original population value. The tAA input is shown in black (data and polynomial interpolation). The simulated glucose and insulin concentrations are shown in red and blue, respectively. The measured concentrations, obtained from (van Sloun et al., 2020) are shown as black asterisk with corresponding standard errors of the means.

**Supplemental Table S1: Sum of squared residuals (SSR), Akaike Information Criterion (AIC), and Bayesian Information Criterion (BIC) of the AA+glucose challenges from literature datasets using the E-DES and E-DES-PROT model as described in the Results section.**

| E-DES | SSR | AIC | BIC | E-DES-PROT | SSR | AIC | BIC |
|---|---|---|---|---|---|---|---|
| | | | | **Glucose + Insulin response** | | | |
| | | | | **Glucose + Insulin response** | | | |
| Leucine + Glucose | 0.9853 | -77.0958 | -72.0634 | Leucine + Glucose | 0.8266 | -75.6618 | -66.8551 |
| Isoleucine + Glucose | 4.2394 | -39.1555 | -34.1231 | Isoleucine + Glucose | 4.7099 | -30.4194 | -21.6125 |
| Lysine + Glucose | 2.1334 | -57.0094 | -51.9771 | Lysine + Glucose | 1.5095 | -60.0042 | -51.1976 |
| Phenylalanine + Glucose | 3.3157 | -45.5451 | -40.5127 | Phenylalanine + Glucose | 3.4446 | -38.5533 | -29.7468 |
| Glycine + Glucose | 1.7085 | -59.0821 | -54.0498 | Glycine + Glucose | 2.0023 | -45.6105 | -37.3638 |
| Proline + Glucose | 1.6715 | -63.3544 | -58.3221 | Proline + Glucose | 1.5434 | -59.4260 | -50.6202 |
| Across all co-ingestion tests | 14.0537 | -7.9954 | -2.9630 | Across all co-ingestion tests | 14.0364 | -2.0275 | 6.7792 |
| **E-DES** | **SSR** | **AIC** | **BIC** | **E-DES-PROT** | **SSR** | **AIC** | **BIC** |
| | **Glucose response** | | | | **Glucose response** | | |
| Leucine + Glucose | 0.5345 | -33.4877 | -31.2279 | Leucine + Glucose | 0.3426 | -33.2711 | -29.3164 |
| Isoleucine + Glucose | 3.1633 | -10.3733 | -8.1135 | Isoleucine + Glucose | 0.6546 | -24.8533 | -20.8982 |
| Lysine + Glucose | 0.4056 | -37.0743 | -34.8145 | Lysine + Glucose | 0.5807 | -26.4106 | -22.4555 |
| Phenylalanine + Glucose | 2.4123 | -13.8971 | -11.6373 | Phenylalanine + Glucose | 1.6784 | -12.6121 | -8.6578 |
| Glycine + Glucose | 0.9126 | -22.9169 | -20.6571 | Glycine + Glucose | 0.5694 | -22.5770 | -19.1826 |
| Proline + Glucose | 0.1894 | -46.9771 | -44.7173 | Proline + Glucose | 0.1350 | -45.3792 | -41.4219 |
| Across all co-ingestion tests | 7.6176 | 1.0517 | 3.3115 | Across all co-ingestion tests | 3.9607 | -1.4509 | 2.5038 |
| **E-DES** | **SSR** | **AIC** | **BIC** | **E-DES-PROT** | **SSR** | **AIC** | **BIC** |
| | **Insulin response** | | | | **Insulin response** | | |
| Leucine + Glucose | 0.4508 | -35.7023 | -33.4425 | Leucine + Glucose | 0.4840 | -28.7772 | -24.8226 |
| Isoleucine + Glucose | 1.0761 | -24.3910 | -22.1312 | Isoleucine + Glucose | 4.0553 | -1.1440 | 2.8106 |
| Lysine + Glucose | 1.7278 | -18.2353 | -15.9755 | Lysine + Glucose | 0.9288 | -20.3042 | -16.3499 |
| Phenylalanine + Glucose | 0.9034 | -26.6643 | -24.4045 | Phenylalanine + Glucose | 1.7662 | -11.9496 | -7.9949 |
| Glycine + Glucose | 0.7959 | -24.5583 | -22.2985 | Glycine + Glucose | 1.4329 | -11.5027 | -8.1081 |
| Proline + Glucose | 1.4821 | -20.2295 | -17.9697 | Proline + Glucose | 1.4085 | -14.8917 | -10.9369 |
| Across all co-ingestion tests | 6.4361 | -1.1393 | 1.1205 | Across all co-ingestion tests | 10.0757 | 10.6873 | 14.6419 |

**Supplemental Table S2: Sum of squared residuals (SSR), Akaike Information Criterion (AIC), and Bayesian Information Criterion (BIC) of the dairy challenges of the randomized single-blind crossover trial study dataset using E-DES and E-DES-PROT model as described in the Results section.**

| E-DES | SSR | AIC | BIC | E-DES-PROT | SSR | AIC | BIC |
|---|---|---|---|---|---|---|---|
| | | | Glucose + Insulin response | | | | |
| | | | Glucose + Insulin response | | | | |
| LF-UHT | 4.7395 | -16.0199 | -12.4584 | LF-UHT | 0.5840 | -47.7081 | -41.4755 |
| LF-PAS | 3.7143 | -20.4073 | -16.8458 | LF-PAS | 0.2709 | -61.5370 | -55.3022 |
| FF-UHT | 6.1975 | -11.1921 | -7.6306 | FF-UHT | 0.7732 | -42.6566 | -36.4240 |
| FF-PAS | 5.7793 | -12.4495 | -8.8881 | FF-PAS | 0.8822 | -40.2827 | -34.0501 |
| Yoghurt | 5.3701 | -13.7713 | -10.2100 | Yoghurt | 1.3470 | -32.6649 | -26.4323 |
| Across all challenges | 25.8008 | 14.4806 | 18.0421 | Across all challenges | 3.8573 | -13.7273 | -7.4947 |
| **E-DES** | **SSR** | **AIC** | **BIC** | **E-DES-PROT** | **SSR** | **AIC** | **BIC** |
| | **Glucose response** | | | | **Glucose response** | | |
| LF-UHT | 4.4449 | -0.1083 | 1.1021 | LF-UHT | 0.2395 | -23.3196 | -21.1998 |
| LF-PAS | 3.2612 | -3.2048 | -1.9946 | LF-PAS | 0.1317 | -29.2981 | -27.1800 |
| FF-UHT | 5.3515 | 1.7479 | 2.9583 | FF-UHT | 0.3138 | -20.6166 | -18.4977 |
| FF-PAS | 5.0361 | 1.1406 | 2.3508 | FF-PAS | 0.4418 | -17.1954 | -15.0767 |
| Yoghurt | 4.1821 | -0.7177 | -0.4926 | Yoghurt | 0.3043 | -20.9242 | -18.8052 |
| Across all challenges | 22.2758 | 16.0092 | 17.2195 | Across all challenges | 1.4311 | -5.4414 | -3.3233 |
| **E-DES** | **SSR** | **AIC** | **BIC** | **E-DES-PROT** | **SSR** | **AIC** | **BIC** |
| | **Insulin response** | | | | **Insulin response** | | |
| LF-UHT | 0.2946 | -18.4126 | -18.0949 | LF-UHT | 0.3446 | -11.1585 | -10.6024 |
| LF-PAS | 0.4530 | -14.9704 | -14.6527 | LF-PAS | 0.1392 | -18.4103 | -17.8542 |
| FF-UHT | 0.8460 | -16.6983 | -15.4879 | FF-UHT | 0.4595 | -8.8565 | -8.3004 |
| FF-PAS | 0.7432 | -11.0099 | -10.6921 | FF-PAS | 0.4404 | -9.1956 | -8.6400 |
| Yoghurt | 1.1881 | -7.2567 | -6.9389 | Yoghurt | 1.0427 | -2.3009 | -1.7449 |
| Across all challenges | 3.5249 | 1.4433 | 1.7611 | Across all challenges | 2.4264 | 4.4557 | 5.0118 |

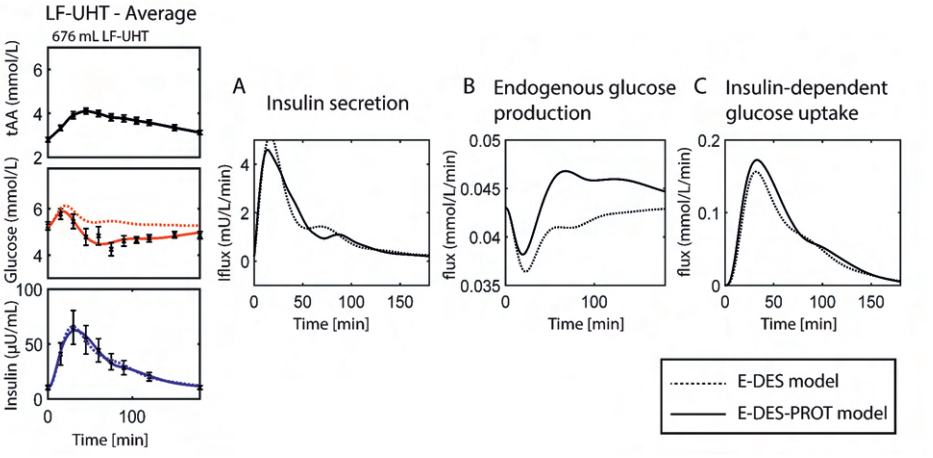


**Supplemental Figure S2: Simulated model fluxes following LF-UHT intake as described in the Results section.** The leftmost column pertains to the average LF-UHT simulation. Panel A, B, C, describe the insulin secretion, endogenous glucose production and insulin-dependent glucose uptake flux, respectively, using the original E-DES model (dashed black) and the E-DES-PROT model (black)

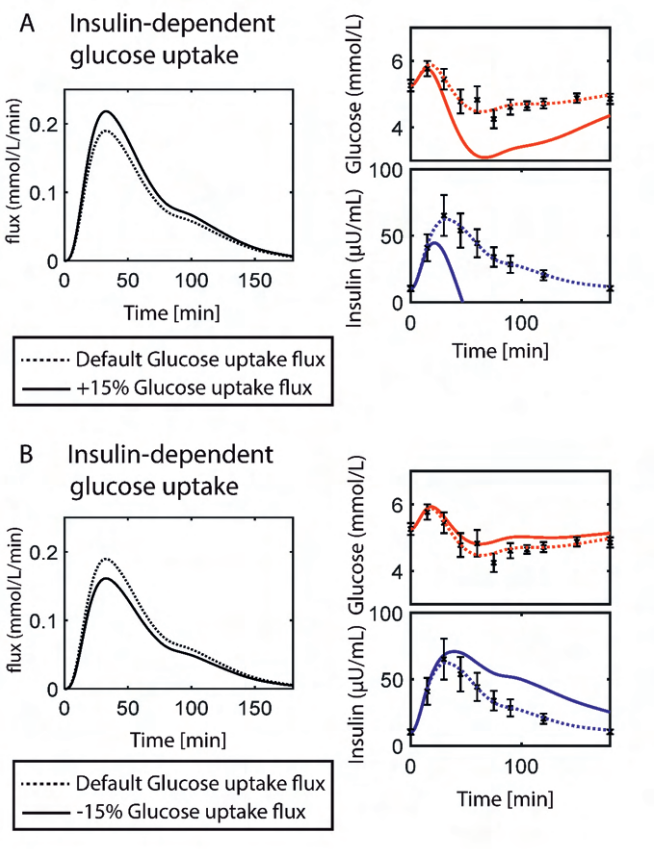


**Supplemental Figure S3: Varying the insulin-dependent glucose uptake flux following LF-UHT intake as described in the Results section.** Panel A and B show a 15% increase and decrease in the insulin-dependent glucose uptake flux, with the corresponding model simulation in red and blue for glucose and insulin, respectively.

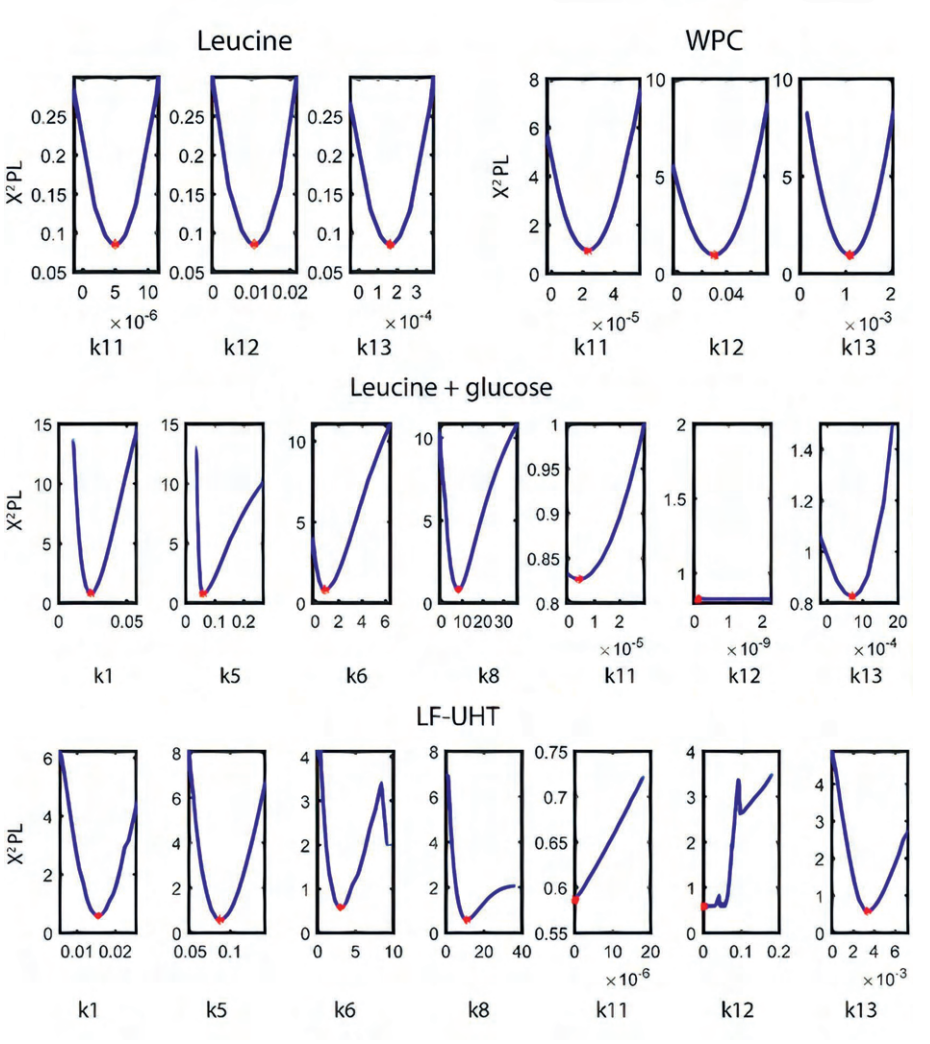


**Supplemental Figure S4: Profile likelihood analysis of leucine, WPC, leucine+glucose, and LF-UHT intake as described in the Limitations of the study section.** The red asterisk indicates the SSR of the model fitted using the optimal parameter values estimated from data, while the blue line corresponds to the error as the other parameter values are being re-estimated after adjusting the parameter value iteratively.

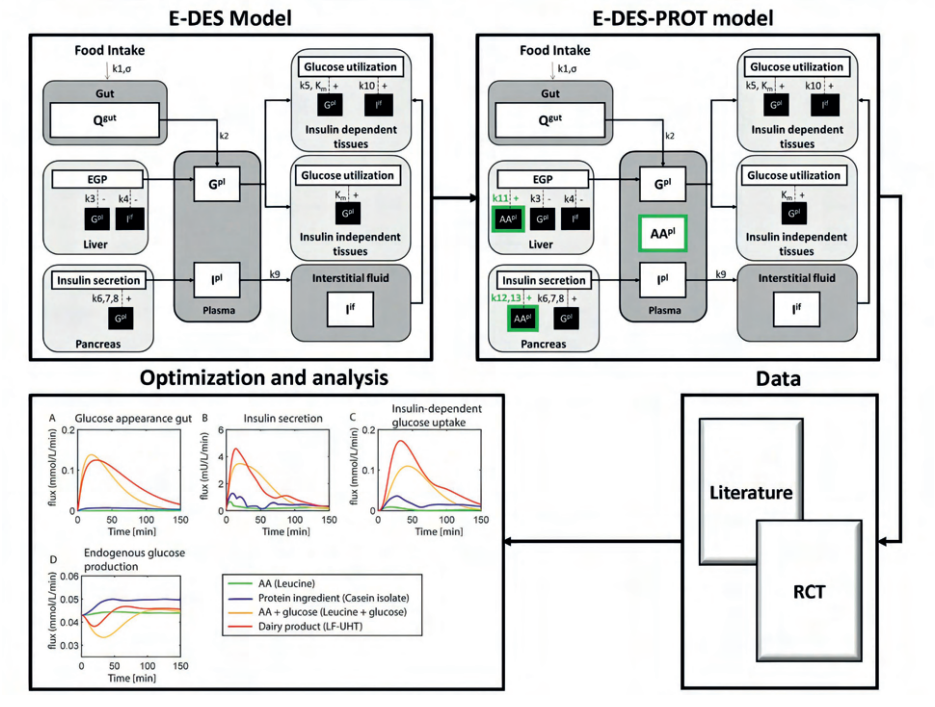


**Supplementary Figure S5: Overview of the study workflow as described in the STAR Methods section.** The E-DES model was extended (E-DES-PROT) to account for the postprandial effects of AAs and protein on glucose and insulin dynamics. Model equations were adjusted and additional parameters were introduced. Postprandial AA, glucose, and insulin time-series data from the literature and the randomized, single-blind crossover trial (RCT; NCT02546141) were used for parameter estimation. The models were evaluated using the sum of squared residuals (SSR), the Akaike Information Criterion (AIC) and Bayesian Information Criterion (BIC). Model fluxes were compared between the E-DES and the newly developed E-DES-PROT model, as well as for various meal challenges.

**Supplementary Table S3: Overview of the datasets described in the STAR Methods section.**

| Author | Challenge | Dosage | N | M/F | Mean Age (yrs) | Mean BMI (kg/m$^2$) | #G | #I | #AA |
|---|---|---|---|---|---|---|---|---|---|
| Kalogeropoulou (Kalogeropoulou et al., 2008) | AA | 7g Leucine | 13 | 6/7 | 24 | 24 | 14 | 14 | 5 |
| | AA+Glucose | 7g Leucine + 25g Glucose | 13 | 6/7 | 24 | 24 | 14 | 14 | 5 |
| Nuttall (Nuttall et al., 2008) | AA | 7.4g Isoleucine | 9 | 3/6 | 33.8 | 28 | 14 | 14 | 5 |
| | AA+Glucose | 7.4g Isoleucine + 25g Glucose | 9 | 3/6 | 33.8 | 28 | 14 | 14 | 5 |
| Kalogeropoulou (Kalogeropoulou et al., 2009) | AA | 11g Lysine | 13 | 6/7 | 30 | 26 | 14 | 14 | 5 |
| | AA+Glucose | 11g Lysine + 25g Glucose | 13 | 6/7 | 30 | 26 | 14 | 14 | 5 |
| Gannon (Gannon et al., 2002) | AA | 4.6g Glycine | 9 | 5/4 | 21-52 | 25.9 | 13 | 13 | 5 |
| | AA+Glucose | 4.6g Glycine +25g Glucose | 9 | 5/4 | 21-52 | 25.9 | 13 | 13 | 5 |
| Nuttall (Nuttall et al., 2004) | AA | 6.0g Proline | 8 | 4/4 | 28 | 23 | 14 | 14 | 5 |
| | AA+Glucose | 6.0g Proline + 25g Glucose | 8 | 4/4 | 28 | 23 | 14 | 14 | 5 |
| Nuttall (Nuttall et al., 2006) | AA | 9.7g Phenylalanine | 6 | 3/3 | 26 | 24 | 14 | 14 | 5 |
| | AA+Glucose | 9.7g Phenylalanine + 25g Glucose | 6 | 3/3 | 26 | 24 | 14 | 14 | 5 |
| Horstman (Horstman *et al.*, 2021) | Protein ingredient | 31g WPC: 24.8g protein, 2g carbohydrate, 1.6g fat | 10 | 5/5 | 66.7± 4.3 | 25.6± 2.6 | 14 | 9 | 14 |
| | Protein ingredient | 29g MCI: 25.2g protein, 2.9g carbohydrate, 0.3g fat | 10 | 5/5 | 66.7± 4.3 | 25.6± 2.6 | 14 | 9 | 14 |
| | Dairy product | 676 mL LF-UHT: 25g protein, 33.8g carbohydrate, 0.7g fat | 10 | 5/5 | 66.7± 4.3 | 25.6± 2.6 | 14 | 9 | 14 |
| | Dairy product | 694 mL LF-PAS: 25g protein, 32.6g carbohydrate, 0.7g fat | 10 | 5/5 | 66.7± 4.3 | 25.6± 2.6 | 14 | 9 | 14 |
| | Dairy product | 694 mL FF-UHT: 25g protein, 32.6g carbohydrate, 25g fat | 10 | 5/5 | 66.7± 4.3 | 25.6± 2.6 | 14 | 9 | 14 |

**Supplementary Table S3: Overview of the datasets described in the STAR Methods section. (continued)**

| Author | Challenge | Dosage | N | M/F | Mean Age (yrs) | Mean BMI (kg/m$^2$) | #G | #I | #AA |
|---|---|---|---|---|---|---|---|---|---|
| | Dairy product | 694 mL FF-PAS: 25g protein, 32.6g carbohydrate, 25g fat | 10 | 5/5 | 66.7± 4.3 | 25.6± 2.6 | 14 | 9 | 14 |
| | Dairy product | 532 mL Yoghurt: 25g protein, 21.3g carbohydrate, 0g fat | 10 | 5/5 | 66.7± 4.3 | 25.6± 2.6 | 14 | 9 | 14 |
| | Dairy product | 97g Cheese: 24.9g protein, 0g carbohydrate, 32.5g fat | 10 | 5/5 | 66.7± 4.3 | 25.6± 2.6 | 14 | 9 | 14 |

Abbreviations are: BMI: Body Mass Index; #G: Number of glucose measurement time-points; #I: Number of insulin measurement time-points; #AA: Number of AA measurement time-points; N: Number of study participants; M: Males; F: Females; WPC: Whey protein concentrate; MCI: Micellar casein isolate; LF-UHT: Low-fat untreated treated milk; LF-PAS: Low-fat pasteurized milk; FF-UHT: Full-fat untreated-treated milk; FF-PAS: Full-fat pasteurized milk

**Supplementary Table S4: Overview of the E-DES-PROT model parameters as outlined in the STAR Methods section.**

| Name | Description | Units |
|---|---|---|
| $k1$ | Rate constant of glucose appearance in the gut | 1/min |
| $k2$ | Rate constant of gut emptying | 1/min |
| $k3$ | Rate constant of ΔG suppression of EGP when $G^{pl} > G_b^{pl}$ | 1/min |
| $k4$ | Rate constant of $I^{if}$-dependent suppression of EGP | 1/min |
| $k5$ | Rate constant of insulin-dependent glucose uptake | 1/min |
| $k6$ | Rate constant of ΔG dependent insulin production | 1/min |
| $k7$ | Rate constant of ∫G dependent insulin production | 1/min |
| $k8$ | Rate constant of $\frac{dG}{dt}$ dependent insulin production | 1/min |
| $k9$ | Rate constant of insulin outflow from plasma to interstitial fluid | 1/min |
| $k10$ | Rate constant of interstitial fluid insulin utilization | 1/min |
| **$k11$** | **Rate constant of ΔAA increase of EGP when $AA^{pl} > AA_b^{pl}$** | **1/min** |

**Supplementary Table S4: Overview of the E-DES-PROT model parameters as outlined in the STAR Methods section. (continued)**

| Name | Description | Units |
|---|---|---|
| ***k*12** | **Rate constant of $\frac{dAA}{dt}$ dependent insulin production** | **1/min** |
| ***k*13** | **Rate constant of ΔAA dependent insulin production** | **1/min** |
| $\sigma$ | Shape factor of the gastric emptying pattern | dimensionless |
| $K_m$ | Michaelis-Menten constant for glucose uptake | mg/dL |

*k*11-*k*13 are included as additional parameters for the E-DES-PROT model, indicated in bold. Abbreviations are: G: Glucose; pl: Plasma; b: Basal; I: Insulin; if: Interstitial fluid; AA: Amino acids.

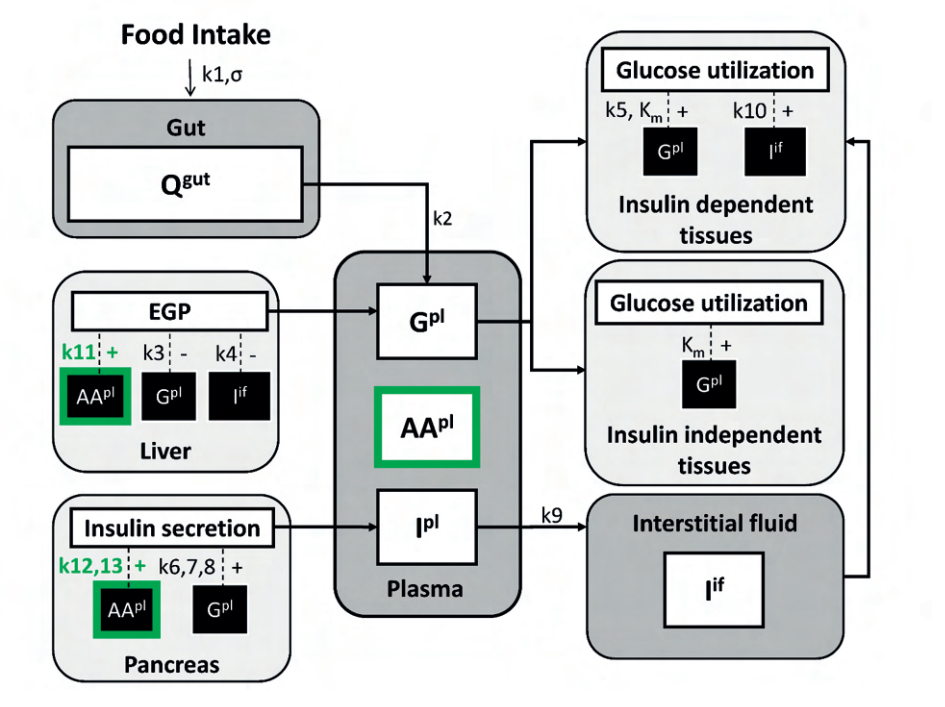


**Supplementary Fig S6: Schematic representation of the E-DES-PROT model as described in the STAR Methods section**. The dark-gray areas show the three model compartments (i.e. the gut, plasma, and interstitial fluid) used in the model. The black arrows denote the model fluxes, with corresponding parameters denoted with k. In the model, glucose enters the system via simulated ingestion in the gut ($Q^{gut}$). Plasma amino acid ($AA^{pl}$) concentration are provided as input via fitted piecewise cubic Hermite interpolating polynomial of the measured AA data. Full model equations are described in Supplemental Section S3.

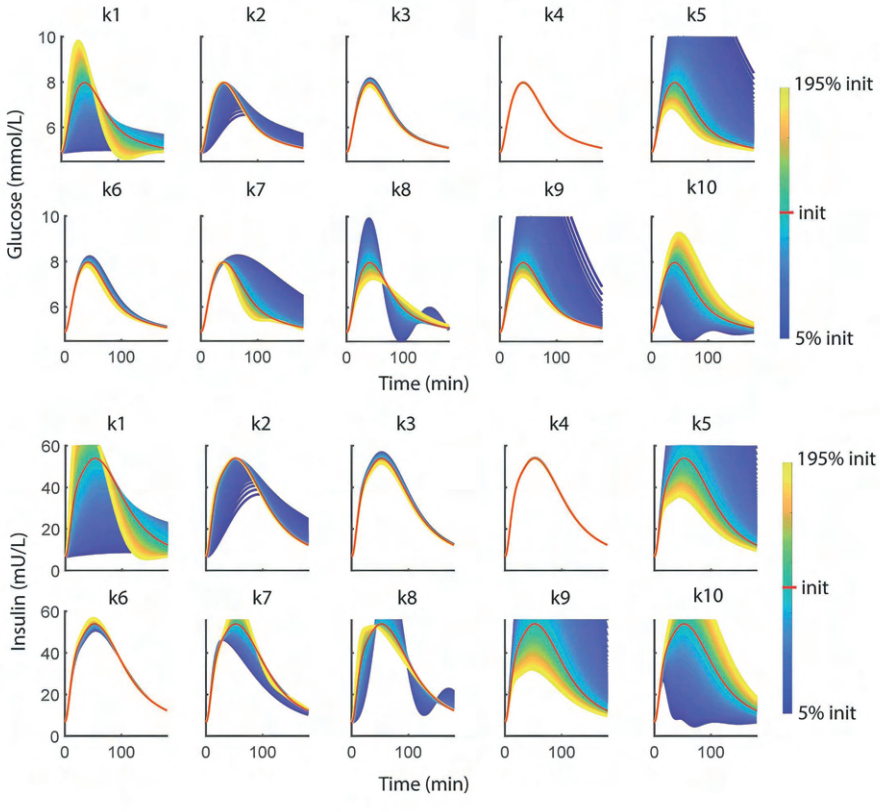


**Supplemental Figure S7: Local parameter sensitivity analysis on the simulated plasma glucose and insulin response following 75g glucose ingestion in the E-DES model as described in the STAR Methods section.** The E-DES model parameters are varied in both directions while maintaining others at a constant value. A threshold of 95% in both directions compared to the average healthy population values was selected as the limit of sensitivity.

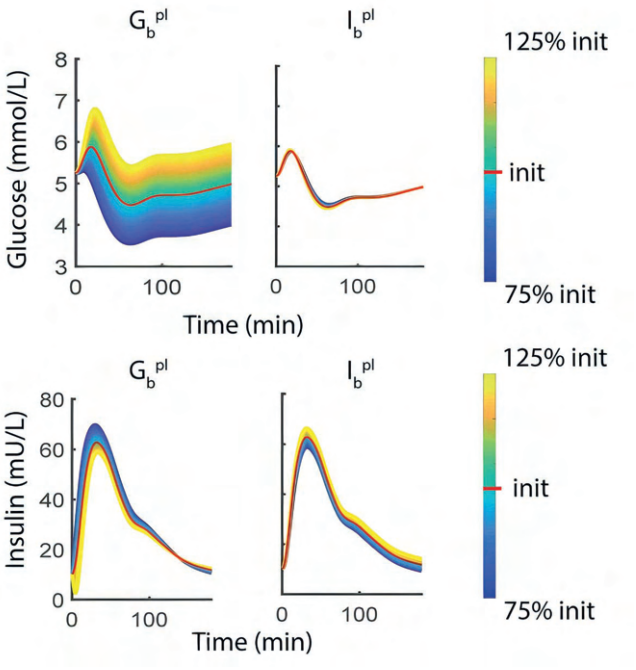


**Supplemental Figure S8: $G_b^{pl}$ and $I_b^{pl}$ sensitivity in the E-DES-PROT model as described in the STAR Methods section.** $G_b^{pl}$ and $I_b^{pl}$ were varied in both directions. A threshold of 25% in both directions compared to the average healthy population values was selected as the limit of sensitivity.

## SUPPLEMENTAL SECTION S1

**Simulated postprandial responses for all individual in the randomized single-blind crossover trial study following ingestion of protein ingredients (WPC, MCI) and cheese as described in the Results section.** The model parameters pertaining to amino acids (AAs, *k*11-*k*13) were estimated, whereas the other model parameters were kept to their original population value. The tAA input is shown in black (data and polynomial interpolation). The simulated glucose and insulin concentrations are shown in red and blue, respectively. The measured concentrations, obtained from (Horstman *et al.*, 2021), are shown as black asterisks with corresponding standard errors of the means. The leftmost column in panel A, B, and C pertains to average study population, whereas the other columns represent the individuals

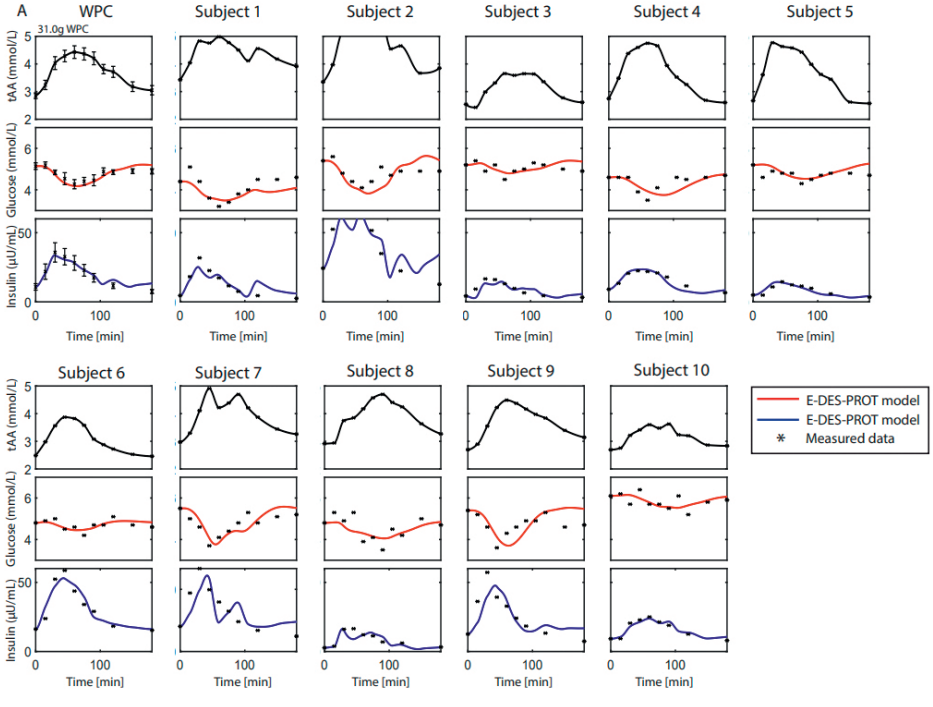

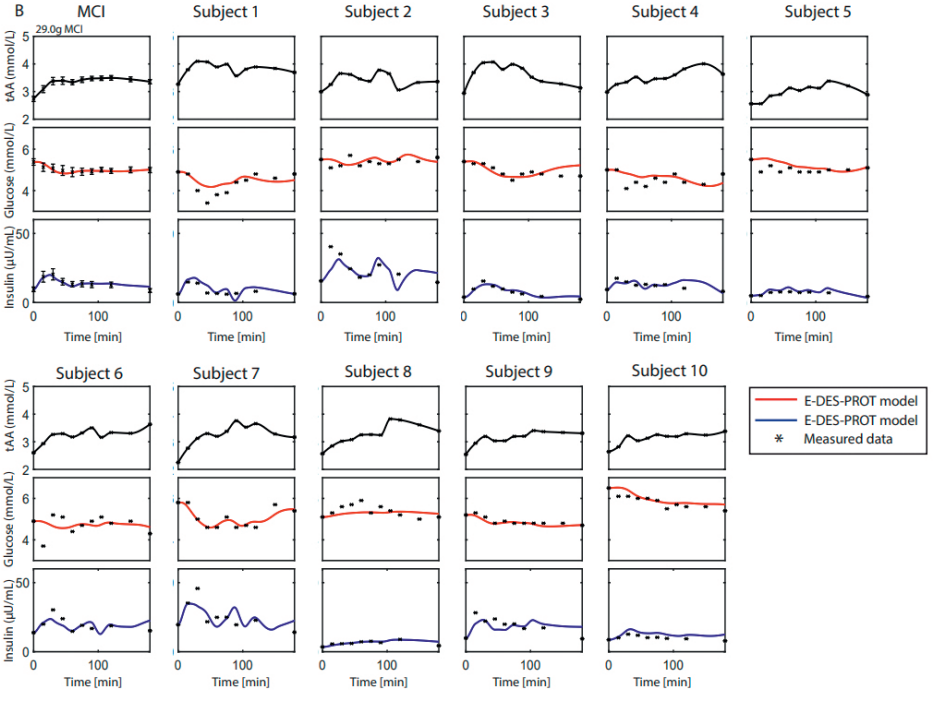
B
MCI
29.0g MCI
Subject 1
Subject 2
Subject 3
Subject 4
Subject 5
Subject 6
Subject 7
Subject 8
Subject 9
Subject 10
tAA (mmol/L)
Glucose (mmol/L)
Insulin (µU/mL)
Time [min]
E-DES-PROT model
E-DES-PROT model
Measured data

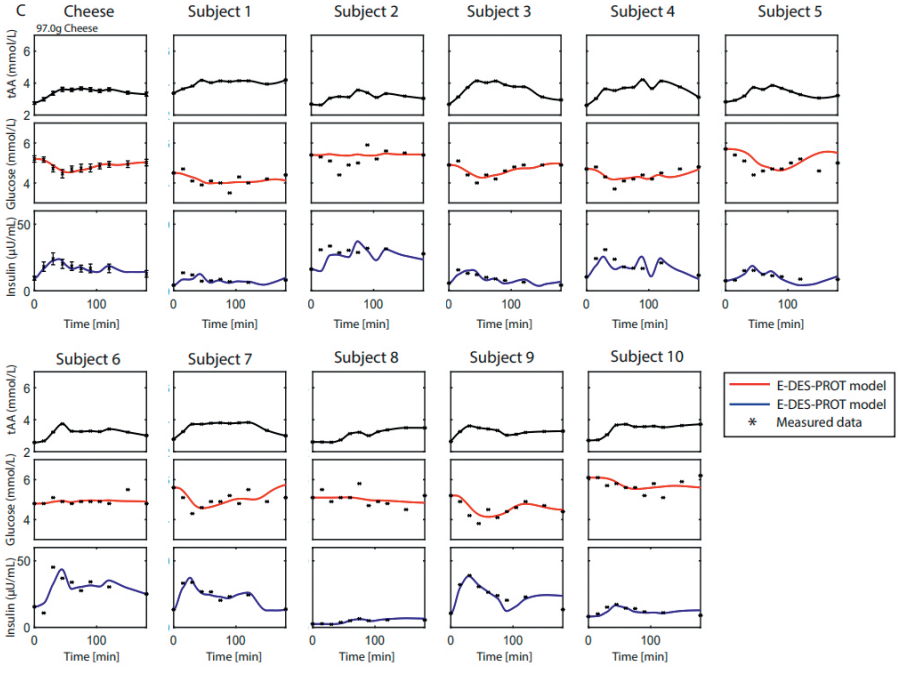
C
Cheese
97.0g Cheese
Subject 1
Subject 2
Subject 3
Subject 4
Subject 5
Subject 6
Subject 7
Subject 8
Subject 9
Subject 10
tAA (mmol/L)
Glucose (mmol/L)
Insulin (µU/mL)
Time [min]
E-DES-PROT model
E-DES-PROT model
Measured data

## SUPPLEMENTAL SECTION S2

**Simulated postprandial responses for all individuals in the randomized single-blind crossover trial study following ingestion of dairy products (LF-UHT, LF-PAS, FF-UHT, FF-PAS, and Yoghurt) as described in the Results section.** The tAA input is shown in black (data and polynomial interpolation). The simulated glucose and insulin concentrations following parameter estimation (*k*1, *k*5, *k*6, *k*8) using the original E-DES model, are shown in dashed red and blue, respectively. The simulated glucose and insulin concentrations following parameter estimation (*k*1, *k*5, *k*6, *k*8, *k*11-*k*13) using the E-DES-PROT model, are shown in red and blue, respectively. The other model parameters were kept to their original population value. The measured concentrations, obtained from (Horstman *et al.*, 2021), are shown as black asterisks with corresponding standard errors of the means. The leftmost column in panel A, B, C, D, and E pertains to average study population, whereas the other columns represent the individuals.

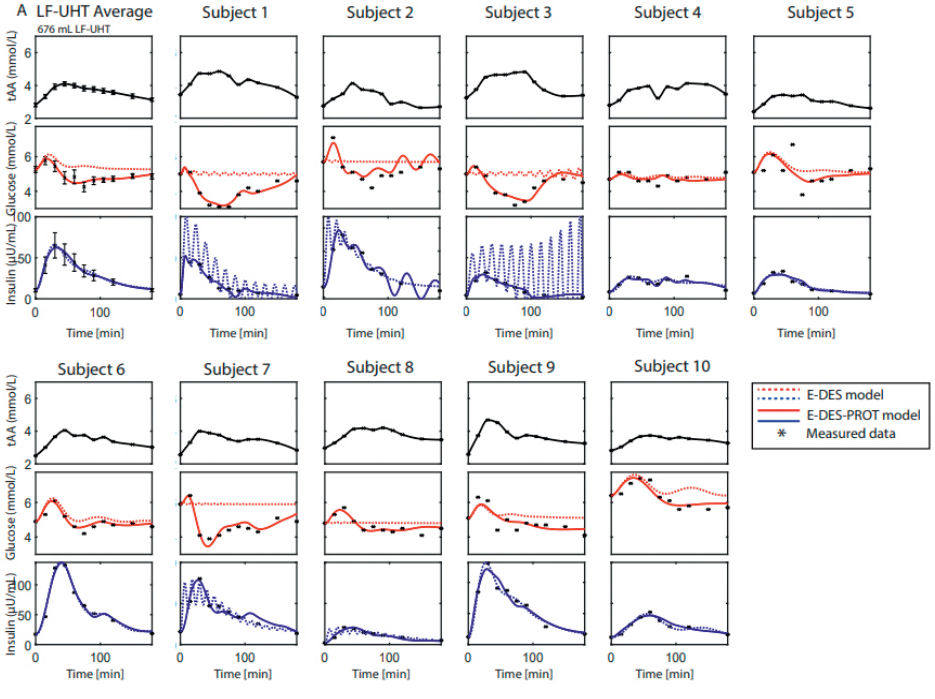

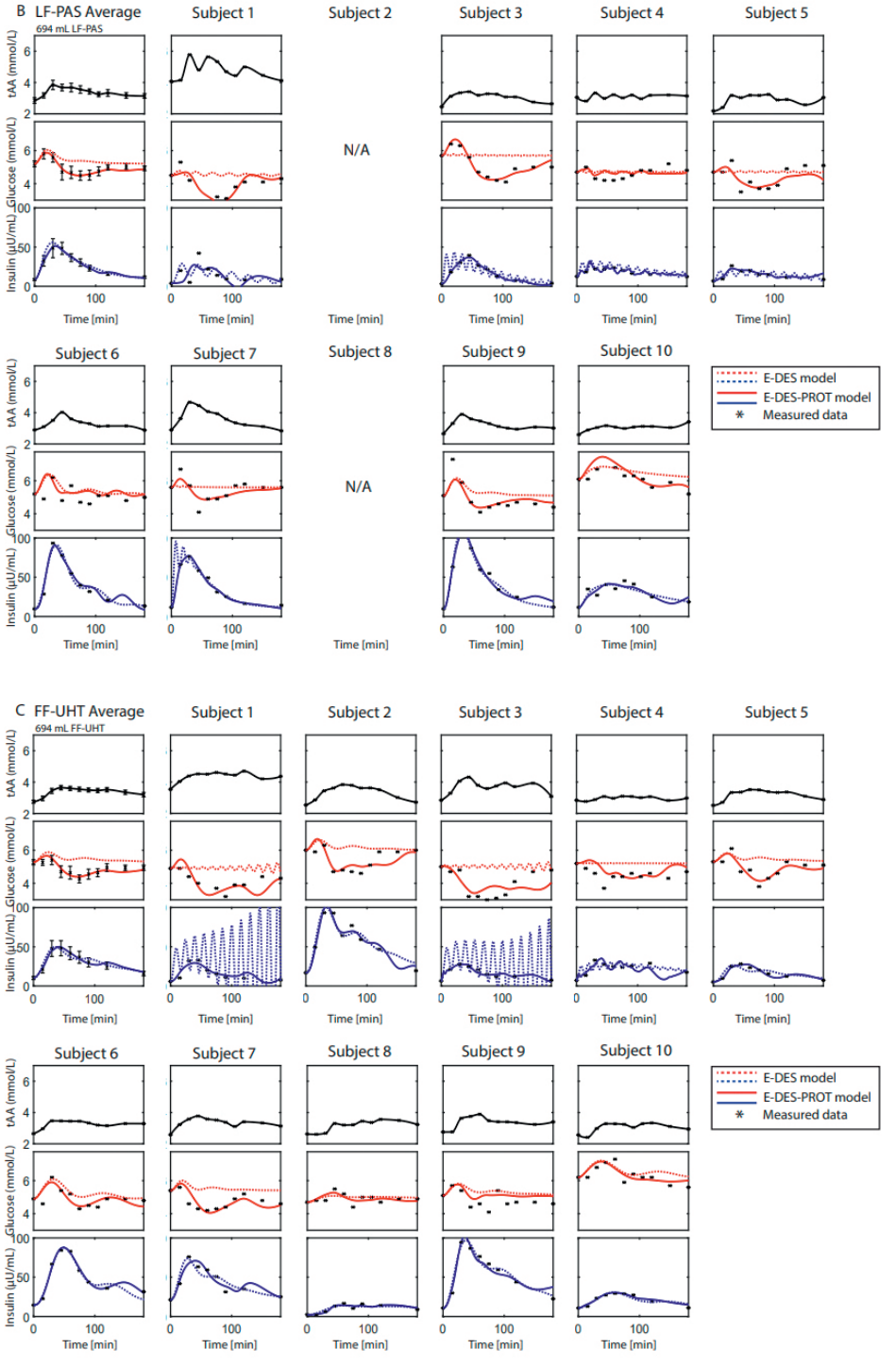
B LF-PAS Average
694 mL LF-PAS
Subject 1
Subject 2
Subject 3
Subject 4
Subject 5
Subject 6
Subject 7
Subject 8
Subject 9
Subject 10
N/A
N/A
tAA (mmol/L)
Glucose (mmol/L)
Insulin (μU/mL)
Time [min]
E-DES model
E-DES-PROT model
Measured data
C FF-UHT Average
694 mL FF-UHT

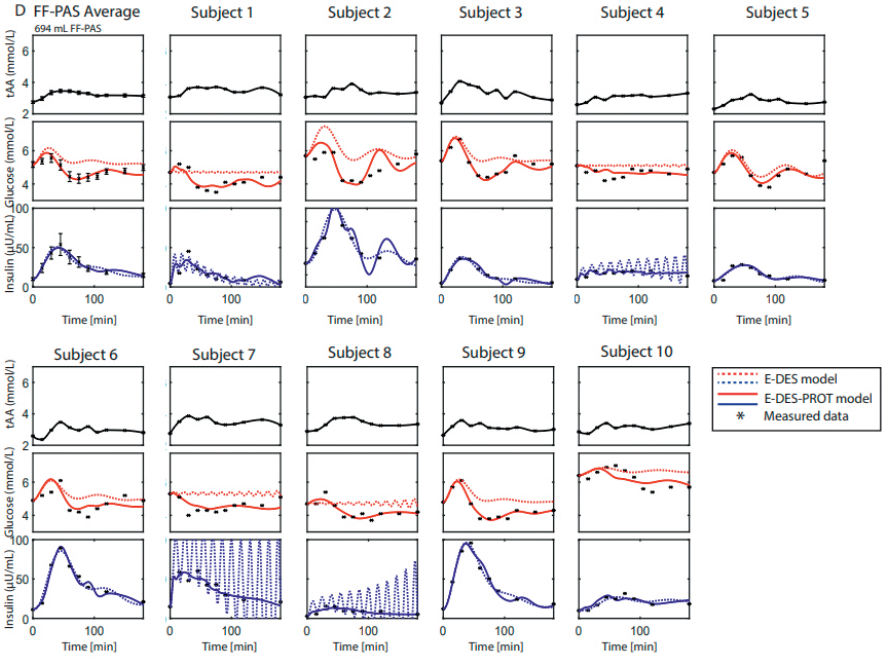
D FF-PAS Average
694 mL FF-PAS
Subject 1
Subject 2
Subject 3
Subject 4
Subject 5
Subject 6
Subject 7
Subject 8
Subject 9
Subject 10
tAA (mmol/L)
Glucose (mmol/L)
Insulin (µU/mL)
Time [min]
E-DES model
E-DES-PROT model
Measured data

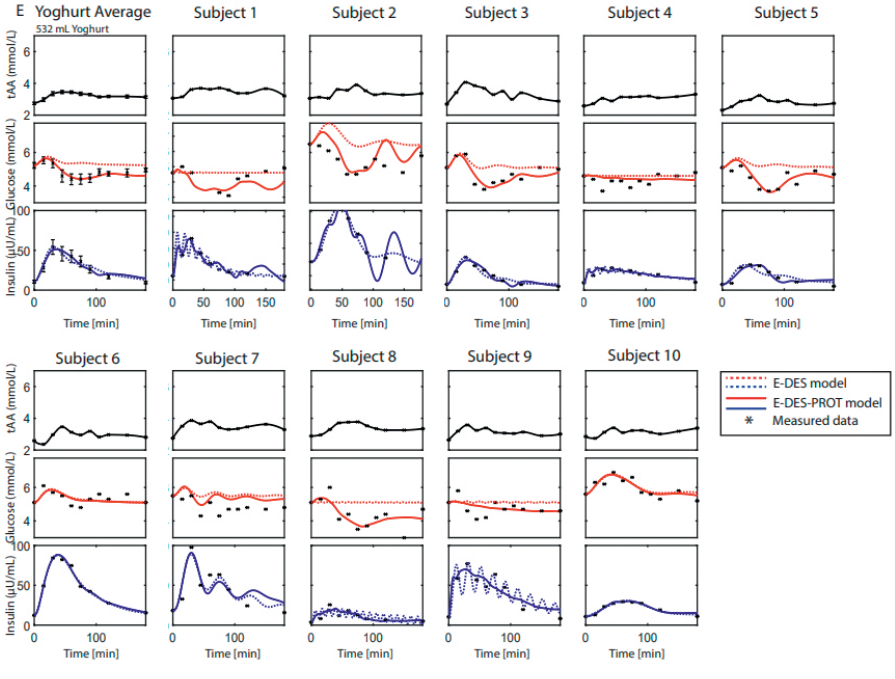
E Yoghurt Average
532 mL Yoghurt
Subject 1
Subject 2
Subject 3
Subject 4
Subject 5
Subject 6
Subject 7
Subject 8
Subject 9
Subject 10
tAA (mmol/L)
Glucose (mmol/L)
Insulin (µU/mL)
Time [min]
E-DES model
E-DES-PROT model
Measured data

## SUPPLEMENTAL SECTION S3

The current model has been adapted from [1].

## E-DES-PROT MODEL STRUCTURE

### Glucose in the gut

$$\frac{dM_G^{gut}}{dt} = m_G^{meal}(t) - m_G^{pl}(t)$$

$$m_G^{meal}(t) = \sigma k_1^{\sigma} t^{\sigma-1} \exp\left(-(k_1 t)^{\sigma}\right) D^{meal}$$

$$m_G^{pl}(t) = k_2 M_G^{gut}(t)$$

### Glucose in the plasma

$$\frac{dG_G^{pl}}{dt} = g^{liv}(t) + g^{gut}(t) - g^{non-it}(t) - g^{it}(t) - g^{ren}(t)$$

$$g^{liv}(t) = g_b^{liv} - k_3\left(G^{pl}(t) - G_b^{pl}\right) - k_4 \beta I^{if}(t) + k_{11}\left(AA^{pl}(t) - AA_b^{pl}\right)$$

$$g^{gut}(t) = \frac{f}{V_G M^b} m_G^{pl}(t) = k_2 \frac{f}{V_G M^b} M_G^{gut}(t)$$

$$g^{non-it}(t) = g_b^{liv}\left(\frac{K_m + G_b^{pl}}{G_b^{pl}}\right)\frac{G^{pl}(t)}{K_m + G^{pl}(t)}$$

$$g^{it}(t) = k_5 \beta I^{if}(t) \frac{G^{pl}(t)}{K_m + G^{pl}(t)}$$

$$g^{ren} = \begin{cases} \frac{c1}{V_G M^b}\left(G^{pl}(t) - G_{th}^{pl}\right), & if\ G^{pl} > G_{th}^{pl} \\ 0, & if\ G^{pl} \le G_{th}^{pl} \end{cases}$$

### Insulin in the plasma

$$\frac{dI^{pl}}{dt} = i^{pnc}(t) - i^{liv}(t) - I^{if}(t)$$

$$^{pnc}(t) = k_6(G^{pl}(t) - G_b^{pl}) + \left(\frac{k_7}{\tau_i}\right)\int (G^{pl}(t) - G_b^{pl})dt + \left(\frac{k_7}{\tau_i}\right) G_b^{pl} + (k_8\tau_d)\frac{dG^{pl}}{dt} + k_{12}\frac{dAA^{pl}}{dt} + {}_{13}(AA^{pl}(t) - AA_b^{pl})$$

$$i^{liv}(t) = k_7 \frac{G_b^{pl}}{\beta\tau_i I_b^{pl}} I^{pl}(t)$$

$$i^{if}(t) = k_9(I^{pl}(t) - I_b^{pl})$$

### Insulin in the interstitial fluid

$$\frac{dI^{if}}{dt} = i^{if}(t) - i^{it}(t)$$

$$i^{it} = k_{10}(I^{if}(t))$$

## E-DES-PROT MODEL INPUTS, FLUXES AND CONSTANTS

Table 1: Overview of the E-DES-PROT model (input) variables

| Name | Description | Units |
|---|---|---|
| $t$ | Time | min |
| $M_G^{gut}$(t) | Glucose mass in the gut | mg |
| $G^{pl}$(t) | Plasma glucose concentration | mmol/L |
| $I^{pl}$(t) | Plasma insulin concentration | mU/L |
| $AA^{pl}$(t) | Plasma amino acid concentration | µmol/L |
| $I^{if}$(t) | Interstitial fluid insulin concentration | mU/L |
| $D^{meal}$ | Glucose intake | mg |
| $M^b$ | Body mass | kg |

Table 2: Overview of the E-DES-PROT model fluxes

| Name | Description | Units |
|---|---|---|
| $m_G^{meal}(t)$ | Glucose mass entering from stomach | mg/min |
| $m_G^{pl}(t)$ | Glucose mass leaving to plasma | mg/min |
| $g^{liv}(t)$ | Glucose production by the liver (EGP) | mmol/L/min |
| $g^{gut}(t)$ | Glucose entering from the gut | mmol/L/min |
| $g^{non-it}(t)$ | Glucose uptake by insulin-independent tissue | mmol/L/min |
| $g^{it}(t)$ | Glucose uptake by insulin-dependent tissue | mmol/L/min |
| $g^{ren}(t)$ | Renal glucose elimination | mmol/L/min |
| $I^{pnc}(t)$ | Pancreas insulin secretion | mU/L/min |
| $I^{if}(t)$ | Insulin flowing into interstitial fluid | mU/L/min |
| $I^{liv}(t)$ | Insulin uptake by the liver | mU/L/min |
| $I^{it}(t)$ | Insulin usage by insulin-dependent tissue | mU/L/min |

Table 3: Overview of the E-DES-PROT model constants

| Name | Description | Units | Value |
|---|---|---|---|
| $G_b^{pl}$ | Basal plasma glucose | mmol/L | $G_b^{pl}(0)$ |
| $I_b^{pl}$ | Basal plasma insulin | mU/L | $I_b^{pl}(0)$ |
| $AA_b^{pl}$ | Basal plasma amino acid | µmol/L | $AA_b^{pl}(0)$ |
| $g_b^{liv}$ | Basal endogenous glucose production | mmol/L/min | 0.043 |
| $G_{th}^{pl}$ | Renal threshold | mmol/L | 9 |
| $V_G$ | Glucose distribution volume in plasma | L/kg | 17/70 |
| β | Unit conversion factor from glucose to insulin | (mmol/L)/(mU/L) | 1 |
| $f$ | Unit conversion factor from mmol to mg glucose | mmol/mg | 0.005551 |
| $\tau_i$ | Integral time constant | min | 31 |
| $\tau_d$ | Derivative time constant | min | 3 |
| $c1$ | Rate constant of glomerular filtration | 1/min | 0.1 |

## E-DES-PROT MODEL PARAMETER VALUES

Table 4: Parameter values for reference simulation: Average LF-UHT

| Name | Description | Units | Value |
|---|---|---|---|
| $k1$ | Rate constant of glucose appearance in the gut | 1/min | 0.0155 |
| $k2$ | Rate constant of gut emptying | 1/min | 0.28 |
| $k3$ | Rate constant of ΔG suppression of EGP when $G^{pl} > G_b^{pl}$ | 1/min | 6.07e-3 |
| $k4$ | Rate constant of $I^{if}$-dependent suppression of EGP | 1/min | 2.35e-4 |
| $k5$ | Rate constant of insulin-dependent glucose uptake | 1/min | 0.087 |
| $k6$ | Rate constant of ΔG dependent insulin production | 1/min | 3.01 |
| $k7$ | Rate constant of ∫G dependent insulin production | 1/min | 1.15 |
| $k8$ | Rate constant of dG/dt dependent insulin production | 1/min | 10.99 |
| $k9$ | Rate constant of insulin outflow from plasma to interstitial fluid | 1/min | 3.83e-2 |
| $k10$ | Rate constant of interstitial fluid insulin utilization | 1/min | 0.28 |
| $k11$ | Rate constant of ΔAA increase of EGP when $AA^{pl} > AA_b^{pl}$ | 1/min | 1.25e-7 |
| $k12$ | Rate constant of dAA/dt dependent insulin production | 1/min | 1.85e-3 |
| $k13$ | Rate constant of ΔAA dependent insulin production | 1/min | 3.40e-2 |
| $\sigma$ | Shape factor of the gastric emptying pattern | dimensionless | 1.34 |
| $Km$ | Michaelis-Menten constant for glucose uptake | mg/dL | 13.2 |

## REFERENCES

[1] Rozendaal, Y.J. (2018). *Model-based analysis of postprandial glycemic response dynamics for different types of food*.

## SUPPLEMENTAL SECTION S4

The MATLAB implementation of the E-DES-PROT model code has been deposited in GitHub (https://github.com/BartvSloun/E-DES-PROT)

# Quantifying postprandial glucose responses using a hybrid modelling approach: combining mechanistic and data-driven models in The Maastricht Study

# 5

**Balázs Erdõs*, Bart van Sloun*, Gijs H. Goossens, Shauna D. O'Donovan, Simone J.M.P. Eussen, Bastiaan E. de Galan, Marleen M.J. van Greevenbroek, Coen D.A. Stehouwer, Miranda T. Schram, Ellen E. Blaak, Michiel E. Adriaens, Natal A.W. Riel , Ilja C.W. Arts.** *These authors contributed equally to this work

*PloS One. 2023 Jul 27:18(7)e0285820*

## ABSTRACT

Computational models of human glucose homeostasis can provide insight into the physiological processes underlying the observed inter-individual variability in glucose regulation. A range of modelling approaches, including ”bottom-up” mechanistic and ”top-down” data-driven techniques have been applied to untangle the complex interactions underlying progressive disturbances in glucose homeostasis. While both approaches offer distinct benefits, a combined approach taking the best of both worlds has yet to be explored. Here, we propose a sequential combination of a mechanistic and a data-driven modelling approach to quantify individuals' glucose and insulin responses to an oral glucose tolerance test, using cross sectional data from 2968 individuals from a large observational prospective population-based cohort, the Maastricht Study. The best predictive performance, measured by $R^2$ and mean squared error of prediction, was achieved with personalized mechanistic models alone. The addition of a data-driven model did not improve predictive performance. The personalized mechanistic models consistently outperformed the data-driven and the combined model approaches, demonstrating the strength and suitability of bottom-up mechanistic models in describing the dynamic glucose and insulin response to oral glucose tolerance tests.

## INTRODUCTION

Maintaining glucose homeostasis within a narrow physiological range is essential for normal body function. When glucose levels are elevated (i.e. following meal intake), the hormone insulin is secreted from pancreatic β-cells to promote glucose uptake in peripheral organs and suppress hepatic glucose production [1]. In individuals with insulin resistance there is an impairment in the uptake of glucose by the insulin-dependent tissues (i.e. muscle, and fat), and in the suppression of hepatic glucose production. The increased demand on pancreatic β-cell to produce and secrete more insulin may eventually lead to β-cell dysfunction, which is the key factor in the development of type 2 diabetes mellitus (T2DM), and is characterized by persistent hyperglycemia [2]. The pathophysiology of T2DM is known to be heterogeneous with differences in the severity of insulin resistance and progression of β-cell dysfunction [3]. Physiology-based mathematical models of the glucose-insulin regulatory system have long been used to provide qualitative and quantitative information on relevant physiological processes governing postprandial glucose and insulin dynamics [4–6]. The Eindhoven-Diabetes-Education simulator (eDES) is a comparatively simple model of human insulin-regulated glucose metabolism describing the most crucial reactions involved in postprandial glucose regulation through a system of coupled differential equations [6, 7]. The reactions described by this model are regulated by rate parameters, which can be estimated from postprandial glucose and insulin time-series data. In our previous work, we successfully applied a parsimonious eDES model estimating only 4 parameters governing gastric emptying, endogenous insulin secretion and insulin-dependent glucose disposal into tissues, to quantify the postprandial glucose and insulin responses following the intake of an oral glucose load in a large population of overweight or obese but otherwise healthy individuals [8]. Our results showed that most of the individuals' responses were accurately estimated with the eDES model, nevertheless we have identified some cases where the mechanistic model struggled to capture the response. While, the intra-individual variability in the postprandial responses can be largely explained by the mechanisms of glucose regulation encoded in the eDES model, it is known that other factors such as diet, physical activity, sleep and stress may affect glucose regulation [9, 10]. However, such factors are not directly included in the eDES model and their implementations within the mechanistic model may be inconvenient requiring excessive experimentation.

Besides physiology-based mathematical models, the application of data-driven prediction models have gained substantial interest in diabetes research, providing insight into factors contributing to, as well as predicting glucose responses to nutrient intake [11–14]. Such approaches aim to exploit the large amounts of heterogeneous data available, to find informative patterns in a data-driven way. Notably, Zeevi and colleagues [14] have shown that a machine-learning model trained on a wide variety of phenotypic information was able to accurately predict the magnitude of postprandial glucose excursions. While mechanistic models of the glucose regulatory system describe the change in glucose (and insulin) levels according to known physiological phenomena, they are limited in their scope and accuracy by the understanding of the underlying physiology as well as the availability of invasive measurements in model building. In comparison, data-driven models allow a convenient framework to integrate diverse data that may have relevance in glucose regulation without the need for a causal understanding. Recently, the bottom up and top down modelling strategies outlined above have been successfully combined to improve simulation accuracy in the field of systems biology [15–17]. Here, we combine a mechanistic model with a data-driven model to identify factors predictive of inter-individual differences in glucose and insulin dynamics following an oral glucose tolerance test (OGTT) in a large group (n=2968) of individuals with various glucometabolic status (including normal glucose metabolism (NGM), prediabetes, as well as T2DM) participating in a population-based cohort study (The Maastricht Study) [18]. The aim of the present study was to investigate the predictive performance (explained variance, error of prediction) in simulating the postprandial glucose and insulin levels following an OGTT in individuals using the mechanistic eDES model, a data-driven model and a hybrid combination of the two. In addition, we compared the predictive performance between the various models and evaluated the factors underlying the inter-individual differences in the responses as derived from the models.

## METHODS

### Data availability

The data of this study derive from The Maastricht Study, but restrictions apply to the availability of these data, which were used under license for the current study. Data are, however, available from the authors upon reasonable request and with permission of The Maastricht Study management team.

## Data

Data from The Maastricht Study, an observational prospective population-based cohort study [18] was used in this work. Briefly, The Maastricht Study focuses on the etiology, pathophysiology, complications, and comorbidities of T2DM, and is characterized by an extensive phenotyping approach. Individuals aged between 40 and 75 years and living in the southern part of the Netherlands were eligible for participation. Participants were recruited through mass media campaigns and from mailings through the municipal registries and the regional Diabetes Patient Registry. Known T2DM status was used in stratifying the recruitment process for efficiency. The present report includes data from the first 3451 participants who completed the baseline survey between November 2010 and September 2013. All examinations were performed within a three-month time window; the OGTT and vascular measurements were performed during different research visits. The study has been approved by the institutional medical ethical committee (NL31329.068.10) and the Minister of Health, Welfare and Sports of the Netherlands (Permit 131088–105234-PG). All participants gave written informed consent.



*Oral glucose tolerance test*

Following an overnight fast, participants underwent a standardized two-hour 75 g oral glucose tolerance test (OGTT) in order to determine glucose metabolism status [18]. Blood samples were taken under fasting conditions (t=0) and 15, 30, 45, 60, 90 and 120 minutes after ingestion of the glucose drink and plasma glucose and insulin concentrations were determined. Individuals relying on external insulin did not undergo the OGTT. Furthermore, individuals with more than two missing samples or missing samples at baseline (t=0) or 2 hour post-load were excluded from the analysis.

*Deep phenotyping features*

A selection of health-related features from The Maastricht Study were used in order to provide a holistic picture of the individuals' health state. These features pertain to health behavior (e.g. diet, physical activity, smoking), cardiovascular health, musculoskeletal health, metabolic and demographic characteristics, body composition and biomarkers. In total 49 features were selected by a set of co-authors who are experts in the field of metabolism/diabetes. The continuous variables were transformed to zero mean and unit variance, while the categorical variables were dummy coded prior to modelling. Details about the measurements can be found in [18]. A complete list of the features used in this work is provided in the S1 Appendix of the Supplementary Material.

## Computational modelling of glucose regulation

*Models*
In the present study, a variety of modelling scenarios were explored, including mechanistic models, data-driven models, and a hybrid combination of both models.

*Eindhoven Diabetes Education Simulator*
The Eindhoven Diabetes Education Simulator (eDES, version 2.0) published by Maas and colleagues [6, 7] was employed in this study. The eDES model is a physiology-based mathematical model of the glucose regulatory system in healthy people and people with type 1 and type 2 diabetes. The eDES model consists of a gut and plasma compartment, in which the change in mass or concentration of either glucose or insulin over time is described using coupled differential equation (full details provided in [8]). The reactions included in the model are controlled by rate parameters, which have been estimated and validated using OGTTs from multiple healthy populations [7]. The eDES model was implemented and analysed in MATLAB 2018b (The Mathworks, Inc., Natick, Massachusetts, United states). Model parameters were estimated through minimizing the sum of squared residuals (SSR) in the model prediction for glucose and insulin using a non-linear least squares solver in MATLAB (*lsqnonlin*).

In order to provide personalized simulation of glucose and insulin concentrations using the eDES model, we implemented the model selection approach that we have developed previously [8]. Briefly, the workflow reduces the number of model parameters estimated to provide an accurate and reliable description of individual postprandial glucose and insulin responses. To obtain the most sensitive, parsimonious and identifiable model parameter set, the following steps were undertaken (full details available in [8]). First, a local parameter sensitivity analysis (LPSA) was performed to identify the most sensitive parameters for estimation. Second, a set of all the possible combinations of 3 or more sensitive parameters were generated. These were then fit on representative responses to oral glucose intake of individuals with different glucometabolic status (i.e. normal glucose metabolism (NGM), impaired fasting glucose (IFG), impaired glucose tolerant (IGT), both IFG and IGT (IFG&IGT), and T2DM); based on the American Diabetes Association (ADA) diagnosis criteria values [19], the most extreme responses of the Maastricht Study dataset, and on the largest and smallest response in the dataset by area under the glucose curve (Min, Max). The initial values for glucose and insulin in the eDES model were set to be equal to the

t=0 measurement of the response, and the setpoint parameters $G_b^{pl}$ (basal plasma glucose) and $I_b^{pl}$ (basal plasma insulin) were also set to these initial values (t=0). The candidate model with the lowest Akaike Information Criterion (AIC) score across the set of representative curves was selected as most parsimonious model, which was further evaluated for identifiability using Profile Likelihood Analysis (PLA) [20]. The estimated model parameters resulting from the model selection pertain to gut emptying ($k1$), insulin sensitivity ($k5$) or insulin secretion ($k6$ & $k8$) described in Table S1 and in more detail in [8].

The parameter space of the personalized eDES model is visualized by reducing the number of dimensions from the number of estimated parameters to two dimensions using principal component analysis (PCA). Prior to PCA, the parameter values were log-transformed and normalized to zero mean and unit standard deviation.



*Gradient boosting regression and training scheme*

The targets of the data-driven prediction model were the postprandial glucose and insulin concentrations following the OGTT or the corresponding glucose and insulin simulation using the mechanistic model depending on the modelling scenario. In order to allow non-linear relationships between the targets and the predictors (i.e. features), we built XGBoost models based on gradient boosting regression (GBR) [21, 22]. GBR works by combining the prediction of many different decision trees that were inferred sequentially by training the tree on the residual of the previous trees. A wide range of phenotypic, demographic and lifestyle characteristics of the individuals (full details in supplementary material) were selected and used as predictors in the gradient boosting regression models.

The GBR models were trained in a nested cross-validation framework in order to provide an unbiased estimation of model performance as described by Cawley and Talbot [23]. Standardization of the numeric features was carried out within each fold to avoid introducing positive bias to the estimates. Hyperparameter tuning was carried out with the options described in Table S3 of the supplementary material. The objective function to be minimized in training was the mean squared error. The reported performance estimates are the mean squared error of prediction (MSE) and the coefficient of determination ($R^2$). The accuracy ($R^2$) and prediction error (MSE) in the model predictions of the outlined scenarios are than evaluated at the time points of the OGTT and compared for the different approaches. The performance estimates were calculated in the outer 5-fold

cross validation (CV), with the inner loop (also 5-fold CV) carrying out a limited hyperparameter search independently of the model training procedure. Relative feature importances are reported as the variance (MSE) reduction weighted by the proportion of samples reaching the node across all trees [24].

*Hybrid approach*

In addition to using the eDES and GBR models separately, we also employed a hybrid approach combining these two models. This hybrid model consists of sequentially joining the prediction of the eDES model and a GBR model. First, the eDES model is used to capture measured postprandial glucose and insulin time series data, from which we determine and store the residuals (i.e. difference between predicted and measured data-points). Gradient boosting regression models are than built to predict these residuals independently per time-point of the postprandial glucose and insulin measurements thereby linking the two models together.

*Modelling scenarios*

A variety of modelling scenarios are evaluated and compared in terms of coefficient of determination ($R^2$) and mean squared error of prediction (MSE). The modelling scenarios are selected in order to allow the comparison of mechanistic with data-driven as well as their sequential combinations. The underlying models used in this work are the Eindhoven Diabetes Education Simulator (eDES) and Gradient Boosting Regression (GBR). All models work by predicting the postprandial glucose and insulin concentrations of the OGTT. The modelling scenarios are detailed below.

- Reference healthy eDES
- Reference GBR
- Hybrid I. (reference eDES + GBR)
- Personalized eDES model
- Hybrid II. (personalized eDES + GBR)

For the Reference healthy eDES scenario, the median glucose and insulin responses to the OGTT in the Maastricht Study are calculated by taking the median of the measurements per time-point of the OGTT across NGM individuals. The eDES model parameters identified in the model selection are then estimated on the median glucose and insulin responses. The Reference GBR scenario consists of GBR models estimated for each time-point of the OGTT response to predict the corresponding glucose and insulin concentrations, using the approach

described in Section Gradient boosting regression & training scheme. In the Hybrid I scenario, a combined approach is used in which the residuals in the individuals' OGTT response resulting from the reference healthy eDES are used as targets for the GBR models, thereby sequentially joining the two approaches. In the Personalized eDES model scenario, the eDES is personalized using the approach described in Section Eindhoven-Diabetes Education Simulator for individuals in the Maastricht Study. For the Hybrid II scenario, the residuals in the individual OGTT responses resulting from the personalized eDES models are used as targets for the GBR models.

## RESULTS

A total of 2968 participants were included in the analysis after excluding individuals with missing data on 2 or more time points of the 7-points OGTT measurements, missing measurement at baseline (t=0) or 2 hours post-load (n=483). Out of the 2968 included individuals 1436 (48%) were normoglycaemic, 906 (31%) demonstrated impaired glucose metabolism (IFG and/or IGT) and 625 (21%) had type 2 diabetes. The characteristics of the study population are depicted in Table 1.



### Prediction task properties

To demonstrate the prediction task, an example of an individual's OGTT response with corresponding simulation using the different modelling scenarios is provided in Fig 1. The various modelling scenarios aimed to capture the measured data, denoted with black crosses. The discrepancy between the simulated glucose and insulin responses (in blue and orange, respectively) and the measured data-points, termed residuals, were summarized across individuals by calculating the error of prediction (MSE) and the explained variance ($R^2$), and were used as comparison between the different modelling approaches in the following paragraph. As observed from this example, the personalized eDES and Hybrid II approaches produced perfect predictions of the first (t=0) glucose and insulin time-points. However, this resulted from the first measurement being supplied to the eDES model as initial values. Therefore, in these scenarios the performance measures (MSE, $R^2$) were not reported.

**Table 1**. Descriptive characteristics of the study population

| | Total | NGM | IFG | IGT | IFG&IGT | T2DM |
|---|---|---|---|---|---|---|
| Characteristic | n=2968 | n=1436 | n=529 | n=134 | n=243 | n=625 |
| Sex (%*male*) | 51 | 39 | 65 | 37 | 55 | 68 |
| Age (*years*) | 59.8 (8.2) | 57.6 (8.3) | 59.7 (7.6) | 60.9 (8.1) | 63.3 (7.1) | 63.1 (7.4) |
| BMI ($kg/m^2$) | 26.8 (4.3) | 25.2 (3.5) | 27.1 (3.9) | 27.1 (4.1) | 28.7 (4.5) | 29.4 (4.7) |
| HbA1c (*mmol/mol*) | 39.3 (6.9) | 35.7 (3.7) | 38.1 (4.1) | 37.0 (4.0) | 40.3 (4.7) | 48.7 (7.0) |
| Matsuda index | 4.0 (2.7) | 5.2 (2.8) | 3.4 (2.0) | 3.4 (1.9) | 2.5 (2.0) | 2.3 (1.7) |

NGM: normal glucose metabolism, IFG: impaired fasting glucose, IGT: impaired glucose tolerance, T2DM: type 2 diabetes mellitus
Matsuda index is calculated as $10000/(G_{t0} * I_{t0} * \overline{G} * \overline{I})^{1/2}$, where $G_{t0}$, $\overline{G}$ and $I_{t0}$, $\overline{I}$ are the t=0 and average glucose and insulin measurements of the 7-point OGTT in *mg/dl* and μU/L, respectively. Calculated when t=0 and t=120 measurements were available. Values are means (standard deviations)

## Modelling Scenarios: Explained variance and error of prediction

An overall comparison of how well the different modelling scenarios (Reference healthy eDES model, Reference GBR, Hybrid I, Personalized eDES model, and Hybrid II) perform in predicting the postprandial glucose and insulin levels is shown in Fig 2 and in Table S2 of the supplementary material. The $R^2$ (Fig 2, panel A) and MSE (Fig 2, panel B) are provided for all the glucose and insulin time-points following the OGTT. The first glucose and insulin time-point for the personalized eDES model and Hybrid II approach are not provided as these are used as initial values for glucose and insulin simulation via the eDES model.

For the Reference healthy eDES scenario, the eDES model parameters $k1$, $k5$, $k6$, $k8$ were estimated on the NGM median OGTT response. The MSE ranged between 1.79 and 29.35 for glucose, 73.95 and 7205.55 for insulin, across all time-points (MSE and $R^2$ values are provided in the supplementary table). The MSE appeared to increase with respect to time, up until the 6th time-point. The $R^2$ ranges between -0.62 and -0.30 for glucose, -0.03 and -0.25 for insulin, across all time-points. The negative explained variance indicates that the model is likely mis-specified for the majority of the OGTT responses. For the Reference GBR scenario, the GBR models were estimated for each time-point of the OGTT responses to predict the corresponding glucose and insulin concentrations using the features outlined in the methods section. The MSE ranges between 0.37 and 4.88 for glucose, 32.59 and 3857.80 for insulin, across all time-points. The MSE appears to increase with time, up until the 6th time-point. The $R^2$ ranges between 0.58 and 0.77 for glucose, 0.21

and 0.46 for insulin, across all time-points. For the Hybrid I scenario, a hybrid approach was used in which the residuals in the individuals' OGTT responses as predicted by the reference healthy eDES are used as targets for the GBR models. The MSE ranges between 0.38 and 4.87 for glucose, 32.73 and 3877.16 for insulin, across all time-points.

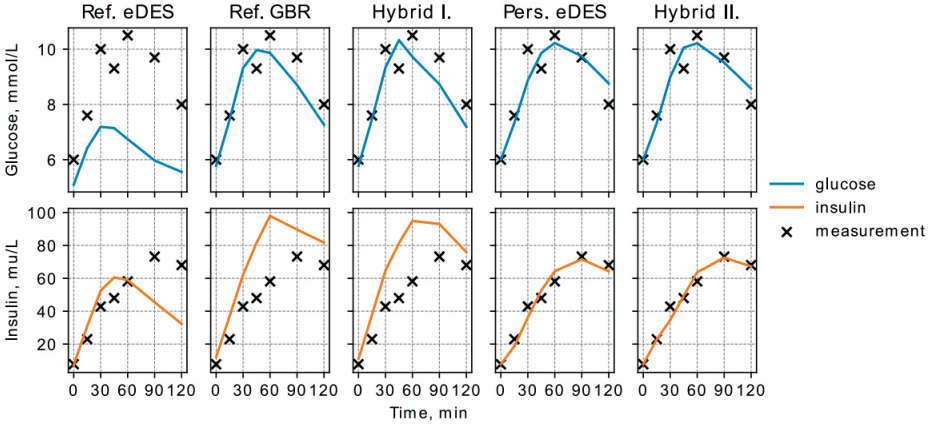


**Figure 1**. Simulated glucose (blue line) and insulin (orange line) responses of a study participant following an OGTT using the modelling scenarios. The crosses denote the measured glucose and insulin concentrations.

The MSE appears to increase with time, up until the 6th time-points. The $R^2$ ranges between 0.58 and 0.77 and 0.21 and 0.45 for glucose and insulin respectively, across all time-points. For the Personalized eDES model scenario, the eDES model is personalized through estimating eDES model parameters 1,5,6,8 for individual OGTT responses in the Maastricht Study. The MSE ranges between 0.49 and 0.77 for glucose, 161.03 and 1177.05 for insulin, across all time-points. The MSE appears to increase with time, up until the last (7th) time-point. The $R^2$ ranges between 0.75 and 0.97 for glucose, 0.78 and 0.91 for insulin, across all time-points. For the Hybrid II scenario, the residuals in the individual OGTT responses obtained by the personalized eDES models are used as targets for the GBR models. The MSE ranges between 0.47 and 0.77 for glucose, 148.30 and 1220.46 for insulin, across all time-points. The MSE appears to increase with time, up until the 7th time-points. The $R^2$ ranges between 0.77 and 0.97 for glucose, 0.79 and 0.91 for insulin, across all time-points.

When comparing the different modelling scenarios, the reference eDES model appeared to perform the worst across all glucose and insulin time-points, showing the largest MSE and the lowest $R^2$. The data-driven XGBoost performed

better than the reference eDES model (81% and 42% decrease in MSE and 248% and 325% increase in $R^2$ for glucose and insulin across all time-points). Combining the reference eDES model with XGBoost (Hybrid I) resulted in an almost identical performance (81% and 42% decrease in MSE and 248% and 323% increase in $R^2$ for glucose and insulin across all time-points). The personalized eDES model performed much better than the reference eDES model or the XGBoost model (96% and 85% decrease in MSE and 296% and 690% increase in $R^2$ for glucose and insulin across all time-points when compared to the reference eDES model). Combining the personalized eDES model with XGBoost (Hybrid II) resulted in an almost identical performance (96% and 85% decrease in MSE and 298% and 693% increase $R^2$ for glucose and insulin across all time-points).

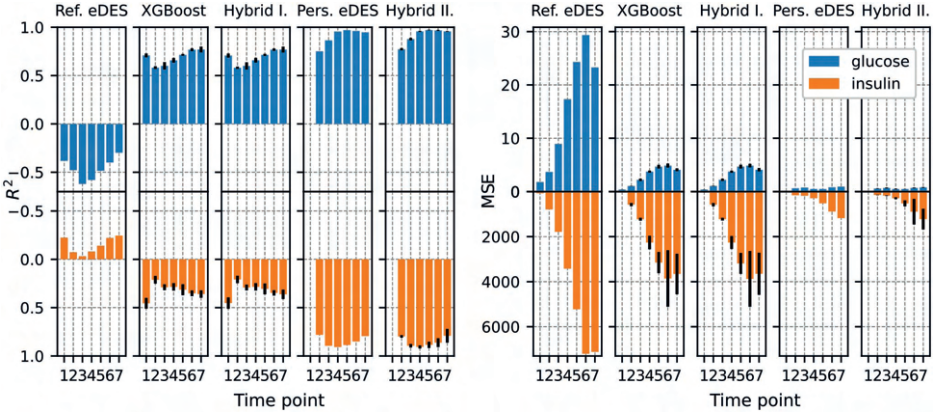


**Figure 2.** Explained variance ($R^2$ ; panel A) and mean squared error (MSE; panel B) per glucose and insulin time-points following OGTT for the modelling scenarios

## Modelling Scenarios: Derivable information

Both the mechanistic models and the data-driven models allow insight into factors underlying the OGTT responses. In the case of the mechanistic eDES model the tuned model parameters represent physiological properties such as gut emptying or insulin secretion. Whereas the data-driven XGBoost models are able to derive the features that were used to predict the responses. Since the reference eDES model represents the population median response, the model parameters provide no distinction between individuals. The personalized eDES models allow a comparison between individuals based on the estimated parameter values. In Fig 3, the individuals in the parameter space of the personalized eDES models are shown after dimensionality reduction via PCA. The estimated parameter set of individuals can be used to quantify inter-individual variability. In addition, the parameters represent physiological processes such as gut emptying or insulin

secretion, therefore where the individuals lie in the parameter space can be directly associated with these physiological properties. However, a detailed exploration of the eDES parameters values is outside of the scope of this work, as the aim here was to explore novel features using an hybrid modelling approach. We previously explored these parameters in [8].

In the case of the XGBoost model, we can calculate the relative feature importances to derive the contribution of each feature to the model prediction. Fig 4 shows the relative feature importances of the 20 most important features (ordered by relative feature importance in the t=0 model) in the XGBoost model predicting the postprandial glucose levels at all time-points. The relative feature importances per insulin time-point are shown in Fig S3.

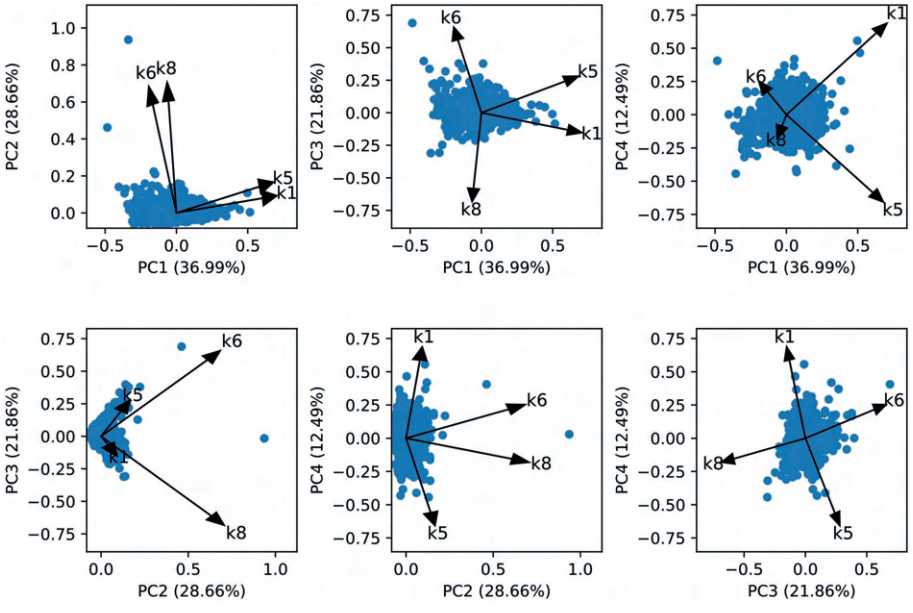


**Figure 3**. Individual parameter sets (n=2968) in the parameter space of the model. The parameter space spanning the direction of the estimated model parameters *k*1, *k*5, *k*6 and *k*8 is shown after dimensionality reduction via principal component analysis. Dots represent the estimated parameter sets of individuals from the Maastricht Study and arrows represent the loadings.

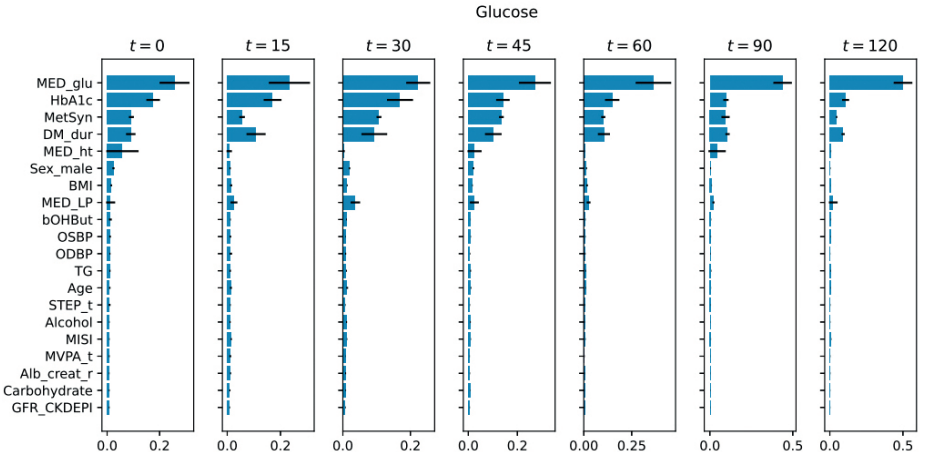


**Figure 4**. Relative feature importances of the 20 most important features for the seven time points of the OGTT (decreasing order by relative feature importance at t=0) in the XGBoost models predicting the postprandial glucose levels. The relative feature importances (x-axes) are calculated as the variance (MSE) reduction weighted by the proportion of samples reaching the node across all trees. Error bars represent the standard deviation across cross-validation folds.

Across all time-points the most important features to the model predictions of glucose levels were whether the individual was taking glucose lowering medication (MED_glu), followed by HbA1c, presence of metabolic syndrome (MetSyn), and diabetes duration (DM_dur). In case of predicting the insulin levels, the most informative features were the presence of metabolic syndrome for all the time-points, BMI and the MISI score for time-points 2-6 and whether the individual was taking glucose lowering medication for time-points 2-4. Additional features seem to add to the model prediction in certain time-points, such as total cholesterol-to-HDL cholesterol ratio (Chol_r) at the 2nd time-point or the inflammation marker IL-8 at the 4th time-point.

The features importances in the data-driven part of the Hybrid I scenario largely agree with those in case of the pure XGBoost model. In the Hybrid II scenario, the personalized eDES models showed good prediction performance, however the data-driven models had low predictive performance (Table S2). Therefore, in contrast to the Hybrid I scenario, the interpretation of the feature importances in the Hybrid II scenario is hindered by a low explained variances observed in the data-driven models (Fig S6 and S7).

## DISCUSSION

In the present study, we investigated various modelling scenarios to predict glucose and insulin concentrations following an OGTT comparing mechanistic modelling with data-driven models as well as the combination of the two approaches in order to evaluate predictive performance (measured as coefficient of determination, $R^2$ and mean squared error of prediction, MSE) and to identify factors underlying inter-individual differences in the responses. In addition, we assessed whether the variance explained by a mechanistic model could be improved by explicitly accounting for additional factors such as body composition, lifestyle related factors, and cardiometabolic health-related parameters, using a data-driven model. We showed that a mechanistic model, tuned on a large number of individual's data from The Maastricht Study was suited to accurately capture individual OGTT responses, whereas the combination with the data-driven model did not improve the prediction further.



The mechanistic glucose model used in this study employs time series data to estimate rate parameters related to glucose metabolism. The reference eDES model, in which selected parameters were estimated on the median OGTT responses, performed the worst of all the modelling scenarios for both $R^2$ and MSE. In this approach, the estimated parameters represented a median OGTT response. Therefore, the large MSE and low $R^2$ were not surprising, given the heterogeneity in individual OGTT responses. Nevertheless, the reference eDES model highlights the flaw in one-size fits all approaches, as well as providing us with a reference model that is not personalized. Using the individualization approach briefly described in the methods, we were able to accurately capture glucose and insulin concentrations using only 4 estimated model parameters. As expected, the model performance in terms of MSE and $R^2$ was much better than the reference eDES model. In addition to being able to capture dynamic glucose and insulin responses, the mechanistic nature of this model provides quantitative information on the encoded processes linked to glucose metabolism. The individualization approach employed on the current data set resulted in the same sensitive, parsimonious, and identifiable parameter set as employed in our previous work, describing the rate constant of glucose appearance in the gut ($k1$), the rate constant of insulin-dependent glucose uptake ($k5$), the proportional rate constant of insulin secretion due to the difference in the actual plasma glucose level compared to baseline ($k6$), and the insulin secretion dependent on the rate of change in plasma glucose ($k8$).

As opposed to mechanistic models of glucose homeostasis, data-driven models make no assumption about the underlying physiological properties of glucose homeostasis. Instead, the large amounts of heterogenous data are explored to find patterns associated with glucose and insulin levels in a hypothesis generating way. Glucose predictor models have been gaining ground in diabetes prevention and management with increasing success [14, 25]. Here, we trained gradient boosting regression models to predict glucose and insulin concentrations after an OGTT using the deep phenotyping features from the Maastricht Study. A nested cross-validation training scheme was used in order to provide unbiased performance estimates. The XGBoost models were able to explain a large part of the variance (Table S2), however their predictive performance was considerably lower than the performance of the personalized eDES models. The explained variances for insulin concentrations were much lower, indicating that the features used in the models are more predictive of glucose, rather than insulin concentrations. In addition, the prediction error of the XGBoost model was much higher than the personalized eDES models. An advantage of the data-driven modelling used in this work is that a large number of features representing a wide range of characteristics can be used as predictors in the models, however in contrast to the mechanistic model, no time-dependency structures are taken into account. This independent time-point-wise modelling of the glucose and insulin concentrations disregard the correlation between glucose and insulin measurements at consecutive time-points of the OGTT in the same individual likely leading to less accurate predictions. Furthermore, as opposed to the eDES model, the XGBoost models did not account for the correlation between glucose and insulin measurements made in the same individual either. The feature importances of the XGBoost models indicate that the most predictive features of glucose concentrations (Fig 4) were well known measures of glucose homeostasis such as HbA1c or a prescription of diabetes medication leading to no novel insights. While the feature importances in the case of insulin predictions (Fig S3) may show some interesting features to contribute to the predictions, however, the low coefficient of determination and high prediction error undermine their relevance.

In an attempt to evaluate whether the glucose and insulin predictions of the eDES model can be further improved by accounting for characteristics of individuals that are not explicitly modeled in the eDES model we combined the prediction of the eDES models with those of XGBoost models. The results of this proof-of-concept study showed that these hybrid models (models Hybrid I and Hybrid II) present little benefit in combining the two models indicated by the lack of

improvement in either $R^2$ or MSE. In the case of Hybrid I the data-driven part of the model is almost equivalent to the standalone XGBoost models (Table S2, Fig S4 and S5) implying there is no benefit to combining the predictions with the reference eDES model. While, in the case of Hybrid II the personalized eDES models performed very well and there seems to be no additional insight gained by adding the data-driven models to the prediction task (Table S2, Fig S6 and S7). The lack of improvement in prediction performance may originate from the lack of time-dependency structure in the data-driven models, the choice of feature set but also from the features used in the data-driven model falling into the same causal pathway as the parameters of the eDES model. While the eDES model does not explicitly account for many of the features used in the data-driven modelling, it does account for high-level physiological processes that may encompass the information in those features, therefore leading to an issue of representations of the same causal pathways. For example, the estimated parameters of the eDES model in this work attribute the variance in the OGTT responses between individuals to differences in gut emptying ($k1$), insulin sensitivity ($k5$) or insulin secretion ($k6$ & $k8$). It is biologically plausible that the effect of certain features (e.g. physical activity) on the glucose and insulin predictions are already realized through one or a combination of parameter estimates of the eDES model (e.g. the value for $k5$; insulin sensitivity). Therefore, combining a mechanistic and a data-driven model in a sequential manner may not be appropriate, instead a parallel approach should be explored. In addition, the mechanistic model, that was employed in this study, was able to accurately describe the responses to standardized OGTTs. However, for complex meals containing varying amounts of macronutrients as well as meals in free-living conditions, the resulting glucose and insulin excursions may not be accurately captured. In such conditions, an approach combining a mechanistic model with a data-driven model may yield more informative results. A strength of this proof-of-concept study was the large and heterogeneous study population from The Maastricht Study. Individuals (n=2968) with varying glycemic regulation including normoglycemia, prediabetes (impaired fasting glucose, impaired glucose tolerant or both conditions) as well as type 2 diabetes were present in the study population. Furthermore, the 7 time-point OGTT facilitates the observation of nuanced dynamics in the glucose and insulin profiles compared to the more prevalent 5 time-point measurements. In addition, the comprehensive profiling of the study participants included health behavior, cardiovascular health, musculoskeletal health, metabolic and demographic characteristics as well as body fat composition and biomarkers. The comprehensive phenotypic information of such a large number of individuals

allowed the use of data-driven models to find patterns that may provide additional insight about the glucose regulation on top of the OGTT response.

## CONCLUSIONS

In the present study, we compared the predictive performance of mechanistic models with well-defined temporal dependencies (eDES), data-driven models with no temporal dependencies (XGBoost) and the sequential combination of the two (Hybrid I and Hybrid II). Our results suggest, that a 4 parameter model with appropriate temporal structure can vastly outperform a naive model built on a cross sectional phenotypic profile of an individual in predicting postprandial glucose and insulin concentrations. In addition, a sequential combination of a mechanistic and a data-driven approach may not be suitable when studying the underlying factors of inter-individual variance. Nevertheless, we show that the eDES model is especially convenient when temporal dynamics in the glucose and insulin responses are to be quantified. Furthermore, the findings presented in this work corroborate our previous results indicating that the personalized eDES models are suitable to capture nuanced dynamics in the responses.

## REFERENCES


1. Sharabi, K., Tavares, C. D., Rines, A. K. & Puigserver, P. *Molecular pathophysiology of hepatic glucose production*. Molecular aspects of medicine **46**, 21–33 (2015).
2. Galicia-Garcia, U. et al. *Pathophysiology of Type 2 Diabetes Mellitus*. International Journal of Molecular Sciences **21**. issn: 1422-0067. https://www.mdpi.com/1422-0067/21/17/6275 (2020).
3. Freeman, A. M. & Pennings, N. *Insulin resistance*. StatPearls (2021).
4. Bergman, R. N., Ider, Y. Z., Bowden, C. R. & Cobelli, C. *Quantitative estimation of insulin sensitivity*. American Journal of Physiology-Endocrinology And Metabolism **236**, E667 (1979).
5. Dalla Man, C., Rizza, R. A. & Cobelli, C. *Meal simulation model of the glucose-insulin system*. IEEE Transactions on biomedical engineering **54**, 1740–1749 (2007).
6. Maas, A. H. et al. *A physiology-based model describing heterogeneity in glucose metabolism: the core of the eindhoven diabetes education simulator (E-DES)*. Journal of diabetes science and technology **9**, 282–292 (2014).
7. Maas, A. *Playing with numbers: the development of an educational diabetes game* (2017).
8. Erdõs, B. et al. *Personalized computational model quantifies heterogeneity in postprandial responses to oral glucose challenge*. PLoS computational biology **17**, e1008852 (2021).
9. Pillon, N. J., Loos, R. J., Marshall, S. M. & Zierath, J. R. *Metabolic consequences of obesity and type 2 diabetes: Balancing genes and environment for personalized care*. Cell **184**, 1530–1544. issn: 0092-8674. https://www.sciencedirect.com/science/article/pii/S0092867421001628 (2021).
10. Tsereteli, N. et al. *Impact of insufficient sleep on dysregulated blood glucose control under standardised meal conditions*. Diabetologia, 1–10 (2021).
11. Woldaregay, A. Z. et al. *Data-driven modeling and prediction of blood glucose dynamics: Machine learning applications in type 1 diabetes*. Artificial intelligence in medicine **98**, 109–134 (2019).
12. Li, J., Huang, J., Zheng, L. & Li, X. *Application of artificial intelligence in diabetes education and management: present status and promising prospect*. Frontiers in public health **8**, 173 (2020).
13. Van Doorn, W. P. et al. *Machine learning-based glucose prediction with use of continuous glucose and physical activity monitoring data: The Maastricht Study*. PloS one **16**, e0253125 (2021).
14. Zeevi, D. et al. *Personalized nutrition by prediction of glycemic responses*. Cell **163**, 1079–1094 (2015).
15. Lee, D., Jayaraman, A. & Kwon, J. S. *Development of a hybrid model for a partially known intracellular signaling pathway through correction term estimation and neural network modeling*. PLOS Computational Biology **16**. Publisher: Public Library of Science, 1–31 (Dec. 2020).
16. Bock, F. E., Keller, S., Huber, N. & Klusemann, B. *Hybrid Modelling by Machine Learning Corrections of Analytical Model Predictions towards High-Fidelity Simulation Solutions*. Materials **14**. issn: 1996-1944 (2021).
17. Van Riel, N. A. W., Tiemann, C. A., Hilbers, P. A. J. & Groen, A. K. *Metabolic Modeling Combined With Machine Learning Integrates Longitudinal Data and Identifies the Origin of LXR-Induced Hepatic Steatosis*. Frontiers in Bioengineering and Biotechnology **8**. issn: 2296-4185 (2021).

18. Schram, M. T. et al. *The Maastricht Study: an extensive phenotyping study on determinants of type 2 diabetes, its complications and its comorbidities*. European Journal of Epidemiology **29**, 439–451. issn: 1573-7284. https://doi.org/10.1007/s10654-014-9889-0 (June 2014).
19. Association, A. D. et al. *2. Classification and diagnosis of diabetes*. Diabetes care **38**, S8–S16 (2015).
20. Vanlier, J., Tiemann, C., Hilbers, P. & Van Riel, N. *Parameter uncertainty in biochemical models described by ordinary differential equations.* Mathematical biosciences **246**, 305–314 (2013).
20. Chen, T. & Guestrin, C. *XGBoost: A Scalable Tree Boosting System in Proceedings of the 22nd ACM SIGKDD International Conference on Knowledge Discovery and Data Mining* (ACM, San Francisco, California, USA, 2016), 785–794. isbn: 978-1-4503-4232-2. http://doi.acm.org/10.1145/2939672.2939785.
21. Friedman, J. H. *Greedy function approximation: a gradient boosting machine*. Annals of statistics, 1189–1232 (2001).
22. Cawley, G. C. & Talbot, N. L. *On over-fitting in model selection and subsequent selection bias in performance evaluation*. The Journal of Machine Learning Research **11**, 2079–2107 (2010).
23. Breiman, L., Friedman, J. H., Olshen, R. A. & Stone, C. J. *Classification and regression trees* (Routledge, 2017).
24. Robertson, G., Lehmann, E. D., Sandham, W. & Hamilton, D. *Blood Glucose Prediction Using Artificial Neural Networks Trained with the AIDA Diabetes Simulator: A Proof-of-Concept Pilot Study*. en. Journal of Electrical and Computer Engineering 2011, 1–11. issn: 2090-0147, 2090-0155. http://www.hindawi.com/journals/jece/2011/681786/ (2011).

## SUPPLEMENTARY MATERIAL

**Table S1:** Explanation of estimated eDES model parameters

| Name | Description | Units |
|---|---|---|
| $k1$ | Rate constant of glucose appearance in the gut | 1/min |
| $k5$ | Rate constant of insulin-dependent glucose uptake | 1/min |
| $k6$ | Rate constant of ΔG dependant insulin production | 1/min |
| $k8$ | Rate constant of $\frac{dG}{dt}$ dependant insulin production | 1/min |

where $G$ is plasma glucose concentration. For details see [1].

[1] Balázs Erdõs et al. “Personalized computational model quantifies heterogeneity in postprandial responses to oral glucose challenge”. In: *PLoS computational biology* 17.3 (2021), e1008852

## S1 APPENDIX: LIST OF PHENOTYPIC VARIABLES

*Anthropometrics*
Age: Age at visit (years), Sex_male: Sex, BMI: Body Mass Index, Body_fat: Total body fat percentage (%), Smoke_never/former: Smoking status (3 categories)

*Demographics*
Ethnicity: Ethnicity, Education_low/medium: Educational level categories

*Health behaviour*
MVPA_t: mean MVPA wake minutes per day total, STEP_t: mean step wake minutes per day total, Wmax: Estimated maximal power output adjusted for body weight ($Wkg^{-1}$), MVPA: moderate to vigorous physical activity per week (*hours/week*), Alcohol: Alcohol total (*g/day*), Protein: Protein total (*g/day*), Energy: Energy (*KJ*), Carbohydrate: Carbohydrates total (*g/day*), Fat: Fat total (*g/day*), Fibre: Dietary fibre total (*g/day*), Dairy: dairy products with probiotics (*g*)

*Medication*
MED_glu: Glucose-lowering medication (oral only), Glucose-lowering medication or insulin, MED_HT: Blood pressure lowering medication (all types),MED_LP: Lipid-modifying medication

*Cardiovascular health*
CVD: history of cardiovascular disease, ODBP: Diastolic Blood Pressure, OSBP: Systolic Blood Pressure

*Metabolic health*
Matsuda index, HIRI index ((*mmol/L*)(*pmol/L*)(*hour*)$^2$), c-peptidogenic index t30, Fasting plasma Glucose (*mmol/L*), glucose tolerance status (WHO), HOMA2, MetSyn: metabolic syndrome, MVD: Microvacular disease, DM_dur: Duration of type 2 diabetes in years, MISI: MISI index (*umol/L/min/pmol/L*),

*Biomarkers*
HDL: Serum HDL cholesterol (*mmol/l*), Chol_r: Total cholesterol-to-HDL cholesterol ratio, HbA1c: HbA1c (*mmol/mol*), Alb_creat_r: Albumin-creatinine ratio (*g/molcreatinine*), bOHBut: 3-hydroxybutyrate (*mmol/l*), CK: Creatine kinase in serum (*U/L*), GFR_CKDEPI: Glomerular filtration rate (*ml/min/*1.73$m^2$), CKDEPI using serum creatinine, FA: Total fatty acids (*mmol/l*), TG: Serum triglycerides (*mmol/l*)

*Inflammation markers*
CRP: C-reactive protein (*g/ml*), IL6: Human interleukin-6 (*pg/ml*), IL8: Human interleukin-8 (*pg/ml*), SICAM1: Soluble intercellular adhesion molecule-1 (*ng/ml*), TNF: Human tumor necrosis factor alpha (*pg/ml*), SAA: Serum amyloid A (*g/ml*)

*Self reported quality of life*
SF36_GH: SF36 general health, SF36_MCS: SF36 Mental component summary score, SF36_MH: SF36 mental health, SF36_PCS: SF36 Physical component summary score

**Table S2**: $R^2$ and MSE of prediction per time point of glucose and insulin in the OGTT in the modelling scenarios

| | | Ref. eDES | | Pers. eDES | | Ref.GBR | | Hybrid I. | | Hybrid II. | |
|---|---|---|---|---|---|---|---|---|---|---|---|
| M | TP | $R^2$ | MSE | $R^2$ | MSE | $R^2$ | MSE | $R^2$ | MSE | $R^2$ | MSE |
| Glucose | 1 | -0.38 | 1.79 | - | - | 0.71 (0.02) | 0.37 (0.02) | 0.71 (0.02) | 0.38 (0.02) | - | - |
| | 2 | -0.48 | 3.69 | 0.75 | 0.62 | 0.58 (0.01) | 1.04 (0.03) | 0.58 (0.01) | 1.04 (0.04) | 0.77 (0.01) | 0.56 (0.05) |
| | 3 | -0.62 | 8.95 | 0.86 | 0.75 | 0.60 (0.04) | 2.20 (0.23) | 0.60 (0.04) | 2.20 (0.22) | 0.88 (0.01) | 0.68 (0.08) |
| | 4 | -0.58 | 17.33 | 0.96 | 0.49 | 0.66 (0.02) | 3.74 (0.20) | 0.66 (0.02) | 3.73 (0.20) | 0.96 (0.01) | 0.47 (0.08) |
| | 5 | -0.49 | 24.32 | 0.97 | 0.49 | 0.71 (0.01) | 4.66 (0.34) | 0.71 (0.01) | 4.68 (0.36) | 0.97 (0.00) | 0.47 (0.03) |
| | 6 | -0.40 | 29.35 | 0.96 | 0.80 | 0.77 (0.01) | 4.88 (0.38) | 0.77 (0.01) | 4.87 (0.34) | 0.97 (0.00) | 0.68 (0.07) |
| | 7 | -0.30 | 23.29 | 0.95 | 0.94 | 0.77 (0.03) | 4.09 (0.26) | 0.77 (0.03) | 4.10 (0.32) | 0.96 (0.00) | 0.77 (0.07) |
| Insulin | 1 | -0.22 | 73.95 | - | - | 0.46 (0.06) | 32.59 (2.50) | 0.45 (0.06) | 32.73 (2.78) | - | - |
| | 2 | -0.07 | 789.97 | 0.78 | 161.03 | 0.21 (0.04) | 585.75 (72.72) | 0.21 (0.04) | 578.41 (75.55) | 0.80 (0.01) | 148.30 (10.93) |
| | 3 | -0.03 | 1788.02 | 0.89 | 182.72 | 0.29 (0.03) | 1227.06 (63.90) | 0.29 (0.03) | 1222.82 (59.75) | 0.89 (0.02) | 179.72 (13.84) |
| | 4 | -0.08 | 3422.29 | 0.91 | 292.46 | 0.29 (0.04) | 2259.30 (299.14) | 0.28 (0.04) | 2260.18 (287.06) | 0.91 (0.02) | 292.76 (41.76) |
| | 5 | -0.14 | 5224.25 | 0.89 | 517.77 | 0.31 (0.06) | 3152.21 (470.09) | 0.31 (0.06) | 3187.93 (464.78) | 0.88 (0.03) | 521.00 (133.79) |
| | 6 | -0.22 | 7205.55 | 0.85 | 882.94 | 0.35 (0.03) | 3857.80 (1256.49) | 0.35 (0.03) | 3877.16 (1238.39) | 0.86 (0.05) | 890.21 (570.07) |
| | 7 | -0.25 | 7120.25 | 0.79 | 1177.05 | 0.36 (0.04) | 3659.74 (899.36) | 0.36 (0.05) | 3647.84 (936.59) | 0.79 (0.07) | 1220.46 (460.50) |

**Table S3:** Hyperparameter search details

| parameter | range | number of equidistant samples |
|---|---|---|
| n_estimators | 150-200 | 10 |
| max_depth | 2-15 | 7 |
| learning_rate | 0.01-0.05 | 11 |
| subsample | 0.7-0.9 | 21 |
| colsample_bytree | 0.48-0.98 | 11 |
| min_child_weight | 1-9 | 8 |

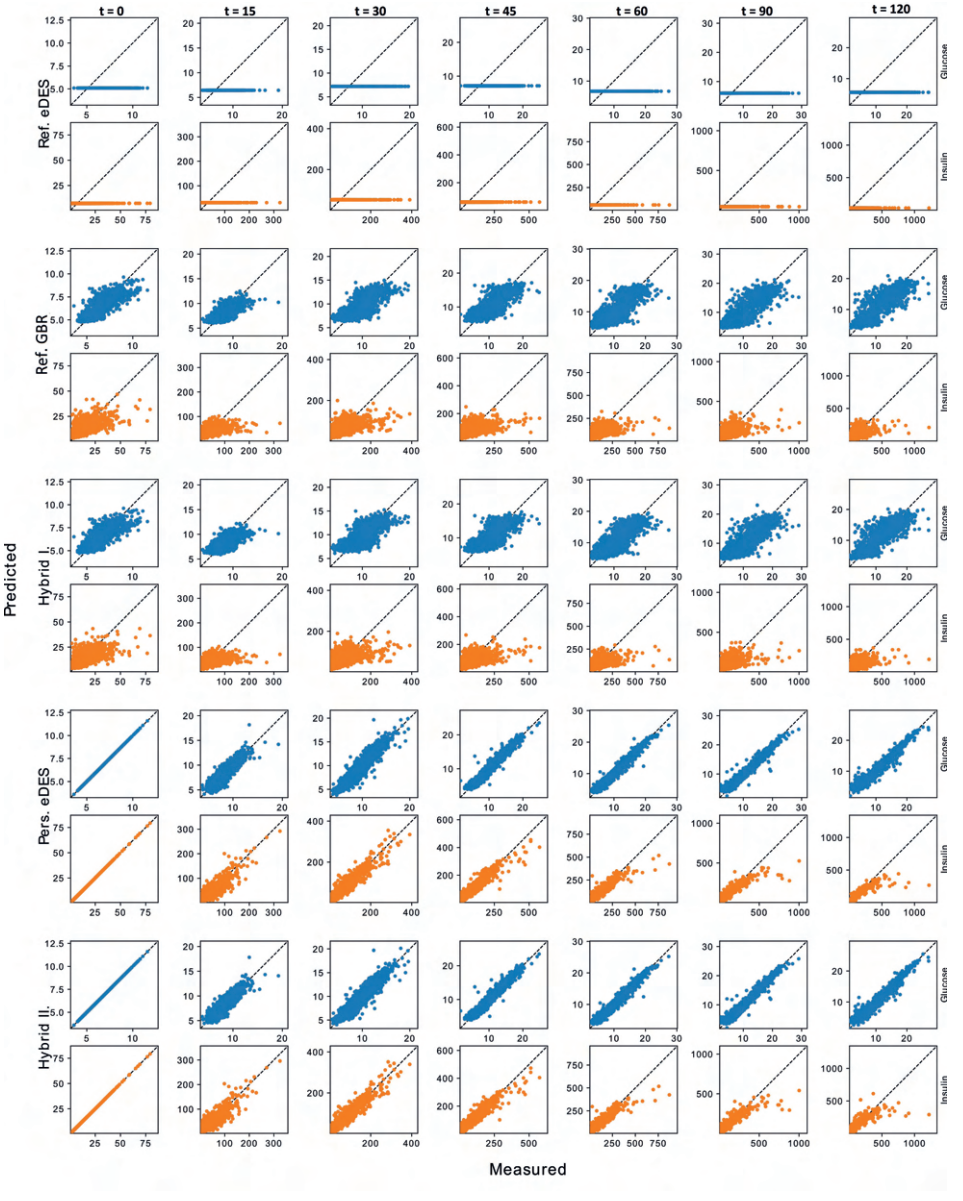


**Figure S1**. Measured versus predicted glucose and insulin concentrations at the time points of the OGTT in the case of the modelling scenarios

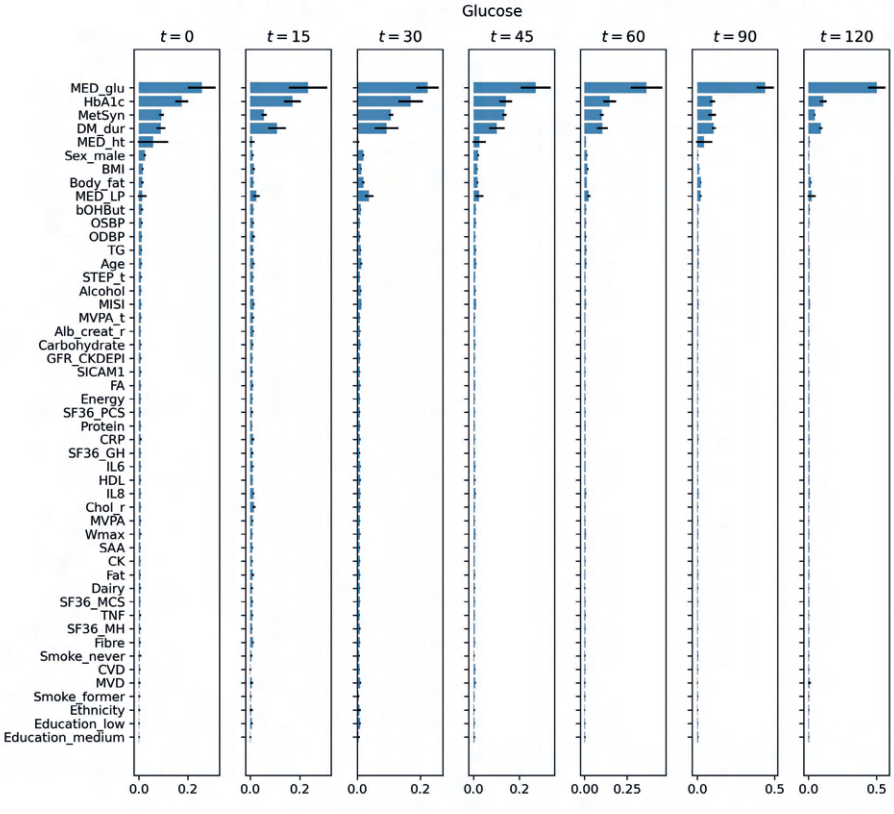


**Figure S2.** Relative feature importances of the features (decreasing order by relative feature importance at t=0) in the XGBoost models in the Ref. GBR scenario predicting the postprandial glucose levels. The relative feature importances (x-axes) are calculated as the variance (MSE) reduction weighted by the proportion of samples reaching the node across all trees. Error bars represent the standard deviation across CV folds.

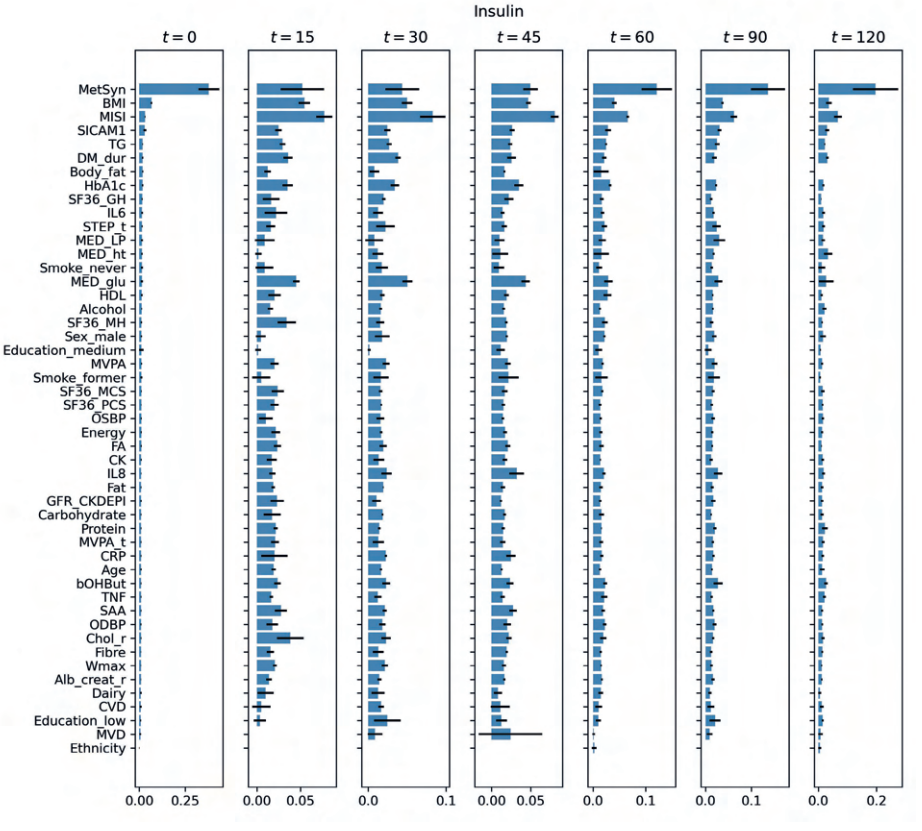


**Figure S3.** Relative feature importances of the features (decreasing order by relative feature importance at t=0) in the XGBoost models in the Ref. GBR scenario predicting the postprandial insulin levels. The relative feature importances (x-axes) are calculated as the variance (MSE) reduction weighted by the proportion of samples reaching the node across all trees. Error bars represent the standard deviation across CV folds.

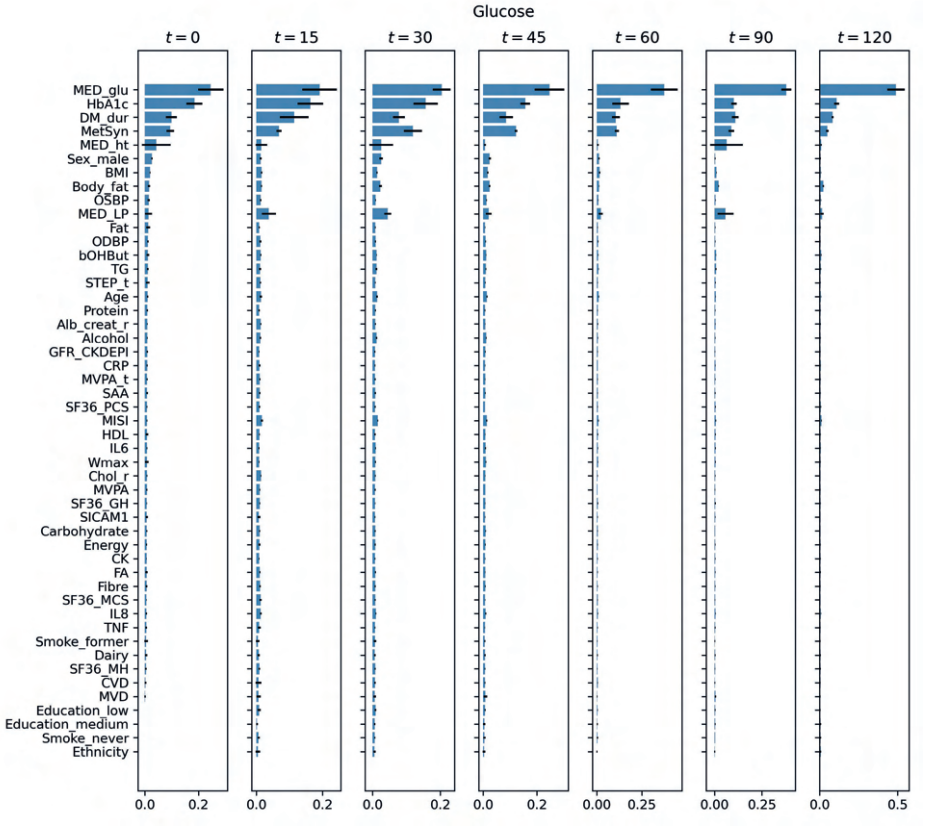


**Figure S4.** Relative feature importances of the features (decreasing order by relative feature importance at t=0) in the XGBoost models of the Hybrid I scenario predicting the postprandial glucose levels. The relative feature importances (x-axes) are calculated as the variance (MSE) reduction weighted by the proportion of samples reaching the node across all trees. Error bars represent the standard deviation across CV folds.

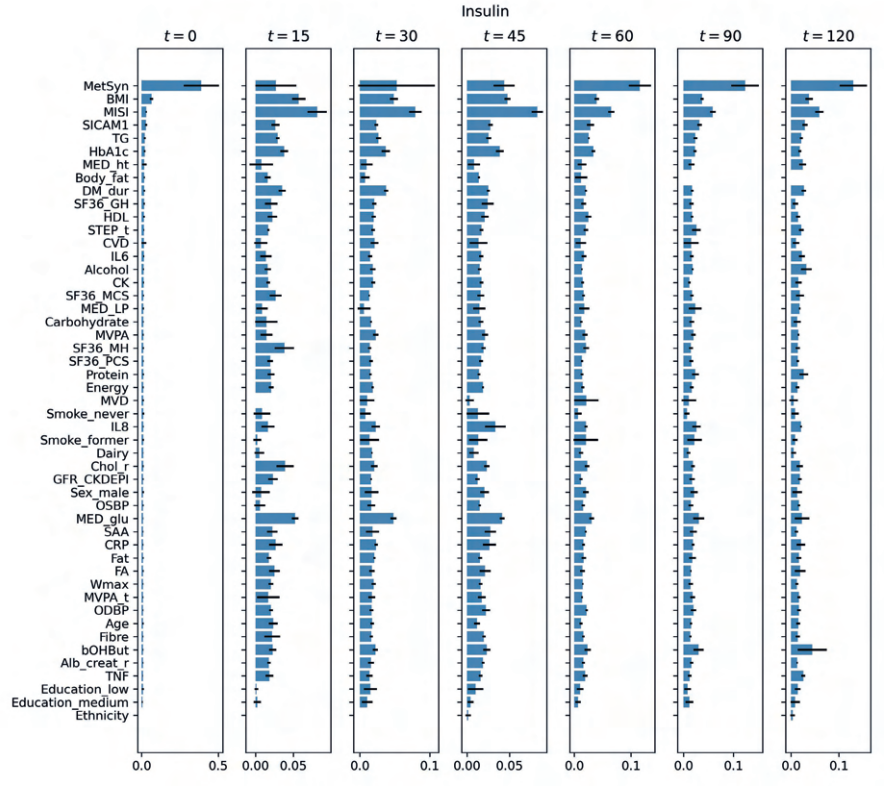


**Figure S5.** Relative feature importances of the features (decreasing order by relative feature importance at t=0) in the XGBoost models of the Hybrid I scenario predicting the postprandial insulin levels. The relative feature importances (x-axes) are calculated as the variance (MSE) reduction weighted by the proportion of samples reaching the node across all trees. Error bars represent the standard deviation across CV folds.

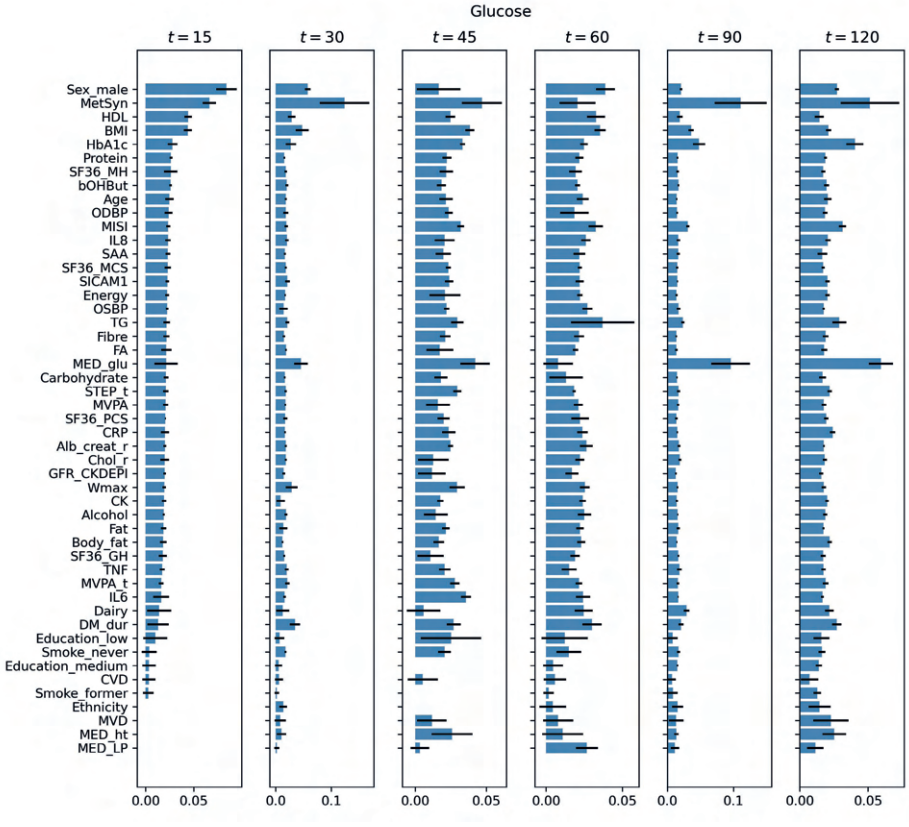


**Figure S6.** Relative feature importances of the features (decreasing order by relative feature importance at t=0) in the XGBoost models of the Hybrid II scenario predicting the postprandial glucose levels. The relative feature importances (x-axes) are calculated as the variance (MSE) reduction weighted by the proportion of samples reaching the node across all trees. Error bars represent the standard deviation across CV folds.

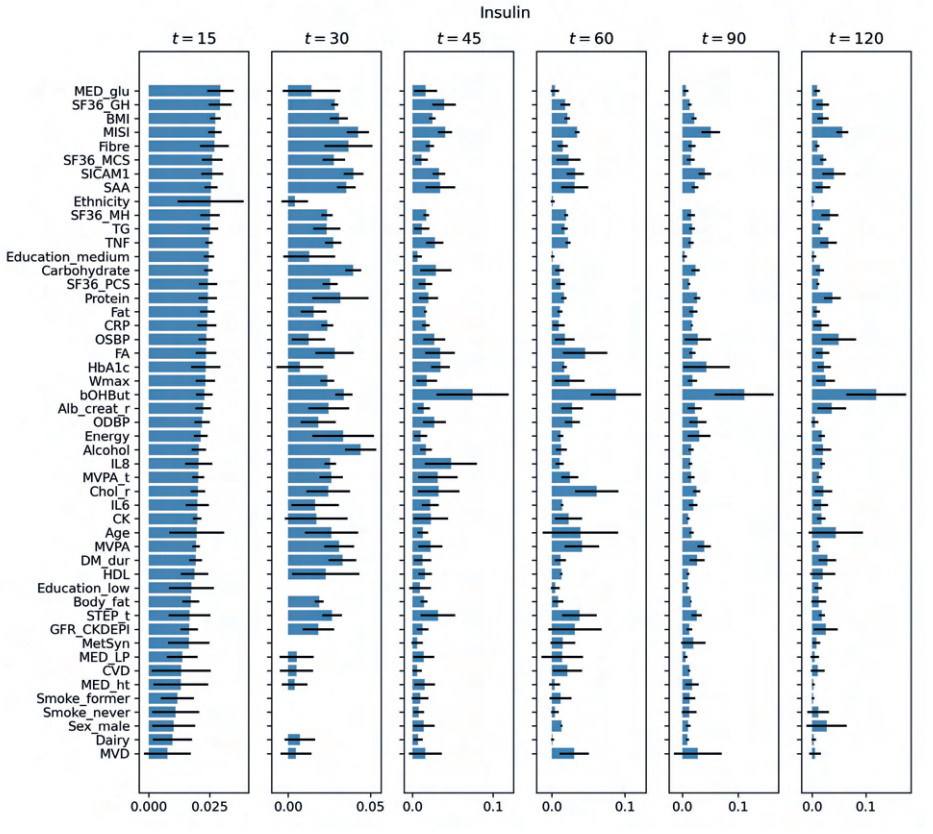


**Figure S7.** Relative feature importances of the features (decreasing order by relative feature importance at t=0) in the XGBoost models of the Hybrid II scenario predicting the postprandial insulin levels. The relative feature importances (x-axes) are calculated as the variance (MSE) reduction weighted by the proportion of samples reaching the node across all trees. Error bars represent the standard deviation across CV folds.

# Predicting the postprandial glucose response in tissue-specific insulin resistant phenotypes: a computational modelling approach



**Bart van Sloun, Gijs H. Goossens, Balázs Erdõs, Seguna D. O'Donovan, Anouk Gijbels, Inez Trouwborst, Kelly M. Jardon, Ellen E. Blaak,Lydia Afman, Natal A.W. van Riel and Ilja C.W. Arts**

*Submitted*

# 7 General Discussion

Computational models are able to provide insight into biological processes that underlie health and disease [1]. Different modelling techniques exist, from the 'bottom up' mechanistic models to the 'top down' data-driven approaches, each having their own advantages and disadvantages [2]. Mechanistic modelling allows simulation of complex biological systems, such as the glucose-insulin regulatory system, which includes various organs and tissues that work together to regulate blood glucose levels to ensure normal body function [3, 4]. The research described in this thesis aimed to further develop and apply various computational modelling techniques for analysis of the glucose-insulin regulatory system. This involved the use of ordinary differential equation (ODE) based mechanistic models and their combination with machine learning. We developed a pipeline for the personalization of a mechanistic model, highlighting the heterogeneity in individuals' responses. Furthermore, we extended the mechanistic model to allow for the description of dietary amino acids (AAs) and protein, and their interactions with circulating insulin and glucose concentrations. This made it possible to accurately describe individual responses to complex meals and investigate physiological differences between individuals with distinct tissue-specific insulin resistance phenotypes. In this chapter, we discuss the various components developed and applied over the course of this thesis.

## MODEL BUILDING

### Personalized models of the glucose regulatory system

The move towards personalized nutritional interventions requires characterization of the large heterogeneity in individuals' glycemic regulation. To explore this heterogeneity, personalized mechanistic models are required that capture individual responses and provide insight into the variability in glucose homeostasis between individuals. In **Chapter 3**, we developed a workflow to transition from describing population averages towards individualized glucose and insulin response patterns, generalizable to other biological models and systems. The workflow involves systematically reducing the number of model parameters to estimate for each individual response to ensure reliable, accurate parameter estimates. The subset of model parameters to be estimated was selected based on the following criteria: the selected parameters had to (i) exhibit high sensitivity, (ii) demonstrate good model fit while maintaining parsimony, (iii) be identifiable.

We assessed the sensitivity of model parameters by increasing and decreasing its value while maintaining the others at a constant value, and inspecting the effect on the resulting model outcome (i.e. glucose and insulin concentrations). A threshold of 75% in both directions (i.e. increase/decrease in parameter values) compared to the average healthy population values was selected as the limit of sensitivity. Parameters that were not sensitive at this threshold were fixed to their respective values [5]. Second, parsimony and model fit were considered. A set of all possible combinations of three or more sensitive parameters was generated. With the set of parameter combinations as 'free parameters', models were selected and fitted on representative responses obtained from individuals that participated in the European DIOGenes study to promote the model to be able to fit a wide range of responses. To impose parsimony, we used the Akaike Information Criterion (AIC) to introduce a penalty term on the number of parameters in the model. The AIC estimates the amount of information lost by a given model, and deals with the trade-off between the goodness of fit and the simplicity of the model (parsimony). We used the AIC in our approach to identify the models with the lowest AIC value. This approach is desired as it discourages overfitting, as the increase in model parameters almost always improves the goodness of fit. Our results described in **Chapter 3** showed that the top five and six parameter models performed only marginally better than the four parameter model. Based on the AIC, the four-parameter model containing parameters $k1$, $k5$, $k6$, $k8$ was selected as the most parsimonious model. These 4 parameters describe the transition of glucose from the stomach to the gut ($k1$), the insulin-dependent glucose uptake to the periphery ($k5$), and the processes representative of insulin secretion ($k6$ and $k8$). Quantifying uncertainty in parameters is essential to understand the predictive power of the model. Mechanistic models are, in principle, prone to overfitting, and it is often not possible to reliably estimate multiple parameters [6]. Therefore, Profile Likelihood Analysis (PLA) was carried out to evaluate how well parameter values can be determined given the available data. The results from the PLA showed that the selected parameters were identifiable, indicating that a unique solution exists in the tested range. The personalized models were capable of simulating a wide variety of postprandial glucose and insulin responses following the intake of a glucose drink (standard Oral Glucose Tolerance Test (OGTT)) in study participants of the DIOGenes study. Each of the 738 personalized models contained a unique parameter set pertaining to the physiological state of the participant's glucose homeostasis.

The model parameters corresponding to insulin secretion ($k6$, $k8$) were found to be lower in individuals with more severe perturbations in glucose homeostasis

such as type 2 diabetes. Furthermore, the insulin secretion parameters showed a significant association with the insulinogeneic index, which is a frequently used measure of insulin secretion. The insulin-dependent glucose uptake parameter ($k5$) was also lower in individuals with more severe impairments in glucose homeostasis compared to individuals with normal glucose homeostasis, and showed a significant association with the Matsuda index (index of whole-body insulin sensitivity). These findings demonstrate that the model structure captures relevant features of the insulin-mediated glucose homeostasis and that the personalized models can distinguish between diverse impairments in the insulin-regulated glucose control.

### Model extension with amino acids

Whilst we showed that the original E-DES model was able to capture a wide variety of postprandial glucose and insulin responses to an OGTT using the individualization workflow described in the previous paragraph, it is unable to provide mechanistic insight in processes underlying complex meal challenges (also containing fat and protein). In **Chapter 4**, we developed a computational model of the human glucose-insulin system, incorporating the effects of amino acids (AAs) and protein on insulin secretion and hepatic glucose production. We used the postprandial time-series data of AAs, glucose, and insulin following ingestion of AAs and AAs in combination with glucose (AA+glucose) extracted from literature as described in **Chapter 2**, as well as additional data from the Postprandial Plasma Amino Acid Concentrations after Dairy Consumption (PARROT) study [7] containing postprandial time-series following ingestion of dried milk protein ingredients and dairy products. To prevent the development of an overly complex model, which might be challenging to parameterize and more prone to overfitting, processes accounting for the postprandial effects of individual and total AAs were modeled using simple linear and derivative terms. The original E-DES model, which does not account for AAs and protein, was unable to accurately capture the postprandial data when AAs or protein were present in the (meal) challenge. Our E-DES-PROT model was not only able to describe postprandial responses to the various challenges, but also showed the ability to reproduce a wide variety of individual postprandial glucose and insulin responses as well. In our work described in **Chapter 4**, we employed a forcing function to describe the rate of appearance of AAs in E-DES-PROT. This means that measured plasma AAs have to be provided to the model as an input. Future work should focus on adding a function that explicitly describes the rate of appearance, allowing simulation of postprandial profiles (e.g. specifying the amount of ingested protein) without the need for measured AAs to be provided

as model input. Here, a (simple) machine learning model might be employed and is worthwhile investigating.

### Hybrid models

Besides the physiology-based mechanistic models, the application of data-driven prediction has gained substantial interest in diabetes research [8]. Mechanistic models of the glucose regulatory system describe the change in glucose and insulin levels according to known physiological phenomena, while data-driven models provide a framework to integrate diverse data that may have relevance in glucose regulation without the need for a causal understanding [9-11]. In **Chapter 3**, we showed that the majority of the individual responses to an OGTT were accurately estimated with the E-DES model. However, we identified some cases in which the model was not able to adequately capture the postprandial responses. While the intra-individual variability in the responses can be largely explained by the mechanisms encoded in the E-DES model, it is known that other factors such as diet, physical activity, sleep, and stress may affect glucose regulation. Therefore, we developed a hybrid model, combining the mechanistic E-DES model with a data-driven machine-learning model to identify factors predictive of inter-individual differences in glucose and insulin dynamics following an OGTT.



We selected and investigated different modelling scenarios in order to compare a mechanistic and data-driven model as well as their sequential combination. In **Chapter 5**, we therefore implemented the model selection approach that was developed in **Chapter 3** to obtain the most sensitive, parsimonious, and identifiable model parameter set. This workflow again resulted in model parameters pertaining to gut emptying ($k1$), insulin sensitivity ($k5$), and insulin secretion ($k6$, $k8$). For machine learning, we used a gradient boosting regression model. In addition to using these models separately, we employed a hybrid approach of combining the two models. Here, the mechanistic E-DES model was used to capture the measured postprandial glucose and insulin time-series data, whereas the stored residuals (i.e. difference between the predicted and measured data) were used as targets for the gradient boosted regression model. As expected, the model performance of the personalized E-DES models was much better than the average reference E-DES model. The gradient boosted regression model was able to explain a large part of the variance, but its predictive power was considerably lower than the personalized E-DES models. To evaluate whether the performance of the E-DES model could further be improved by accounting for characteristics of individuals that are not explicitly modeled in the E-DES model, we combined the predictions of the E-DES model with those of

the gradient boosted regression model. The results, however, showed that this hybrid combination provided little benefit in terms of prediction accuracy over the personalized E-DES models.

The lack of improvement in prediction performance may stem from the choice of feature set, including features falling into the same causal pathway as the E-DES model parameters. The mechanistic E-DES model was able to accurately describe the responses to standardized OGTTs. For complex meals containing varying amounts of macronutrients as well as meals in free-living conditions, the resulting glucose and insulin excursions may not be accurately captured. Here, a hybrid combination of a mechanistic and data-driven model may yield more informative results and may provide directions for improvement of the mechanistic model.

## MECHANISTIC INSIGHT

Mechanistic models consist of coupled ordinary differential equations (ODEs) that describe how the concentrations of various biological entities in the system change over time [12]. Such equations are typically constructed using *a priori* information of the underlying biological system to define how the key players interact, allowing investigation of the underlying processes. The behavior of the mechanistic models is governed by the equations themselves, defining how species interact, and the set of parameter values, which define the rate at which the reactions occur. Computer-based numerical solvers allow estimation of these parameters by fitting model simulations to measured time-series data, such as postprandial metabolomics data. This ensures that parameters, describing states of the underlying biological system, can be identified directly from data. Mechanistic models thus enable the analysis of the dynamics of the system and provide insight in the presence of perturbations [13].

The use of mechanistic models to analyze measured time-series data is not a novel concept. The glucose minimal model developed by Bergman et al. [14] in 1979 was used to approximate insulin sensitivity and β-cell function using plasma glucose and insulin measurements following a frequently sampled intravenous glucose tolerance test. The Bergman model formed the basis of many other models including E-DES. The E-DES model has been used to describe the dynamics of glucose homeostasis in healthy, type 1 and type 2 diabetic populations [15]. While the E-DES model performs well in response to oral glucose challenges, interactions

with other nutrients that affect postprandial glucose metabolism, such as amino acids (AAs), are not considered. AAs have distinct effects on glucose regulation in various phenotypes, which we extensively described showed in **Chapter 2** [16]. In **Chapter 6**, the time-series data extracted in **Chapter 2**, as well as additional data obtained from the PARROT study [7], allowed us to develop a model that was used to explore underlying physiological processes between distinct tissue-specific phenotypes in response to a high-fat mixed meal. The results from this study [17] highlight the beneficial relationship between experimental data and computational modelling, with the model being a powerful tool for interpretation and quantification of meal challenge data. The model predicted a faster glucose appearance from the gut in individuals with liver insulin resistance, as well as increased insulin secretion and insulin-dependent glucose uptake compared to individuals with muscle insulin resistance. A better understanding of how individuals respond to diet at the mechanistic level may eventually lead to more personalized dietary advice and targeted nutritional intervention, which, I believe will be essential in advancing personalized nutrition.

## CONCLUSION AND FUTURE PERSPECTIVES



Mechanistic models are regularly applied across disciplines to study dynamic behavior of biological systems and, unlike black box machine learning algorithms, allow for physiological interpretability of their parameters. Currently, the majority of mechanistic models have been applied on population average data. In the present work, we developed personalized mechanistic models and showed their ability to capture postprandial responses more accurately compared to population level mechanistic models. Also, these mechanistic models provided quantitative information on relevant features of individuals' metabolic health such as gastric emptying, endogenous insulin secretion, and insulin-dependent glucose disposal.

This modelling framework, where we move from population to individual models, may prove beneficial in revealing (the mechanisms underlying) early deteriorations in the glucose regulatory system at the individual level using parameters that are relatively easy to determine. Furthermore, insight into the biological mechanisms underlying tissue-specific insulin resistance phenotypes is important, as the severity of insulin resistance at the tissue level may play a role in the differential response to lifestyle (i.e. dietary interventions [18]) and pharmacological interventions that aim to increase cardiometabolic health

and/or insulin sensitivity. Future studies should therefore investigate how individuals respond to different diets (or other interventions) at the mechanistic level. In this way, personalized models could allow for individualized assessment of intervention success but also prevent further deteriorations in the glucose regulatory system (e.g. by providing dietary advice), thus supporting the transition towards personalized nutrition.

Towards this goal, we extended a mechanistic model of the glucose-insulin system with the postprandial effects of AAs and protein, which were shown to impact postprandial glucose metabolism [16]. Future studies should focus on incorporating the effects of dietary fat in the model [19], which would then cover the three macronutrient classes (carbohydrates, fat, protein). This would allow *in silico* prediction of glycemic responses of individuals (represented by the individualized models) to modified or new food products. In addition, it would make it possible to simulate how changes in physiological processes (i.e. described by model parameters) modulate glycemic responses to particular foods. As such, personalized models might contribute to more personalized dietary advice and targeted nutritional interventions.

Another opportunity lies in the use of data-driven techniques. Future studies should also focus on integrating machine-learning with the mechanistic models, to include additional individual features that are not taken into account by the mechanistic models [20, 21]. Such hybrid combinations of mechanistic and data-driven models might prove valuable in providing further insight into the biology underlying inter-individual differences in glucose homeostasis. This could allow for the most accurate prediction of metabolic responses at the individual level, thus creating a 'digital twin'. In this respect, open science is also important, as (our) models are dependent on good quality data. Therefore, researchers should be stimulated to make their datasets and model codes publicly available to allow further advancements in science.

## REFERENCES


1. Collin, C.B., T. Gebhardt, M. Golebiewski, T. Karaderi, M. Hillemanns, F.M. Khan, A. Salehzadeh-Yazdi, M. Kirschner, S. Krobitsch, E.-S.P. consortium, et al., *Computational Models for Clinical Applications in Personalized Medicine—Guidelines and Recommendations for Data Integration and Model Validation.* Journal of Personalized Medicine, 2022. **12**(2): p. 166.
2. Ellis, J.L., M. Jacobs, J. Dijkstra, H. van Laar, J.P. Cant, D. Tulpan, and N. Ferguson, *Review: Synergy between mechanistic modelling and data-driven models for modern animal production systems in the era of big data.* Animal, 2020. **14**: p. s223-s237.
3. Palumbo, P., S. Ditlevsen, A. Bertuzzi, and A. De Gaetano, *Mathematical modeling of the glucose–insulin system: A review.* Mathematical Biosciences, 2013. **244**(2): p. 69-81.
4. Mari, A., A. Tura, E. Grespan, and R. Bizzotto, *Mathematical Modeling for the Physiological and Clinical Investigation of Glucose Homeostasis and Diabetes.* Front Physiol, 2020. **11**: p. 575789.
5. Maas, A.H., *Playing with numbers: the development of an educational diabetes game.* Technische Universiteit Eindhoven, 2017.
6. Gábor, A. and J.R. Banga, *Robust and efficient parameter estimation in dynamic models of biological systems.* BMC Syst Biol, 2015. **9**: p. 74.
7. Horstman, A.M.H., R.A. Ganzevles, U. Kudla, A.F.M. Kardinaal, J.J.G.C. van den Borne, and T. Huppertz, *Postprandial blood amino acid concentrations in older adults after consumption of dairy products: The role of the dairy matrix.* International Dairy Journal, 2021. **113**: p. 104890.
8. Woldaregay, A.Z., E. Årsand, S. Walderhaug, D. Albers, L. Mamykina, T. Botsis, and G. Hartvigsen, *Data-driven modeling and prediction of blood glucose dynamics: Machine learning applications in type 1 diabetes.* Artif Intell Med, 2019. **98**: p. 109-134.
9. Baker, R.E., J.-M. Peña, J. Jayamohan, and A. Jérusalem, *Mechanistic models versus machine learning, a fight worth fighting for the biological community?* Biology Letters, 2018. **14**(5): p. 20170660.
10. Choi, R.Y., A.S. Coyner, J. Kalpathy-Cramer, M.F. Chiang, and J.P. Campbell, *Introduction to Machine Learning, Neural Networks, and Deep Learning.* Translational Vision Science & Technology, 2020. **9**(2): p. 14-14.
11. van Riel, N.A., *Dynamic modelling and analysis of biochemical networks: mechanism-based models and model-based experiments.* Brief Bioinform, 2006. **7**(4): p. 364-74.
12. Gratie, D.-E., B. Iancu, and I. Petre, *ODE Analysis of Biological Systems*. 2013. p. 29-62.
13. Niarakis, A. and T. Helikar, *A practical guide to mechanistic systems modeling in biology using a logic-based approach.* Brief Bioinform, 2021. **22**(4).
14. Bergman, R.N., Y.Z. Ider, C.R. Bowden, and C. Cobelli, *Quantitative estimation of insulin sensitivity.* Am J Physiol, 1979. **236**(6): p. E667-77.
15. Maas, A.H., Y.J. Rozendaal, C. van Pul, P.A. Hilbers, W.J. Cottaar, H.R. Haak, and N.A. van Riel, *A physiology-based model describing heterogeneity in glucose metabolism: the core of the Eindhoven Diabetes Education Simulator (E-DES).* J Diabetes Sci Technol, 2015. **9**(2): p. 282-92.

16. van Sloun, B., G.H. Goossens, B. Erdos, M. Lenz, N. van Riel, and I.C.W. Arts, *The Impact of Amino Acids on Postprandial Glucose and Insulin Kinetics in Humans: A Quantitative Overview.* Nutrients, 2020. **12**(10): p. 3211.
17. van Sloun, B., G.H. Goossens, B. Erdos, S. O'Donovan, A. Gijbels, I. Trouwborst, K.M. Jardon, E.E. Blaak, L. Afman, N.A. van Riel, et al., *Predicting the postprandial glucose response in tissue-specific insulin resistant phenotypes: a computational modeling approach*. Unpublished manuscript, 2022.
18. Trouwborst, I., A. Gijbels, K.M. Jardon, E. Siebelink, G.B. Hul, L. Wanders, B. Erdos, S. Péter, C.M. Singh-Povel, J. de Vogel-van den Bosch, et al., *Cardiometabolic health improvements upon dietary intervention are driven by tissue-specific insulin resistance phenotype: A precision nutrition trial.* Cell Metabolism, 2023. **35**(1): p. 71-83.e5.
19. O'Donovan, S.D., B. Erdős, D.M. Jacobs, A.J. Wanders, E.L. Thomas, J.D. Bell, M. Rundle, G. Frost, I.C.W. Arts, L.A. Afman, et al., *Quantifying the contribution of triglycerides to metabolic resilience through the mixed meal model.* iScience, 2022. **25**(11): p. 105206.
20. van Riel, N.A.W., C.A. Tiemann, P.A.J. Hilbers, and A.K. Groen, *Metabolic Modeling Combined With Machine Learning Integrates Longitudinal Data and Identifies the Origin of LXR-Induced Hepatic Steatosis.* Frontiers in Bioengineering and Biotechnology, 2021. **8**.
21. Yazdani, A., L. Lu, M. Raissi, and G.E. Karniadakis, *Systems biology informed deep learning for inferring parameters and hidden dynamics.* PLOS Computational Biology, 2020. **16**(11): p. e1007575.

# 8 Addendum

# IMPACT PARAGRAPH

Computational modelling is a powerful tool that has greatly improved our understanding of the human system. Computational models can be combined with (biological) datasets to perform *in silico* predictions across different spatial and temporal scales. The increasing amount of data allows the development of models that link different levels of biological organization to study complex system behavior and provide insight into the processes underlying health and disease. In this thesis, "Modelling of postprandial glucose and insulin dynamics: the role of amino acids", we focused on personalizing computational models of the glucose-insulin regulatory system and investigating factors influencing this system, in particular the effects of amino acids (AAs).

## Personalized complex meal models

The increasing prevalence of obesity and overweight, defined as abnormal or excessive fat accumulation, has a large impact on health and well-being [1]. Obesity results from an imbalance between energy intake and energy expenditure and is one of the major causes of insulin resistance. An increased insulin secretion by the pancreatic β-cells can often compensate for insulin resistance. However, over time, the increased demand on the β-cells to produce more insulin may lead to β-cell dysfunction and the development of type 2 diabetes mellitus (T2DM), which is characterized by high blood glucose levels [2]. Type 2 diabetes mellitus (T2DM) may eventually lead to disorders of the circulatory, nervous, and immune system, adversely affecting the life of patients as well as causing a large socio-economic impact. Large efforts are being undertaken by governmental and public health bodies to educate the general public on the importance of a healthy lifestyle, including diet and physical activity [3, 4]. While nutritional and lifestyle interventions may improve glucose homeostasis, a large heterogeneity exists in an individual's response to such interventions, which can be attributed to differences in genetic, environmental, and lifestyle factors [5]. In this thesis, we transitioned from a population average glucose homeostasis model (E-DES) to a personalized model, enabling insight into inter-individual differences in glucose metabolism. Together with an extension made to the model that allows for description of AAs and protein (E-DES-PROT), we can now describe and simulate the response of a person to a complex meal. This makes our work interesting for both consumers as well as for the food industry. The mechanistic nature of the model allows study and comparison of physiological processes contributing to postprandial glucose and insulin dynamics. A better understanding of how individuals respond to various foods at the mechanistic level may lead to

personalized dietary advice as well as targeted nutritional interventions. It also provides the opportunity to adjust and develop new food products with varying macronutrient composition targeted for specific phenotypes. This might further contribute to improved healthcare and reduction of the socio-economic impact of metabolic diseases such as T2DM. In addition, mechanistic models can easily be modified and adapted for various conditions, allowing researchers to simulate their own experiments or procedures, potentially reducing costs and the use of animal experiments.

### Hybrid models

While the intra-individual variability in postprandial glucose and insulin responses can be largely explained by mechanisms of glucose regulation encoded in mechanistic models, it is known that other factors such as body composition, diet, physical activity, and cardio-metabolic health related parameters may also affect glucose regulation [6, 7]. Zeevi et al. [8] showed that large inter-individual differences exist in response to identical meals, and that a machine learning model trained on a wide variety of phenotypic information was able to accurately predict the magnitude of postprandial glucose excursions. Machine learning methods allow a convenient framework to integrate diverse data that may have relevance in glucose regulation without the need for a causal understanding. While machine learning based approaches are useful for prediction, they only provide limited insight into the biology underlying inter-individual differences in glucose homeostasis [9]. Thus, a hybrid approach in which machine learning is combined with mechanistic modelling may circumvent the disadvantages of these standalone methods. Such a hybrid approach may yield more insight into the biology underlying inter-individual differences in glucose homeostasis. In our work, we developed and applied, for the first time, a hybrid combination of a machine-learning model with the mechanistic E-DES model to identify factors predictive of inter-individual differences in glucose and insulin following a glucose drink in a large group of individuals with various glucometabolic status. Whilst, a naïve sequential combination may not be suitable when studying underlying factors of inter-individual variance, a parallel approach should be explored in glycemic responses following complex meals containing varying amount of macronutrients as well as meals in free-living conditions. In the future, hybrid models may play a crucial role in the advancement towards ‘digital twins’ by providing simulative decision-support.

### Open source data and software

Open science is the movement to make scientific research and its results accessible to allow verification of scientific claims by others, but also to allow data from many different sources to be integrated to obtain new insights. There is a growing realization that scientific research depends more and more on computer code for simulation, calculations, analysis, visualization, and general data processing. It is important to have access to this code as well as to usable datasets. This allows researchers, for example, to apply models to their own data and further build and improve upon them. In our work, we made the computational modelling code publically available and detailed the computational software with corresponding versions and libraries. Furthermore, the modelling individualization pipeline was made available and was constructed in a generalized manner, requiring no biological insight to implement. As such, these computational techniques can be readily applied to other systems or models for analysis. We extracted dynamic time-series data from papers spanning over multiple decades going back to the late 60's. We made this data reusable and publically available to support data-sharing and allowing other researchers to use and employ the data.

## REFERENCES


1. Panuganti, K.K., M. Nguyen, and R.K. Kshirsagar, *Obesity*, in StatPearls. 2022.
2. Wondmkun, Y.T., *Obesity, Insulin Resistance, and Type 2 Diabetes: Associations and Therapeutic Implications.* Diabetes, metabolic syndrome and obesity : targets and therapy, 2020. **13**: p. 3611-3616.
3. Gorski, M.T. and C.A. Roberto, *Public health policies to encourage healthy eating habits: recent perspectives.* Journal of healthcare leadership, 2015. **7**: p. 81-90.
4. Whitsel, L.P., *Government's Role in Promoting Healthy Living.* Prog Cardiovasc Dis, 2017. **59**(5): p. 492-497.
5. Gijbels, A., I. Trouwborst, K.M. Jardon, G.B. Hul, E. Siebelink, S.M. Bowser, D. Yildiz, L. Wanders, B. Erdos, D.H.J. Thijssen, et al., *The PERSonalized Glucose Optimization Through Nutritional Intervention (PERSON) Study: Rationale, Design and Preliminary Screening Results.* Front Nutr, 2021. **8**: p. 694568.
6. Pillon, N.J., R.J.F. Loos, S.M. Marshall, and J.R. Zierath, *Metabolic consequences of obesity and type 2 diabetes: Balancing genes and environment for personalized care.* Cell, 2021. **184**(6): p. 1530-1544.
7. Tsereteli, N., R. Vallat, J. Fernandez-Tajes, L.M. Delahanty, J.M. Ordovas, D.A. Drew, A.M. Valdes, N. Segata, A.T. Chan, J. Wolf, et al., *Impact of insufficient sleep on dysregulated blood glucose control under standardised meal conditions.* Diabetologia, 2022. **65**(2): p. 356-365.
8. Zeevi, D., T. Korem, N. Zmora, D. Israeli, D. Rothschild, A. Weinberger, O. Ben-Yacov, D. Lador, T. Avnit-Sagi, M. Lotan-Pompan, et al., *Personalized Nutrition by Prediction of Glycemic Responses.* Cell, 2015. **163**(5): p. 1079-1094.
9. Alber, M., A. Buganza Tepole, W. Cannon, S. De, S. Dura-Bernal, K. Garikipati, G. Karniadakis, W. Lytton, P. Perdikaris, L. Petzold, et al., *Integrating machine learning and multiscale modeling—perspectives, challenges, and opportunities in the biological, biomedical, and behavioral sciences.* npj Digital Medicine, 2019. **2**.

## SUMMARY

A complex regulatory system is in play to maintain and control blood glucose levels under different physiological conditions. Currently existing whole-body mechanistic models of the glucose regulatory system generate quantitative information on glucose-insulin dynamics whilst capturing the mechanistic link between glucose and insulin. However, these models do not include the effect of amino acids (AAs), which have been recognized as important dietary components influencing glucose regulation in various health phenotypes. Incorporating the postprandial effect of AAs and protein is essential given their impact on both acute and long-term postprandial glucose metabolism. In addition, these mechanistic models have mainly been used to describe population averages, thus disregarding the heterogeneity in individual responses. In this thesis, we used a computational modelling approach to allow personalized simulation of postprandial glucose, insulin, and AA responses following challenge tests containing AAs or protein in various health phenotypes using a whole-body mechanistic model of glucose homeostasis. Furthermore, we explored whether the addition of a data-driven model could improve the predictive performance of the mechanistic models.

In **Chapter 2**, we performed a systematic literature search to identify intervention studies reporting glucose and insulin concentrations following acute ingestion and/or intravenous infusion of AAs in healthy adults and those living with obesity and/or type 2 diabetes (T2DM). We identified and extracted glucose and insulin time-series data from 55 studies that examined the effects of leucine (n=6), isoleucine (n=1), alanine (n=6), glutamine (n=1), arginine (n=28), lysine (n=1), glycine (n=2), proline (n=1), phenylalanine (n=1), glutamate (n=3), branched-chain AAs (n=4), and multiple individual AAs (n=1) on glucose and insulin concentrations. The data showed that oral ingestion of most individual AAs induced an insulin response but did not alter glucose concentrations in healthy participants. Specific AAs, such as leucine and isoleucine, when co-ingested with glucose exerted a synergistic effect on the postprandial insulin response, and attenuated the glucose response more compared to glucose intake alone in healthy participants. Furthermore, oral AA ingestion as well as intravenous AA infusion was able to stimulate an insulin response and decrease glucose concentrations in T2DM and obese individuals. The extracted glucose and insulin time-series data was made publicly available.

The postprandial glucose and insulin responses to identical meals can vary significantly across individuals. Certain dynamic features of these responses have been shown to be indicative of the state of the glucose regulatory system and therefore relevant for targeted lifestyle intervention. Currently, this heterogeneity is overlooked due to a lack of methods to quantify the interconnected dynamics in the glucose and insulin time-courses. In **Chapter 3**, we personalized a physiology-based mechanistic model of the glucose regulatory system to elucidate the heterogeneity in individuals' postprandial responses to an oral glucose tolerance test (OGTT) using a large population of people who have overweight or obesity ($n$ = 738) from the DIOGenes study. To transition from population averages towards describing individual response patterns, we developed a systematic parameter selection pipeline that may also be generalized to other biological systems. We showed that personalized models were able to capture the postprandial glucose and insulin responses more accurately compared to the population-level models. Furthermore, the estimated model parameters captured relevant features of individuals' metabolic health such as gastric emptying, endogenous insulin secretion, and insulin-dependent glucose disposal into tissues. The latter two also showed a significant association with the Insulinogenic index and the Matsuda insulin sensitivity index, respectively.

While physiology-based mechanistic models perform well in response to oral glucose challenges, interactions with other nutrients, like AAs and protein have not been considered yet. In **Chapter 4**, we developed a mechanistic model of the glucose homeostasis that incorporates and captures the postprandial effects of AAs and protein intake. New terms, accounting for the effect of AAs on insulin secretion and liver glucose production were introduced and the model was applied to postprandial glucose and insulin time-series data following different AA challenges (with and without co-ingestion of glucose), dried milk protein ingredients, and dairy products. We showed that this novel model was able to accurately describe the postprandial glucose and insulin dynamics, whilst providing insight into the physiological processes underlying meal responses.

While both "bottom-up" mechanistic and "top-down" data-driven techniques offer distinct benefits in untangling the complex interactions underlying disturbances in glucose homeostasis, a combined approach has yet to be explored. In **Chapter 5**, we used a sequential combination of a mechanistic and a data-driven modelling approach to quantify individuals' glucose and insulin responses to an OGTT, using cross-sectional data from a large observational population-based cohort, the Maastricht Study. We showed that the addition of

a data-driven machine learning model did not improve predictive performance. The personalized mechanistic models consistently outperformed the data-driven and the combined model approaches, demonstrating the strength and suitability of “bottom-up” mechanistic models in describing the dynamic glucose and insulin responses to OGTTs.

Tissue-specific insulin resistance phenotypes (predominantly muscle or liver) have been shown to interact with diet to determine changes in metabolic outcome and have shown distinct glycemic responses to challenge tests. In **Chapter 6**, we applied our novel model (developed in Chapter 4), to simulate and understand mechanistic differences between muscle insulin resistance and liver insulin resistance, using postprandial glucose, insulin, and AA time-series data following a high-fat-mixed meal in individuals from the PERSON study. We showed that our model accurately simulated glucose and insulin response following ingestion of a high-fat mixed meal, and predicted a difference in physiological processes such as gastric emptying and insulin-dependent glucose uptake into tissues, and insulin secretion between tissue-specific insulin-resistant metabolic phenotypes. Insight into the biological mechanisms underlying tissue-specific insulin resistance phenotypes is important due to the differential response to lifestyle and pharmacological interventions aimed to increase cardiometabolic health and/or insulin sensitivity. Personalized models could therefore play a key role in the transition towards precision nutrition, not only by assessing the effects of an intervention, but also providing dietary advice aimed to prevent (further) deteriorations in the glucose regulatory system.

# ACKNOWLEDGEMENTS

My journey as a PhD candidate has come to an end. It was a time filled with memorable moments, in which I forged lifelong friendships. A PhD is never a solitary endeavor, so I want express my gratitude to all those who directly or indirectly contributed to the research presented in this thesis and supported me throughout my years as a doctoral student.

First and foremost, I would like to thank my promotor, **Ilja**, for granting me the opportunity to pursue a PhD position in the field of Systems Biology. Collaborating with **Natal** and **Gijs** as members of my supervision team, we successfully carried out this challenging project. I am grateful for all the guidance, valuable insights, and engaging discussions we had. I would like to thank **Michael** for his supervision during the first year of my PhD. Your knowledge and experience with mechanistic models and machine learning was a true inspiration. You were always eager to help and offer your support, even after you pursued a different career path. **Shauna**, you were also a tremendous help, offering practical insights and setting realistic expectations (a.k.a. the "office cloud of doom").

I would like to thank the members of the assessment committee: **Prof. Dr. Ir. Ralf Peeters**, **Prof. Dr. Barbara Bakker**, **Dr. Aurélie Carlier**, **Prof. Dr. Peter Hilbers**, and **Dr. Lex Verdijk** for taking the time and effort in reading and assessing my dissertation.

The research conducted in this PhD was carried out under the TiFN theme: "The biology behind perceivable consumer benefits; Glucose (M)apping". Thank you **Ellen** for taking a leading role in this consortium, providing a collaborative and supportive environment. **Gabby**, your support in data handling was truly invaluable. I would like to thank all co-authors for their contribution to the chapters in this thesis. **Johan** and **Cécile**, your curiosity and genuine interest in computational models and application to nutrition was truly appreciated, and allowed me to look at my work from different perspectives. **Kelly**, **Inez**, **Anouk**, and **Lisa** – thank you for the many conversations and enjoyable moments together. Also Kelly, thank you for helping me out in organizing the blood samples, especially considering my 'occasional' moments of chaos.

I would like to thank all the people at MaCSBio for the welcoming environment, the good laughs and the many scientific and non-scientific discussions. Thank you **Claudia** for the assistance, and of course, for the enjoyable chats we have

had. A big shout-out to my office buddies **Balázs**, **David** and **Charlie**. We shared many great moments together, from dressing up as pirates for the PhD boat party "Pirates of the Maasribbean", to enjoying the energetic 24-h loop of Paul Stanley's 'Live to win' in the office (I'm still puzzled that you didn't threw me out). I genuinely could not have done this without you guys. Thanks for everything! Balázs, you were a great support during my time as a PhD student and kept me sane throughout this challenging project. Our collaboration was truly exceptional! I still remember clearly the time we wrote a paper in a matter of days, fueled by caffeine. I cannot help but wonder if we will ever witness the moment when Luffy uncovers the One Piece. I for sure know whom to contact first when he does.

I also want to thank my colleagues at the Rabobank - **Sina**, **Chenming**, **Reinhardt**, **Jelena**, **Cenk**, **Rao**, **Arjen**, **Hakan**, **Karen**, **Benay**, and **Dariya** for creating a welcoming environment for me during the final stages of my PhD.

Nu even een switch naar het Nederlands. Ik wil mijn familie en vrienden bedanken voor de steun, gezelligheid, en de nodige afleiding. **Niels**, **Maud**, **Sanne**, **Danique**, **Robin**, **Glenn**, en **Frank** – bedankt voor de vele jaren van plezier en uitjes met de Treinlimbocellos, dat allemaal begon bij de Student Council waar we als jonge studenten allemaal ons uiterste best deden om een bijdrage te leveren aan de universiteit. Heel mooi om te zien hoe we ons over de jaren ontwikkeld hebben.

Ik wil de leden van de Geitenclub Iris XI – **Daan**, **Kevin**, **Guus**, **Robbert**, **Ivo**, **Jelle**, **Nick**, **Moos**, **Patrick**, **Randy**, **Glenn**, **Harm**, **Joep**, **Remco**, en **Vince** – bedanken voor de jaren van vriendschap en gezelligheid. Of het nu een avondje bij café 't Heukske is, of ons jaarlijks uitje met de geitjes, het is altijd genieten. Ik heb al zin in ons volgende uitstapje. Helaas hebben we ook afscheid moeten nemen van onze dierbare vriend **Joep Nizet**. Ik ben dankbaar voor de waardevolle vriendschap die we met hem hebben mogen delen.

**Niels**, wat tof dat we zo dicht bij elkaar woonden. Ik herinner me nog goed onze regelmatige uitstapjes naar de Gouverneur, hoewel de ochtenden daarna soms iets minder aangenaam waren. **Maud**, onze academische reis begon bij GW, waar we vooral veel klaagden en het spel 'sla je pc aan stukken' speelden. Mooi dat we de master en PhD samen hebben doorlopen. Ik wil jou en Niels dan ook bedanken voor de gezelligheid, gastvrijheid en vriendschap.

**Daan**, **Marc**, **Erik**, **Dennis**, en **Tom** – bedankt voor de nodige afleiding en plezierige momenten, zeker wanneer ik worstelde met de druk van het publiceren. Jullie zijn echte vrienden!!

**Femke**, wat ben ik blij om jou als schoonzusje te hebben. Samen genieten van Temptation Island of losgaan bij de bodypump, het is altijd leuk met jou. Wat fijn dat we nu zo dicht bij elkaar wonen in het mooie Eindhoven. Ik kijk ernaar uit om de groei van **Feline** van dichtbij te mogen meemaken. **Yala**, jouw enthousiasme kent geen grenzen. Bedankt voor de vele knuffels!

**Ruud** en **Jelle**, mijn paranimfen en mijn beste vrienden. Jelle, we hebben heel wat avonturen meegemaakt over de jaren heen, genoeg om een boek over te schrijven. Heerlijk dat we ons moeiteloos tot vijf uur in de ochtend kunnen amuseren als we met z'n tweeën op stap gaan. Wǒ de péngyǒu! Ook wil ik je bedanken voor het ontwerp van de omslag van mijn proefschrift, het is echt heel mooi geworden. Ruud, wat ben ik ontzettend trots op jou wat jij allemaal in korte tijd bereikt hebt. Je bent een echte inspiratie, en ik weet dat ik altijd op jou kan rekenen (ook voor auto advies).

**Pap en mam**, ik weet niet waar ik moet beginnen. Of het nu gaat om advies, een luisterend oor of een warme knuffel, jullie zijn er altijd. Ik kijk er dan ook altijd naar uit om weer terug naar Echt City te komen. Bedankt voor de voortdurende aanmoediging, steun, en de vrijheid om mijn dromen na te jagen. Ik kan me werkelijk geen betere ouders wensen. Bedankt voor alles wat jullie voor me hebben gedaan en nog steeds doen!

# PUBLICATIONS

**Sloun BV**, Goossens GH, Erdos B, Lenz M, Riel NV, Arts ICW. The Impact of Amino Acids on Postprandial Glucose and Insulin Kinetics in Humans: A Quantitative Overview. Nutrients. 2020 Oct 21;12(10):3211

Erdős B, **van Sloun B**, Adriaens ME, O'Donovan SD, Langin D, Astrup A, Blaak EE, Arts ICW, van Riel NAW. Personalized computational model quantifies heterogeneity in postprandial responses to oral glucose challenge. PLoS Comput Biol. 2021 Mar 31;17(3):e1008852.

**van Sloun B**, Goossens GH, Erdõs B, O'Donovan SD, Singh-Povel CM, Geurts JMW, van Riel NAW, Arts ICW. E-DES-PROT: A novel computational model to describe the effects of amino acids and protein on postprandial glucose and insulin dynamics in humans. iScience. 2023 Feb 18;26(3):106218.

Erdős B, **van Sloun B**, Goossens GH, O'Donovan SD, Eussen SJMP, de Galan BE, van Greevenbroek MMJ, Stehouwer CDA, Schram MT, Blaak EE, Adriaens ME, van Riel NAW, Arts ICW. Quantifying postprandial glucose responses using a hybrid modeling approach: Combining mechanistic and data-driven models in The Maastricht Study. PLoS One. 2023 Jul 27;18(7):e0285820.

**van Sloun B**, Goossens GH, Erdõs B, O'Donovan SD, Gijbels A, Blaak EE, Afman L, van Riel NAW, and Arts ICW. Predicting the postprandial glucose response in tissue-specific insulin resistant phenotypes: a computational modeling approach (submitted)

# ABOUT THE AUTHOR

Bart van Sloun was born on May 31, 1992 in Sittard, the Netherlands. After completing his pre-university education at the Connect College in Echt, Bart pursued a degree in Health Sciences at Maastricht University. During his studies, he conducted a research project at the Department of Biomedical Engineering, focusing on the Hodgkin-Huxley model of action potentials. In September 2015, Bart pursued a Master's degree in Systems Biology at Maastricht University. He undertook an internship at the Department of Cardiology, where he worked on a project investigating the structure-function relationship in heart muscle cells using a unique approach of experimental and computational biology under the supervision of Dr. Jordi Heijman. Bart continued as a PhD candidate at the Maastricht Centre for Systems Biology. His research centered around computational modeling of glucose dynamics in humans, with a specific emphasis on amino acids, under the supervision of Prof. Dr. Ir. Ilja Arts, Prof. Dr. Ir. Natal van Riel, and Dr. Gijs Goossens. In October 2022, Bart joined the Rabobank as a data-scientist. In his current role, he assesses the performance and compliance of credit risk model.